NASA TECHNICAL MEMORANDUM

NASA TM X-73,181

NASA TM X-73,181

FY 1976 PROGRESS REPORT ON A FEASIBILITY STUDY EVALUATING THE USE OF SURFACE PENETRATORS FOR PLANETARY EXPLORATION

M. B. Blanchard, V. R. Oberbeck, T. E. Bunch, R. T. Reynolds, T. N. Canning, and R. W. Jackson

Ames Research Center
Moffett Field, Calif. 94035

November 1976

1. Report No.	2. Government Accession No.	3. Recipient's Catalog No.
NASA TM X-73,181		

4. Title and Subtitle	5. Report Date
FY 1976 PROGRESS REPORT ON A FEASIBILITY STUDY EVALUATING THE USE OF SURFACE PENETRATORS FOR PLANETARY EXPLORATION	6. Performing Organization Code

7. Author(s)	8. Performing Organization Report No.
M. B. Blanchard, V. R. Oberbeck, T. E. Bunch, R. T. Reynolds, T. N. Canning and R. W. Jackson	A-6814

9. Performing Organization Name and Address	10. Work Unit No.
Ames Research Center Moffett Field, Calif. 94035	186-68-76-06
	11. Contract or Grant No.

12. Sponsoring Agency Name and Address	13. Type of Report and Period Covered
National Aeronautics and Space Administration Washington, D.C. 20546	Technical Memorandum
	14. Sponsoring Agency Code

15. Supplementary Notes

16. Abstract

This report summarizes activities performed by Ames Research Center, Sandia Corporation, and a group of potential experiment investigators funded by NASA Headquarters during FY 1976 to examine the feasibility of employing penetrators for exploring Mars. During this time a committee of scientists chaired by Dr. James Westphal, evaluated the penetrator concept as a tool for planetary exploration. Eight areas of interest for key scientific experiments have been identified by this committee. These include: seismic activity, imaging, geochemistry, water measurement, heatflow, meteorology, magnetometry, and biochemistry. In seven of the eight potential experiment categories this year's progress included: conceptual design, instrument fabrication, instrument performance evaluation, and shock loading of important components. Most of the components survived deceleration testing with negligible performance changes. Components intended to be placed inside the penetrator forebody were tested up to 3,500 g and components intended to be placed on the afterbody were tested up to 21,000 g.

A field test program was conducted using tentative Mars penetrator mission constraints. Drop tests were performed at two selected terrestrial analog sites to determine the range of penetration depths for anticipated common Martian materials. Minimum penetration occurred in basalt at Amboy, California. Three full-scale penetrators penetrated 0.4 to 0.9 m into the basalt after passing through 0.3 to 0.5 m of alluvial overburden. Maximum penetration occurred in unconsolidated sediments at McCook, Nebraska. Two full-scale penetrators penetrated 2.5 to 8.5 m of sediment. Impact occurred in two kinds of sediment: loess and layered clay.

Although previous information indicated no important disturbance in the soil surrounding the penetrator during impact, and therefore the soil in the immediate vicinity was suitable for in-situ analysis by instruments on-board the penetrator, detailed laboratory analyses of the soil in a 0 to 1 cm zone adjacent to the penetrator's skin revealed that this zone is modified during penetration and is therefore not suitable for in-situ analysis.

In summary, this year's activity has revealed three important results: (1) Deceleration g loads of nominally 2,000 for the forebody and 20,000 for the afterbody do not present serious design problems for potential experiments, (2) Penetrators have successfully impacted into terrestrial analogs of the probable extremes of potential Martian sites, and (3) To avoid contaminated and chemically modified soil samples for penetrator experiments performing in-situ analyses, some kind of sample collector will be necessary. Although a number of problem areas have been identified for future study, none appear insurmountable.

17. Key Words (Suggested by Author(s))	18. Distribution Statement
Penetrators Planetary exploration Mars	Unlimited STAR Category – 91

19. Security Classif. (of this report)	20. Security Classif. (of this page)	21. No. of Pages	22. Price*
Unclassified	Unclassified	286	$8.75

*For sale by the National Technical Information Service, Springfield, Virginia 22161

TABLE OF CONTENTS

FY 1976 PROGRESS REPORT ON A FEASIBILITY STUDY EVALUATING THE USE OF SURFACE PENETRATORS FOR PLANETARY EXPLORATION

M. B. Blanchard, V. R. Oberbeck, T. E. Bunch, R. T. Reynolds,
T. N. Canning, and R. W. Jackson

Ames Research Center

SUMMARY

This report summarizes activities performed by Ames Research Center, Sandia Corporation, and a group of potential experiment investigators funded by NASA Headquarters during FY 1976 to examine the feasibility of employing penetrators for exploring Mars. During this time a committee of scientists chaired by Dr. James Westphal, evaluated the penetrator concept as a tool for planetary exploration. Eight areas of interest for key scientific experiments have been identified by this committee. These include: seismic activity, imaging, geochemistry, water measurement, heatflow, meteorology, magnetometry, and biochemistry. In seven of the eight potential experiment categories, this year's progress included: conceptual design, instrument fabrication, instrument performance evaluation, and shock loading of important components. Most of the components survived deceleration testing with negligible performance changes. Components intended to be placed inside the penetrator forebody were tested up to 3,500 g and components intended to be placed on the afterbody were tested up to 21,000 g.

A field test program was conducted using tentative Mars penetrator mission constraints. Drop tests were performed at two selected terrestrial analog sites to determine the range of penetration depths for anticipated common Martian materials. Minimum penetration occurred in basalt at Amboy, California. Three full-scale penetrators penetrated 0.4 to 0.9 m into the basalt after passing through 0.3 to 0.5 m of alluvial overburden. Maximum penetration occurred in unconsolidated sediments at McCook, Nebraska. Two full-scale penetrators penetrated 2.5 to 8.5 m of sediment. Impact occurred in two kinds of sediment: loess and layered clay.

Although previous information indicated no important disturbance in the soil surrounding the penetrator during impact, and therefore the soil in the immediate vicinity was suitable for in-situ analysis by instruments on-board the penetrator, detailed laboratory analyses of the soil in a 0 to 1 cm zone adjacent to the penetrator's skin revealed that this zone is modified during penetration and is therefore not suitable for in-situ analysis.

In summary, this year's activity has revealed three important results: (1) Deceleration g loads of nominally 2,000 for the forebody and 20,000 for the afterbody do not present serious design problems for potential experiments, (2) Penetrators have successfully impacted into terrestrial analogs of the probable extremes of potential Martian sites, and (3) To avoid contaminated and chemically modified soil samples for penetrator experiments performing in-situ analyses, some kind of sample collector will be necessary. Although a number of problem areas have been identified for future study, none appear insurmountable.

INTRODUCTION

The Space Science Board of the National Academy of Sciences has recommended that surface penetrators be considered as standard tools for exploration of the solar system (ref. 1). A number of other studies (refs. 2–8) have also concluded that surface penetrator missions to Mars would provide useful scientific results. During FY 1976, NASA Headquarters funded three activities designed to assess the feasibility of using surface penetrators to emplace useful scientific experiments on the Martian surface: (1) Ames Research Center performed a field test program to evaluate penetrator systems, penetration depths, and environmental effects of penetration into terrestrial analogs of Martian surface materials. This effort was divided into two principal activities: (a) A contract with Sandia Laboratories for testing instrument components in the laboratory and penetrators in the field; and (b) Analytical studies performed in the Ames Space Science Division laboratories on contamination of impacted rocks, site selection, and penetrability. (2) Selected investigators performed feasibility studies of candidate scientific instruments potentially capable of operating from penetrators. (3) Dr. James Westphal was appointed to chair and select an ad hoc committee of scientists to evaluate the usefulness of penetrators as devices to explore Mars and other planets.

In April, 1976, a meeting of the Westphal committee and principal investigators was held in Albuquerque, New Mexico to review progress. In July, 1976, the Westphal committee met and prepared their report evaluating the feasibility of the surface penetrator concept. The following is a summary of work carried out by Ames and Sandia personnel, and a summary of reports (appendices A–M of this report) by investigators funded by NASA Headquarters to study feasibility of various candidate scientific instruments that could be emplanted by penetrators.

SCIENTIFIC RATIONALE

A prime objective of NASA's planetary programs is to study the origin and evolution of planetary bodies in the solar system. Current models of planetary evolution require a wide variety of data. Planetary surface models require data in the areas of geochemistry of the crust, geologic structure, and meteorologic activity. Planetary interior models require data in the areas of seismic activity, heat flow, and magnetic fields.

Surface penetrators are capable of providing data in each of these six areas. In fact, penetrators offer a unique capability for obtaining unusually high quality data in three of these areas. This uniqueness is a consequence of a penetrator's ability to pass through overburden material into underlying rock units. This action insures: (1) Adequate coupling to enable measurement (free from noise produced by meteorological activity and solar radiation) of a broad spectrum of seismic events, (2) Meaningful geochemical measurements from geologic formations rather than wind blown surface materials, and (3) Subsurface temperature measurements at depths below the influence of diurnal and annual fluctuations. The combination of high quality seismology, in-situ subsurface geochemistry, and heat-flow, along with an imager on the penetrator afterbody to observe surface processes, provides a unique instrument capable of acquiring prime scientific data from widely separated regions on a planet during one relatively low-cost mission.

The use of multiple penetrators (up to six) launched from one orbiting spacecraft allows several probes to be used for landing sites selected to provide data for global studies (e.g., seismic network) and allows a few additional probes to be used for unusually interesting sites (e.g., polar caps) that would have otherwise not been selected because the landing environment would endanger a mission devoted to a single landing craft.

The Westphal committee (ref. 9) found that penetrators offer a superior way to answer key science questions about planetary bodies. Their studies show that a penetrator mission would be worthwhile and should be considered as a logical follow-on to Viking. An exploration program of this nature would substantially enhance the value and success of subsequent surface-roving and sample return missions to Mars by dramatically improving the data base on which these missions are planned.

MISSION CONCEPT

The use of surface penetrators to deliver scientific instruments to a planet is a recent addition to NASA's inventory of planetary exploration methods. The basic concept of penetrators (refs. 2 and 3) is that a properly shaped vehicle can impact a surface at a moderately high velocity and then dissipate its kinetic energy by penetrating several meters beneath the surface. Thus, the vehicle does not require complicated systems to make a soft landing and the deceleration loads are held to acceptable levels. On a planetary body, part of the vehicle is designed to remain at the surface to provide a platform for both the communication antenna and some sensors. An umbilicus is unfurled to provide electrical connections to the more deeply buried forebody.

The technology of surface penetrators has been developed by the U.S. military and all the essential characteristics of planetary penetrators have been demonstrated on test or operational devices.

Mars Penetrator Design Features

The basic design features of a Mars surface penetrator are shown in figure 1. The rocket shape is necessary to assure penetration of the surface and stable flight through the ground. Most of the scientific instruments and the supporting subsystems are mounted inside the cylindrical section. The antenna and some shock-hardened sensors are mounted on the afterbody.

The vehicle is powered by a combination of a radioisotopic-thermoelectric-generator for steady loads and a rechargeable battery for peak loads. Communications to Earth are accomplished via a radio relay link to an orbiting spacecraft. Scientific data from the instruments will be collected and stored in a memory until a communication session with the orbiter allows the data to be sent to Earth. Instrument operations will be controlled from Earth and sequenced by an onboard computer.

A typical Mars mission would include 4 to 6 surface penetrators and a single spacecraft to carry them. After arrival at Mars, the penetrators would be separately targeted to preselected sites

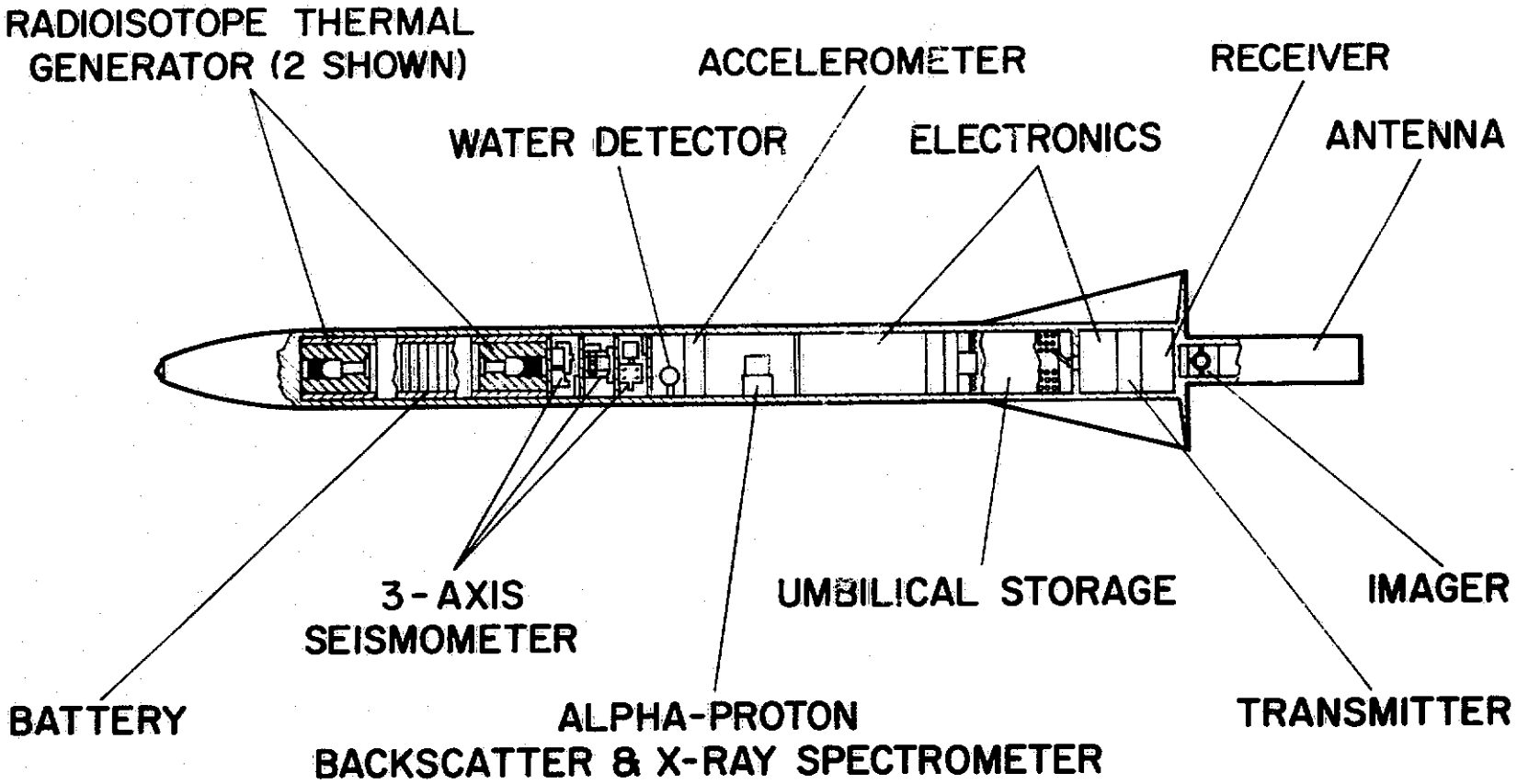

Figure 1.- A possible penetrator configuration.

as shown in figure 2 to establish a network of surface and subsurface stations. Once established, each penetrator in the network would be scheduled for daily communication sessions with the orbiter for at least a Martian year.

INSTRUMENT FEASIBILITY STUDIES

Science Justification for Selected Experiments

Certain types of experiments are generally considered useful to answer basic geophysical, geochemical, and biological questions necessary for understanding planetary and biological evolution. NASA Headquarters selected seven candidate experiments to study for a penetrator which satisfy major requirements for important planetary experiments: seismometry, imaging, geochemistry, water detection, heat flow, magnetometry, and biochemistry experiments.

Passive seismic instruments carried by a number of penetrators and emplaced at widely separated places on Mars can provide basic information characterizing the major structural features of the planet's interior. The presence and structure of a core, mantle, and crust can be determined. The diversity of surface geologic structure suggests that current geologic processes can also be studied using passive seismic techniques. An array of penetrators can provide an ideal seismic network because subsurface burial insures good seismic coupling of the instruments to the subsurface material.

Imaging experiments are usually the first source of information from which surface processes on a planet may be observed. They provide an indication of both meteorologic and geologic activity as evidenced by major landforms, and also provide a framework within which all other measurements may be interpreted. High-resolution images can be obtained from a camera on the afterbody of the penetrator. This is possible because the afterbody separates from the forebody at the time of penetration and remains on the surface. Imagery of the terrain surrounding several penetrators could provide substantially more information than is currently available for Mars and could thus augment the imagery obtained from Viking at two local sites in assessing the interaction between the planet's atmosphere and lithosphere.

Geochemical experiments can be more effective when performed from penetrators than from other spacecraft and landers. The surface of Mars is covered by deposits comprising a mixture of material excavated from coherent formations beneath the regolith by meteorite impact and volcanic processes, and fragmental materials carried by wind and water from other regions. Geochemical data can be most easily related to interpretation of known geologic events when large formations can be sampled completely and directly. For example, during lunar exploration the most meaningful rock samples were collected only from craters that penetrated through the overburden and excavated blocks from underlying formations. Penetrators can be emplaced beneath regolith deposits on Mars into coherent formations. In-situ geochemical analyses of such formations will provide important information on the geologic history of the planet.

Experiments to detect free and bound water are desirable for at least two reasons: First, water is considered vital to life processes and exploration for biological activity is a major goal for Martian studies. Second, many ancient Martian surface features suggest that a considerable amount of water

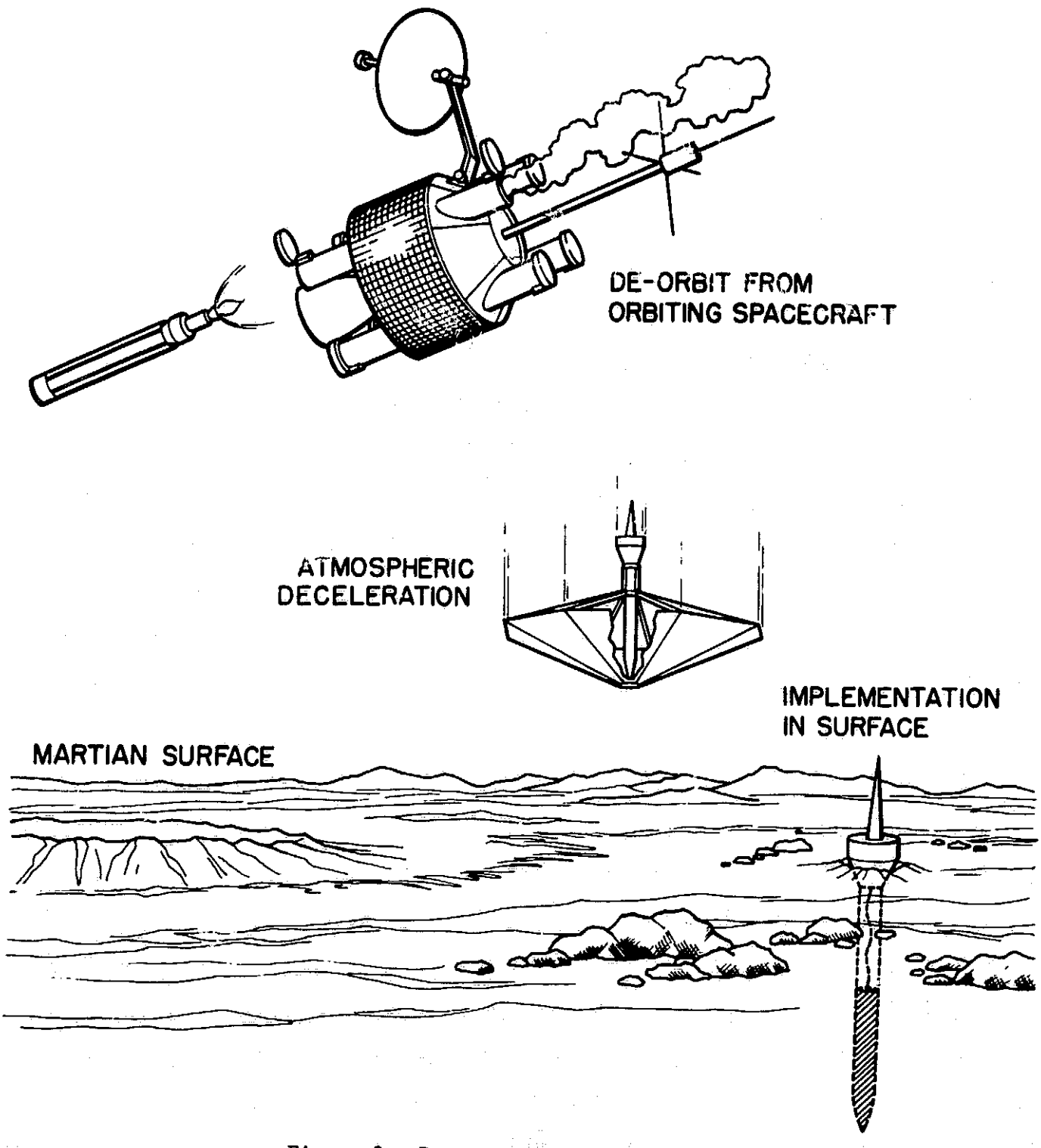

Figure 2.- Penetrator deployment on Mars.

was once present on the surface, and recent evidence from Viking has shown that the polar caps are covered with water ice. Detection and location of water stored in the Martian regolith is therefore an important task for reconstructing the meteorologic and geologic history of the planet.

Heat-flow experiments are important because they provide direct measurements of the thermal state of a planet. These measurements can be used to deduce the degree of differentiation of a planet. Heat flow information in conjunction with geochemical, seismic, and magnetic data, is essential to determine a complete picture of the planetary interior and its history.

Magnetometer experiments are important because they can reveal physical properties of the planet's interior. Refined simultaneous measurements of the magnetic field from a network of penetrators and from a supporting orbiter spacecraft can yield information on the size, composition, and dynamics of a liquid metal core. Analysis of diurnal field measurements will make it possible to distinguish global and local magnetic fields and relate them to local geologic features. Electrical conductivity and temperature profiles can be derived from magnetometer measurements for the crust and mantle.

A major objective of solar system exploration is the search for extraterrestrial life and for conditions suitable for life development. This is the primary objective for Viking. Certainly, positive or inconclusive results from Viking will indicate that further experiments should be considered for subsequent missions. Penetrators could be used as reconnaissance tools to locate regions where life-sustaining environments are better developed. Experiments designed to detect life-related compounds can help to characterize the distribution, origin and evolution of life. The current Viking results suggest that subsurface biochemical exploration may be more suitable for detecting life than surface studies because the surface environment is so severe and changes rapidly. The need for simple and specific tests for life, or life-related compounds, seems certain from current interpretations of Viking data.

Summaries of Progress for Candidate Experiments

Seismic experiment– Several studies evaluating candidate seismometers for a penetrator mission have been performed: (a) Triaxial transducers compatible with the volume available have been identified; (b) Performance of two commercially available accelerometers were compared with a standard; (c) One commercially available accelerometer and an inertial mass suspension system were shock tested at the Sandia test facilities. Details of these studies are reported in Appendix A.

Four preliminary designs of three-axis instruments thought suitable for a Martian seismic investigation were identified. All are based on transducers that measure displacement rather than velocity because they yield greater response at very low frequencies. Viscous damping provided by fluids is likely to be employed for protection of the suspended mass against deceleration forces and as a conductive medium for resistance-bridge transducers. A rigid caging system similar to that used for the Viking seismometer and a limiting stop for the test mass are also being considered to protect the inertial masses from impact forces.

Two commercially available transducers were tested under controlled laboratory conditions and compared to the response of a Benioff I-90 system during a 6-3/4 magnitude earthquake in Peru. The commercial instruments have been found to be more sensitive than the Viking

seismometer. A commercial bubble tiltmeter and an inverted pendulum seismometer passed shock testing to 2,000 g with no changes in performance.

Surface imaging experiment– Cameras attached to the penetrator afterbody provide the means for useful study of soil characteristics, microcratering, aeolian processes, water and carbon dioxide condensation processes (i.e., fog and frost), dust storms, site characterization, and determination of position and orientation of the after-body by star observations. Details of an imaging device with these capabilities are reported in Appendix B.

A 100 X 100 element Fairchild CCD array was subjected to an acceleration of 19,500 g perpendicular to the plane of the array. The results after the shock test showed the device operated normally, except that the photogate appeared to be open. It was concluded that no damage to the basic device was directly attributable to the shock and that contamination and poor quality control were responsible for the problem. A device built to flight standards should have survived without damage.

Geochemical experiments– Two types of geochemical experiments were investigated: the alpha, proton, and X-ray instrument, and the γ-ray spectrometer.

Alpha, Proton, and X-ray Instrument. Since the first chemical analyses were performed on the lunar surface from Surveyor by an α-backscatter experiment, improvements on the technique have continued. For the penetrator the experiment would include alpha, proton, and X-ray analysis modes. With these three modes the experiment is capable of measuring all of the major elements (except hydrogen) and many of the minor and trace elements in a soil sample. Details of the experiment are contained in Appendix C.

Work to adapt the alpha particle instrument for a penetrator mission has proceeded in four areas: (a) Miniaturized "mini" and "micro" alpha instruments have been conceptually developed but not built. The "micro" design is tailored to the penetrator envelope assuming the soil immediately adjacent to the penetrator's skin would be analyzed. Since recent soil modification studies have shown this zone to be unsuitable for analysis, the "micro" instrument concept will either have to be revised or one of several methods employed to remove the affected soil layer. (b) Four potentially shock-critical components of the instrument have been identified. These are: solid state semiconductor detector, alpha source, collimator and film, and Joule-Thomson cryostat. (c) Environment testing of two of these four critical components was performed. Shock testing of silicon detectors at 90° (in-plane) and 45° angles has been successful at the 3,500 g levels. Cantilever-suspended collimators survived shock tests at 3,300 g; however, the suspended films did not. No alpha source or cryostat was available for shock testing. (d) Because CdTe X-ray detectors can be operated at ambient penetrator temperatures, they offer an advantage over cooled Ge detectors. Progress by others on CdTe detectors is being closely monitored to see if the CdTe can replace the Ge detector now planned for the "micro" instrument.

γ-Ray Spectrometer. The lunar-orbiting γ-ray spectrometer experiment flown on Apollo 15 and 16 provides a basis from which to project performance for a similar spectrometer capable of operating from a penetrator. This instrument complements an alpha, proton, X-ray instrument since the soil is analyzed to an effective depth of >10 cm, whereas the alpha, proton, X-ray instrument analyzes an effective depth of <1 mm. The γ-ray instrument will be able to measure Th, K, Fe, Ti, Mg, Si, O, and H. If signal/noise ratios can be improved, it may be possible to include Al, U, and Ca. Details of this spectrometer are reported in Appendix D.

Possible detectors for this instrument include cooled Ge, CdTe, photodiode-scintillator, and phototube-scintillator. After a design and performance trade-off study, the phototube-scintillator (PMT) was selected for testing. Three 5 cm PMT's and three 3.5 cm PMT's were shock tested. One of the larger PMT's collapsed when subjected to 3,500 g applied 12.4° off the central axis, otherwise the PMT's survived undamaged. A CsI scintillation crystal and a CdTe crystal were also successfully shock tested. An integrated detector assembly consisting of a 5 cm CsI crystal mated with a 3.5 cm PMT is planned for shock testing soon.

The RTG power source generates radiation fluxes of neutrons and γ-rays which will detrimentally affect the sensitivity of the proposed experiment. The γ-ray emission results from impurities in the Pu 238 fuel and daughter products from the decay of the Pu 238. The dominant γ-ray emission (2.614 MeV) can be reduced if specially processed Pu 238 is used. The neutron flux generated by the RTG can produce measurable activation in a scintillation detector and in the materials from which the penetrator is made. The calculated RTG background interference does not preclude the proposed experiment, but it demonstrates that a special effort should be devoted to shielding methods.

Any hydrogen present in the soil will interact with secondary neutrons from cosmic rays or the neutron flux from the RTG to produce the 2.23 MeV hydrogen line. The γ-ray instrument can provide a useful measurement for soil water because the minimum detectable level for hydrogen is estimated to be about 0.3% by weight.

Water detection experiment– Various techniques have been considered to measure soil moisture. The use of a pulsed neutron source (14 MeV), combined with a γ-ray detector, has been briefly examined and is reported in Appendix H. The use of neutrons generated by cosmic rays or by the RTG has also been examined and is reported in Appendix D. However, during the past year emphasis has been placed on a P_2O_5 type of hygrometer. Details of this study are reported in Appendix E. In this experiment a commercial Beckman P_2O_5 electrolytic hygrometer sensor element was evaluated in terms of its general operating characteristics and the feasibility of redesign and reconfiguration. It was subjected to shock tests at Sandia. The Beckman sensor element survived these tests in terms of electrical and mechanical integrity although recalibration tests showed that instrument sensitivity and dynamic range were reduced. After careful reconfiguration and conditioning of the P_2O_5 element, five of these sensors survived several shock tests and two aerial drop tests in full-scale penetrators experiencing decelerations up to 20,000 g. Additional tests of redesigned sensors were performed using a simulated Martian atmosphere (70% CO_2, 30% Ar, at pressures between 2–10 torr) containing water vapor at the ppm level. The sensor elements performed generally satisfactorily in terms of electrical integrity and sensitivity. However, evidence of uneven flow through the sensor element at a pressure range between 2–5 torr resulted in interruptions of the instrument measurements. In summary, the tests showed the sensor element responded to water vapor only and with sufficient sensitivity to function as a hygrometer in the Martian environment.

During the same period an alternate sensor (solid polymer electrolytic) that can function in either the conductance, or conductance-electrolysis mode was also studied. The solid polymer electrolytic has potential advantages over the P_2O_5 which includes wider dynamic range, better mechanical and chemical stability, and more versatile configurations.

Heat flow experiment– Most of the FY76 heat flow activity has been devoted to analyzing the influence of the natural and artificial phenomena that could interfere with a viable heat flow experiment. These analyses included an assessment of first-order effects of the following: annual and daily temperature fluctuations at the surface, energy stored in the penetrator by virtue of the temperature differences when implanted, energy deposited along the bore hole and in the penetrator skin during penetration, free convection in the bore hole, and heat produced by the RTG. Studies describing the effect a penetrator has on local soil temperature are reported in Appendices K and L.

The feasibility of making a viable heat flow measurement from a penetrator in the Martian soil has been examined mathematically and is reported in Appendix F. The similarities in deployment geometry and expected subsurface temperature variations between the lunar heat flow experiments and the proposed Mars penetrator system suggest that comparable methods could be used. To examine the difficulties involved in making such measurements, two numerical simulations of feasible penetrator deployment configurations were computed for a time cycle of one Martian year. The simulations show that the principal factors necessary for a successful Mars penetrator heat flow measurement include substantial penetration (>4 m preferably) and deployment of accurate temperature sensors (±0.05 K) at favorable locations. No hardware for the penetrator heat flow experiment has been built.

Magnetometer experiment– Preliminary performance requirements for a magnetometer to be operated onboard a penetrator on Mars were established. Details of this instrument are reported in Appendix G. A single-axis flux-gate sensor capable of performing within these constraints was built and tested. The sensor was mounted parallel and perpendicular to the direction of shock and experienced shock levels up to 21,000 g. No sensor mechanical or electrical properties were affected by the shock tests.

Biological experiments– Attention has been concentrated on the development of simple experimental concepts which can use the subsurface, multi-site, and long-life characteristics of the Mars penetrators. Details are given in Appendix H. In addition to providing information relative to planetary biology these experiments may also yield data beneficial to the geosciences.

FIELD TEST PROGRAM

Penetration Test Results

The objectives of the FY76 field test program were to determine the following: (1) The range of penetration depths for anticipated Martian materials at selected terrestrial analog sites, (2) The alteration of physical and chemical properties in the soil caused by the impacting penetrator, (3) The amount of contamination introduced to the soil by the penetrator during impact, and (4) The effect of full-scale testing on penetrator subsystems (e.g., telemetry) and sensors.

Terrestrial analog sites were selected to represent anticipated Martian materials in which the penetrator would experience maximum and minimum penetration depths. Maximum penetration occurred at the test site in McCook, Nebraska, and minimum penetration occurred at the site in Amboy, California.

The McCook, Nebraska, site was selected because it simulated penetration into wind deposited sediments (silts and sands) on Martian plains. During January 1976, two full-scale penetrators were dropped from an aircraft and two 0.58-scale penetrators were fired with an air gun into the McCook site. One set (full-scale and 0.58-scale) landed in a deposit of dense laminated silt and clay. Total penetration was 2.5 m for the full-size penetrator and 1.7 m for the 0.58-scale penetrator. Decelerations were measured at 300–400 g for the full-scale penetrator and estimated at 800–900 g for the 0.58-scale penetrator. The other set of penetrators landed in the desired loess sediment. Total penetration was 8.5 m for the full-scale and 4.6 m for the 0.58-scale penetrators. Peak decelerations were estimated at 100–200 g for the full-scale penetrator and measured at 400–600 g for the 0.58-scale model. At the McCook site, all penetrations were less and decelerations were greater than anticipated because the top 30 cm of soil was frozen. Results of the McCook field operations are described in Appendix I.

The Amboy, California, site was selected because it simulated penetration into Martian basalt flows. Several sites were investigated (refs. 10 and 11) in order to find one having a thin regolith that would be suitable as an analog to a lava flow on Mons Olympus. A regolith thickness of less than 1 m was selected using impact cratering theory. A model simulation study (ref. 6), using impact velocities specified in the mission plan and penetration equations, indicated total penetration into the underlying lava would be little affected by this layer of overburden. These simulations were confirmed by the full-scale field tests. During April 1976, four full-scale penetrators were dropped from an aircraft into the Amboy test site. The first penetrator impacted at a slightly higher velocity (213 m/s) than the mission model (150 m/s). Its total depth of penetration was 1.2 m. The amount of basalt penetrated was 0.9 m and the amount of alluvial overburden penetrated was 0.3 m. The second penetrator impacted at 152 m/s and its total depth of penetration was 0.9 m. The amount of basalt penetrated was 0.4 m and the amount of alluvial overburden penetrated was 0.5 m. Two other penetrators achieved similar results, although overburden thicknesses were greater. In three of the drops, total penetration was less than the penetrator length and the afterbody remained on the aft end of the penetrator. All penetrators had "off-the-shelf" telemetry packages not designed for hard rock penetration and, consequently, all failed on impact. Because of these failures, complete deceleration records were not obtained. However, calculations indicate that the penetrators experienced about 2,000 g during penetration of the alluvial overburden. Results of the Amboy field operations are described in Appendix M.

Soil Modification and Contamination Effects

Studying the effects produced in the soil (refs. 12–15) caused by the penetrator passing through the soil has proved to be very important for three reasons. First, the metal surface of the penetrator abrades and thus introduces contaminants to the environment. Second, the temperature levels reached in the soil in the immediate vicinity of the penetrator (0–2 mm) are sufficiently high that phase changes occur and thus change the elemental and mineralogical composition. Third, a zone of sediment mixing occurs in a boundary layer (0–1 cm thick) surrounding the penetrator as it passes through the soil. Within this mixing zone soil particles are rotated, crushed, and dragged along by the penetrator to their final stopping place.

It is clear that a thorough analysis describing the environment surrounding the penetrator is required before a sample recovery mechanism can be designed. The viability of potential geochemical and water detection experiments is affected by both the introduction of contaminants

and the phase changes occurring in the sediments. A preliminary report describing those changes observed in the soil for the full-scale penetrator landing in the loess is included in Appendix J. Analyses are continuing in an effort to describe the changes in the layered strata (interbedded clay and silt layers) where full-scale and 0.58-scale penetrators also impacted at McCook. Also, analyses are just beginning to determine the changes in the basalt where four full-scale penetrators impacted.

A brief summary of the preliminary report describing the changes observed in the soil for the full-scale penetrator impact site in the loess follows:

(1) The region 0–50 μm from the penetrator's skin is characterized by a glass layer. The elemental analyses have shown increases in Fe, Cr, Mo, Ni, and Ca (?) and decreases in Si, Al, K, and Na. The mineralogical analyses have shown the following minerals were introduced or newly formed: α Fe alloy, Cu-Sn alloy, cristobalite, opal; and the following minerals were destroyed: calcite, mica, kaolinite, illite, and montmorillonite.

(2) The region 50 μm–1 mm from the penetrator's skin is characterized by sintered and crushed sediment. The elemental analyses have shown increases in Fe, Cr, Mo, Ni, and Na, and decreases in Si, Al, and Ca (?). The mineralogical analyses have shown the following minerals were introduced or newly formed: α Fe alloy, hematite, ϵ Fe_2O_3, geothite, lepidocrocite, limonite, lechatelierite, and opal; and the following minerals were destroyed: calcite, kaolinite, illite, and montmorillonite.

(3) The region 1–2 mm from the penetrator's skin is characterized by a crushed and mixed sediment. The elemental analyses have shown increases in Fe, Cr, Mo, and Ni, and no decreases were observed. The mineralogical analyses have shown only a pressure-sensitive transformation from calcite to aragonite.

(4) The region 2 mm–1 cm from the penetrator's skin shows extensive mixing of soil particles and all pre-existing structure has been destroyed. No chemical or mineralogical changes were observed.

SHOCK TESTING

To assess the ability of scientific instruments to survive the high decelerations of penetration, a shock testing program was carried out. Sensors and devices were procured, fabricated, and subjected to acceleration pulses in a horizontal air-gun. The operation of this air-gun requires propelling a light piston (containing the test item) by rapid compression of a cushion of air between this light piston and a heavier driver piston. During this test the acceleration rises smoothly to a peak and diminishes smoothly to zero in a sine-wave-like fashion. Because the actual deceleration experienced by components in the full-scale penetrator is nearly a square-wave, rather than a sine-wave, the shock effects observed during these tests may be underestimated. A test facility to correct this deficiency is being designed. The results of all tests through May 1976 are shown in table 1. Test levels of 2,000 g for forebody devices and 20,000 g for afterbody devices were selected from preliminary studies of the highest loads expected. Most of the sensors tested so far have survived the required acceleration with negligible changes.

TABLE 1.– SHOCK TEST RESULTS

Device tested	Max. acceleration	Results
Water detection experiment		
Hygrometer P_2O_5 sensor	18,000 g 200 g loess test[a] 2,200 g basalt test[a]	No change in operation
Solid polymer sensor	2,200 g basalt test[a]	
α-Proton experiment		
30 μ thick disk detector	3,500 g in plane of detector 3,500 g at 45° to plane	
500 μ thick ring detector	3,500 g in plane 3,500 at 45° to plane	No change in performance
Source collimator	3,300 g normal to axis, cantilevered	
Oxide films in collimator	3,300 g in plane of film	Failed
γ-Ray experiment		
3.5 cm diam. photomultiplier tubes (3)	2,000 g along axis 3,500 g 20° from axis	No change in resolution Gain change less than 2
5.0 cm diam. photomultiplier tubes (3)	2,000 g along axis 3,500 g 12.4° from axis	One 5 cm tube broke at 3500 g
CsI scintillation crystal (5 cm diam. X 5 cm long)	2,100 g along axis	No change in resolution 10% gain change
CdTe crystal	2,200 g	No visible change
Seismic experiment		
Single axis seismometer 2 axis bubble sensor Levelling motor	2,200 g along axis 700 g normal to axes 2,100 g	No changes
Magnetic field experiment		
Single axis sensor	21,000 g along axis 21,000 g normal to axis	No change
Imaging experiment		
100 X 100 ccd array	19,500 g normal to array	Electrical problems due to poor workmanship

[a]Mounted inside penetrator.

CONCLUSIONS

To summarize this year's work, three important points should be noted: Full-scale penetrators have successfully impacted into terrestrial analogs of two extremes of potential Martian rock types (least and most penetrable). Some kind of an active or passive sample collector will be needed to provide uncontaminated and unmodified rock and soil samples for in-situ analysis. Deceleration loads of 2,000 g for the forebody and 20,000 g for the afterbody do not appear to present serious design problems for potential experiments.

Further, certain items have been identified as requiring special attention in the near future. The most important of these are the following:

- Design, build, and test telemetry and power systems that operate reliably in a full-scale penetrator to at least the 2,000 g level.

- Conceptually develop and analyze a thermal control system capable of keeping onboard penetrator experiments operational over a wide range of Martian subsurface environments.

- Compare the effectiveness of passive (e.g., ramp and entrapment designs) and active (e.g., auger design) methods for collecting uncontaminated soil and rock samples.

- Perform terrestrial analog full-scale penetrator drop tests and determine soil modification effects for a permafrost environment.

- Prepare a preliminary map of the surface of Mars delineating the surface materials' "penetrability." These data will be used to develop a preliminary Mars site selection plan in cooperation with other planetary investigators.

Penetrators are superior to other landing devices (i.e., hard and soft landers), for some measurements, principally because they penetrate overburden material into underlying rock units. The concept offers unique high quality seismology, in-situ subsurface geochemistry and heat flow measurements. These measurements, combined with an imager on the afterbody to monitor surface processes, offer a unique exploration tool capable of acquiring prime scientific data from widely separated regions of a planet during one relatively low cost mission.

The Ames penetrator project team enthusiastically endorses the Westphal report (Appendix N), recommending a 1981 penetrator mission to Mars.

REFERENCES

1. Space Science Board: Opportunities and Choices in Space Science. National Academy of Science, 1974.

2. Sandia Labs.: Mars Penetrator: Subsurface Science Mission. Contractor's Report No. SAND 74-0130, August 1974, NASA-Ames Contract No. RA88365A.

3. Hughes Aircraft Co.: Pioneer Mars Surface Penetrator Mission – Mission Analysis and Orbiter Design. Summary Report NAS2-8424, August 1974.

4. Jet Propulsion Lab.: Mars Polar Orbiter/Penetrator Study Report. Rep. 760-120-B, October 30, 1975.

5. Ames: Mars Science Missions in the Post-Viking Era: Possible Contributions of Pioneer-Type Missions. Working Report, August 1974.

6. Quaide, W. L., Oberbeck, V. R., Blanchard, M. B., and Morrison, R. H.: Penetrators: Multiple Subsurface Probes for Mars and Other Planetary Bodies. v. 56, Trans. of Am. Geophys. Union, 1975.

7. Quaide, W. L., Oberbeck, V. R., Morrison, R. H., Aggarwal, H. R., and Blanchard, M. B.: Mars Penetrators: A Preliminary Analysis of Their Value for Near Surface Science. Intnl. Colloq. of Planetary Geology, Expanded Abstracts, Rome, Italy, September 22–30, 1975.

8. Quaide, W. L., Oberbeck, V. R., Blanchard, M. B., and Reynolds, R. T.: Status Report on Feasibility of Using Penetrators in Planetary Exploration. (Memo to NASA-Hq. Planetology Program Principal Investigators from NASA-Ames, May 14, 1976).

9. Westphal, J. A., Currie, D., Fruchter, J., Head, J., Helsey, C., Lister, C., Niehoff, J., and Tillman, J.: Final Report and Recommendations of the Ad Hoc Surface Penetrator Science Committee, NASA-OSS, Planet. Prog. Div., August 1976.

10. Greeley, R., and Bunch, T. E.: Basalt Models for the Mars Penetrator Mission: Geology of the Amboy Lava Field, California. NASA TM X-73,125, 1976.

11. Bunch, T. E., Quaide, W. L., and Polkowski, G.: Initial Basalt Target Site Selection Evaluation for the Mars Penetrator Drop Test. NASA TM X-73,111, 1976.

12. Blanchard, M. B., and Shade, H.: The Effect of a Planetary Surface Penetrator on the Soil Column Surrounding the Impacting Body. NASA TM X-62,428, 1975.

13. Shade, H. D.: Preliminary Analysis of Soil Modification Found After 0.58-Scaled Penetrator Impaction on August 4, 1975, at Sandia Lab., New Mexico. LFE Report TLW 6142A, 1975.

14. Shade, H. D., and Polkowski, G. R.: Analysis of Core Material Obtained from McCook, Nebraska. LFE Report TLW 6148B, 1976.

15. Polkowski, G. R.: Procedures for Preserving Subsurface Fabric and Textures in Soil Adjacent to an Impacted Penetrator. LFE Report TLW 6149, 1976.

APPENDIX A

STUDY OF HARDWARE
FOR A
PENETRATOR-EMPLACED SEISMIC STATION

Wayne Miller

California Institute of Technology

Report of Progress, Contract NSG 7160

A Study of Hardware for a Penetrater-Emplaced Seismic Station

During the period covered by this contract (July 1, 1975 to June 30, 1976) a number of studies and experiments have been undertaken which are preliminary to the development of a penetrater-emplaced seismic station. Specifically we have: 1. studied tri-axial transducer designs which will fit within the required envelope; 2. conducted pier tests on two commercially available accelerometers; 3. prepared one of the commercially available accelerometers, an inertial mass-suspension system of our own design and some candidate centering motors for shock testing at the Sandia test facility.

Figures 1 through 4 are schematic representations of instruments which we feel are good candidates for meeting the requirements of volume and sensitivity. All are designs which are based on instruments which we have built in the past for other applications. Most of the designs are shown without transducers or facilities for damping. It is anticipated that displacement transducers will be used in each design because of their greater response at very low frequencies over that of velocity transducers. However velocity transducers are not ruled out and in fact an auxiliary velocity transducer (coil and magnet) may be added as part of a feedback design used for instrument centering and stabilization.

Viscous damping will be achieved by liquid filling the instrument which also acts as a protection against the forces of acceleration experienced upon impact with the planetary surface. In addition the liquid may serve as the dielectric for a capacitive bridge transducer or as the conductive media for a resistive bridge transducer. Liquid viscous damping, provided the components are properly designed, is proportional to velocity, as is electro-magnetic damping, however the elimination of magnetic devices will avoid stray magnetic fields which might adversly effect other experiments aboard the penetrater.

Figure 1 shows a co-axial, tri-axial suspension based upon a design previously used as a compact down-hole system. Resistive or capacitive bridge transducers are shown. A negative length spring will be used on the vertical to effect the equivalent of a greater spring extension in the small envelope and the period may be lengthened by incorporating an iron disk on the mass with a small magnet fixed to the frame. This technique is shown in more detail in Figure 2.

The vertical component shown in Figure 2 is, in principle, identical to the vertical component in Figure 1. The bi-axial horizontal instrument is a simple pendulum with period lengthening. A model of this design has been constructed to demonstrate the technique. The attraction between the magnet on the mass and the iron ring on the frame effects the cancellation of system restoring force with the resultant increase in the natural period from 0.3 sec to 1.0 sec. Because the instrument period varies inversely as the square of the restoring force, 0.9 of the system restoring force is transferred to the frame. Thus, an auxiliary displacement

transducer may be added by the addition of force sensing transducers between the iron ring and the frame. The horizontal components shown in Figure 3 incorporate a bi-axial, inverted pendulum.

Whatever suspension system is finally settled upon, the design must be capable of withstanding the forces encountered upon impact. This may be accomplished by using a rigid caging system as was done in the Viking instrument, or by building compliance into the suspension. An example of this latter technique, applied to an inverted pendulum, is shown in Figure 4. This is a schematic of a model which has been built for testing in the Sandia Laboratory's shock facility. Here the acceleration force is transferred to a limit stop. It is planned to test this device at 2000 g's.

As was mentioned, all of the designs discussed would use fluid damping and this fluid may act as an electrolyte between transducer plates and the common mass. The variable resistance of the electrolyte forms two arms of an alternating current bridge. This is the form of the transducer used with the bi-axial bubble tiltmeter, still to be discussed, and such a transducer was tested on the inverted pendulum to be shock tested. An electrical schematic of the bridge circuit is shown in Figure 5 for two axes. Although the bubble tiltmeter uses a common carrier oscillator, different frequencies on each axis would help eliminate cross-coupling of the axes.

Our studies of transducers applicable to a penetrator has also included commercially available units, two of which seem promising. The first of these is the Autonetics Model SE541A biaxial tiltmeter, shown in Figure 6. In principle, the tiltmeter

sensor is simply the ancient sprit level, in which the position of the bubble or void in a body of fluid is used to indicate the attitude of the fluid container with respect to gravity. The fluid is a methyl or ethyl alcohol or an alcohol and glycerin mixture. The position of the bubble is detected by a resistive bridge, as previously discussed. The weight of the bubble assembly is approximately 25 grams and its power consumption less than 0.1 milliwatt.

According to the manufacturer, the limit of resolution is of the order of 4×10^{-7} degree at 1Hz which is equivalent to 7×10^{-9}g. The small size, biaxial nature and high sensitivity make it a good candidate for a seismic instrument aboard a penetrater if it can be packaged to withstand the anticipated g forces. We have packaged it in a jig for shock testing at Sandia, first at 1000 g's and, if it survives, at 2000 g's.

The other commercial accelerometer which we have investigated is the Systron-Donner force-balance accelerometer, Model 4841. The primary application of this device is as a strapdown sensor for guidance systems. A drawing of the unit is shown in Figure 7 along with an operational block diagram. The inertial pendulum is maintained nearly at its mechanical zero position by the high gain amplifier and servo loop. This unit is primarily a high frequency (greater than 50Hz) device so much of our effort was to determine its low frequency characteristics.

If this unit has sufficient sensitivity for the application it is of particular interest to us because of its inherent feedback. We anticipate including signal shaping circuitry in the feedback

loop and thus may control the low frequency response of the device in the manner discussed in our previous reports on this subject. The weight of the unit is roughly 250 grams per axis and the power comsumption of the electronics supplied by the manufacturer is about 120 mw. The suspension of the inertial mass is by a diamond bearing which the manufacturer claims is purely elastic. So far, however, with our pier testing we have been unable to verify this.

Both the Autonetics bubble tiltmeter and the Systron-Donner accelerometer are being pier tested with their recordings compared to standard instruments. We have two test sites, one on the CIT campus and one at the CIT Kresge Laboratory about 4 km west of the campus. The bubble is simultaneously tested at the Kresge and campus sites. At the Kresge facility the bubble's frequency response is shaped electronically to equal the magnification of a Benioff, 1-90 system over the range of roughly 2 sec. to 20 sec. (Figure 8) to determine its long period characteristics. At the campus facility, very little response shaping is used so that its short period and wideband characteristics may be compared to the Viking instrument, a more or less conventional geophone (Figure 10). The force balance accelerometer is also being tested at the campus site and compared against the Viking and bubble instruments.

Figure 9 shows a Peruvian earthquake of magnitude 6 3/4 recorded at Kresge on the bubble and the Benioff system. Figure 9a and 9b show the beginning of the event (time scales are not the same on the two recordings) and Figures 9c and 9d show long period waves arriving some 13 munutes later. Figure 11 compares the

short period characteristics of the bubble with the Viking for a local event. The wide band characteristics of the bubble are evident as indicated by the presence of 6 sec. microseisms, which are absent on the Viking record, and the high frequency signatures of the local event and the train. Also shown, in Figure 11a, is a record of the same event as it appears after being processed by the Viking data compression system. This system extracts the envelope of the event and also makes a count of the number of times the signal made a position crossing of the zero axis, as a measure of the harmonic content of the event. The sampling interval in each case is one sample per second. Some kind of data compression will also be needed for the seismic penetrator experiment.

A comparison of the Viking instrument, the bubble and the force balance accelerometer is made in Figure 12 for a teleseism. Here again, the wideband characteristics of the bubble are evident. The record of the force balance accelerometer, however, is disturbing due to the lack of 6 sec. microseisms. The response curves of Figure 10 show that in the region of 6 seconds (arrows) the response of the bubble and the force balance accelerometer are within a few db. However, Figure 12 and other recordings of the force balance accelerometer, do not show 6 sec. microseisms, indicating that the response is not as shown in Figure 10. The 6 sec. microseisms represent an acceleration of the order of 10^{-7}g and their absence on the record could be interpreted to mean that the diamond suspension of the force balance accelerometer is not purely elastic at these g levels. Records supplied by Systron-Donner seem to show 6 sec. microseisms although no comparison instrument was operated at the time the recordings were made. This question is presently unresolved, problems

in the instrumentation are not ruled out, and is still being investigated.

Fig. 13 is from one of our previous reports and shows what we thought could be accomplished with an advanced Viking type instrument or what would have to be done in order to extend its response to that necessary to observe the free modes of Mars. The dotted area has been added to indicate the response that we have shown the bubble to have. It may, in fact, have much greater sensitivity than this since the manufacturer claims a resolution of greater than 10^{-8} g at a 1 Hz bandwidth. If the shock tests are successful the limits of sensitivity will be investigated further. If the lack of 6 sec. microseisms on the recordings from the force balance accelerometer is in fact due to instrumentation problems, it too, would have a response within the dotted area in Fig. 13 and a shock test of this instrument would be in order.

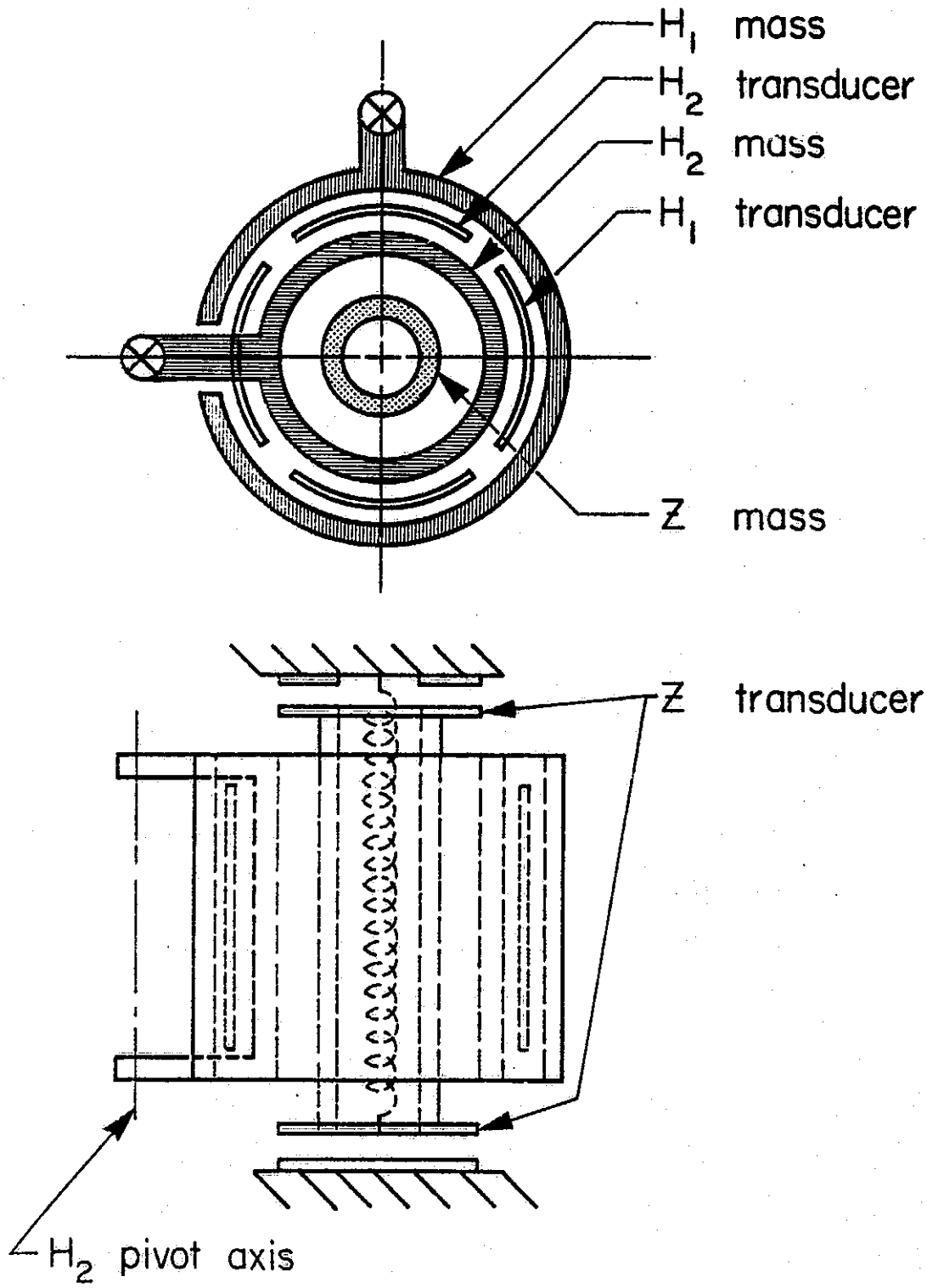

Triaxial Suspension System

FIGURE 1

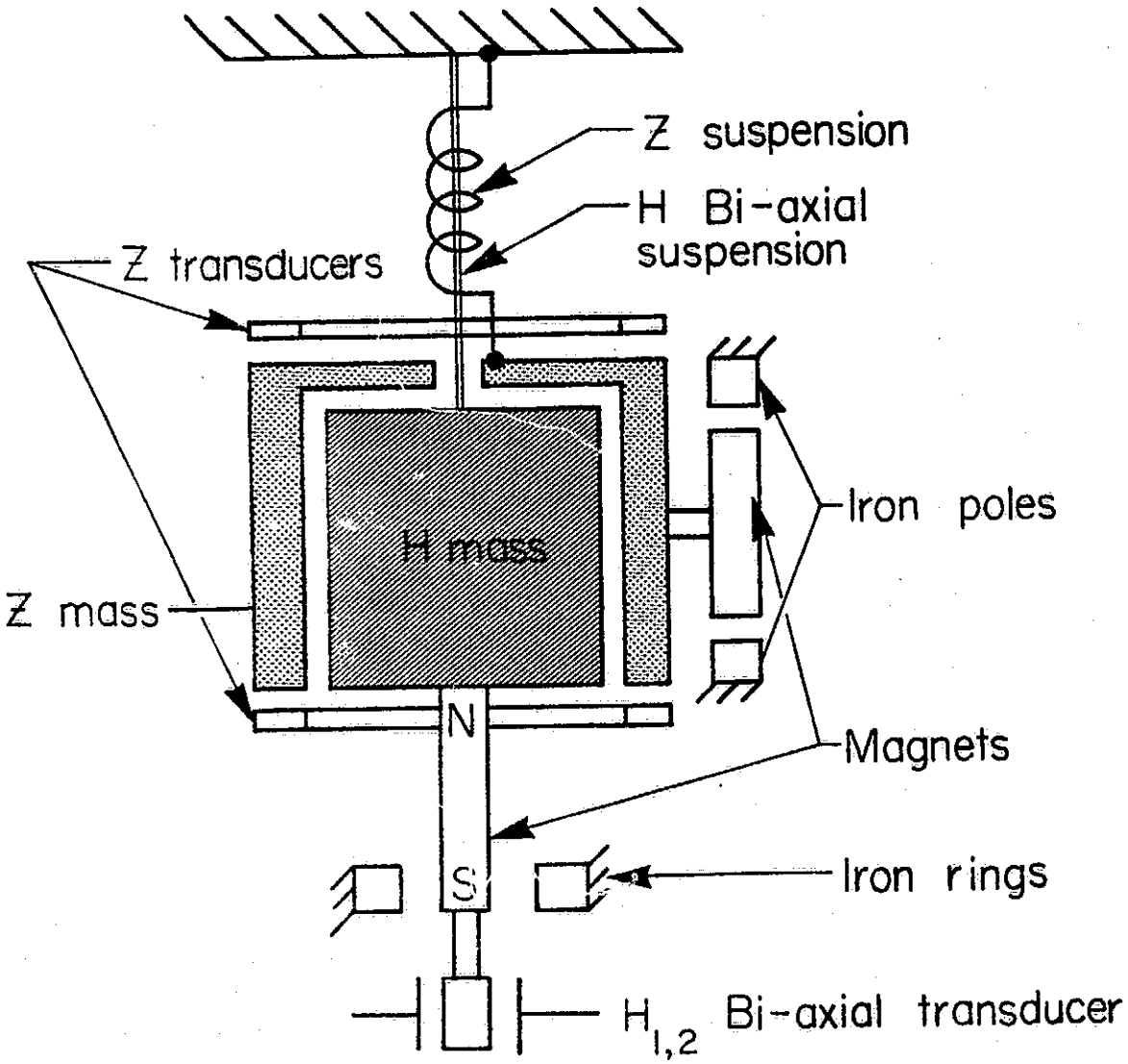

Triaxial Suspension System
with period lengthning

FIGURE 2

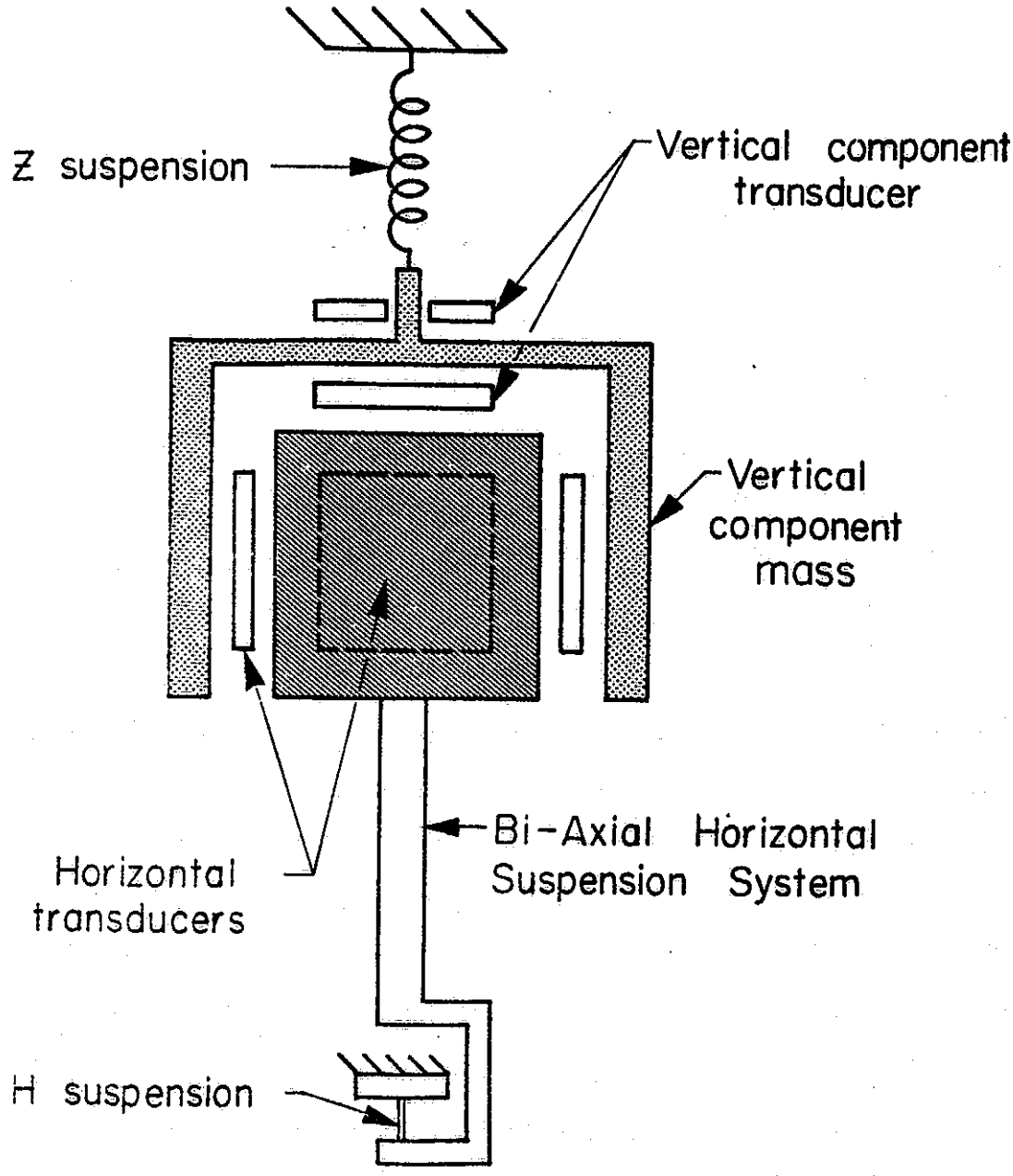

Triaxial Suspension System

FIGURE 3

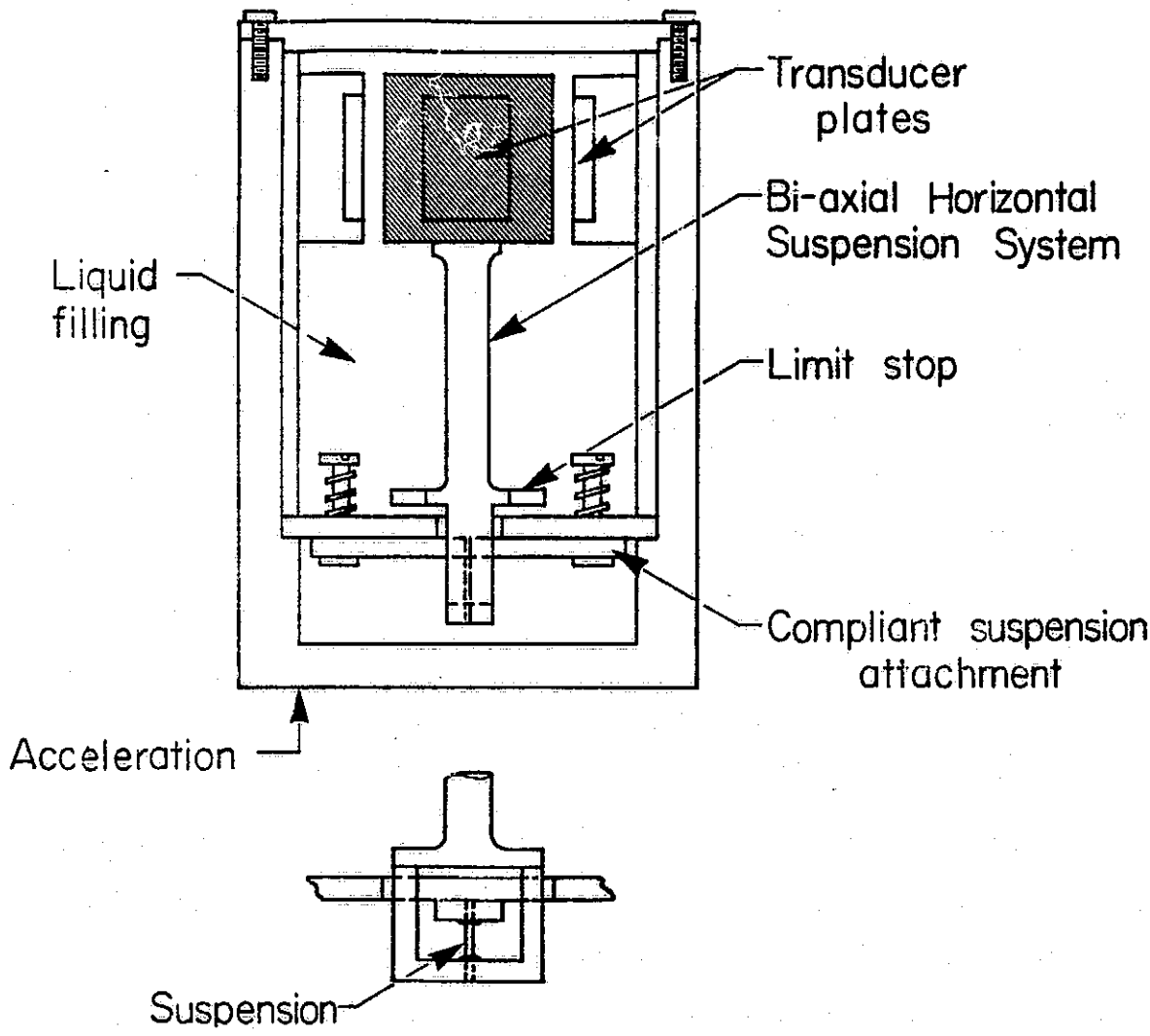

Experimental Bi-axial Horizontal Seismometer

FIGURE 4

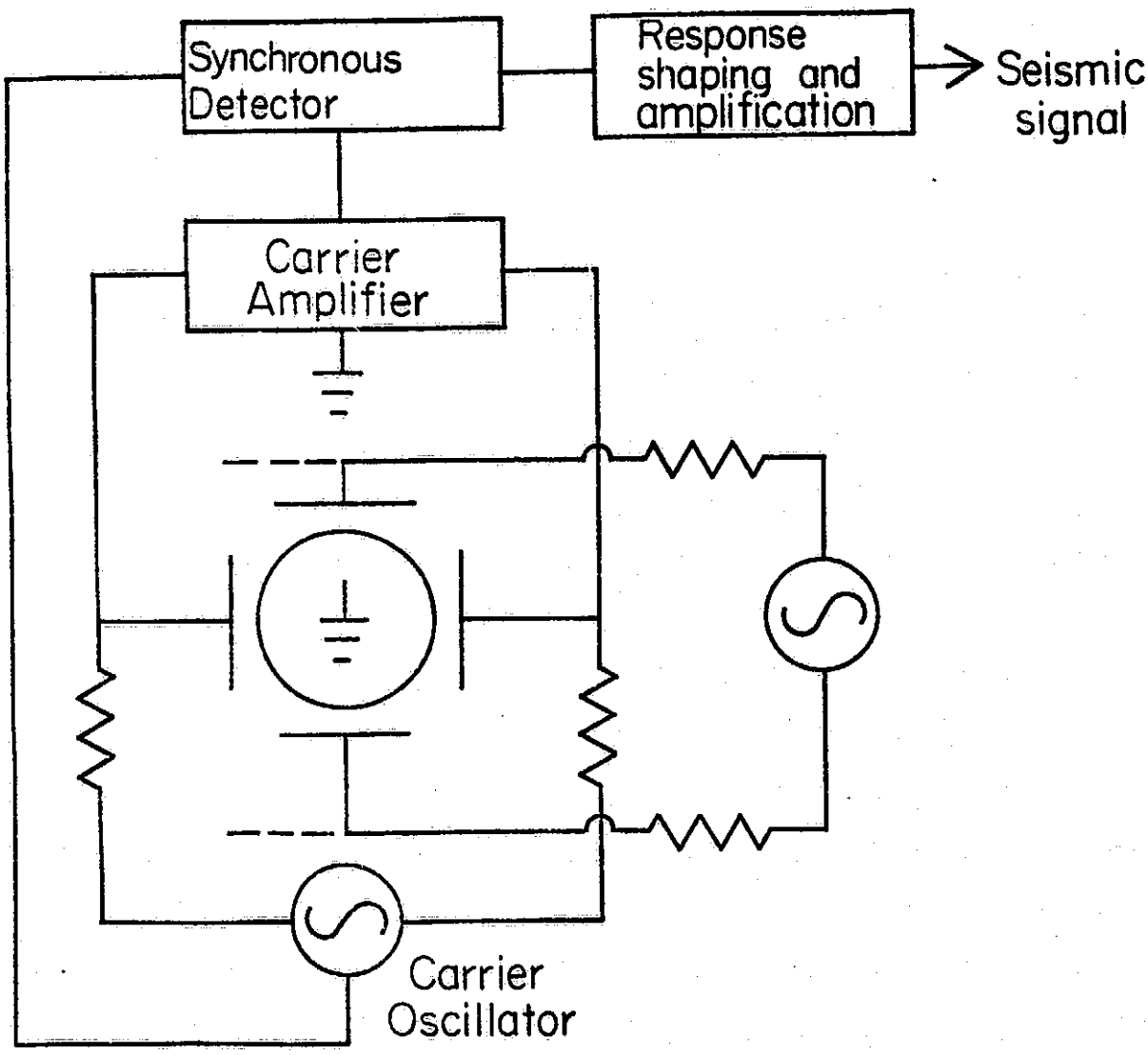

Seismometer System Block Diagram

FIGURE 5

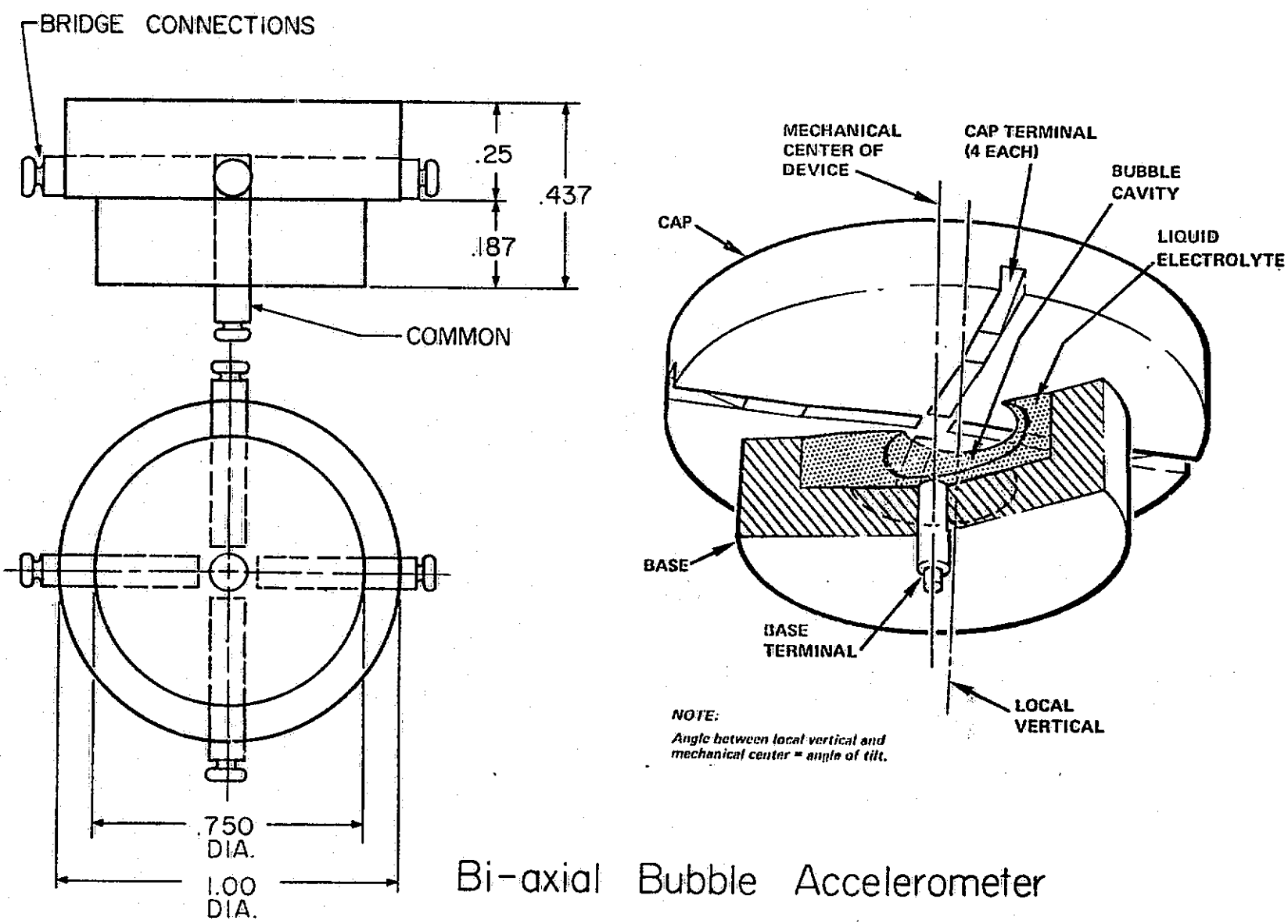

Bi-axial Bubble Accelerometer

FIGURE 6

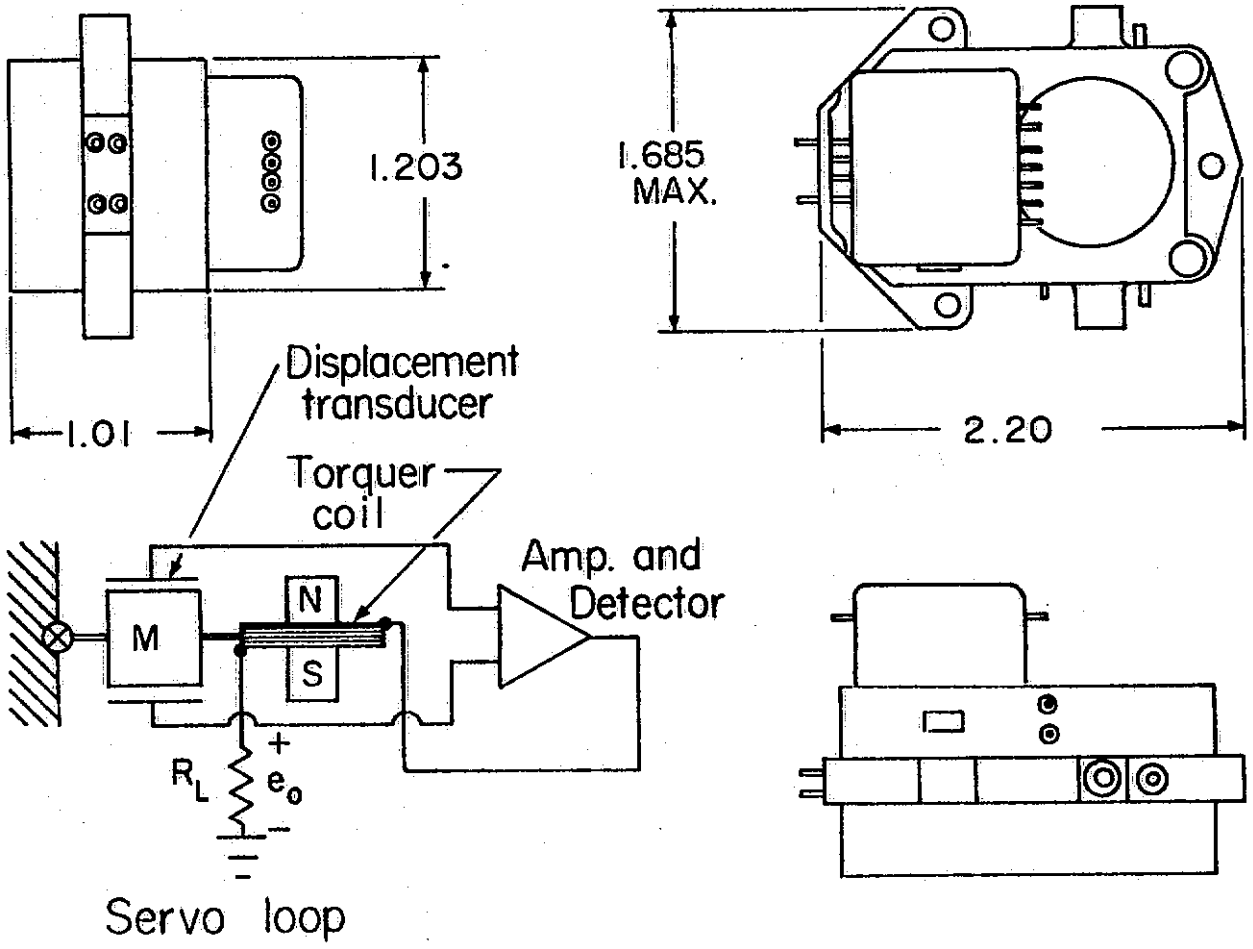

Force Balance Accelerometer

FIGURE 7

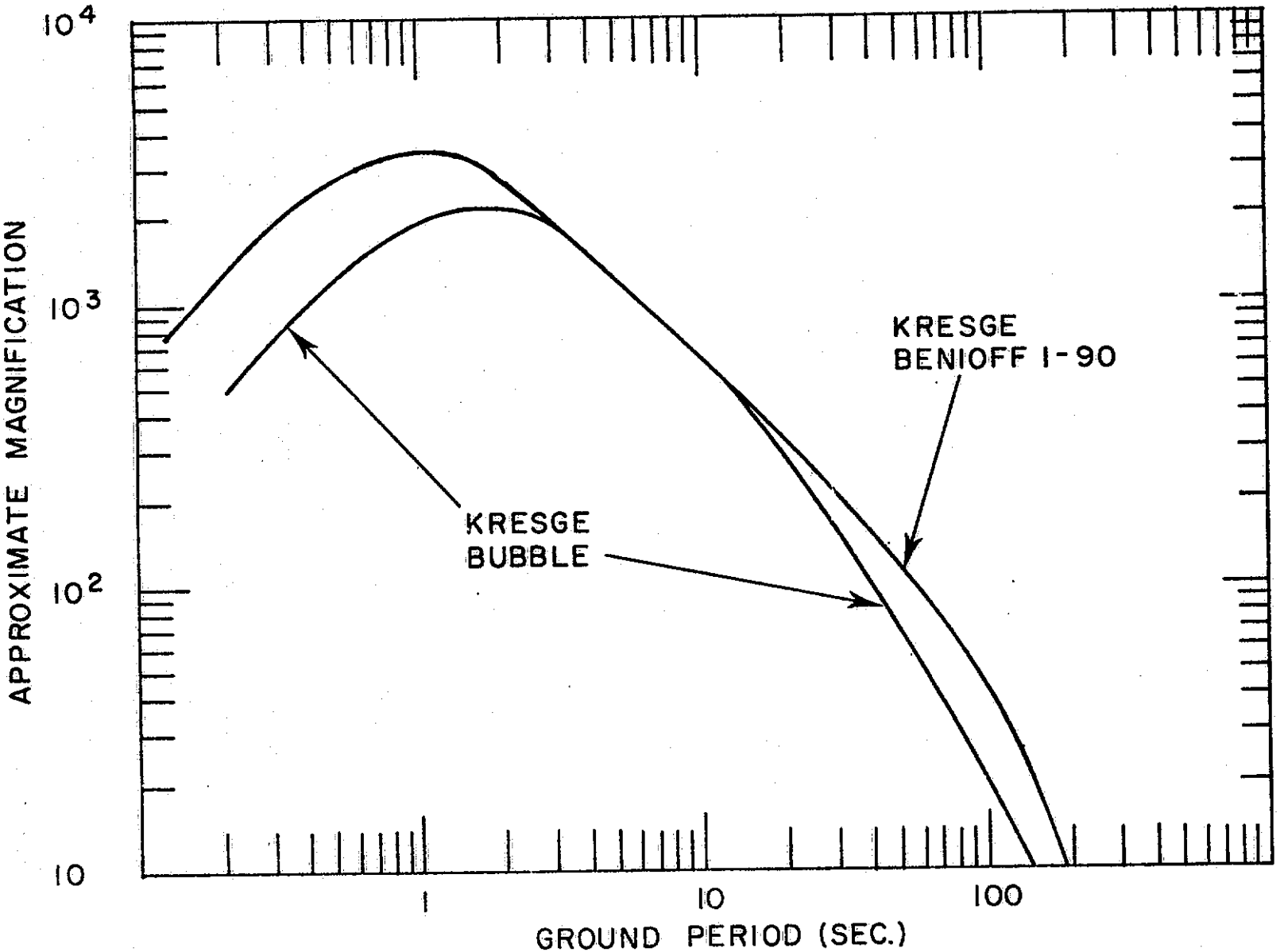

COMPARISON CHARACTERISTICS AT KRESGE TEST SITE

FIGURE 8

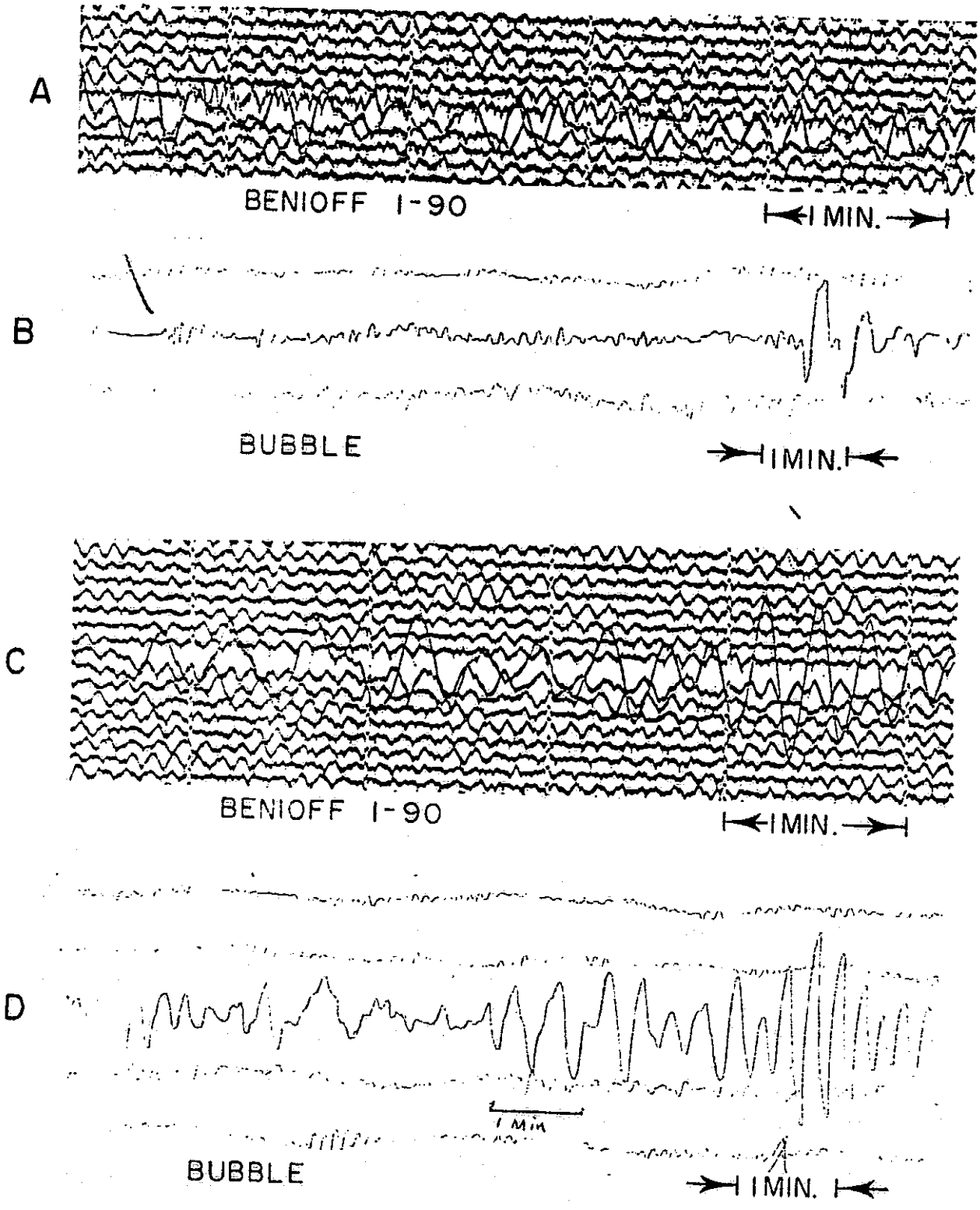

MAGNITUDE 6 3/4 (PERU) RECORDED AT KRESGE TEST SITE

FIGURE 9

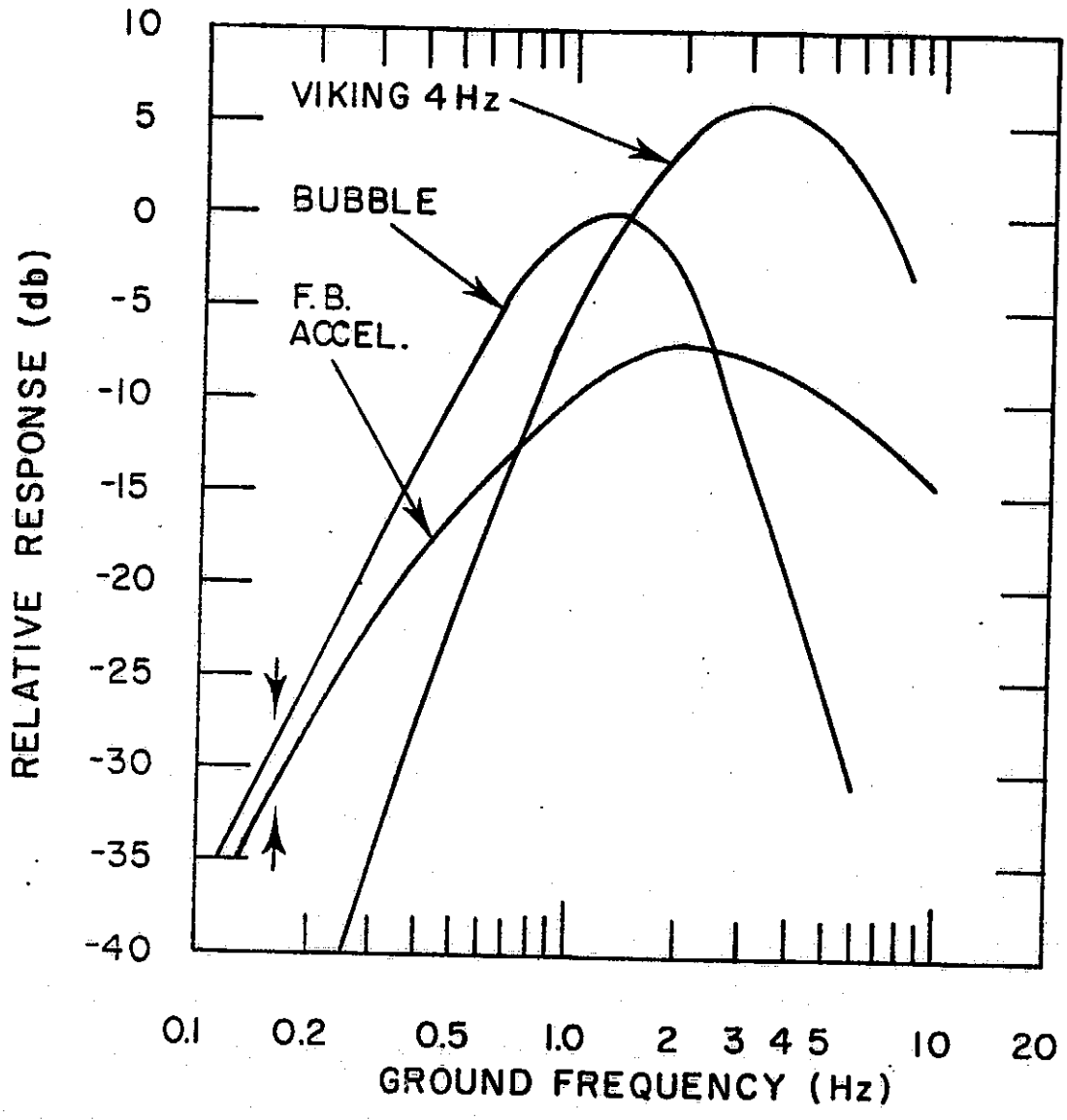

COMPARISON CHARACTERISTICS
AT CIT CAMPUS TEST SITE

FIGURE 10

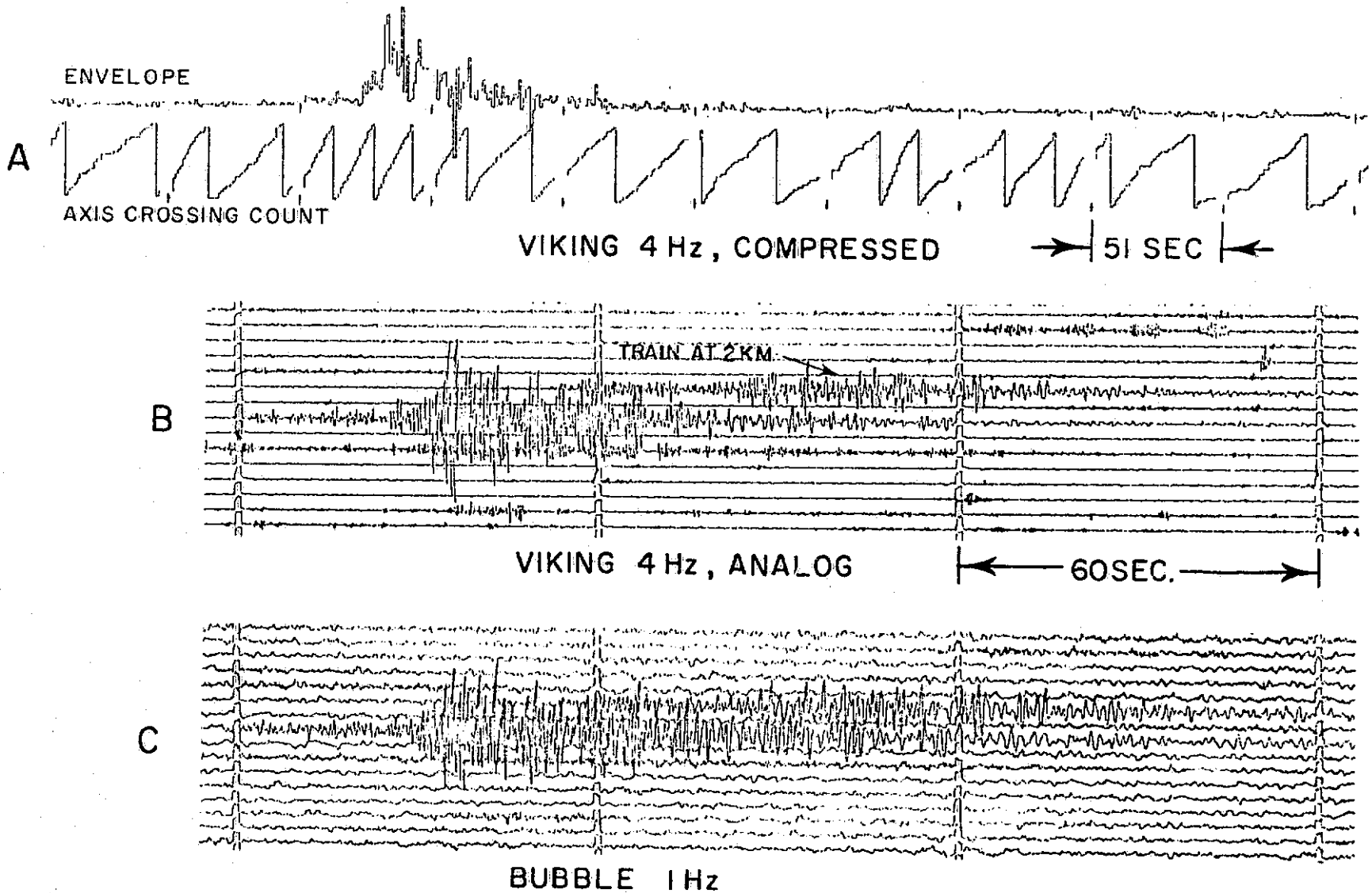

LOCAL EVENT AT 200 KM
RECORD AT CIT CAMPUS TEST SITE

FIGURE II

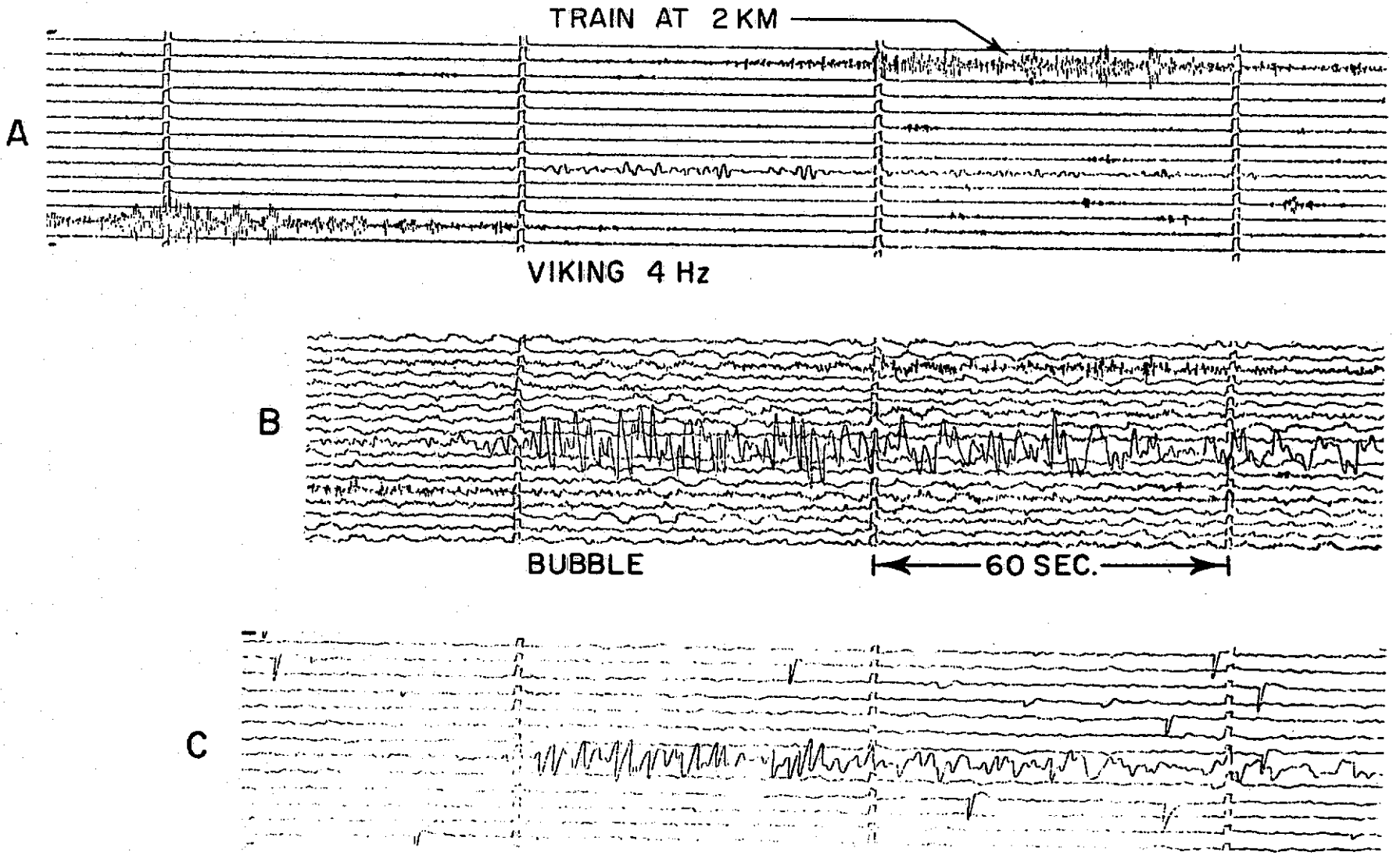

BAJA CALIFORNIA EVENT RECORDED AT CIT CAMPUS TEST SITE

FIGURE 12

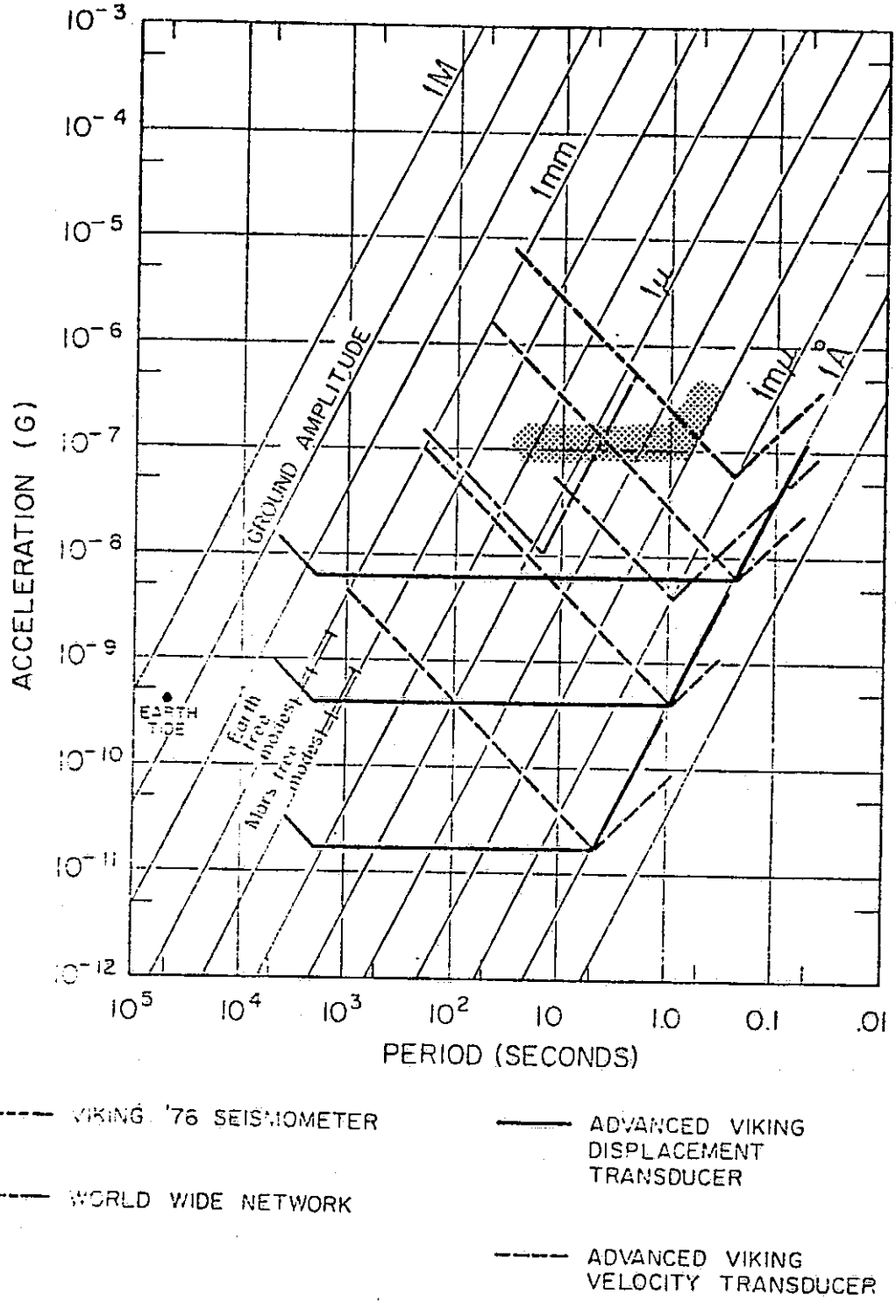

SENSITIVITIES OF SEISMIC SYSTEMS

FIGURE 13

APPENDIX B

SURFACE IMAGING EXPERIMENT FOR PENETRATOR AFTERBODY

Geoffrey Briggs

Jet Propulsion Laboratory

Example Instrument

Approximately 4 camera units on Penetrator afterbody

190 x 244 element CCD detector in each unit

8-bit digitization of each element

3.7×10^5 data bits per frame

No spectral filters--wideband response

12° x 16° field of view for each unit

About 1.5 millirad per pixel

Acceleration Test Results

A 100 x 100 element CCD array was subjected to acceleration of 19,500 g perpendicular to the plane of the array.

The results of testing the Fairchild 100 x 100 CCD area array after the shock test are as follows:

1. The device operated normally after the shock test except that the photogate appeared to be open. This allows photocharge to bleed down in a completely uncontrollable fashion.

2. The device was delidded and visually inspected, with the following results:

   a. Much debris was discovered to have been encapsulated within the device; a section of gold bond wire and several chunks of conductive epoxy being most notable. One piece of conductive epoxy was found lying on the gate structure of the device.

   b. One (of several) substrate aluminization connections was vaporized, apparently from excessive current flow. A redundant parallel aluminization strip had obviously been overstressed.

   c. One gold ball bond appeared to have been broken in bonding or handling prior to packaging. The wire was sheared at the top of the ball bond, but was being held in place at the edge of the ball by the glue used to bond the lid to the case.

   d. All other bond wires appeared to be OK. No obvious damage had occurred to the chip or the package. No evidence of deformation of bond wires was evident.

Potential Far Field Observations

1. Site Characterization

   In principle, Penetrators could be targeted to many diverse regions on Mars where relatively closeup observations of land forms from a different aspect that can be obtained from orbit would seem to have obvious value to geologists. Example land forms of particular interest are dunes, rock formations, layered deposits, arroyo beds, landslides, cliffs and volcanic forms.

2. Dust Storms

   Although the Viking Lander cameras may provide the first surface images of dust storms it is likely that Penetrator cameras, commanded when orbital imaging indicates the presence of dust clouds, could contribute usefully to the study of this phenomenon. The combination of orbital imaging and IR data together with the surface images could be a powerful means of understanding how dust storms begin, propagate and decay.

3. Condensate Clouds

   The manner in which seasonal water ice clouds form in the tropical areas, typically in the vicinity of volcanos and canyons, will not be well studied by either Viking, or probably, by a Mars Polar Orbiter. Imaging at different times of day, principally in the morning, on successive days at sites where clouds occur could help understand this phenomenon, particularly if a meterology package is included in the payload. The pictures could determine whether the clouds form at high or low altitude and whether surface condensation plays any role.

Star Observations

A Penetrator imaging system could be used to determine the position and orientation of the probe. This would have particular value for the seismic experiment. The area array cameras can be used for long exposures, particularly at night when temperatures are low, and therefore should be able to detect bright stars. We estimate that an exposure of about 100 seconds would be needed so that the images would be smeared over a few pixels, an effect for which compensation could be made. The principal errors in determining the location and orientation are likely to arise because the aft-body orientation is not identical to that of the forebody and because the camera alignment with respect to the aft-body may change on landing.

CONCLUSIONS

1. No damage to the basic device was directly traceable to the shock. The photo-gate problem is probably related to the conductive junk on the chip surface and the substrate connection overstress.

2. A device built to flight standards, without the junk and bad workmanship, should have survived without damage.

Potential Near Field Observations

1. Soil Characteristics

   Other Penetrator measurements are more useful if they are related to the site context as ascertained in far field observations and Orbiter imaging. One would look for evidences of particle sorting, ripples and layering. Sites on volcanos might be at a sufficiently high altitude that aeolian covering is slight so that the lava type may be distinguished. In arroyo sites the degree of rounding of any observable rocks will be of interest to see whether water ran for a long period or if the channels were cut by episodic floods.

2. Microcratering

   In any areas where the bed rock is exposed small craters may have been preserved in which case their areal density and state of preservation would be of interest in connection with cratering rates, secondary cratering, erosional and filling rates.

3. Eolian Processes

   During a 2 year-long mission some movement of the soil may occur as a result of winds. Occasional imaging could provide observations of how the dust is deposited and removed near small scale positive and negative topographic features which would be relevant to the problem of Martian albedo feature generation.

4. Condensation Processes

   In winter and in the early morning hours surface condensation of water and CO_2 ices may be observed at some sites. The determination of the temporal history of ices (which would involve several images) would be of considerable interest since there are many poorly understood problems involving water processes and polar cap phenomena (e.g. does wind drifting of CO_2 ice play an important role in determining the rate of retreat of the caps).

Camera Development

Work is in progress at the Naval Research Laboratory to fabricate a complete camera unit (lens, CCD detector, electronics, and mechanical support) and shock test the unit up to 20,000 g's. The tests and evaluation will be finished in October 1976.

APPENDIX C

REPORT ON STATUS
OF
ALPHA PARTICLE INSTRUMENT
WITH
ALPHA, PROTON, AND X-RAY MODES
FOR A PENETRATOR-TYPE MARS MISSION

Anthony L. Turkevich

T. E. Economou

University of Chicago

Ernest J. Franzgrote

Jet Propulsion Laboratory

Report on Status of Alpha Particle Instrument with Alpha, Proton, and X-ray Modes for a Penetrator-Type Mars Mission

Anthony L. Turkevich and T. E. Economou
Enrico Fermi Institute, University of Chicago,
Chicago, Illinois 60637
and
Ernest J. Franzgrote
Jet Propulsion Laboratory, Pasadena, California 91103

Abstract

The scientific objectives of a chemical analysis on a Penetrator-type Mission are discussed. The status of the development of the Alpha Particle technique with alpha, proton, and X-ray modes is presented via a reprint of an article appearing in Nuclear Instruments and Methods. Recent shock tests on components have shown that detectors and collimators can survive accelerations comparable to those expected on Penetrator implantations. The collimator films need further development. The recent soil penetration tests indicate that the material around an implanted Penetrator may be contaminated and modified. These tests suggest that a sample acquisition mode be developed for this type of chemical analysis.

I. Introduction and Technique Status

As part of the general development program of the Planetology branch of the Office of Space Sciences of NASA, the alpha particle technique of chemical analysis that provided the first chemical analyses of the lunar surface on the Surveyor Missions is being developed for future space missions. This development has proceeded in two directions - miniaturization, and development of higher accuracies and sensitivities than were achieved on the lunar missions in 1967-1968. The present status of this program of technique development is summarized in the accompanying reprint of an article appearing in NUCLEAR INSTRUMENTS AND METHODS (ref. 1).

This status can be summarized by the statements that:

1. It is technically feasible to identify and determine more than 99% of the atoms (other than H) in a sample on an automated mission. The problem of hydrogen determination is discussed in an accompanying report.

2. Many minor and trace elements can be determined down to ppm levels.

3. Sensitivities and accuracies are continually being improved.

Although the enclosed reprint addresses itself primarily to the possibilities on a soft lander of the Viking type, the accuracies and sensitivities quoted there can be approached on a Penetrator-type mission.

II. Scientific Objectives of a Chemical Analysis Program on a Penetrator Mission.

A chemical analysis experiment on a Penetrator Mission should, of course, take account of the special characteristics of such a mission:

1. the possibility of measurements below the surface of the site, and thus:

a) be less subject to aeolian-affected surface material

b) have the opportunity of detecting stored volatiles (H_2O, CO_2)

c) conceivably make possible stratigraphic measurements along the length of a penetrator.

2. the possibility of measurements at several sites on one mission and, particularly, at sites relatively inhospitable to soft landing missions (i.e. rugged terrain, edges of polar caps, etc.

At any one site the scientific objectives of a chemical analysis can be divided into two categories:

1. Chemical characterization of the material at a penetrator site. By this is meant the determination of all the principal chemical elements with an accuracy of ± <0.5% by atom.

This objective would make possible, via stoichiometry, the following first order deductions about the site:

a) the general chemical nature of the material

(i.e. oxide, carbonate, silicate, hydrated oxide, and relative amounts of each).

b) the normative mineral composition of the material.

c) the state of oxidation of the material.

d) the acidity of solutions in contact with the material.

e) the amount of water and/or carbon dioxide in the material.

Information about these items could be deduced, even without the direct determination of hydrogen, by the alpha particle technique as was demonstrated by the Alpha Particle Mars Preprototype Instrument (even without an X-ray mode) (ref. 2). The possibility of greater sensitivity for hydrogen than is achievable by this technique is described in an accompanying report.

2. Addressing Specifically Martian Problems.

a) the nature of the atmosphere-surface interaction. Such an interaction has been very prominent in the earth's surface history, and may well have had an important role in the history of Mars.

b) is sub-surface material a storehouse for volatiles (e.g. H_2O and CO_2)? The importance of a determination of volatiles in subsurface Martian material has been emphasized often enough not to merit further comment here.

c) are chemical elements of significance for life (e.g. C, N) present?

d) clues to gross geochemical history of the planet (e.g. via Mg/Al, K/Ca, Na/Mg, Fe/Mg ratios).

e) following up on Viking results.

3. Analysis of the local atmosphere, for example, for N_2 and Ar.

III. Adaptation of the Alpha Particle Instrument for a Penetrator Mission.

This has proceeded along the following lines:

a. Miniaturization of the instrument. In addition to the "Mini-Alpha" instrument described in the reprint, a model has been built of a "Micro Alpha" instrument (fig. 1). This concept has been described previously (ref. 3). A working instrument has not actually been built, but the figure illustrates the miniaturization that is possible--adequate to fit easily into the confines of a penetrator envelope. This version of Micro Alpha was designed to examine a sample through a port in the wall after emplantation of the penetrator. As discussed below, this concept of instrument operation will be reconsidered in the light of recent penetrator test results showing appreciable soil modification upon emplantation in certain soils.

b. Identification of critical components of an instrument that should be checked for compatibility with the environmental constraints of a Penetrator Mission. For an alpha particle instrument these appear to be:

1. Solid state semiconductor detectors
2. Alpha sources
3. Source collimator and films
4. Joule-Thomson cryostat for cooling the Ge X-ray detector.

The principal environmental requirements of a

Penetrator Mission to Mars are survival of sterilization and of accelerations up to 2000 g.

c. Environmental tests to identify problem areas in this list of components.

Measurements had previously shown that semiconductor silicon detectors of the type being considered could be sterilized (ref. 2). Measurements have also been made showing that the intrinsic Ge detectors (of the type useable in the X-ray mode) could survive sterilization (ref. 4).

Many years ago, silicon detectors had been shown to survive acceleration of up to 1800 g. More recently some of these detectors have been tested with the air gun at Sandia at accelerations of up to 3500 g. Included were samples of the proposed thin alpha (30 μ thick) and proton (300 μ) detectors. Examples of the detector behavior before and after testing are shown in fig. 2 and 3. The results of these shock tests on detectors are summarized in Table I.

A CdTe detector, of the type being considered for the X-ray mode (see below) has been shock tested by A. Metzger of Jet Propulsion Laboratory. It appears to have suffered no damage at 2200 g (private communication).

A few collimators and collimator films have also been subjected to shock tests (Table I). The cantilever suspended collimators survived; however the films did not. The cause of the failure is being investigated and conceivably could be flexing of the collimators. This will be studied further, although

possible changes in orientation of the instrument in the penetrator (see below) may alter the critical direction of these shock tests.

There has been no opportunity to test alpha sources, since these are not available.

d. Tests on Cd/Te X-ray detector. The operational advantages for a Penetrator Mission of an ambient temperature semiconductor X-ray detector over a Joule-Thomson cooled Ge detector are so great that an effort is being made to keep abreast of developments in this detector field. Although such detectors are at present inferior in resolution to cooled (to less than -120°C) Ge detectors, they are rapidly being improved. K. Zanio of Hughes Aircraft, a leader in this field of research, provided a detector to make possible familiarization with the characteristics of such a detector. Fig. 4 shows a spectrum of ^{241}Am photons obtained with this detector at -5°C. The resolution illustrated is already comparable to that with proportional counters. Zanio (ref. 5) has been able to achieve a resolution of 1.9 keV at 29 keV and has seen the 3.9 keV L X ray of iodine. Work at other laboratories (see fig. 5) shows that 1.5 keV FWHM resolution can be achieved at 5.9 keV with such detectors at 20°C!

TABLE I.

SHOCK TESTS ON COMPONENTS OF ALPHA PARTICLE INSTRUMENT

DETECTORS			
Proton (500 μ)	2	pass 3500 g	(Perp)
Alpha (30 μ)	2	pass 3500 g	(Perp)
Proton (500 μ)	2	" "	(Angle, 45°)
Alpha (30 μ)	1*	" "	(Angle, 45°)
Collimators	4	pass 3300 g	
Films (VYNS, Al_2O_3)	3	failed at below 3300 g	

*One of the thin alpha detectors was damaged in operation before shock testing.

IV. Sampling Considerations on a Penetrator Mission.

The original concept of performing a chemical analysis by the alpha particle technique on a Penetrator Mission involved examination of a sample through an opening in the wall. This motivated the instrument configuration of Micro Alpha (illustrated in Fig. 1). This approach had the virtue of simplicity and was encouraged by the results of visual observation that showed little or no soil modification around emplanted small-scale penetrators.

The recent full-scale tests in moist loess in Nebraska (see ref. 7) indicate that this approach is unreliable. In the case of the test where the soil has been examined, the material just outside the emplanted penetrator had been converted to a glass (up to about 50 μ) and both contaminated grossly with nose cone components (Fe, Co, Ni, Mo) in non-proportional amounts, and modified even in the relative amounts of purely soil constituents. These chemical changes appear to peter out beyond 2 mm, but certainly make untrustworthy a mission operation that involves examination of the material just outside the penetrator.

Thus a credible alpha particle experiment for a Penetrator Mission will require either a sample acquisition procedure or the preparation of a clean sample outside the penetrator. The former approach appears more realizable at present. For example, a spring-driven drill might be used to bring in a sample from which the contaminated portion could either be

removed, or diluted enough to be suitable for analysis inside the penetrator. This appears feasible from a loess-type material; its feasibility from a basalt-like material needs to be investigated. The molybdenum content of the nose cone of the penetrator appears to be high enough, the molybdenum content of most natural materials low enough, and the analytical sensitivity of the technique good enough so that contamination of the sample could be monitored at significant levels.

References

1. Thanasis E. Economou and Anthony L. Turkevich. "An Alpha Particle Instrument with Alpha, Proton, and X-ray Modes for Planetary Chemical Analyses." Nuclear Instru. and Methods (in press) (preprint enclosed).
2. Thanasis E. Economou, Anthony L. Turkevich, James H. Patterson. "An Alpha Particle Experiment for Chemical Analysis of the Martian Surface and Atmosphere," J. Geo. Res. 78, 781-791 (1973).
3. see, e.g. James A. J. Cutts. "Evaluation of the Feasibility of Experiments for a Mariner Class Mars Polar Orbit Mission with Multiple Penetrator Surface Probes," Preliminary Draft, Dec., 1975, Planetary Sciences Division, Science Applications, Inc., 2835 Lake Street, Pasadena, Calif. 91101.
4. Ernest J. Franzgrote and Louis Wang, to be published (1976).
5. K. Zanio, H. Montana and K. Krajenbrink. "Cadmium Telluride X-Ray Spectrometer," Appl. Phys. Lett. 27, 159 (1975).
6. A. J. Dabrowski, J. Chwaszczewska, J. Iwanczyk, R. Triboulet and Y. Marfaing. "Spectrometer Performance of n-Type Cadmium Telluride," I.E.E.E. Transaction NS 23, 171-175 (1976).
7. W. L. Quaide, M. B. Blanchard, V. R. Overbeck, and R. T. Reynolds. "Status Report on Feasibility of Using Penetrators in Planetary Exploration," 1976 May 14, Ames Research Center, Moffett Field, California 94035.

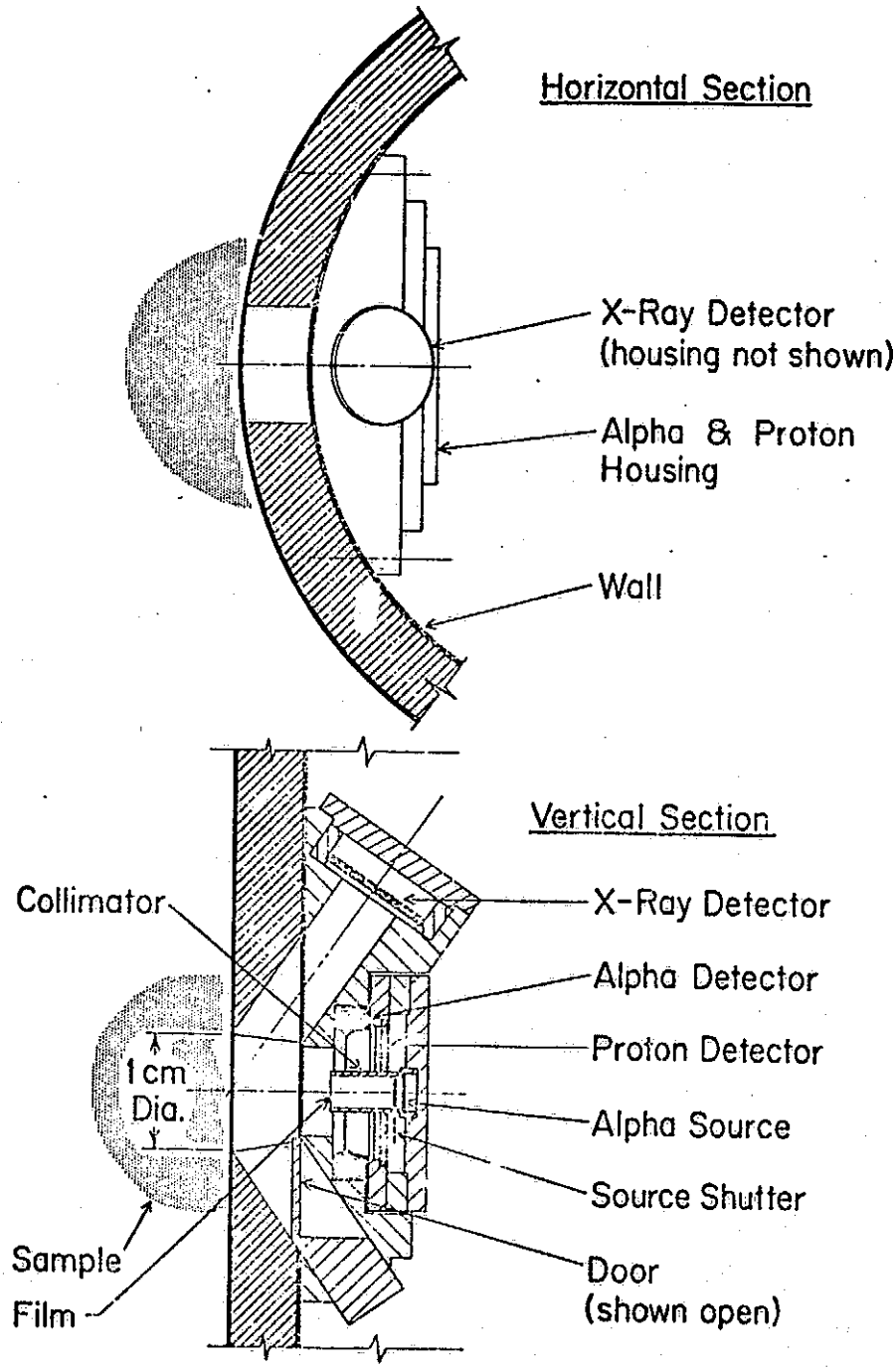

Figure 1. "Micro Alpha" - Possible Geometrical Relationships of Sources, Detectors and Sample for an Alpha Particle Instrument on a Penetrator Mission. The sample is examined through an opening in the penetrator wall.

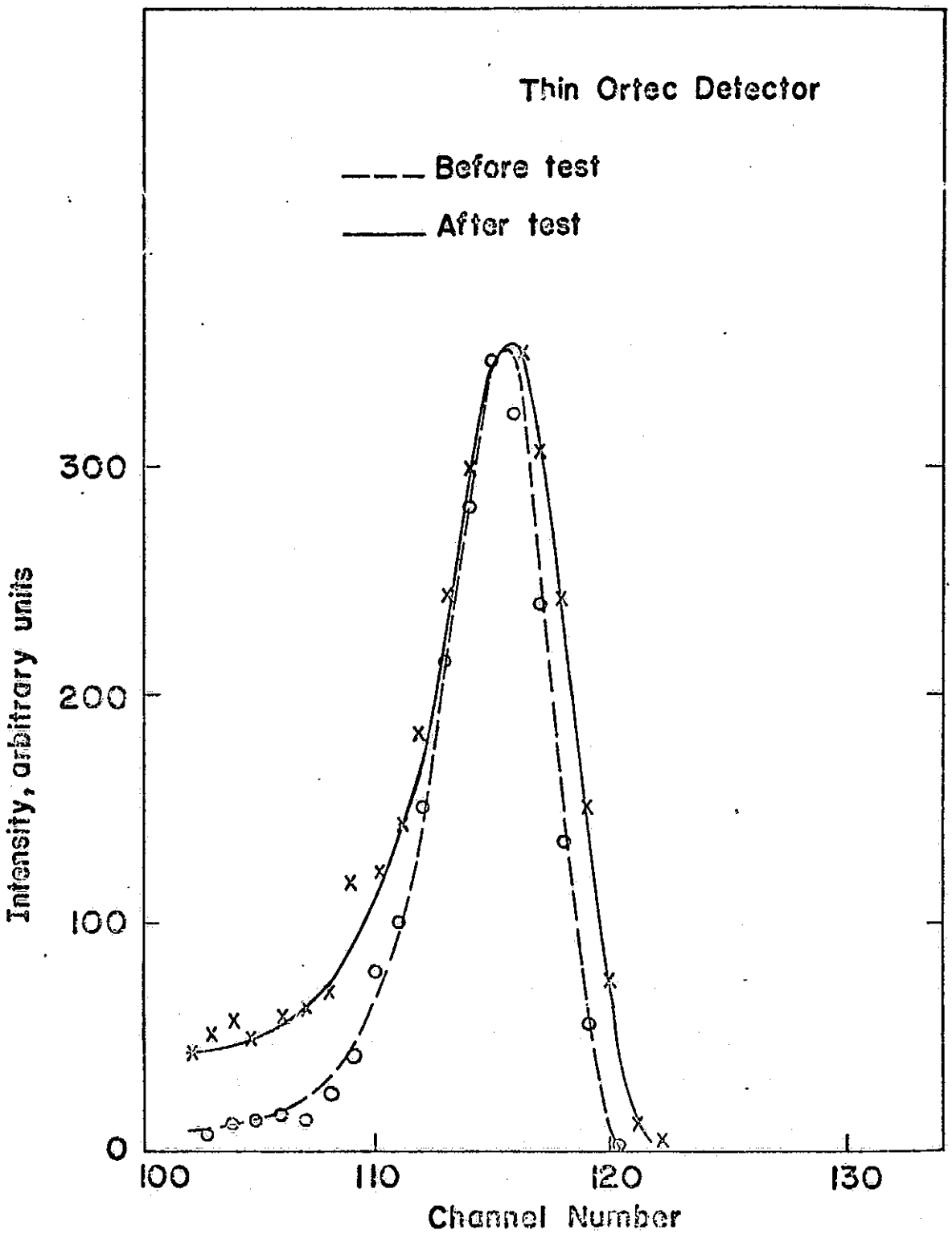

Figure 2. Behavior of Thin (Alpha) Detector before and after subjection to 3500 g along plane of detector.

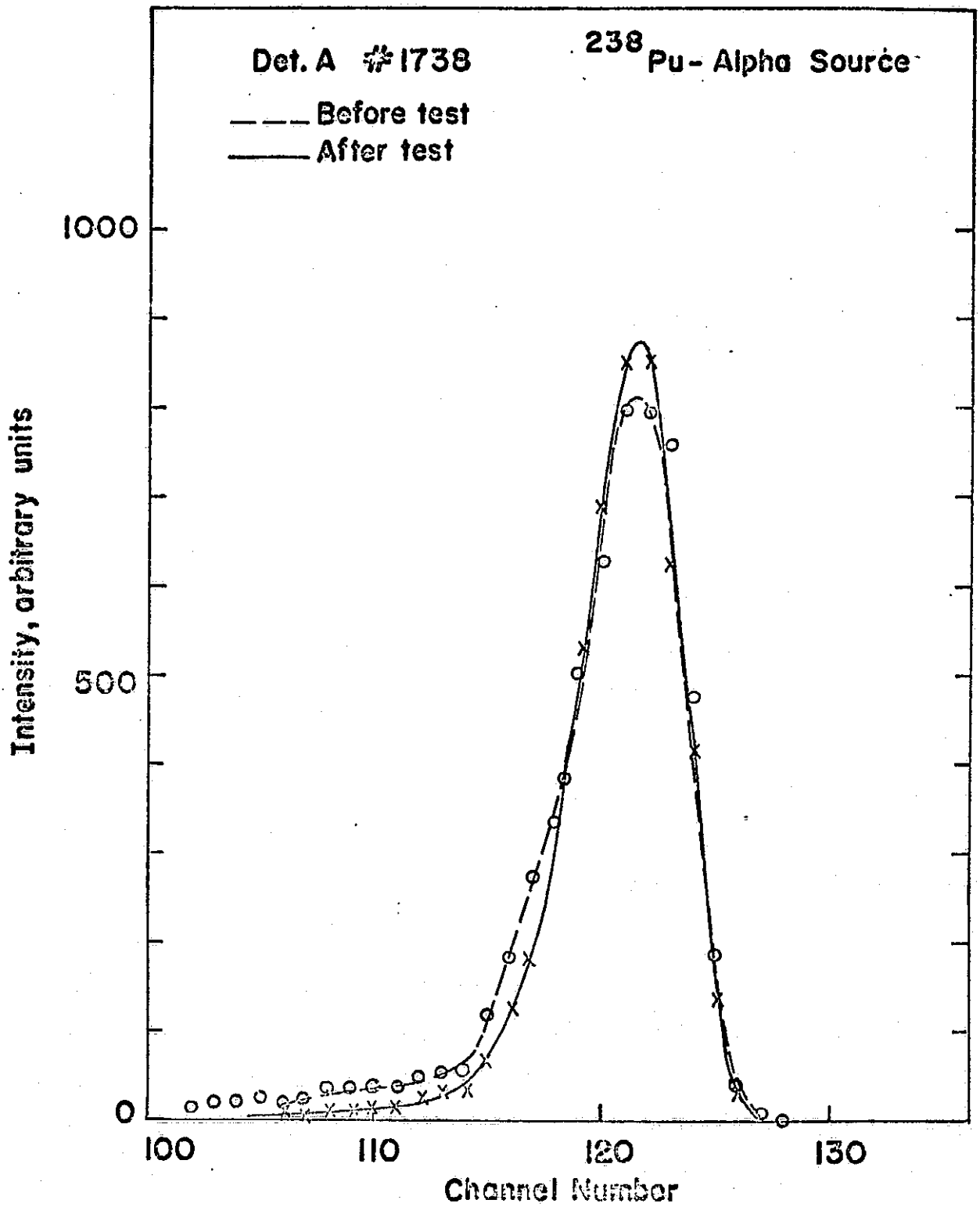

Figure 3. Behavior of Proton Detector before and after subjection to 3500 g along plane of detector.

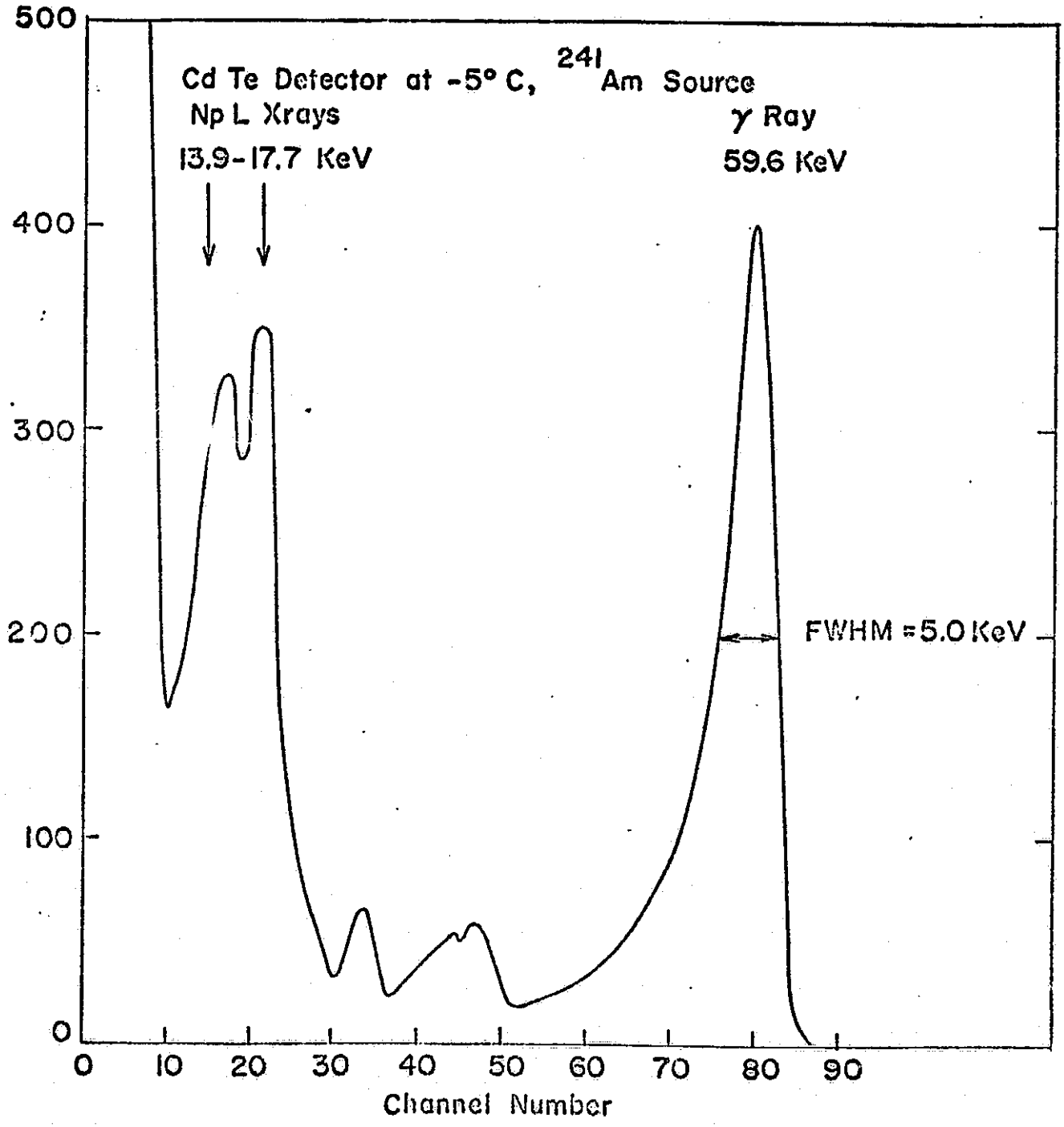

Figure 4. Response of CdTe detector to ^{241}Am Source at -5°C.

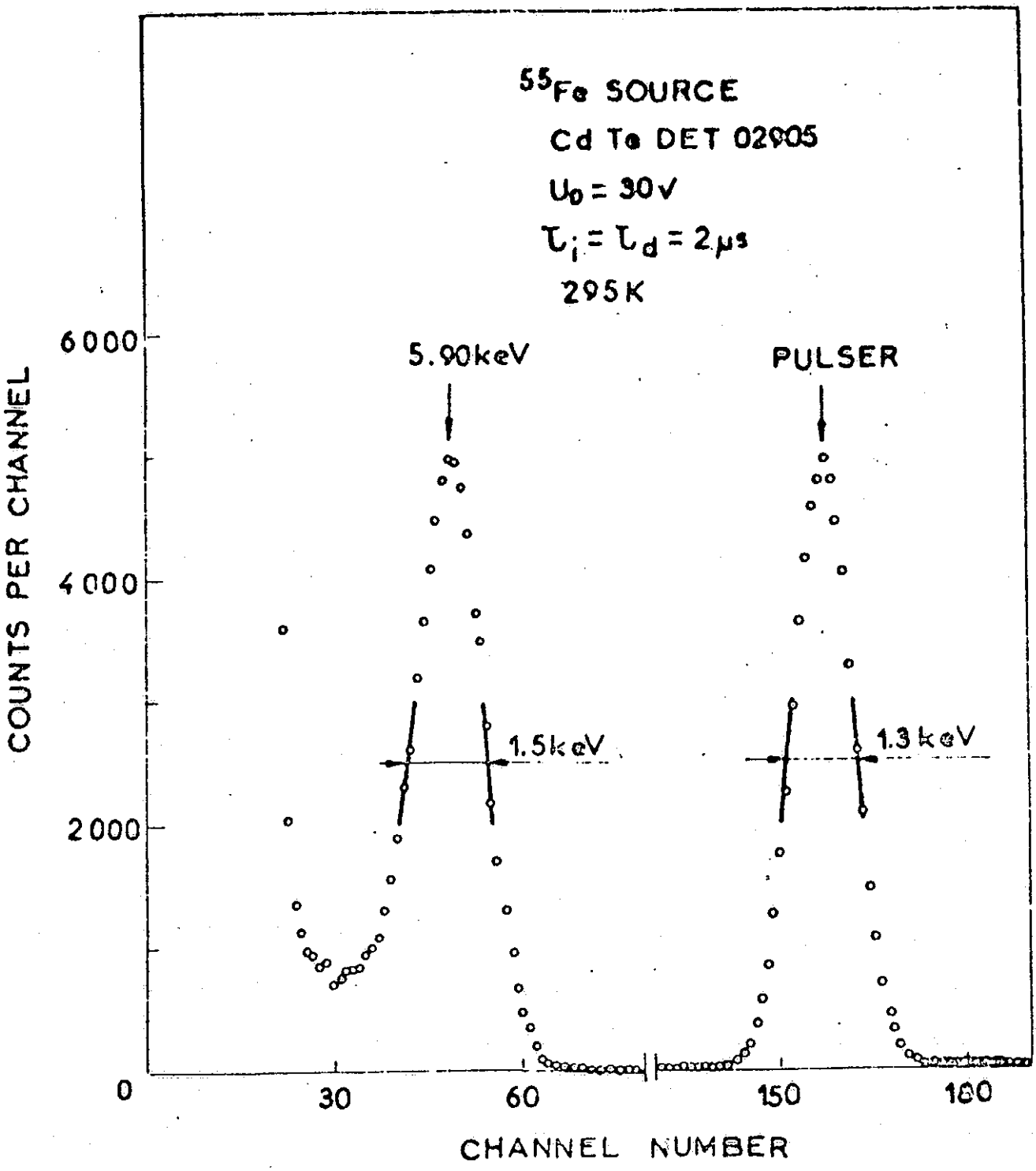

Figure 5. Response of n-type CdTe detector to ^{55}Fe detector to ^{55}Fe X rays (ref. 5).

APPENDIX D

DEVELOPMENT STATUS OF A GAMMA RAY SPECTROMETER FOR A MARS PENETRATOR MISSION

Albert E. Metzger

Richard H. Parker

Jet Propulsion Laboratory

APPENDIX G

DEVELOPMENT STATUS OF A GAMMA RAY SPECTROMETER FOR A MARS PENETRATOR MISSION

Albert E. Metzger and Richard H. Parker

Jet Propulsion Laboratory
4800 Oak Grove Drive
Pasadena, CA 91103

ABSTRACT

This report describes a gamma-ray spectrometer capable of making a chemical analysis on a Mars Penetrator mission. The science objectives are discussed. The components of flux expected are extrapolated from the performance and data analysis of the Apollo lunar-orbiting experiments. Elements which can be detected include Th, U, K, by their naturally occurring gamma-ray emission, and most major elements with an abundance greater than 1-2% which are characteristically excited by cosmic radiation. Bound and free water can be detected in the form of H, both by observing the $H(n,\gamma)D$ line and by observing the line shapes of other neutron induced lines after neutron moderation by hydrogen. The gamma-ray spectrometer technique samples a volume on the order of a cubic meter so that material alteration in the immediate vicinity of the penetrator is not an impediment.

The selection criteria for the gamma-ray detector to be employed is reviewed as well as results of acceleration tests on typical components. Several designs of a detector assembly are compared leading to the selection of one which is now being fabricated as an integrated feasibility test unit.

Finally, potential intereference by the RTG used for electrical power on the Penetrator is discussed and future tests are described.

Introduction

The lunar-orbiting gamma-ray spectrometer experiment flown on Apollos 15 and 16 provides a basis from which to project the functional requirements, performance, and data analysis techniques for a gamma-ray spectrometer which could be incorporated in a surface penetrator probe. Figure 1 shows a gamma-ray spectrum obtained in lunar orbit and the constituent contributions into which it has been analyzed. These are a) a strong, featureless continuum which is the result of a multiple scattering cascade produced by high energy cosmic ray particles in the lunar surface, b) primary cosmic ray induced radiation in the detector, c) radiation induced in the detector by secondary, mostly lunar albedo, neutrons, d) lines of activated species produced in the local mass around the detector by both cosmic ray particles and secondary neutrons, e) bremsstrahlung produced by high energy interplanetary electrons interacting with material in the vicinity of the detector, f) the cosmic gamma-ray flux, g) component resulting primarily from the interaction of cosmic ray particles with spacecraft material, to which can be added any residual natural radioactivity, and finally, but most importantly for this experiment, h) the spectrum of discrete lines containing the lunar compositional information. These components are more fully discussed in Bielefield et al., 1976. Their separation has been accomplished through the analysis of various modes of operation of the Apollo experiment, the irradiation and post-flight measurement of detectors on the Apollo 17 and Apollo-Soyuz missions, accelerator experiments and theoretical calculations.

The discrete-line lunar spectra have been analyzed for their characteristic gamma-ray emission intensities by several techniques, viz., a spectrum unfolding routing based on a set of library functions, photopeak analysis, integration over selected energy intervals, and correlations with lunar sample compositions (Bielefeld, et al., 1976). A physical model based on the neutron energy flux distribution, reaction cross sections and gamma-ray yields serves to translate the computed photon flux into concentrations (Reedy, Arnold and Trombka, 1973).

The effective depth of sampling by gamma-ray spectroscopy amounts to several tens of centimeters. Emplaced below the surface in a penetrator it will therefore see a large volume of material unaltered by the emplacement process. In this important respect it complements a combined alpha scattering/x-ray fluorescence instrument which can sample only a thickness of microns to about a millimeter.

The observed intensities of the various gamma-ray signal and background components will be altered by locating the experiment one to several meters below the surface rather than at some tens to hundreds of kilometers above it. The characteristic gamma-ray lines, which arise from the decay of the primordial radioactive nuclei as well as from reactions induced by the incident cosmic ray flux, will be enhanced relative to an orbital experiment by the ratio of solid angles. This amounts to an increase by a factor of about 3 in comparison to the Apollo experiment. An additional enhancement occurs below the surface for induced reactions, since the intensity of neutron flux which gives rise to this component builds up with increasing penetration to a maximum at 80-100 g/cm^2 and then begins to decline (Figure 2). At one meter, the gamma-ray emission due to induced activity will be about five times greater than at the surface. In the same

manner, the background components arising from multiply-scattered cascade reactions and from other secondary particles of the cascade will be similarly increased by the increase in solid angle, as well as by the depth dependence of the secondary multiplication process. The primary cosmic ray flux will be largely dissipated in the first meter of surface material so that radioactivity from this source in the detector and surrounding materials will be considerably reduced. Both the bremsstrahlung from interplanetary electrons and the cosmic gamma-ray contributions will be eliminated. Radiation from the radioiosotopic thermoelectric generator (RTG), which is to serve as the power source of the penetrator, is an important consideration and will be treated separately below.

Objectives

Chemical information about planetary bodies is of fundamental importance in characterizing their present nature, past history and the overall evolution of the solar system. Some of the desired information about Mars, such as the general nature of major topographical areas (including basin floors, old crater plains and shield volcanoes) can be obtained as well or better from orbital surveys with analytic instruments such as the gamma-ray spectrometer (Haines, Arnold and Metzger, 1976). Certain other objectives are practical only by means of a surface or subsurface experiment. The latter include the association of a measured composition with small scale local characteristics - such as topography, albedo, heat flow, etc., the occurrence of compositional variations with depth which may represent a distinctive earlier period of Martian history, now overlaid by more recent deposits resulting from processes of erosion and transport, and the detection of permafrost which may exist a meter or two below the surface.

The elements to be measured by the instrument described below, will be thorium, potassium, iron, titanium, magnesium, silicon, oxygen and hydrogen. Except for the latter, which is absent in that part of the moon surveyed to date, all were identified in the Apollo data with significant sensitivities. The most likely additions to this list, if the net signal to background ratios can be improved, either by the environment for the experiment or by instrument design, are aluminum, uranium and calcium.

Choice of Detector Type

Several possibilities for the choice of gamma-ray detector existed at the start of this task. These included:

1. Ge detector and cooler
2. CdTe detector
3. Scintillator-photodiode
4. Scintillator-phototube (PMT)

The germanium detector was eliminated from consideration (despite being the best choice in terms of sensitivity) due to the engineering difficulties associated with cooling a detector of the required size for periods of an hour or longer. The CdTe detector, with resolution comparable to the scintillator-PMT combination, was reluctantly excluded (despite the advantages of lower weight, smaller volume and ruggedness it offers) due to the high cost and uncertain prospects of developing the 5-10 cm^3 detector volumes required to measure gamma rays which have energies up to 10 MeV.

The photodiode-scintillator approach was rejected due to the inability of photodiodes to provide the required energy resolution for the low level light pulses from the scintillator. By process of elimination we arrived at the phototube-scintillator class of detector assembly. The design was further defined

by a choice of CsI(Na), instead of NaI(Tl) with its slightly better resolution, because of the superior ruggedness of the former.

The size of the scintillator is dictated by trading the requirements for good counting statistics (large area and adequate photon detection efficiency) against system constraints of small volume and low mass. The size of the phototube is also dependent on optimizing the conflicting requirements of good energy resolution, which calls for a diameter of 5 cm or greater, versus mechanical strength, and a sufficiently small volume, and mass.

Acceleration Tests

We have tested the two most critical components which might be incorporated for a gamma-ray spectroscopy experiment in a penetrator mission, i.e., the photomultiplier tube (PMT) and a scintillation crystal of CsI(Na). The maximum deceleration loads expected are 2000 g for 13 ms - corresponding to a one-meter penetration in a porous basaltic rock. Tests were performed at the Sandia Corporation in Albuquerque, New Mexico, using a drop table facility for levels up to 1000 g and their 5.5" air gun for levels above 1000 g. Two EMR-543 2" PMT's successfully experienced multiple loads up to 2000 g for 7 ms along the PMT cylindrical axis and, for one of them, also along a vector at 12.4° to this axis. A third 2" PMT (S/N 17811) catastrophically failed at 3500 g for 7 ms at 12.4° to the PMT axis after successfully passing lower levels. Three EMR-541 1-3/8" PMT's successfully completed loads up to 2000 g for 7 ms axially and one at 20° to the cylindrical axis. One 1-3/8" PMT (S/N 20266) successfully experienced a load of 3500 g for 7 ms at 20° to the PMT axis. The 2" CsI crystal successfully experienced a load of 2100 g for 6 ms along the cylindrical axis. The monitored values of energy resolution and gain for one tube of each type and the crystal are shown in Tables 1, 2, and 3. In every case, from the measurement at Sandia prior to the first shock

test through the post-test measurement at JPL, resolution was essentially unchanged and gains were not affected by more than a factor of two. Gain changes of less than a factor of about five are not serious as they can be compensated by a simple command capability. A picture of one of the PMT's tested is shown in Figure 3. The complete test report is included here as an appendix.

A CdTe crystal was also shocked at 2000 g. Microscopic inspections showed no evidence of any damage. A subsequent test with an active CdTe detector was not pursued after our decision to concentrate on a scintillation detector was made.

Integrated Detector Assembly

Having shown that the sensor components for a scintillation detector can survive the mission shock levels, the next task is to fabricate and test a combined crystal/PMT assembly.

The detector assembly choices considered were:

a) 2" x 2" diam. scintillator and 2" PMT

b) 2" x 2" diam. scintillator and 1-3/8" PMT

c) 3" x 1" diam. scintillator and 1-3/8" PMT

Both a) and c) offer resolution for the 662 keV line of Cs-137 less than 9% while b) will have poorer resolution (predicted as $\leq$ 13.5%) due to light losses at the diameter mismatch. The counting efficiency of c) is expected to be about 2.5 times lower than that of a) or b) and thus require 2.5 times more power (as operating time) in order to provide the same counting statistics. The overall length of a) is 25.6 cm (10-3/16") that of b) 18.4 cm (7-1/4"), and that of c) 21 cm (8-1/4"). Since the arrangement of the assembly in the penetrator must be with the detector-PMT axis aligned parallel to the penetrator axis, the end area of the detector is shielded by the penetrator mass from Martian material. Thus the ratio of efficiency factor for the 2" x 2" scintillator to the 3" x 1" scintillator is larger than might be expected from end-on detection.

Table 4 presents a summary comparison of the three assemblies. From scientific considerations a) is the best choice, while relative to system integration, b) or c) are better. Assembly b) offers good efficiency, minimum length and intermediate mass at the cost of energy resolution. Since assembly b) represents a reasonable compromise as the requirements for science and engineering are presently understood, and in order not to exclude future consideration of either case a) or c), it has been decided to choose case b) since the latter is also the most mechanically susceptible of the three. Thus the 2" x 2" diameter scintillator with a 1-3/8" PMT will be shock tested in the air gun facility at Sandia in August 1976. This integrated system, which is being fabricated by EMI, is shown in Figure 4.

The integrated assembly will occupy a volume of 334 cc with an estimated weight of 1.3 kg. The flange will not be needed for a flight unit. With the Apollo gamma-ray spectrometer as a baseline, the power required for an entire instrument will be not more than 1.2 watts and may be reducible to 0.8 w. This is without considering the functional relationship between the gamma-ray and alpha-x-ray instrument, namely, that most of the electronic systems can be shared if weight, volume, and power must be kept to an absolute minimum (Harrington, and Metzger, 1969). In the latter case, not more than 300 mw of power would have to be assigned specifically to gamma ray spectrometer subsystems. With the integrated assembly of Figure 4, the additional electronics required by the spectrometer could easily be placed around the photomultiplier tube without exceeding the $2\frac{1}{2}$" o.d. (sans flange) of the design or adding to the existing length.

RTG Effects

The RTG power source generates radiation fluxes of neutrons and gamma-rays which will both degrade and enhance the sensitivity of the gamma-ray experiment. Gamma-ray

emission results from impurities in the processed Pu-238 fuel as well as daughter products from the decay of the Pu-238 itself. The dominant gamma-ray line (2.614 MeV) can be reduced by as much as a factor of 20 compared to the Pioneer 10 and 11 RTGs if a specially processed grade of Pu-238 (i.e. medical grade) is utilized. While a final judgment will be deferred until RTG tests can be made under conditions which approximate the geometry of use, the use of the medical grade of fuel is expected to be a necessity. There will still be some gamma ray background from the decay of the fuel and this contribution will build up with time, but preflight (and possibly in-flight) calibration tests will provide a good identification of this component, which incidentally emits no flux of gamma rays above 2.61 MeV.

The neutron flux generated by an RTG rated at 15 thermal watts will be about 10^5 n/s (4π) with a spectral distribution from thermal to MeV energies. Such a neutron flux can produce measurable activation in a scintillation detector. A laboratory experiment in which a NaI detector was exposed to a Cf-252 source to simulate the neutron flux of an RTG, gave a very pronounced 15-hour decay from Na-24 after removal of the detector from the source (Campbell, 1975). Scaling the neutron flux level, the source-detector separation, and detector efficiency to the projected penetrator configuration gives a detector background rate which reaches a steady state rate of approximately 100 c/s MeV at 1 MeV after nine months in space. The rate will be higher if multiple penetrators are in proximity, but will decay toward a one penetrator steady state value upon separation of each penetrator from the mother spacecraft. This calculation makes no provision for neutron attenuation in the mass between the RTG and the detector or for the use of neutron shielding at either the RTG or instrument. For example, if the neutron attenuation crossection in the penetrator material has an effective value of 0.7 barns, then the neutron flux on the detector will be reduced by a factor of 20.

The neutron flux from the RTG will also activate the material of the penetrator with a resultant production of gamma rays. To estimate the magnitude of this effect, the entire mass of the penetrator was taken to be iron, with a one meter separation between the RTG and the detector. With consideration of the solid angle of the penetrator mass relative to the RTG, and of the absorption of gamma-rays from the place of production to the detector, a one barn cross-section, and making an allowance for mass voids in the penetrator, a counting rate of 200 c/s was computed. This is about the same level of activity expected at 1 MeV in the absence of an RTG, and amounts therefore to a serious enhancement of the background with a resultant degradation in sensitivity by $\sqrt{2}$ on average, somewhat more with the inclusion of detector activation. However, this estimate reflects a generalized worst case situation in which neither neutron attenuation by the mass of the penetrator, nor the use of shadow shielding to reduce the neutron flux has been considered. Both will materially reduce the activation effect of the neutron flux. In summary, the calculated RTG background interference does not preclude conduct of the experiment, but is significant and serious enough for concern and for attention to methods, principally via the use of limited neutron shielding, of reducing the level to a fraction of that from the cosmic ray flux.

Hydrogen Detection

In addition to the elements identified in the Apollo gamma-ray lunar data, the scintillation detector is also sensitive to a line from the reaction $H + n \rightarrow D$ (E_γ = 2.23 MeV). This line was apparently seen in the Apollo data as a result of lunar albedo neutrons interacting with a plastic scintillator placed around the NaI detector for the purpose of vetoing charged particles. Any hydrogen present in, for example, H_2O, near the surface of Mars will interact with secondary neutrons from cosmic rays or the neutron flux of the RTG to produce this line. An illustration of this is shown in the spectrum of Figure 5, the result of a laboratory simulation test in which a Ni target enclosed in a volume of water was irradiated by a Cf-252 source. The gamma-ray spectrum was measured by a 3" x 3" NaI detector. A characteristic neutron capture line of Ni

is seen at 8.99 MeV with its two escape peaks, but the dominant feature is the 2.23 MeV line of hydrogen. Applying normalization factors for the neutron flux level, the energy moderating effect of the hydrogen concentration on the neutron energy spectrum, detector size, counting time, source-detector geometry, and expected backgrounds due to the scattering and activation reactions from the cosmic ray flux and the RTG neutron flux, we estimate a 3σ minimum detectable limit for the detection of hydrogen of about 0.3% by weight (2% by atom).

Future plans

During this first year, our principal effort has deliberately been devoted to the selection of the most suitable sensor and a demonstration of its feasibility in terms of the specified shock environment. This has been largely done as described above and will be completed with a successful test of the integrated assembly. Following this, the value of including an anti-coincidence shield to suppress the charged particle count and the possibility of using NaI instead of CsI will be addressed. At the same time we intend to continue some consideration of other possible sensors such as CdTe. When thermal profiles for the penetrator after emplacement become available, the opportunity to use a high resolution germanium detector will be re-evaluated if the predicted temperature is low enough so that a cooler such as the small Joule-Thompson system being developed for a combined alpha scattering/x-ray fluorescence experiment (Franzgrote, 1976) could be used to cool the detector to a satisfactory operating temperature of 125°K.

In the coming year we intend to emphasize studies of the type shown in Figure 5 and discussed in the section on RTG effects in order to define the science capability of this experiment more precisely. Besides laboratory simulation tests and calculations, we will be seeking access to an actual and/or simulated

RTG for tests to verify our estimates of characteristic line production as well as the magnitude of detector and local (penetrator) activation background. A neutron transport calculation will be performed as part of this effort. Another useful experiment will be to surround a detector with several tens of centimeters of monoelemental or rock material placed in a flux of protons 1 GeV or greater in energy. Such a measurement will simulate the response of a subsurface gamma-ray spectrometer to the incident cosmic ray flux. We have performed similar accelerator tests before, most recently at the Argonne National Laboratory's Zero Gradient Synchrotron where a variety of detectors and thick targets were irradiated with 6 GeV protons for the purpose of studying the resultant prompt and delayed induced activities as an analogue to the cosmic ray flux incident on the surface of planetary bodies.

Finally, by placing the gamma-ray source and detector on the order of 0.5-1 meter apart and with the line of sight well shielded from directly incident gamma-rays, a measurement of the degree of gamma-gamma scattering is a well established technique for determining the density of the surrounding medium. This added capability of a gamma-ray spectrometer experiment will be investigated relative to the characteristics of the RTG and the penetrator configuration.

Table 1

PMT or Crystal	Acceleration/Duration[a] (g)/(ms)	Orientation of Axis to Accel.	Resolution (%)	Gain (Relative)
2" S/N 17785	Pre-JPL/NA	NA	9.20	381
	0-Sandia/NA	NA	8.50	509
	252/21	0°	8.60	487
	950/6	0°	8.76	478
	1500/4.5	0°	8.55	493
	2000/7	0°	8.40	488
	2050/6	12.4°	8.75	507
	Post-JPL	0°/12.4°	9.00	317

Table 2

PMT or Crystal	Acceleration/Duration[a] (g)/(ms)	Orientation of Axis to Accel.	Resolution (%)	Gain (Relative)
1-3/8" S/N 20266	Pre-JPL/NA	NA	19.36	2.98
	0-Sandia/NA	NA	15.57	4.80
	240/20	20°	16.60	4.33
	620/9	20°	14.28	6.77
	900/6.5	20°	15.21	6.88
	~3500/~7	20°	15.55	6.66
	Post-JPL	20°	14.42	4.60

a - The duration is the full width at one-tenth maximum

Table 3

PMT or Crystal	Acceleration/Duration[a] (g)/(ms)	Orientation of Axis to Accel.	Resolution (%)	Gain (Relative)
2" CsI(Na) S/N HA-634	Pre-JPL/NA	NA	10.31	15.9
	0-Sandia/NA	NA	10.70	16.3
	900/6.5	0°	11.01	14.6
	2100/6	0°	10.52	14.5
	Post-JPL	0°	10.88	12.4

a - The duration is the full width at one-tenth maximum

Table 4

Detector Assembly	Scintillator Size	PMT Diameter	Resolution (%)	Efficiency*	Mass*	Volume*	Length (cm)
a)	2" x 2" Dia.	2"	≤ 9	2.5	2.5	3.0	25.6
b)	2" x 2" Dia.	1-3/8"	≤13.5	2.5	2.3	1.8	18.4
c)	3" x 1" Dia.	1-3/8"	≤ 9	1.0	1.0	1.0	21.0

* Relative to c)

References

Bielefeld, M. J., Reedy, R. C., Metzger, A. E., Trombka, J. I., and Arnold, J.R. (1976), "Surface Chemistry at Selected Lunar Regions", Proc. Seventh Lunar Sci. Conf., Geochim. Cosmochim. Acta, in press.

Campbell, R. (1975) - private communication.

Franzgrote, E. (1976) - private communication.

Haines, E. L., Arnold, J. R., and Metzger, A. E. (1976), "Chemical Mapping of Planetary Surfaces", IEEE Transactions Geoscience Electronics, in press.

Metzger, A. E., and Harrington, T. M. (1969), "Addition of a Gamma Ray Spectrometer to the Alpha Scattering Experiment as Designed for the Surveyor Mission", Technical Report 32-1423, Jet Propulsion Laboratory, Pasadena, California.

Reedy, R. C., and Arnold, J. R. (1972), "Interaction of Solar and Galactic Cosmic-Ray Particles with the Moon", J. Geophys. Res., 77, 537.

Reedy, R. C., Arnold, J. R., and Trombka, J. I. (1973), "Expected γ-ray Emission Spectra from the Lunar Surface as a Function of Chemical Composition", J. Geophys. Res., 78, 5847.

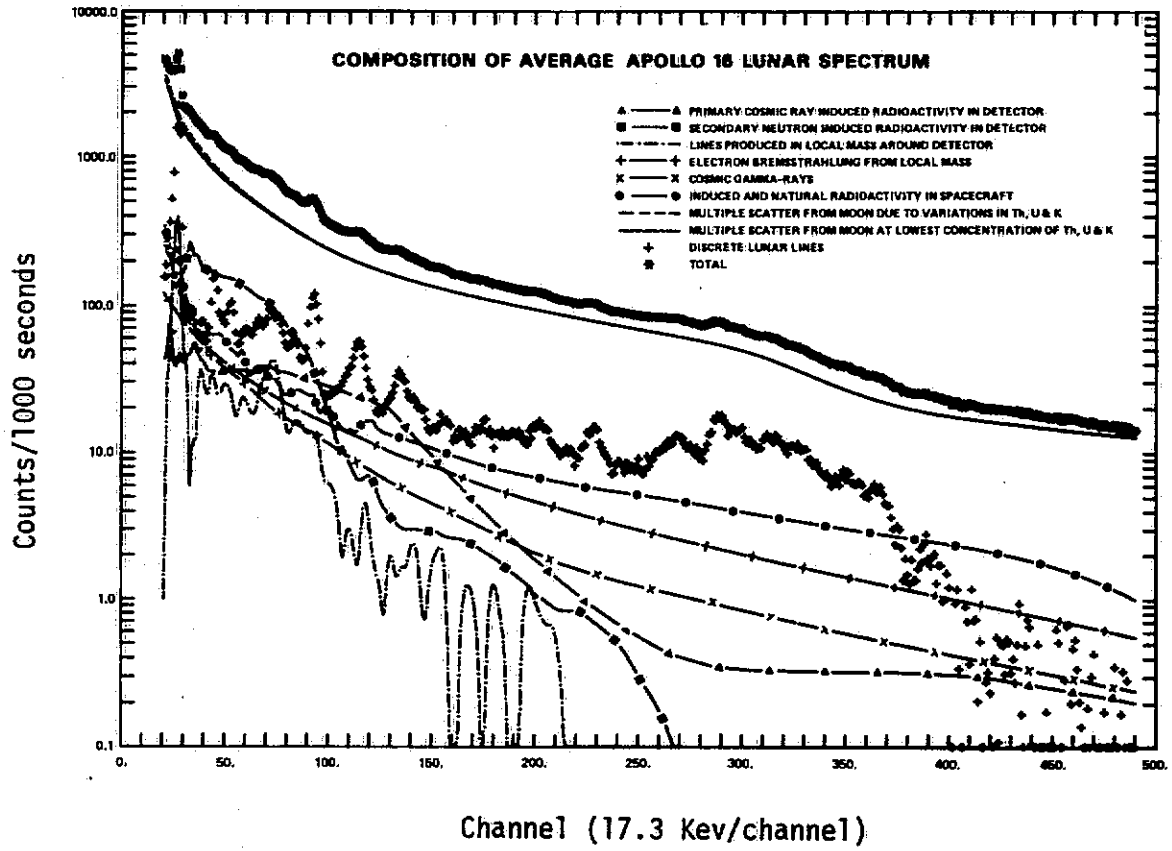

Figure 1. Apollo Gamma Ray Spectrum (total spectrum, background components, and line spectrum shown)

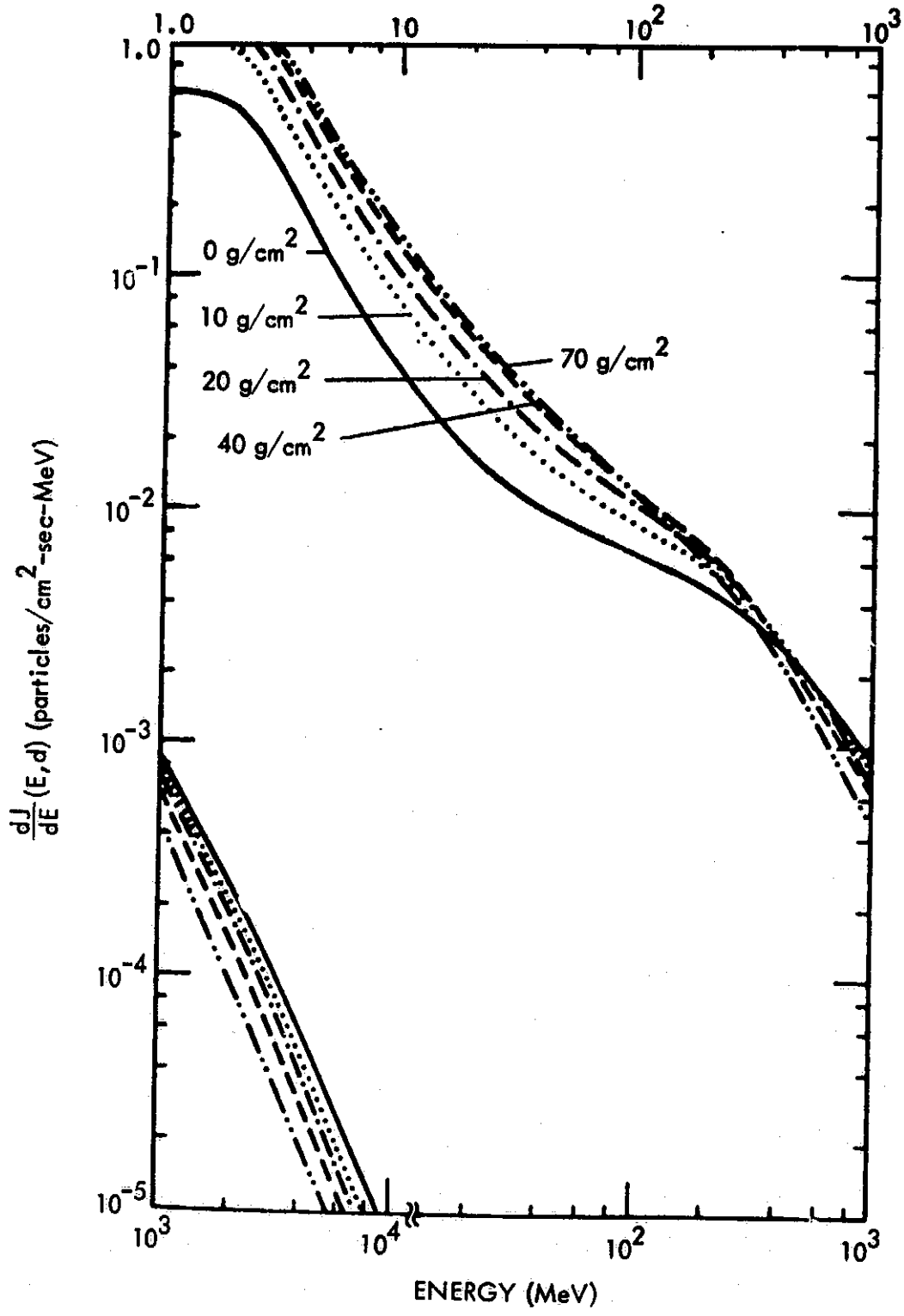

Figure 2. Lunar Differential Particle Fluxes at Depth produced by Cosmic Rays (Reedy and Arnold, 1975)

Figure 3. 1-3/8" Photomultiplier Tube

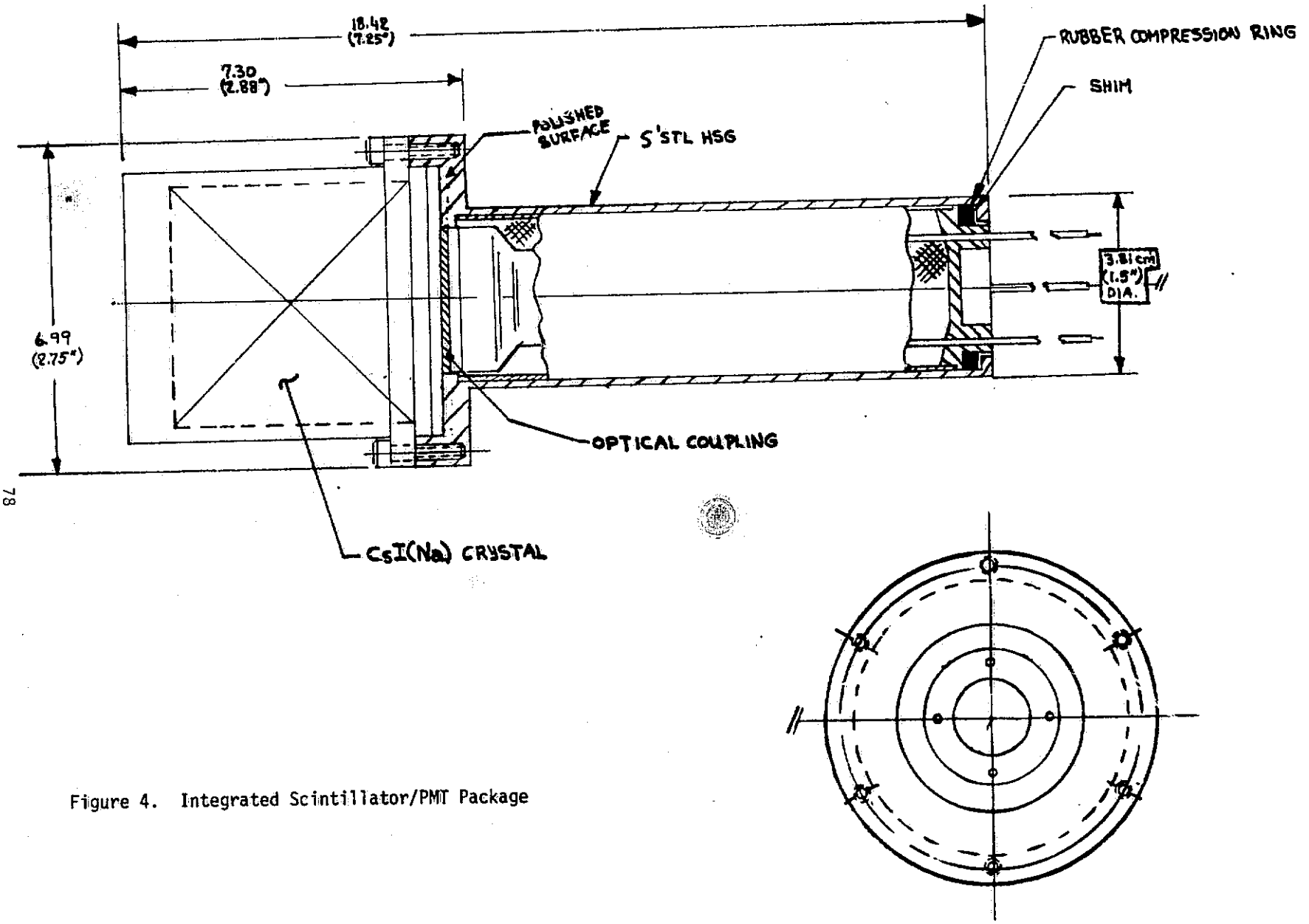

Figure 4. Integrated Scintillator/PMT Package

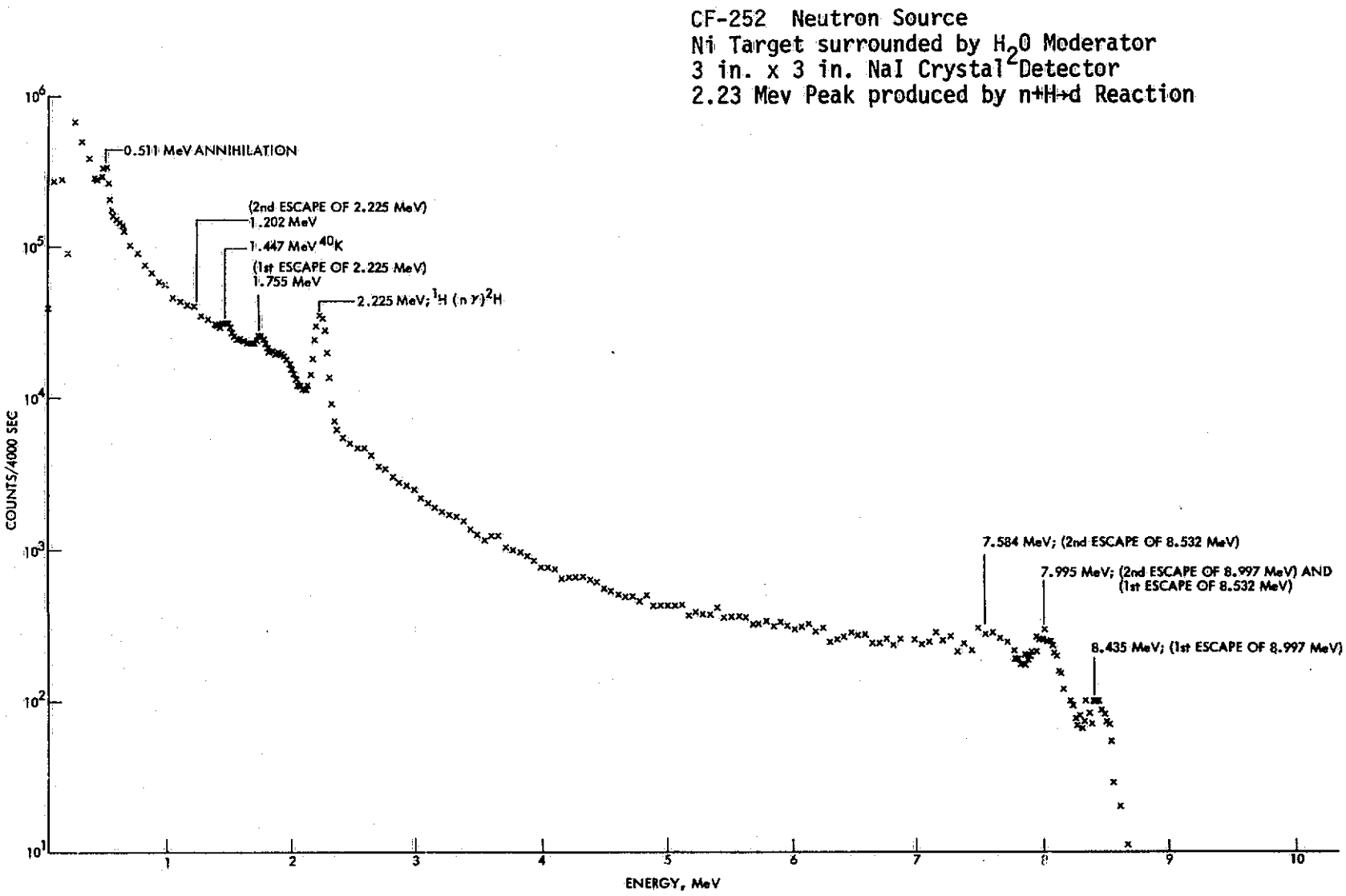

Figure 5. Spectrum from Irradiated Ni Target Surrounded by Water

APPENDIX D-1

REPORT ON ACCELERATION TESTS OF GRS COMPONENTS

Introduction and Summary

The Ames Research Center is conducting a study of a surface penetration mission to Mars. Under this study we have tested the two most critical components which might be incorporated in a gamma ray spectroscopy (GRS) experiment on such a penetrator mission. These are the photomultiplier tube (PMT) and a scintillation crystal of CsI(Na). The masimum deceleration loads expected are 2000g for 13ms--corresponding to a 1 meter penetration in a porous basaltic rock. Tests were performed at Sandia Corporation in Albuquerque, NM, using a drop table facility for levels up to 1000g and the 5.5" air gun for levels above 1000g. Two EMR-543 2" PMTs successfully experienced loads up to 2000g for 7ms along the PMT cylindrical axes and also one PMT along a vector at 12.4° to the PMT axes. One 2" PMT (S/N 17811) catastrophically failed at 3500g for 7ms at 12.4° to the PMT axis. Three EMR-541 1-3/8" PMTs successfully completed loads up to 2000g for 7ms axially and one at 20° to the PMT axes. One 1-3/8" PMT (S/N 20266) successfully experienced a load of 3500g for 7ms at 20° to the PMT axis. The 2" CsI crystal successfully experienced a load of 2100g for 6ms along the cylindrical axis and since we have shown that the components can survive the mission shock levels, the next task is to fabricate and test a combined crystal/PMT assembly. This attempt is scheduled for August 1976.

Methods

Three reject 2" and three 1-3/8" PMT were purchased from EMR Photoelectric. The tubes were rejected for non-mechanical reasons and were adequate for the functional tests. A 2" diameter by 2" high cylindrical CsI(Na) scintillation crystal was purchased from Harshaw Chemical Company. The PMTs were characterized at JPL and Sandia as to gain and resolution prior to and after shock testing using the electronics diagrammed in Figure 1. The crystal was characterized as to gain and resolution after a 20 minute warm up using the same preamp and amplifier, while Sandia provided the power supply, pulser and multichannel analyser. NBS calibrated isotopes (^{22}Na - 511 keV and 1.278 MeV; ^{137}Cs - 662 MeV) were used to excite both a 2" NaI(TI) crystal (lab-standard) for the PMT characterizations and the CsI(Na) being shock tested.

The components were potted in aluminum test fixtures with damp brown sugar. The fixtures were then placed in a vacuum oven and heated to +55°C while pumping for 4 hours. This potting technique has been used routinely at Sandia for tests up to 20,000g. During the packing of the 2" PMTs much of the excess rubber near the photocathode end of the tube was scraped off. However, this had no apparent effect on the tubes' response characteristics.

Five fixtures were used--four for the PMTs and one for the CsI crystal. Two of the fixtures were such that the acceleration loads were at angles to the tube axes. For the 2" (model 543) tubes and 1-3/8" (model 541) the angles were 12.4° and 20° respectively. The alignment accuracy during the potting is estimated to be 0.5°. Both other PMT fixtures held simultaneously a 2" and 1-3/8" PMTs. The crystal fixture was an available Sandia device which allowed the crystal to be shocked along the cylindrical axis. Since the fixtures were longer than standard, single piston air gun firing were required. This means that tests below 1300g could only be performed on the drop table. Figures 2 and 3 show typical acceleration curves for the drop table and air gun, respectively.

Results

Table 1 shows the test results. In every case, from the measurement at Sandia prior to the first shock test through the post-test measurement at JPL, resolution was essentially unchanged and gains were not affected by more than a factor of 2. Gain changes of less than a factor of 5 are not serious as they can be compensated by a simple command capability. All the pre-shock data at JPL show higher resolution for the PMTs and most show a lower gain than any of the other data. This is not considered to be representative of changes in the components since that data was taken under somewhat different circumstances. Thus a combination of noisy power lines and differences in crystal/PMT optical coupling is thought to explain this variation. This early set of data nevertheless does show the same relative characteristics between PMTs which is seen throughout all the tests.

In order to obtain an indication of a margin, one PMT of each size was tested at 3500g for 7ms. The air gun acceleration data for the 1-3/8" firing (#16) was lost due to an accelerometer malfunction. However, all settings were identical to

the previous firing and we assume the acceleration level and duration were likewise identical. Acceleration level and duration uncertainties of ±10% are assumed for test #16. Since the 1-3/8" PMT passed this severe test, it appears that extreme confidence is warranted for EMR 541 PMTs to survive a penetrometer mission impact. The 2" PMTs all met the maximum levels required for a penetrometer mission but the margin is less than 75%. Again a high level of confidence is warranted for EMR 543 PMTs. Further fatigue examination will be performed on the PMTs by Dr. Otmar Sackerlotsky at EMR's Princeton, New Jersey facilities.

The 2" CsI(Na) scintillation crystal visually appears to have displaced a small amount of the reflectance powder between the crystal and glass cover. However, no damage occurred in the crystal and the energy resolution was not affected. Thus a high degree of confidence can be placed in the ability of CsI(Na) crystals to survive a penetrometer mission impact.

Conclusions

GRS components can survive the predicted environment if they are properly integrated into an instrument. The next step in demonstrating the feasibility of a GRS experiment on a penetrator mission is to shock test a detector assembly which consists of the crystal and PMT optically coupled to each other. This is scheduled for August 1976.

Our sincere appreciation is expressed to the personnel at Sandia Corporation for their assistance and cooperation during these experiments. In particular, Mr. Eric Reece and Mr. Bill Burns were indispensable.

Richard H Parker

2/20/76

revised 6/10/76

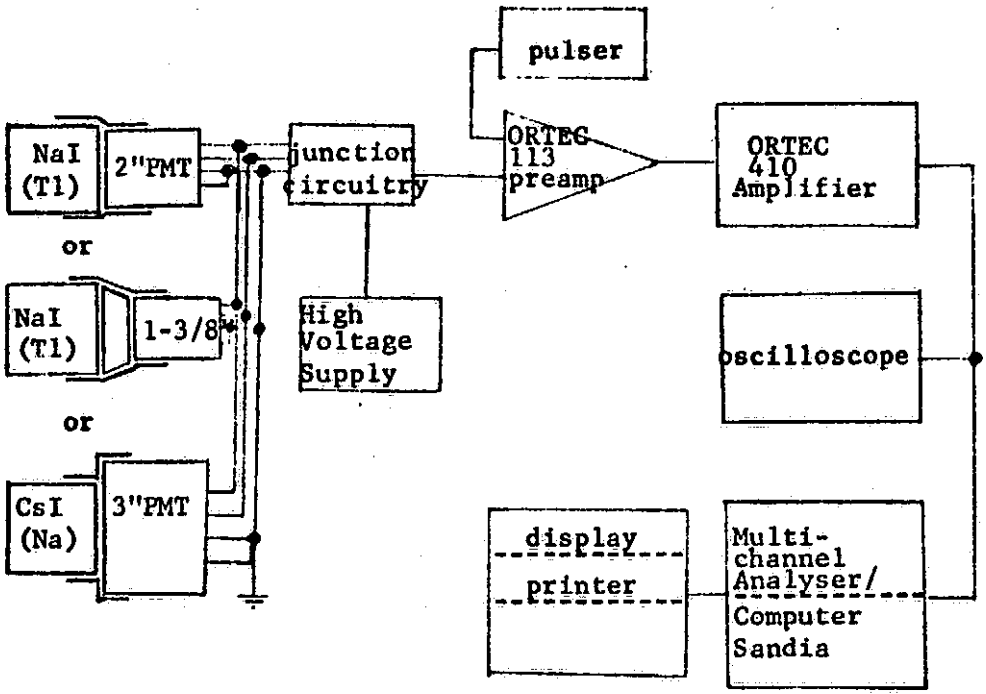

Figure 1

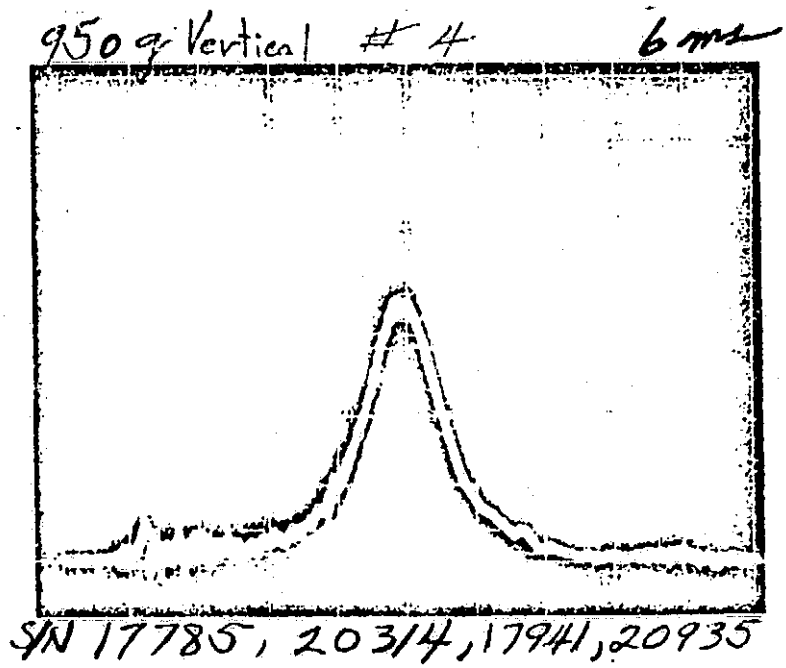

Figure 2

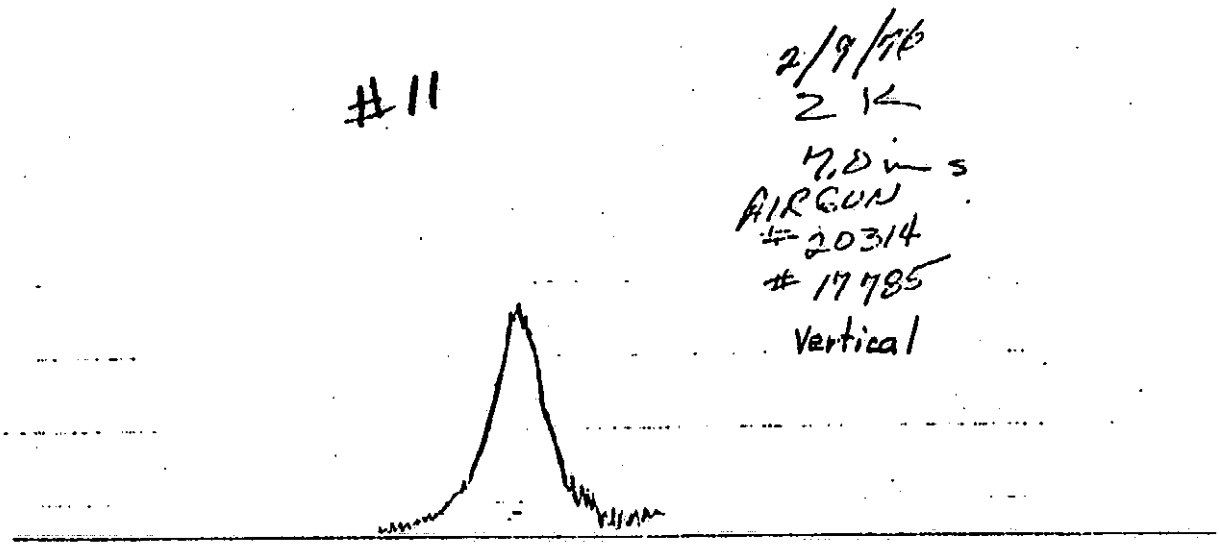

Figure 3

Table 1

PMT or Crystal	Acceleration/Duration[a] (g) / (ms)	Orientation of Axis to Accel.	Test Number	Resolution/Gain (%)/(relative)
1-3/8" S/N20266	pre-JPL/NA	NA	--	19.36/2.98
	0-Sandia/NA	NA	--	15.57/4.80
	240/20	20°	3	16.60/4.33
	620/9	20°	5	14.28/6.77
	900/6.5	20°	8	15.21/6.88
	~3500/~7	20°	16	15.55/6.66
	post-JPL	20°	--	14.42/4.60
1-3/8" S/N20314	pre-JPL/NA	NA	--	18.82/2.67
	0-Sandia/NA	NA	--	14.47/2.67
	252/21	0°	1	17.54/1.63
	950/6	0°	4	14.82/2.72
	1500/4.5	0°	6	16.61/2.34
	2000/7	0°	11	15.41/2.78
	1950/8	20°	14	15.66/2.77
	post-JPL	0°/20°	--	15.49/1.85
1-3/8" S/N20935	pre-JPL/NA	NA	--	19.11/4.61
	0-Sandia/NA	NA	--	15.49/10.4
	400/14	0°	2	15.35/9.61
	950/6	0°	4	16.14/9.26
	2000/7	0°	7	15.65/10.3
	1550/4	20°	10	15.29/10.1
	post-JPL	0°/20°	--	14.95/6.86
2" S/N17785	pre-JPL/NA	NA	--	9.20/381
	0-Sandia/NA	NA	--	8.50/509
	252/21	0°	1	8.60/487
	950/6	0°	4	8.76/478
	1500/4.5	0°	6	8.55/493
	2000/7	0°	11	8.40/488
	2050/6	12.4°	12	8.75/507
	post-JPL	0°/12.4°	--	9.00/317
2" S/N17811	pre-JPL/NA	NA	--	9.89/105
	0-Sandia/NA	NA	--	8.45/111
	240/20	12.4°	3	8.80/112
	620/9	12.4°	5	8.73/112
	900/6.4	12.4°	8	8.95/112
	3500/7	12.4°	15	failed
2" S/N17941	pre-JPL/NA	NA	--	11.39/54.3
	0-Sandia/NA	NA	--	10.61/64.9
	400/14	0°	2	10.18/71.7
	950/6	0°	4	10.41/71.7
	2000/7	0°	7	10.36/75.7
	1300/4	12.4°	9	10.18/73.1
	post-JPL	0°/12.4°	--	10.25/45.2
2" CsI(Na) S/N HA-634	pre-JPL/NA	NA	--	10.31/15.9
	0-Sandia/NA	NA	--	10.70/16.3
	900/6.5	0°	8	11.01/14.6
	2100/6	0°	13	10.52/14.5
	post-JPL	0°	--	10.88/12.4

a - The duration is the full width at one-tenth maximum.

APPENDIX E

MARS PENETRATOR WATER DETECTOR

REPORT OF FY76 WORK

Duwayne M. Anderson
National Science Foundation

John F. South

Fraser P. Fanale
Jet Propulsion Laboratory

Allen R. Tice
Cold Regions Research and Environmental Laboratory

MARS PENETRATOR WATER DETECTOR

Report of FY76 Work

Duwayne M. Anderson
John F. South
Fraser P. Fanale
Allen R. Tice

Abstract

Water on Mars is of interest for a variety of planetological reasons. The experimental evidence for water in the Martian atmosphere and polar caps, and other evidence together with theoretical considerations suggest that there may be large amounts of water in permafrost and hydrated minerals in the regolith. The penetrator vehicle provides an opportunity to measure soil moisture conditions below the surface of the regolith.

Various techniques have been considered to measure soil moisture, with greatest emphasis given to a P_2O_5 type hygrometer. A standard Beckman P_2O_5 electrolytic hygrometer sensor element was evaluated from the point of view of its general operating characteristics and the feasibility of redesign and reconfiguration. It was also subjected to a preliminary shock test at the Sandia Laboratories in their 5.5 inch gas gun. The standard Beckman element survived these tests in terms of electrical and mechanical integrity although recalibration tests showed that the instrument sensitivity to water vapor and its dynamic range was reduced. After reconfiguration and careful conditioning of the P_2O_5 element, five of these sensors survived several shock tests and two actual aerial drops with decelerations up to 20,000 G's. During these tests, the redesigned sensors were evaluated in a simulated Mars atmosphere (70% CO_2, 30% Ar, 2 to 10 torr) containing water vapor at the parts per million level. Performance in general was satisfactory, from the points of view of electrical integrity, sensitivity and capacity. However, in the pressure range of 2 to 5 torr, evidence of uneven flow through the element with a resultant interruption in the steady instrument reading was obtained, indicating the need for additional design work on the sensor tube. Detailed analysis of the gases passing out of the sensor showed that the instrument responded only to water

vapor and that it had sufficient sensitivity to adequately function as a hygrometer in the Martian environment, in addition to its demonstrated ability to serve as an integrating quantitative water detector. This test also showed that water vapor absorption and electrolysis was complete under simulated Martian conditions.

During the course of these activities, a possible alternative to P_2O_5 as the active sensor was examined. It is a solid polymer electrolytic that can function in the conductance mode or in the conductance/electrolysis mode. Its potential advantages include a wider dynamic range, better mechanical and chemical stability, and ease and variety of configuration.

I. Introduction

There is now little doubt as to the occurrence of water on Mars. It has been confirmed as a constituent of the Martian atmosphere in quantities roughly corresponding to saturation with respect to ice. The radiometric temperature regime determined by measurements from the Mariner orbiters have established the fact that Mars is a "permafrost" planet where ice and water vapor are the predominant phases of water. The liquid phase can be only temporarily stable, if at all, in localized areas. Other forms of water expected to be found on Mars include various adsorbed phases, interlayer and zeolitic water contained in clay minerals of the regolith, crystalline hydrates, and other combined forms.

The marked interruption in the retreat of the polar ice cap, combined with changes in its radiometric temperature observed by Mariner 9, is consistent with the view that much, if not all, of the underlying Martian polar caps is composed of water ice. Observations of what appears to be ephemeral frost and of low-lying clouds having temperatures consistent with water ice crystals add support to the view that water ice may be of common occurrence, particularly in the regolith where it may have created an ice-cemented permafrost.

Terrestrial permafrost is formally defined with reference to ground temperature only. Composition, including relative water and ice contents, is considered only in the classification of permafrost into such categories as unfrozen, ice-rich, ice-cemented, dry, etc. Of course in common usage, the term permafrost generally is taken to imply the presence of ice. It is necessary to make distinctions, however, and in considering the situation, vis-a-vis Mars, there seems to be little justification for departing from the conventional terminology of terrestrial permafrost. Thus, the temperature regime of the planetary surface and regolith is of primary concern.

It may be useful to pursue this point a little farther, inasmuch as the variation of regolith temperature with depth is central to the issue at hand, and also is of interest in considering the instrumentation of a planetary penetrator for thermal measurements. Figures 1 and 2 show the essential aspects of the terrestrial permafrost condition. The near surface thermal regime is illustrated in Figure 1. Points a and b are the mean annual minimum and mean annual maximum surface temperatures, respectively. Point c defines the

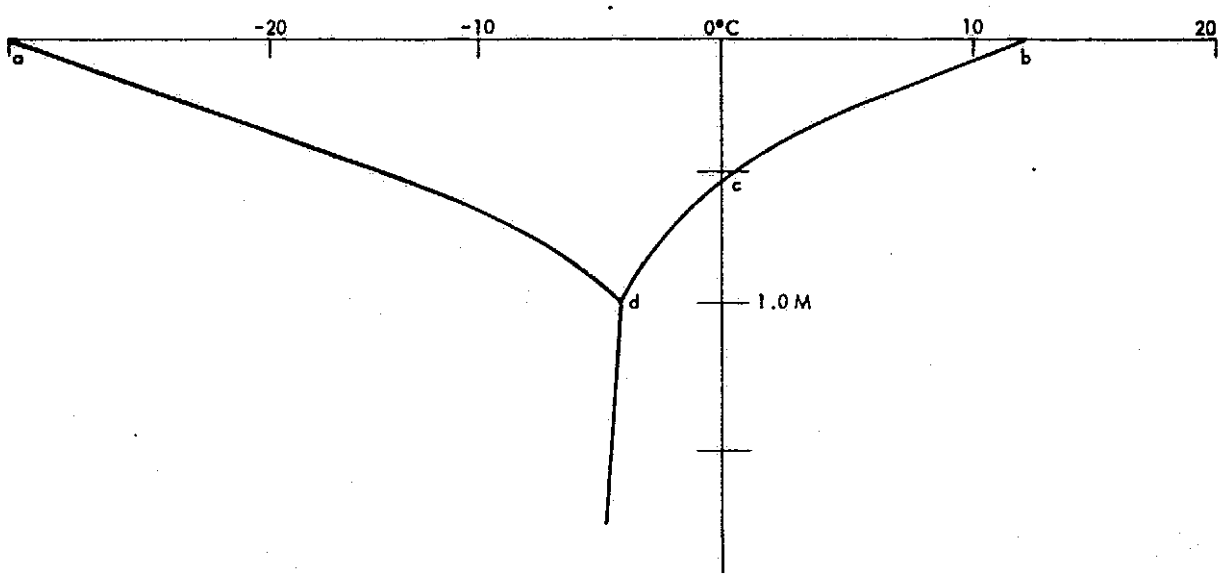

Figure 1. Thermal regime of permafrost, near surface (temperature vs depth)

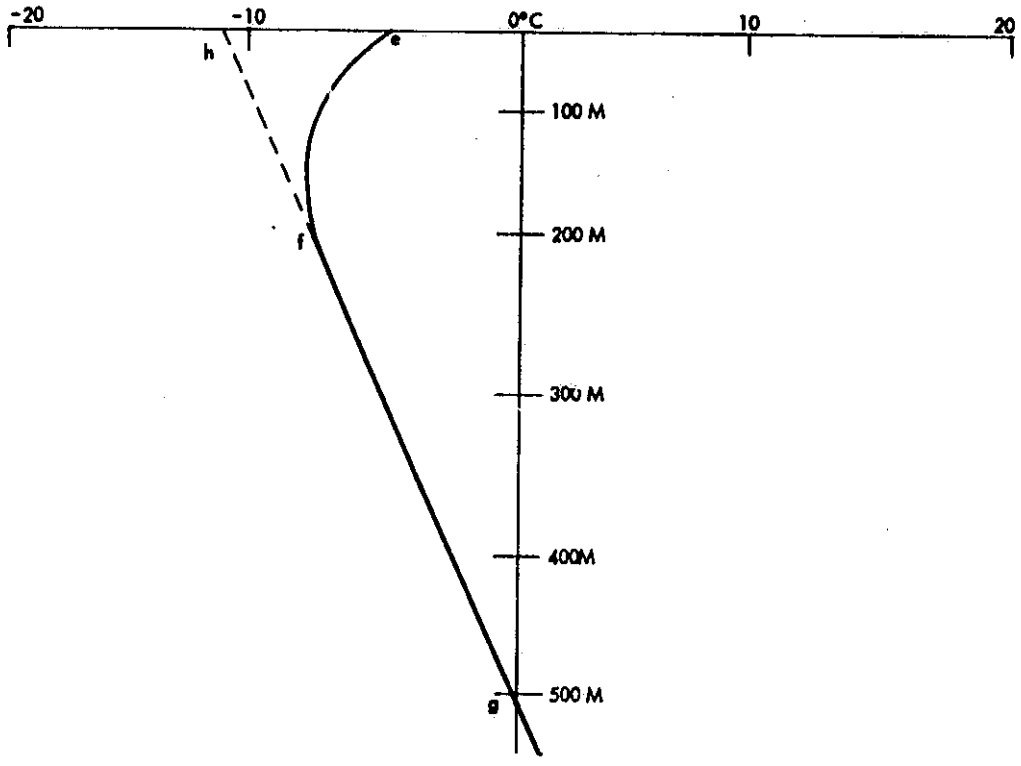

Figure 2. Thermal regime of permafrost, at depth (temperature vs depth)

average depth of annual thaw and the top of the permafrost table. These three points obviously vary somewhat from year to year, but when five year running means are employed, they can be reasonably stable points of reference. Point d is the depth of zero annual temperature fluctuation. Notice that below this depth the temperature gradient with increasing depth is shown as negative. This is characteristic of the north polar regions; its significance will become apparent when Figure 2 is examined.

Figure 2 illustrates the thermal regime at depth of the permafrost near Prudhoe Bay, Alaska. Point e is the mean annual temperature at the depth of zero annual temperature fluctuation and coincides with poind d in Figure 1. From point e to point f, the negative temperature gradient gradually declines and becomes positive and linear from point f to point g. This has been the result of the imposition of warmer surface temperatures caused by the major climatic warming that has caused the disappearance of the continental ice sheets that formerly covered much of the earth's land surface. By extrapolating

the linear portion of this temperature-depth relationship upward, an earlier mean annual temperature of about -12 °C can be reduced. From point g downward, the positive temperature gradient with increasing depth becomes greater due to the difference in thermal conductance between the frozen permafrost above and the unfrozen ground below.

While different with respect to the temperatures associated with these various points, the situation on Mars, it seems certain, must be qualitatively similar to that illustrated in Figures 1 and 2. Thus, a measurement of temperature with depth, possibly by means of temperature transducers placed at intervals along the penetrator umbilical, is very desirable, even necessary, for a complete interpretation of the water content data obtained at the penetrator depth. Of course, it will not be possible, in general, to define the curves with one penetrator. The data shown in Figures 1 and 2 were obtained from carefully instrumented drill holes that penetrated quite far beneath the lower boundary of the permafrost. Nevertheless, even incomplete data of this type would be useful. An obvious complication, of course, is that several months to a year may be required to damp out the thermal perturbations accompanying implantation.

Returning to a brief recitation of the evidence for the existence of water on Mars, there are reports of spectroscopic evidence of hydrated silicate minerals among the constituents of the Martian surface, in addition to the measured levels of water vapor and the observation of ice clouds in the atmosphere and of temperatures that ensure the stability of ground ice. A number of specific minerals, montmorillonite for example, have been postulated as being present. More recently, detailed examination and analysis of sinuous channels visible in the Mariner Mars imagery have led to the belief that these channels were formed or subsequently shaped by the movement of a fluid that is thought most likely to be running water. This implies either atmospheric precipitation or the melting and subsequent run-off of water from ground ice, or perhaps both. In any case, the evidence for the presence of soil water and perhaps massive ground ice is very strong.

As mentioned previously, the levels of water vapor known to be present in the atmosphere are at or very nearly at saturation with respect to ice. Therefore, the measured quantities of atmospheric water give little information on the quantities of soil water and ice that might be present in the regolith, beyond a certain indication of the presence of water in one or more of its possible forms. Present measurements of the polar caps do not reveal nearly as much water as can be inferred from the considerations mentioned above. The question, then, is: Were such large amounts of water as would seem to be required ever present on the surface of Mars, and if so, where is that water now? Theoretical considerations suggest that extensive ice-cemented permafrost, mineral hydrates and adsorbed water present in the regolith can account for the missing water. A long-term climatic periodicity may account for variations in the distribution of water over time and space. Thus, the measurement of water in all its possible forms and in several different representative locations is a matter of high scientific priority.

The mission concept that has been advanced to make these measurements is an assemblage of planetary penetrator vehicles. Sample measurements could then be taken at the emplacement depth at each site.

A good soil water detector in this case would be

1) Specific for water
2) Sensitive enough to detect quantities as low as 0.1% by weight
3) Able to discriminate among the various possible forms of water present
4) Relatively direct in concept and implementation and
5) Compatible with a hard landing, planetary penetrator vehicle

The amounts of ice, frost, snow, adsorbed and chemically bound water, ideally, should be determined at various times, locations, and depths in the planetary regolith in order to address the most important questions pertaining to the hydrology of Mars.

A number of analytical approaches offer a means of approaching this objective, notably thermal evolution, infrared and microwave spectroscopy, gas chromatography, neutron moderation and gamma ray scattering and several chemical methods. However, for reasons outlined elsewhere (Mars Surface Penetrator Mission Instrument Status, Ames Research Center, Feb. 1975), a method involving thermal evolution of soil water followed by its detection and measurement in the form of water vapor has been chosen as an approach that satisfies all the above criteria and that probably could be brought to the flight-qualified stage within two to three years. This is a report of work performed toward that end during FY76. As will become apparent, a flight qualified water vapor detector based on this approach is quite clearly within reach.

II. Water Analysis Objectives

Recognizing certain difficulties inherent in the configuration and characteristics of a penetrator vehicle, particularly the acquisition of a measured quantity of undisturbed Martian regolith material, a basic, minimum set of objectives that seem clearly attainable has been formulated. These are the measurement of the ambient water vapor content of the atmosphere adjacent to the emplaced penetrator, and the semiquantitative measurement of the water/ice content in the surrounding regolith. Semiquantitative here means a classification of water content as essentially none, a little, or a lot, as may be the case if the site is completely dry, if it contains amounts consistent with the presence of absorbed water and mineral hydrates, or if it contains amounts of water consistent with the presence of ice-cemented permafrost. This information will be determined as a function of the depth and location of each penetrator vehicle.

III. Water Detector Selection

As mentioned in the introduction, the criteria for selection of the P_2O_5 electrolytic hygrometer water detector are:

1) Specificity for water
2) Sensitivity

3) Discrimination among types of soil water
4) Simplicity
5) Spacecraft compatibility

The P_2O_5 hygrometer suits the selection criteria well. An alternate sensor element consisting of a solid polymer electrolyte (SPE) has also been identified and given a preliminary evaluation. A hygrometer of either type is capable of providing the two essential measurements in the objective.

IV. Hygrometer Work in FY76

During the past year, activities have concentrated on demonstrating the survivability of a P_2O_5 sensor when subjected to acceleration pulses at levels expected during typical penetrator impacts on Mars. Part of this work has been accomplished using the 5.5 inch air cannon at Sandia Laboratories. It was also possible during this period to utilize actual drop tests of a penetrator vehicle into loess and basalt targets.

A. Sensor Construction and Operational Principles

The P_2O_5 electrolytic hygrometer sensor element consists basically of a pair of rhodium wires spirally wound and encased in a plastic tube. The tube has an axial hole of approximately 0.020-inch diameter to permit sample gas passage. The inner surface of the tube and the wires are initially wetted with phosphoric acid, then electrolyzed to produce the dry, conditioned P_2O_5 absorbent/electrolyte.

When a water-containing sample gas flows through the tube, the highly hygroscopic P_2O_5 absorbs the water vapor quantitatively, if the flow rate is properly regulated, again producing phosphoric acid. An electric field imposed by an emf applied across the wires then electrolyzes the absorbed water, with a current that is exactly proportional to the rate of electrolysis of the absorbed water. This is one of the best features of the P_2O_5 sensor; the charge transferred is directly proportional to the amount of water in the sample and may be computed from first principles; no calibration is required except as a check on the operational system in which the sensor element is incorporated.

B. Shock Tests

In a penetrator mission, a basic concern for any type of sensor is its ability to survive shock loads typical of those expected during planetary implantation. Accordingly, a determination of sensor survivability was set as the first objective of the FY76 feasibility study. To accomplish this it was necessary to obtain or construct several P_2O_5 sensor elements, to arrange for shock loading tests at some convenient facility and to construct the necessary mounting hardware, etc., as needed. In order to take advantage, on short notice of an early opportunity to use the 5.5-inch air cannon at Sandia Laboratories, a commercial Beckman P_2O_5 sensor was obtained and mounted in a stainless steel projectile of suitable dimensions. The response of this element to varying concentrations of water vapor was determined in the calibration-standards facility at Sandia Laboratories before and after firing at a velocity that, on impact, gave a shock pulse of 2,000 G.

Subsequent examination and testing revealed that the sensor suffered no mechanical damage. It was also electrically intact but there was a noticeable reduction in its sensitivity to water vapor at low concentrations with a very large reduction in sensitivity at high concentrations. This is exactly what is to be expected if the phosphoric acid substrate suffered dislodgement and rearrangement. No special precautions were taken to prevent this and it very likely did occur. Since there are a number of ways of preventing this in a reconfigured sensor, this problem was not considered to be particularly troublesome. What is most significant is that the mechanical and electrical integrity of the element was preserved, demonstrating at the outset the basic feasibility of the approach.

Time and funds that could be devoted to this effort were extremely limited during FY76. Consequently, it was necessary to plan the program so that it would be possible, again on very short notice, to provide an instrument at any time there appeared an opportunity for further shock testing. As it happened, these opportunities were more numerous than expected. Lead times, however, were short (as expected) and improvisations were necessary. In the paragraphs

that follow, each test will be described briefly. A summary is presented in Table 1. In every case, the sensor element survived the shock pulse and operated satisfactorily in subsequent tests.

The second test was also conducted with the 5.5-inch air cannon at Sandia Laboratories. A standard Beckman sensor element was placed in a reconfigured mount designed so the load would be optimally applied; i.e., perpendicular to the axis of the sensor winding. The purpose of this test was to determine if the sensor element possessed sufficient mechanical strength in its standard configuration to withstand the maximum predicted impact for the penetrator after body (20,000 G's). For this test the element was not charged with phosphoric acid. After firing in the 5.5-inch air cannon at the appropriate velocity, physical examination and electrical tests demonstrated that the sensor survived undamaged; mechanical integrity and electrical continuity was maintained.

At about the time these tests were completed, an opportunity appeared to place an operating flight prototype hygrometer unit on prototype penetration vehicles for actual drop tests. Accordingly, two prototype hygrometer units were built and configured to fit in the front portion of the penetration vehicle, just ahead of the ballast. Each test package consisted of a section of sensor tube, an operational amplifier to convert sensor current into a signal voltage, and a battery package to supply amplifier power and a sensor emf for absorbed water electrolysis. Each unit was conditioned to minimize the possibility of phosphoric acid redistribution by bringing them to a very low moisture concentration, approximately 0.3 ppm, and sealing them off in glass. This was done also to maintain the current at low enough levels to ensure battery life through the rather long pre- and post-test periods when the test package was inaccessible. A small current flowed continually after each sensor element was sealed. This current is thought to be due to a continuous cycle of electrolysis and catalytic recombination of the low level residual water trapped in the sealed sensor tube. The presence of this current was very useful as it provided a ready indication of satisfactory sensor operation and served as an initial indication of survival when the element was recovered. The two test packages were taken to Sandia in

Table 1. Summary of P_2O_5 electrolytic hygrometer response to shock tests

	Sensor Element				
	1	2	3	4	5
Description	Standard Beckman P_2O_5 hygrometer sensor. Standard potting in black bakelight case	Bare Beckman P_2O_5 hygrometer tube, standard length, in 5.5 inch air cannon mount	Operating shortened Beckman P_2O_5 hygrometer tube in flight prototype configuration	Operating shortened Beckman P_2O_5 hygrometer tube in flight prototype configuration	Bare Beckman P_2O_5 hygrometer tube, standard length in 5.5 inch air cannon mount sealed at about 1.5 ppm water
Maximum shock pulse experienced	2,000 G (air cannon)	21,000 G (air cannon)	17,000 G (air cannon) (also air dropped in basalt at Amboy test 2,500 G)	300 G (Nebraska drop test)	18,000 G (air cannon)
Result	Survived	Survived	Survived	Survived	Survived
Remarks	Survival verified by inspection and electrical continuity test. Calibration shifted, probably due to P_2O_5 displacement.	Survival verified by inspection and electrical continuity test.	Survival and operational performance verified by post shock tests.	Survival and operational performance verified by post shock tests.	Survival and operational performance verified by post shock tests.

early January 1976. Sensor element No. 3 (Table 1) was taken to the air cannon facility for high G tests.

A sequence of tests was run on sensor No. 3 with the air cannon, programmed at 5,000, 10,000, 15,000, and, finally, 17,000 G's. After each test, the P_2O_5 sensor signal voltage was checked and found to be unchanged at the nominal level of the recombination current, a level corresponding to about 0.3 ppm water. These tests demonstrated conclusively that an operating hygrometer, with an operating sensor, could survive successive shocks up to 17,000 G with no shift in calibration.

A similar sequence of air cannon tests was conducted on a full length, standard Beckman sensor element (sensor element No. 5) in the same configuration as sensor element No. 2. The maximum shock pulse in this instance was 18,000 G's. The sensor element was conditioned by drying in a stream of nitrogen containing 3 ppm water vapor to minimize the possibility of redistribution of P_2O_5 during the test. When sealed off, the dynamic equilibrium created by the electrolysis-catalytic recombustion process established a water vapor concentration of about 1.5 ppm in the sensor element. Electrical conductance measurements taken before and after each test again showed no shift in calibration.

Sensor element No. 4 survived a drop test in Nebraska loess. Penetration exceeded 25 feet corresponding to a deceleration of about 300 G's; consequently, it was no surprise that this sealed sensor also survived and showed no shift in calibration. In late January, sensor elements Nos. 3, 4 and 5 were taken to the Cold Regions Research and Engineering Laboratory in Hanover, New Hampshire, for testing under a simulated Martian environment.

C. Simulated Mars Environment Tests

A stainless steel environmental chamber measuring 27 cm long and 10 cm in diameter was used to contain a simulated Martian atmosphere (Figure 3). The top was constructed of plexiglas with a 2.5-cm glass "o" ring

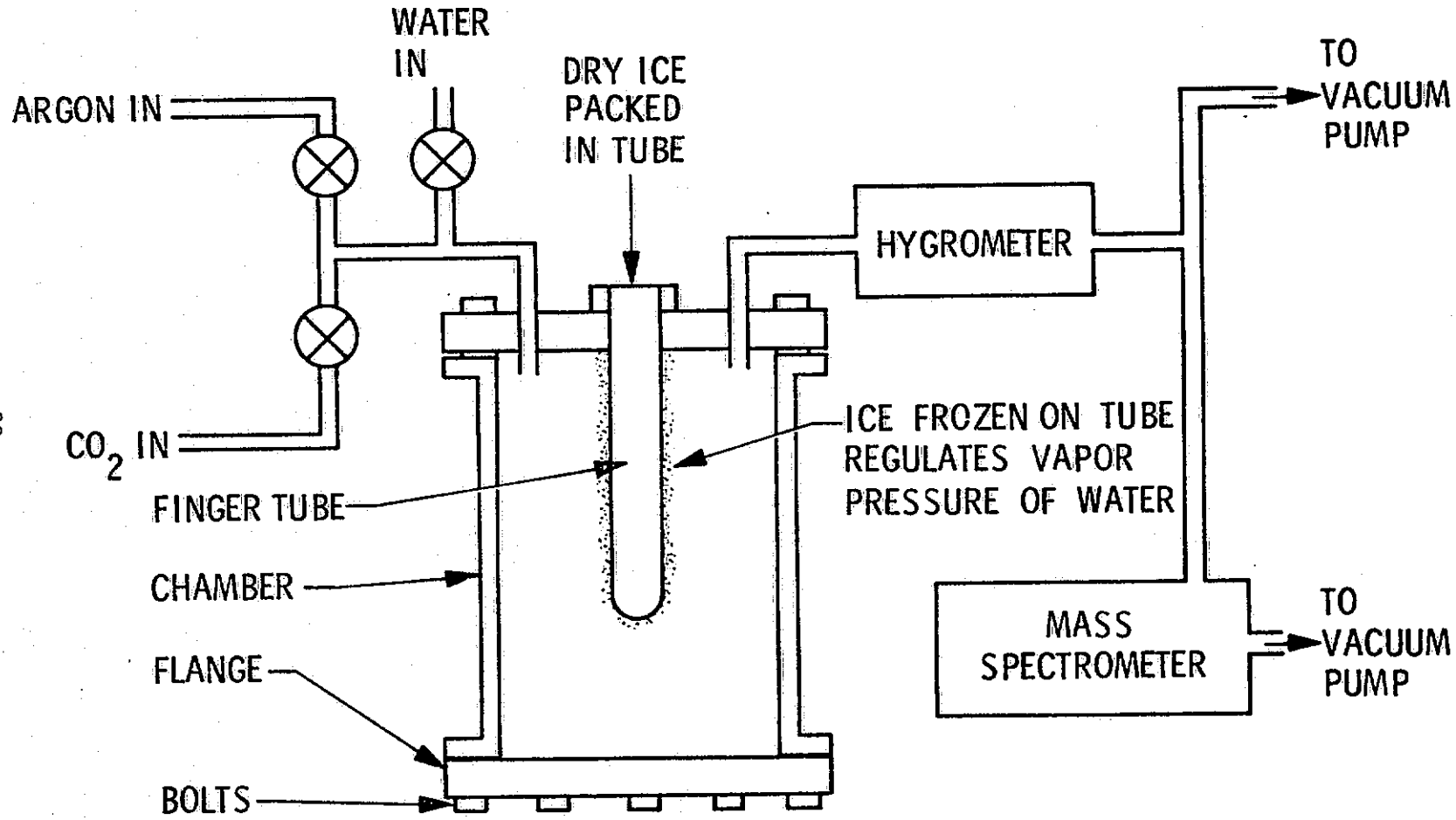

Figure 3. Simulated Mars Atmosphere Chamber

sealed finger tube extending through to a depth of 13 cm. Valved lines were installed in the top to introduce water vapor, argon and carbon dioxide gases. Sensor element No. 3 was physically mounted on the exterior of the chamber so that interior gases could be directed through it. The lines were valved in a manner that allowed the hygrometer to be isolated from both the vacuum system and the chamber while the system was being either evacuated or purged. A precision metering valve was installed to control the portion of outlet gas admitted into the mass spectrometer. Cryogenic pumps were used to evacuate the system and a large capacity ion pump evacuated the mass spectrometer. All the associated stainless steel lines were heated to about 150 C. A quartz Bourdon tube pressure measuring system was used to record the chamber pressures.

A simulated Martian atmosphere was created as follows: The environmental chamber was evacuated to a pressure of about 5×10^{-4} torr. A cold finger tube was then packed with powdered dry ice and a valve was opened to admit water vapor into the chamber. When an amount of frost considered to be sufficient covered the finger tube, the water vapor inlet was closed and the chamber was re-evacuated. The chamber was again isolated from the vacuum pumps and carbon dioxide gas was admitted to a pressure of 7.88 torr; 3.37 torr of additional argon was then admitted, making a total pressure of 11.25 torr.

The testing of sensor element Nos. 3, 4 and 5 proceeded as follows: The valves isolating the hygrometer from the vacuum sink and the simulated Mars atmosphere were opened. The variable leak to the mass spectrometer was partially opened until a pressure of 9×10^{-6} torr existed at the ion source. A computer-aided data logger was started and data from m/e 12 through m/e 250 were continually recorded at a scanning rate of 2/min until the initial chamber pressure of 11.25 torr was reduced to about 3 torr.

The mass spectrometer data for m/e 44 (CO_2) and m/e 18 (H_2O) obtained with sensor element No. 3 are shown in addition to chamber pressure vs time in Figure 4. The CO_2 spectra decreased somewhat linearly with pressure until an apparent partial blockage of the sensor tube reduced the signal level to background; however, the effect was momentary and the signal increased again. The

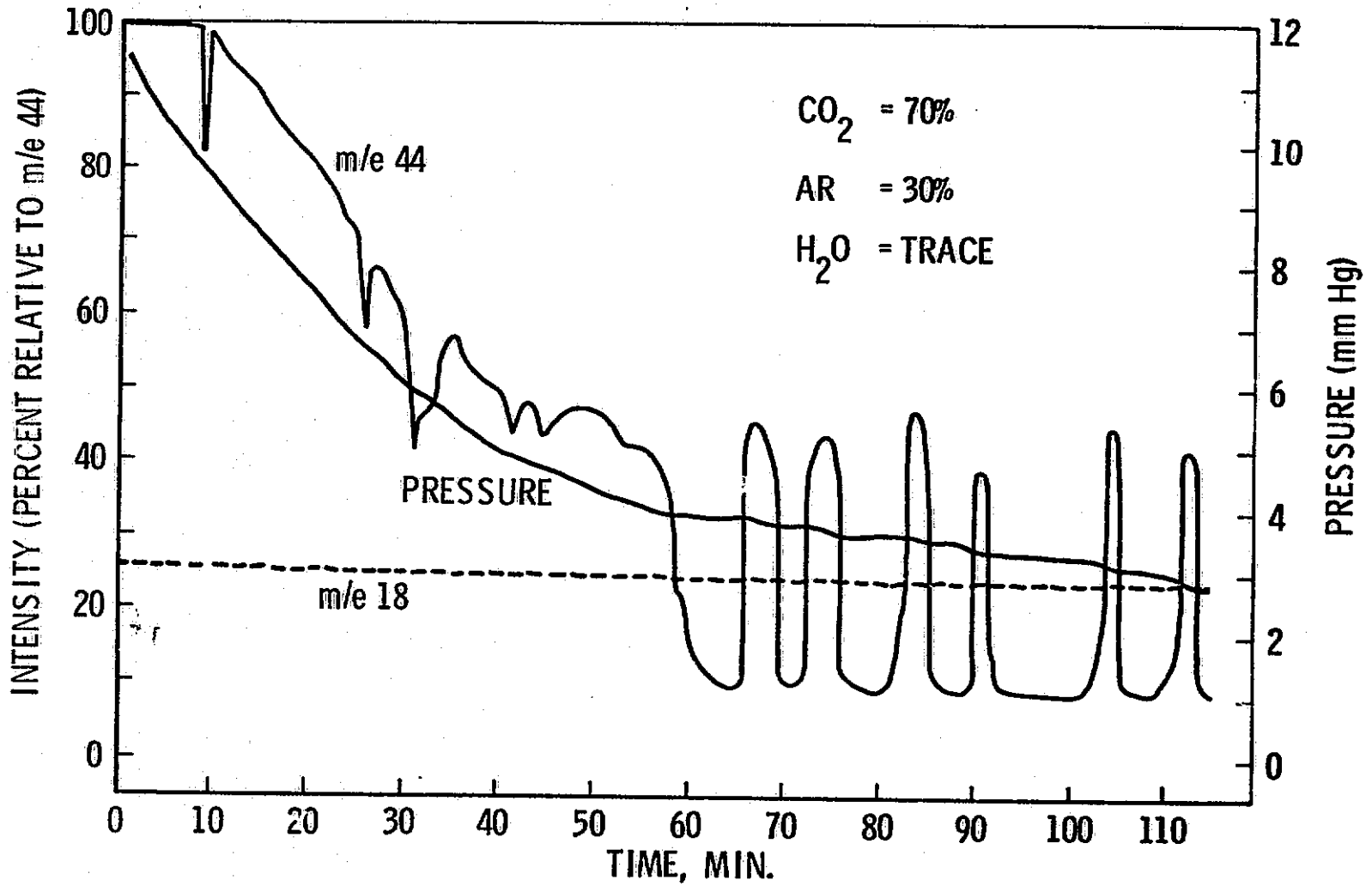

Figure 4. Planetary Penetrometer Hygrometer (Simulated Mars Atmosphere)

chamber pressure remained roughly constant at these points, confirming this deduction. The water peak remained constant throughout the whole run, indicating that the water vapor entering the sensor was quantitatively absorbed and electrolyzed; the constant very low water content shown in Figure 4 is the mass spectrometer-background spectrum.

The corresponding P_2O_5 sensor element current is shown in Figure 5. The current mirrors the reduction in flow rate as the simulated Martian atmosphere in the chamber flowed out through the hygrometer. Slightly obscuring the smooth relationship is the peak at 20 minutes, which resulted when dry ice was partially depleted and then replenished in the finger tube. When the simulated atmospheric pressure dropped below 4 torr, a level lower than that expected on Mars, intermittent flow occurred. This is visible in the sensor element response current, the Bourdon tube pressure measurements, and also the mass spectra. This observation indicates the desirability of an increase in sensor tube diameter in the next redesign.

Sensor element No. 5, subsequent to its series of shock tests, was then tested with results similar to those obtained with sensor element No. 3. The sensor current decreased with the flow until the pressure reached approximately 4 torr, when intermittent flow began.

Finally, sensor element No. 4 was subjected to this same sequence of tests using the simulated Martian atmosphere. Again, the results were similar: all three sensor elements performed well throughout the normal range of Martian conditions. No post shock calibration shifts were observed.

By mid-April another opportunity for actual penetrator drop tests arose, when two penetrator vehicles were available. Sensor element Nos. 3 and 4 were mounted in these vehicles following the tests described above. Sensor element No. 3 was dried in a vacuum and resealed at about 15 ppm water vapor, roughly one order of magnitude higher water content than in its earlier shock tests.

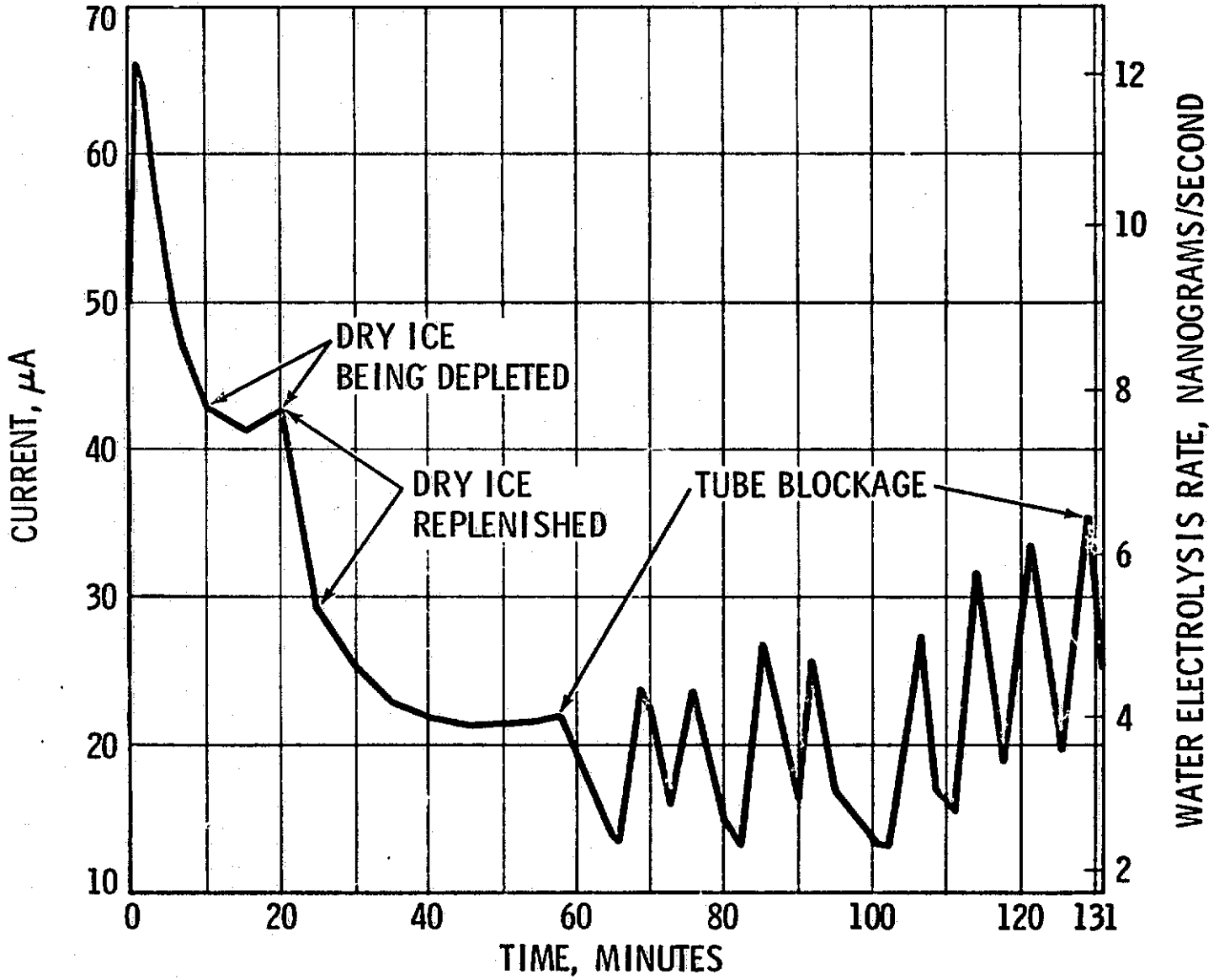

Figure 5. Water Detector Sensor Current (Short Sensor Tube)

While sensor element No. 4 was being prepared for this test, an intermittent short developed at one end of the sensor. There was no time to correct this otherwise minor problem, so an experimental, alternative hygrometer element consisting of a solid polymer electrolyte was substituted for the P_2O_5 sensor No. 4. This element is a sulphonated polymeric material that can function either in the conductance or the conductance/electrolytic modes, depending upon the strength of the imposed electric field. It has a very wide dynamic range and can be employed in a variety of geometrical configurations. It also has good mechanical and chemical stability. Therefore, it was not difficult to choose a configuration that matched the characteristics of the existing electronic package. The resulting operating hygrometer was found to have a dynamic range and electrical characteristics so that power drain was not a concern. Consequently, it was mounted on the second penetrator so that it was exposed to ambient humidity throughout the entire testing period.

The penetrator vehicle carrying the SPE hygrometer was dropped on 14 April and the vehicle carrying the P_2O_5 sensor element No. 3 was dropped on 15 April at Amboy, California. Both vehicles gave their respective hygrometers a very hard ride, coming to rest at depths of 3 ft. and 6 ft., respectively, in basalt. Neither hygrometer was damaged. Both sensors and their associated electronics packages, including their battery packs, survived these shock pulses (estimated in excess of 2,000 G's) in excellent operating condition. Figure 6 shows typical data. The steady electrolysis current resulting from the continuous electrolytic decomposition of the low concentration of water vapor in the sealed element No. 3 and its catalytic recombination is shown at intervals during the period for January to April 1976. The two readings before and after the shock test on 6 January show sensor element No. 3 survived that test and did not change its calibration. It was monitored until 26 February with no significant change. It was then opened and thoroughly tested at the Cold Regions Research and Engineering Laboratory, as described above. It was resealed on 2 April and the current was read before and after the Amboy drop. The variation in the readings in this case arose because of an inability to control the temperature at which these readings were taken. The variation in the catalytic recombination rate with

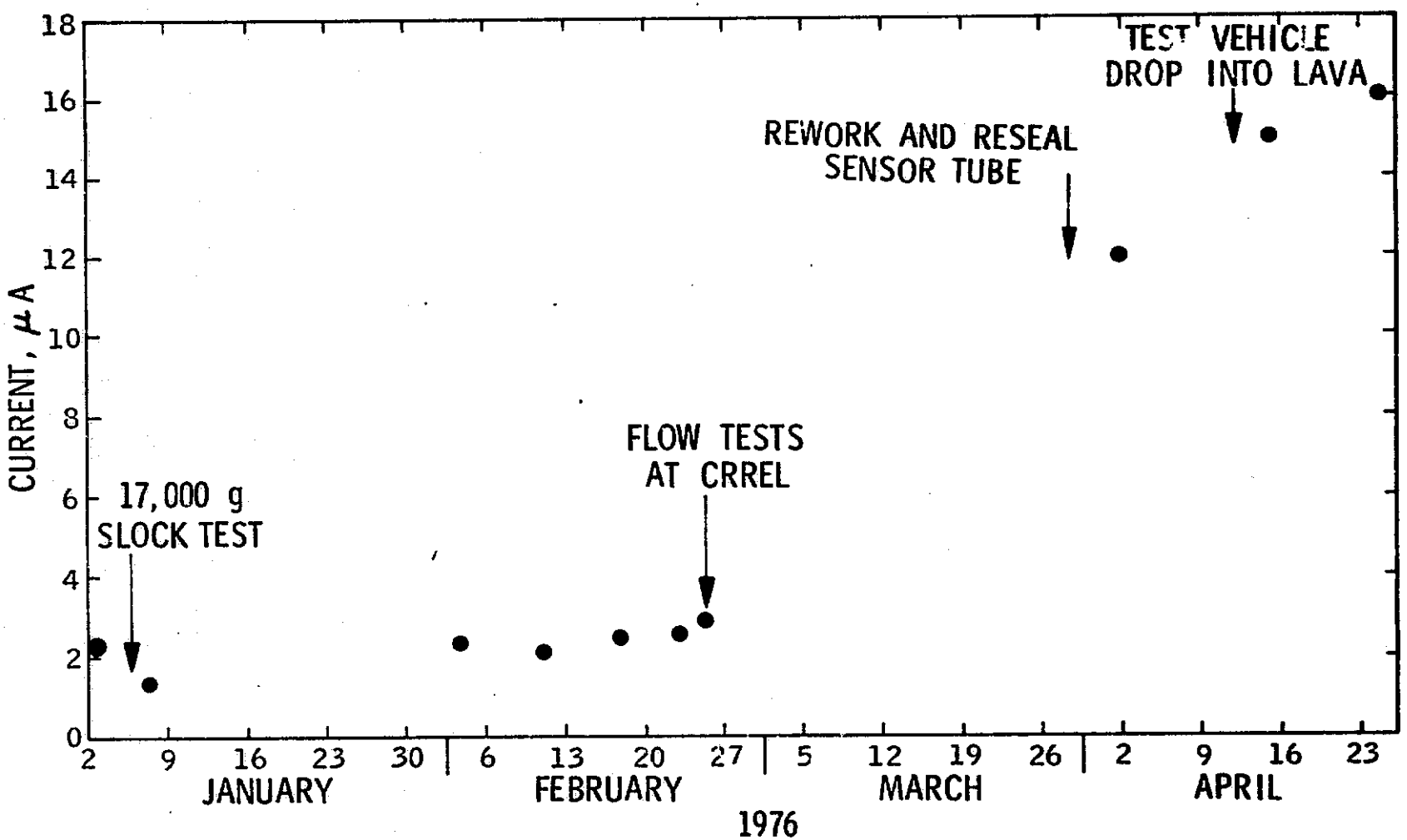

Figure 6. Recombination Current of Residual Water (Sealed Short Sensor Tube)

temperature is the source of the scatter in these data points. Taking this into consideration, it is concluded that the element survived the Amboy drop unharmed, with its calibration essentially unchanged.

The SPE sensor element also survived unharmed and is still responding to ambient fluctuations of atmospheric water vapor content in an apparently normal way. One of the disadvantages of this sensor is that it is not possible to derive its sensitivity from first principles, as is the case with the P_2O_5 element. It is therefore dependent upon empirical calibration. The degree to which its calibration may be subject to shifts has not been determined. Additional work is required in order to establish its characteristics in this respect.

V. Development Tasks on the P_2O_5 Sensor Element

A. Immediate Development Tasks

The immediate development tasks remaining on the P_2O_5 sensor element include:

1) Improve flow rate regulation at low differential pressures
2) Enlarge the diameter of the sensor tube to eliminate intermittent flow at low pressure gradients
3) Shorten the dryout time constant of the sensor
4) Compensate (or eliminate) catalytic recombination
5) Determine effect of long exposure to vacuum on the P_2O_5 substrate
6) Determine effect of sterilization on the P_2O_5 substrate.

B. Additional Development Tasks

Additional development tasks to be performed include:

1) Fabricate redesigned P_2O_5 hygrometer sensor elements, sense amplifiers, flow control orifice, flow meter and vacuum plenum
2) Assemble and integrate these components and subsystems into a planetary soil water analysis instrument

3) Perform performance evaluation tests and shock tests of redesigned soil water analyzer system

4) Design and fabricate a sample induction system consisting of sample access, sample oven with appropriate valves, gates and mating assembly to join with soil-water analysis instrument

5) Test and evaluate combined sample induction system and planetary soil-water analysis instrument using simulated Martian soil in simulated Martian atmospheres and at Martian regolith temperatures

VI. Summary and Conclusions

The general suitability of the phosphorous pentoxide (P_2O_5) hygrometer for detecting and measuring soil water released during heating has been pointed out in a similar discussion held at the Ames Research Center in February 1975. This report updates the earlier one and gives an account of FY'76 activities. These activities have been devoted principally to an investigation of the ability of a conventionally configured P_2O_5 sensor element to survive landing shocks typical of a penetrator impacting the surface of Mars. In addition to tests involving the sensor elements alone, several operational hygrometers with associated electronic and battery packages were tested. In all, five different elements were subjected to a series of shocks up to about 20,000 G's, including actual penetrator drop tests. Operating hygrometer elements survived penetrator vehicle implantations into both a soft loess and hard basalt targets.

Tests of these sensors in a simulated Mars atmosphere demonstrated their ability to detect and measure water vapor at the low levels expected on Mars. It was also shown that the absorption and analysis of atmospheric water under Martian conditions was quantitative and complete. Pre- and post-shock tests showed that it is possible to precondition the sensor elements so that post-shock calibration shifts do not occur. Analysis by mass spectroscopy showed that the instrument responded only to water vapor in the simulated Martian atmosphere.

During the course of this work, a possible alternative to P_2O_5 as the active medium by which water vapor absorption and electrolysis is accomplished was examined. It is a sulphonated polymeric material that can function in either the conductance mode or in the conductance/electrolysis mode, depending upon the electrical field strength employed. Its potential advantages include a wider dynamic range, better mechanical and chemical stability, and ease and variety of possible configurations. Testing and evaluation of this material is continuing.

There seems to be little doubt that the P_2O_5 sensor element can be successfully employed as a hygrometer and an integrating water detector in the measurement of water that is thermally evolved from samples of the Martian regolith. There are a number of development tasks remaining, however. These consist of some relatively minor but nevertheless essential redesign and reconfiguration work on the sensor element itself and a major effort to solve the problems of sample acquisition, sample handling, and adequate sample definition. This work should be undertaken without delay if this instrument is to be available for consideration for an early planetary penetrator mission.

APPENDIX F

LUNAR HEAT FLOW DATA ANALYSIS

AND

FEASIBILITY OF A MARS PENETRATOR HEAT FLOW MEASUREMENT

Stephen Keihm

Marcus Langseth

Lamont-Doherty Geological Observatory

LUNAR HEAT FLOW DATA ANALYSIS AND THE FEASIBILITY OF A MARS PENETRATOR HEAT FLOW MEASUREMENT

Stephen Keihm and Marcus Langseth

Lamont-Doherty Geological Observatory

INTRODUCTION

Similarities in deployment geometry and expected subsurface temperature variations between the lunar heat flow experiments and the proposed Mars penetrator system suggest that comparable methods of analysis could be required to measure heat flow via the penetrator scheme. In particular, the proposed configuration of a high conductance penetrator trailed by umbilicus within an open hole, basically similar to the lunar geometry, implies that radiative as well as conductive thermal linkages will have to be taken into account in any analysis of penetrator and umbilicus temperature measurements.

The discussion will be divided into two parts. First, we review the methods used to analyse the lunar heat flow measurements with emphasis on the interpretation of the long-term subsurface temperature histories. In the second part, using two specific models as examples, we will show how similar methods of analysis might be employed to interpret a Mars penetrator heat flow measurement. For the analysis presented, it is assumed that temperature sensors are deployed along the penetrator umbilicus.

LUNAR HEAT FLOW ANALYSIS AND SUBSURFACE TEMPERATURE HISTORIES

Figure 1 shows the four emplacement geometries at the Apollo 15 and 17 heat flow sites. Each heat flow probe, consisting of two 50 cm sections, was deployed into a predrilled epoxy borestem of 2.5 cm diameter. Probe emplacement depths varied from about one meter at the Apollo 15 probe 2 site to 2.3. m at both Apollo 17

stations. Temperature difference measurements of .001°K accuracy were made over distances of 28 and 48 cm within each probe section. Absolute temperature measurements were provided at eight locations over the one meter probe length. Additional temperature measurements were provided at the Apollo 17 site at depths of 15 and 65 cm by thermocouples embedded in the electronics cable. Detailed descriptions of the experiment design and preliminary results can be found in references 1 and 2.

At 3 of the 4 stations, reliable temperature gradient determinations were made within thirty days following deployment. At the Apollo 15 site, only the bottom probe 1 section gradient measurement could be used initially due to significant diurnal variations seen by the other sensors. Later filtering analysis of diurnal, annual, and transient variations provided a steady-state gradient measurement at the probe 1 upper and probe 2 lower sections. No gradient measurements could be made at the upper section of probe 2, which protrudes above the lunar surface and was off scale.

Our best measure of the regolith bulk thermal properties was provided by analysis of the long period subsurface temperature variations which sampled a large volume of regolith material surrounding each probe. Numerical models of the *in-situ* probe configurations demonstrated that the sensitivity of temporal variations to probe and near probe thermal properties decreases with decreasing frequency. For example, variations of annual frequency, induced by the earth-sun orbital eccentricity, produce very small periodic gradients in the probe and are nearly completely dependent on the bulk properties of a relatively large volume of regolith exterior to the probe. The higher frequency diurnal variations, on the other hand, are significantly altered by the probe-borestem presence and, subsequently, analysis in terms of regolith thermal properties cannot be considered reliable.

In Figure 2 is shown 3.5 years of subsurface temperature histories at the Apollo 15 probe 2 station. The large amplitude variations are of diurnal frequency

and are attenuated below the noise level of the data at a depth of 80 cm. Also apparent at all sensors shown is a component of annual frequency. These longer period variations are attenuated much less effectively than the diurnal and are detectable to depths of about 2 m at the Apollo 17 site. A long period transient component can also be recognized in all probe temperature histories and can be most clearly seen in the Apollo 17 data which contain no diurnal components. (Figure 3.) The transient temperature rises are characterized by larger magnitudes and earlier onset at the shallower sensors. The effect is due to a change in mean surface temperature caused by astronaut disruption of the thermal and radiative surface properties surrounding each probe.

Conductivity estimates based on the long period variations required a filtering of the data. The Apollo 15, 45 cm depth data are shown as an example in Figure 4a. As a first step, a finite Fourier transform was calculated for a 38 lunation window (Figure 4b). Diurnal components could be easily identified and the spectrum smoothed to remove them (smoothed solid curve of Figure 4a). The resultant filtered data contain only the annual and transient components. The annual components were then identified and removed, using a second Fourier transform over a three year window (Figure 4c), resulting in the pure transient history shown as the dashed curve of Figure 4a.

Because the depth attenuation of the annual components provided our best method of conductivity measurement, the precise identification of annual amplitudes merits further elaboration. The three year Fourier transform of the 45 cm probe 1 data shown in Figure 4c illustrates that significant power is present at the lowest frequencies (including the annual, n=3) due to the long-term transient. Transient contribution at the annual frequency must be accurately assessed in order to define the true annual component. One method used was to interpolate from the surrounding frequencies which are totally due to the transient component. It is critical to this

method that at least two years of data be available for the Fourier analysis. Otherwise, the transient background must be extrapolated to differentiate between transient and annual contributions at the fundamental frequency. Even with more than three years of data at the 15 site, the problem of transient component contribution at the annual frequency became critical at deeper sensor locations at which the transient contribution was many times larger than the true annual component. For this reason, we resorted to a trial-and-error method in which feasible sets of annual components were subtracted from the data until no variation of annual period could be discerned by eye. Using this method, we were able to identify annual components to within ±.015°K, well within the noise of the data. It should be noted that a similar approach may be required for the Mars penetrator situation in which large transients are produced by the RTG and significant annual variations can be expected as deep as 5 m.

Apollo 15 and 17 annual component results are shown in Figure 5. The data at all stations fit the theory of exponential attenuation with depth appropriate to a homogeneous medium (reference 3). The slopes of the straight line fits are a function only of the annual frequency and thermal diffusivity. The range of satisfactorily fitting diffusivity values are shown in the figure. At the Apollo 17 site, the depth of probe deployment limited the number of discernible annual components. The identified component at 15 cm is based on thermocouple measurements. Again, however, the available data are very well fitted by the exponential attenuation theory for a uniform medium. The resultant best fitting diffusivity values at all sensors were converted to thermal conductivities using other measurements of regolith density and specific heat (references 4 and 5). Resultant conductivity and heat flow deductions are shown in Figure 6.

Notice on the left that the conductivity values deduced from the annual component analysis (vertical bars) are significantly lower than preliminary estimates,

which were based upon a 36-hour transient response to 0.002W power sources within the gradient housings at either end of each probe section. The main source of error in the short-term measurements was the limited sampling volume on which the results depended. The thermal characteristics of the probe-borestem system and about 2-3 cm of adjacent regolith material controlled the 36-hour temperature response. Uncertainties in numerical model parameters, such as axial heat dissipation by radiation along the probe, were difficult to evaluate. In addition, the thermal properties of the small volume of adjacent regolith material sampled may have been altered to an unknown extent during the drilling process. The fact that the difference between the short-term and long-term measurements increases with depth suggests that the difference may be due to increasing compaction of the regolith around the drill stem as the stem penetrated deeper and deeper. In this context, it should be emphasized that disruption of adjacent material will likely occur to an even greater extent during the penetration of a Mars probe. Thermal, as well as chemical, contamination can be expected and care must be taken that any proposed method of conductivity measurement be of sufficient duration to sample well beyond the contact layer.

Differences between the preliminary (dashed lines) and final (solid lines) heat flow values shown on the right result almost entirely from differences between the preliminary (short-term) and revised (annual wave) conductivity deductions. The identification of diurnal, annual, and transient components was used to refine our preliminary estimates of the steady-state mean temperature profiles; but in no cases were the initial gradient estimates altered by more than 5%. The long-term analysis did, however, allow gradient determinations to be made at probe 2 and the upper section of probe 1 at Apollo 15 where significant diurnal and annual fluxes had not permitted preliminary gradient estimates to be made.

SIMULATION OF A MARS PENETRATOR HEAT FLOW MEASUREMENT

The proposed Mars penetrator design and deployment geometry can be expected to result in subsurface temperature measurements whose temporal variations contain the comparable components observed on the moon. The major difference is expected to be in the considerably larger magnitudes of the annual and transient variations. The eccentricity and obliquity of Mars lead to annual surface temperature variations of many tens of degrees at most latitudes. For example, at -20°S, peak-to-peak-surface variations of 50-60°K can be expected. Assuming reasonable diffusivity values, periodic fluxes 5-30 times the flux due to steady-state heat flow could occur at depths up to two meters. The presence of a 20-watt power source implies temperature rises on the order of tens to hundreds of degrees within the penetrator body within 30 days following deployment. Radiation along an open hole above the penetrator will result in significant effects within three meters of the penetrator body over the course of one Mars year.

The primary significance of such large transient and annual variations is that the difficulties of a heat flow interpretation will be reversed from those of the lunar experience. The magnitude of the temperature rise within the penetrator will be controlled by losses to the surrounding material and should provide an excellent measurement of the thermal conductivity. The presence of large annual variations at umbilicus depths would provide a second conductivity estimate appropriate to the depths of the proposed sensor locations. The measurement critical to a heat flow experiment will be the steady-state temperature gradient determination. To explore the difficulties involved in making such a measurement, two numerical simulations of feasible penetrator deployment configurations have been run over a time period of just over one Martian year. Temperature sensors were assumed to be located at one-meter intervals along the umbilicus with the deepest sensor one meter from the penetrator tail. Open-hole configurations were assumed although the possibility of convection processes and possible phase changes of trapped gas were not.

The primary goal of the models was to examine the feasibility of making a reliable temperature gradient measurement in the presence of large annual and transient variations. In both models, a surface temperature of 200°K mean and a variation of 30°K amplitude and annual period was used. A cooldown period was simulated by assuming that all kinetic energy of the pre-impact penetrator was evenly deposited within a radial zone of two cm thickness along the hole. In both models a nominal regolith gradient of 1.0°K/m was assumed.

In the first model, designated M1, a penetration depth of 5 m into material of conductivity 4 x 10^{-4} W/cm°K was simulated. The evolution of hole wall temperature profiles (which are very well coupled to adjacent umbilicus sensors) are shown in Figure 7. It is obvious that no reliable gradient measurement could be made from the profiles alone, even if temperature sensors were spaced closely enough to describe the profile in such detail. Annual wave effects within the upper 2 m are enormous and profiles at greater depth are washed out by the RTG effects before substantial cooldown to adjacent regolith conditions can take place.

The situation improves considerably, however, if a full year of sensor temperature histories are available. The "measured" gradient value of 1.25°K shown between 0.85 and 1.85 m depths is based on filtering analyses applied to the simulated umbilicus sensor temperature histories shown in Figure 8. Values in parentheses above each of the depth labels give distances from the penetrator tail in meters. At the 0.85 m depth, nearly three meters from the penetrator tail, effects from the RTG begin to be felt only near the end of one Martian year. The large variation consists almost entirely of the annual component. At the sensor one meter below (1.85 depth), the annual component can be easily recognized although transient effects have become significant in the second half of the Martian year. At the deepest sensor (2.85 m depth, 0.95 m from the penetrator tail), RTG effects are totally dominant and the data are useless for the estimation of steady-state gradient. To obtain mean

temperatures at the two shallower sensors, similar component separation techniques as were utilized for the lunar experiment were employed. The results at the 1.85 m sensor are shown in Figure 9.

With the annual component filtered out, it can be clearly seen that the RTG effects were not felt until about 140 days following deployment, allowing cooldown equilibration to have been effectively completed, and yielding the mean temperature estimate indicated. A similar analysis of the .85 m sensor history resulted in the steady-state gradient calculation of 1.25°K/m shown in Figure 7. Admittedly, the result is artificial in that the simulation is characterized by a pure harmonic variation and thermal property homogeneity. The results do, however, show that the gradient measurement is feasible even in the presence of significant annual and transient variations.

The second model, designated M2, assumes a more favorable penetration depth of 8.8 m into material of slightly lower conductivity, 2×10^{-4} W/cm°K. In such a case, the gradient measurement could be made with significantly more confidence as illustrated in the temperature profile evolution shown in Figure 10. For this case, a nearly representative gradient measurement could be made between depths of 2.5 and 4.5 m within about four days following deployment. Analysis of a year's worth of temperature history data, however, will lead to refinement of any preliminary estimate and increased confidence provided by mean temperature determinations at other depths. The "measured" value of 1.08°K/m is based on a least square fit to the mean temperatures at five subsurface locations determined from analysis of the temperature histories shown in Figure 11. The lower conductivity regolith limits the significant annual variations to depths less than three meters and the deeper penetration permits essentially transient free temperature histories to depths of about four meters. Mean temperature values are obtained at the 4.5 and 5.5 m depths by noting the absence of significant annual variations and utilizing the data prior to the transient onset, but well past the significant cooldown equilibration.

In Figure 12 are shown the thermal diffusivity deductions based on the annual amplitude attenuation for the two models. Very reliable results can be obtained using data with significant annual components for either model. Note, however, that if the results depend on the measurement of small annual components, other methods of analysis must be relied upon (such as the penetrator temperature rise) to estimate the thermal conductivity.

CONCLUSIONS AND RECOMMENDATIONS

Within the constraints of the previous analysis, it appears that the principal factors necessary for a successful Mars penetrator heat flow measurement are substantial penetration, at least four meters, and the deployment of accurate ($\pm 0.05^{\circ}K$) temperature sensors at favorable depths. Unless the hole is partially filled following penetration, sensors within one to two meters of the penetrator tail will very likely be useless for the purposes of a gradient measurement. The coupling of the annual variations of the open hole umbilicus to the exterior regolith material implies that annual flux variations can be accounted for, assuming that temperature data are available for a significant portion of the Martian year. Assuming sufficient penetration, the success probability of such a heat flow measurement would then most likely depend upon the number of sensors deployed at favorable depths along the umbilicus.

Certainly other factors must be investigated to reliably assess the feasibility of measuring heat flow via the penetrator scheme. The presence of trapped and adsorbed gaseous phases within the Martian regolith could be significant factors in the exchange of heat between regolith and atmosphere during the diurnal and annual cycles. The presence of significant amounts of permafrost could be significant in controlling the penetrator temperature response to the RTG, and thus lead to errors in conductivity determinations based on this response. RTG-driven convection of gaseous phases present in an open hole above the penetrator tail could conceivably

mask any gradient measurement. Convective effects are now being investigated with simulation models at NASA-Ames (T. Canning, personal communication).

It should also be pointed out that the analysis discussed in this report presumes the emplacement of temperature sensors at known spacing along the umbilicus. The engineering difficulties in assuring a "taut" umbilicus need to be investigated, as well as alternative methods of deploying sensors capable of making a reliable measurement of the steady-state temperature gradient. One such method to be examined from both an engineering and theoretical viewpoint is the radial deployment of sensors 10-20 cm from the penetrator body following emplacement. The critical evaluation, from the theoretical standpoint, would be the equilibration time of the sensors relative to the onset of masking effects from the impact and RTG-induced thermal transients. The effects of thermal coupling along a radial extension arm connecting sensors and the penetrator body would also require analysis.

REFERENCES

1. Langseth, M.G., Clark Jr., S.P., Chute Jr., J.L., Keihm, S.J., and Wechsler, A.E., Heat Flow Experiment, Chapter 11, Apollo 15 Preliminary Science Report, NASA SP 289, 1972.

2. Langseth, M.G., Keihm, S.J., and Chute Jr., J.L., Heat Flow Experiment, Chapter 9, Apollo 17, Preliminary Science Report, NASA SP 330, 1973.

3. Carslaw, H.S. and Jaeger, J.C., Conduction of Heat in Solids (pp. 64-69), Oxford at the Clarendon Press, 1959.

4. Carver III, W.D., Apollo Drill Core Depth Relationships, The Moon 10, pp. 183-194, 1974.

5. Hemingway, B.S., Robie, R.A., and Wilson, W.H., Specific Heats of Lunar Soils Basalt and Breccias from Apollo 14, 15, and 16 Landing Sites Between 90 and 350°K. Proc. Fourth Lunar Sci. Conf., Geochimica et Cosmochimica Acta, Suppl. 4, Vol. 3, pp. 2481-2487, 1973.

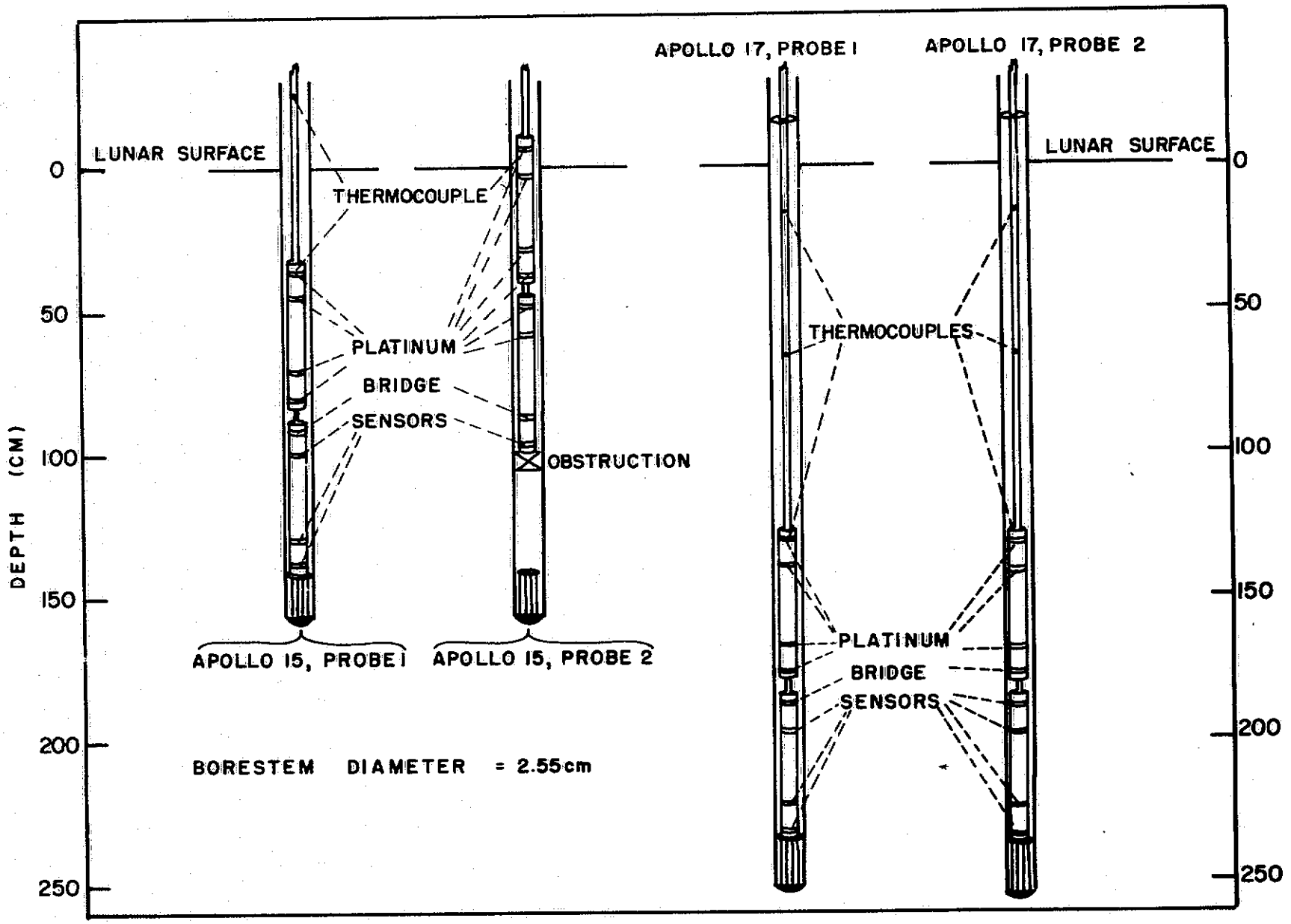

Figure 1. Emplacement geometries and temperature sensor locations at the Apollo 15 and 17 heat flow sites.

HEAT FLOW EXPERIMENT - APOLLO 15, PROBE 2

TEMPERATURES THROUGH LUNATION 42

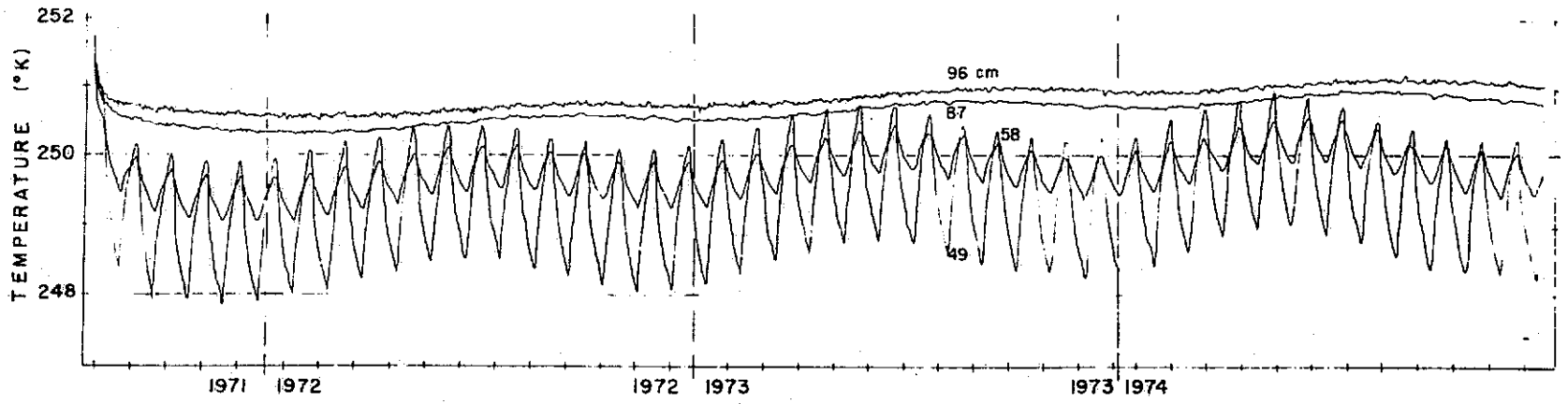

Figure 2. Three and one-half years of subsurface temperature histories at the Apollo 15 probe 2 station.

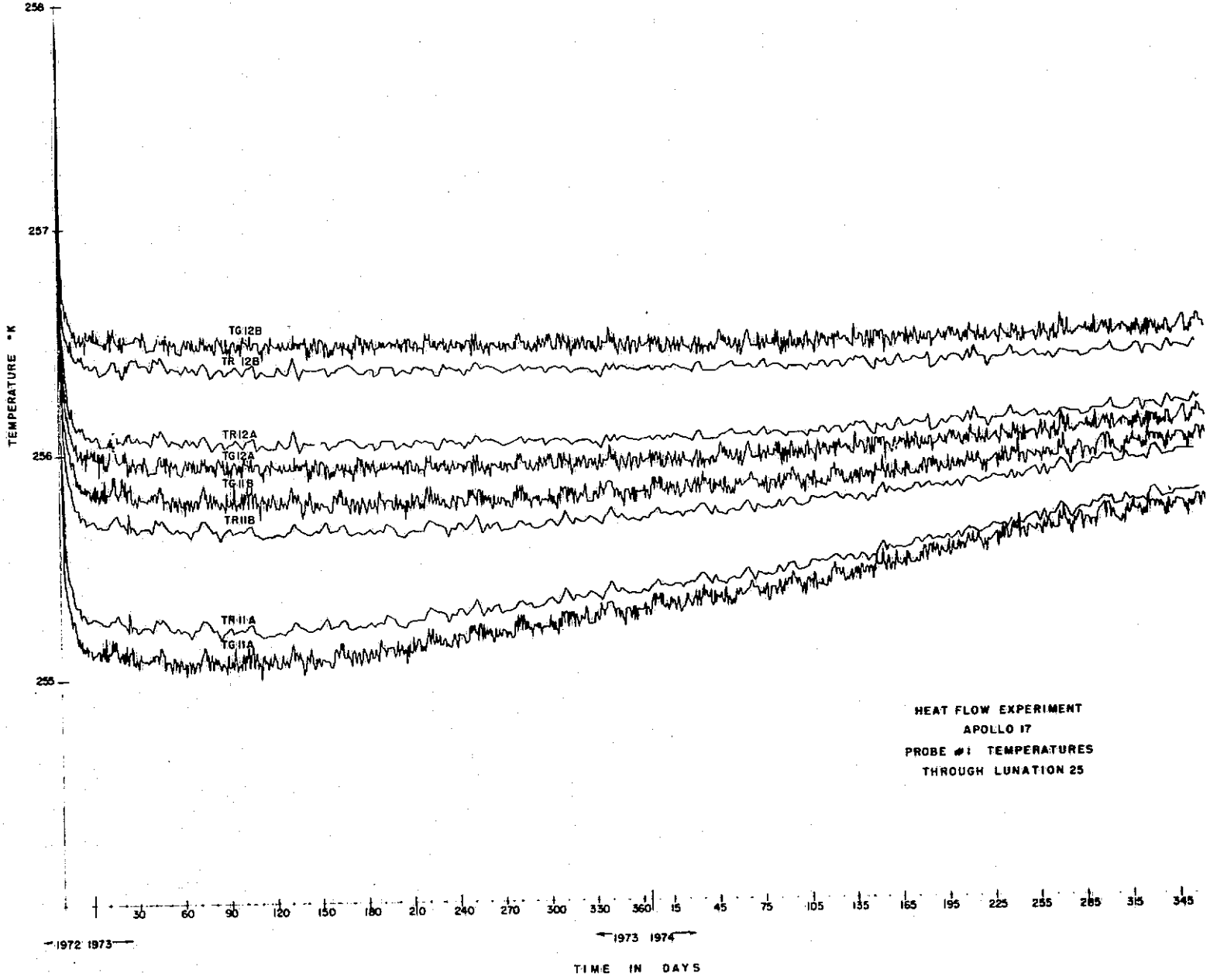

Figure 3. Two years of subsurface temperature histories at the Apollo 17 probe 1 station.

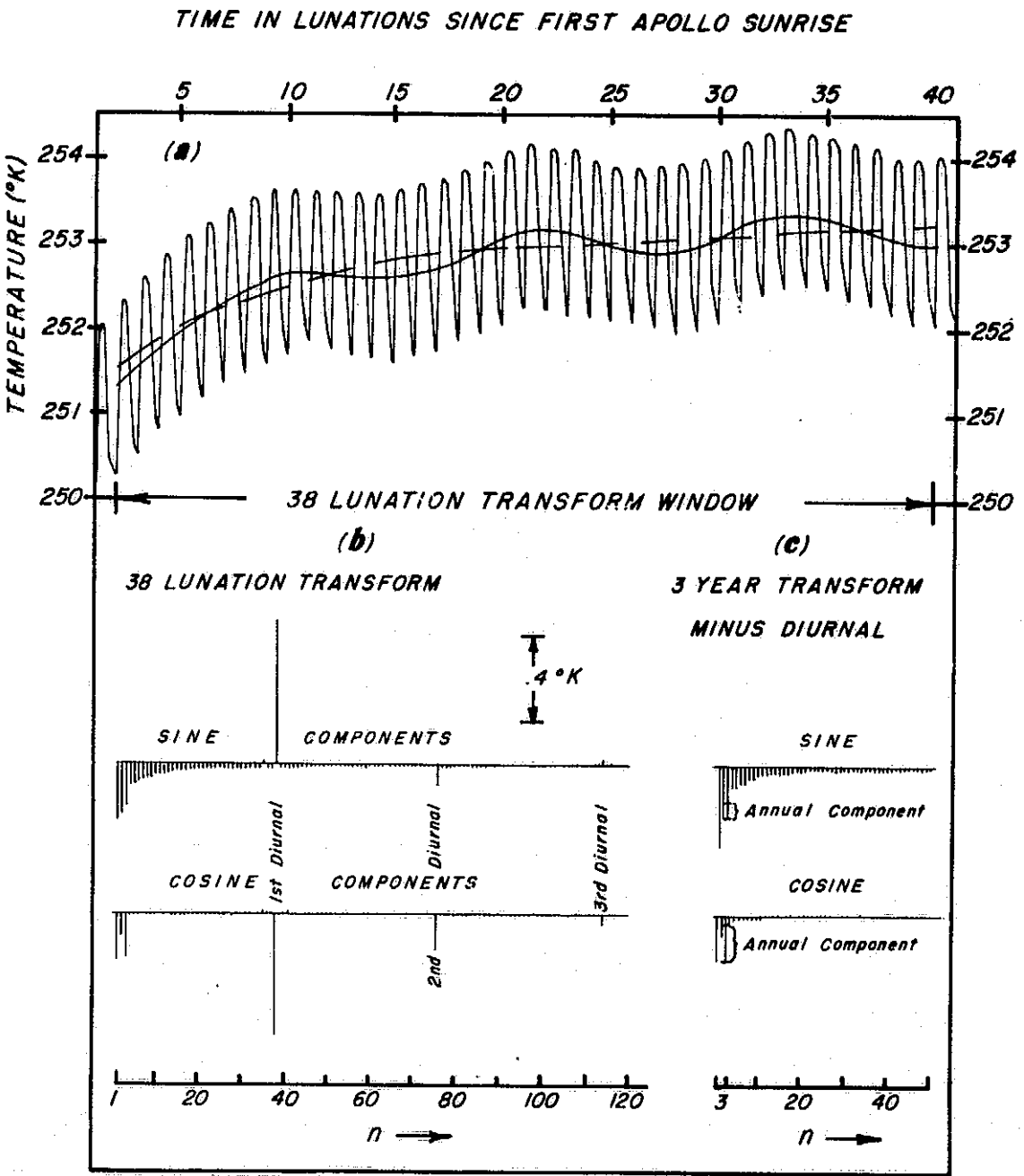

Step-by-step filtering analyses of the Apollo 15 probe 1 sensor at 45 cm depth: (a) Temperatures vs. time. The curve with the high frequency diurnal variations present represents the unfiltered real time data. The smoothed solid curve results when the diurnal variations are filtered out. The dashed line shows the pure transient response after both annual and diurnal variations have been removed. (b) Thirty-eight lunation frequency spectrum used to identify and remove the diurnal components. (c) Three-year frequency spectrum of the diurnal free temperature history. The component at n=3 consists of both an annual and a transient contribution.

Figure 4. Filtration Analysis.

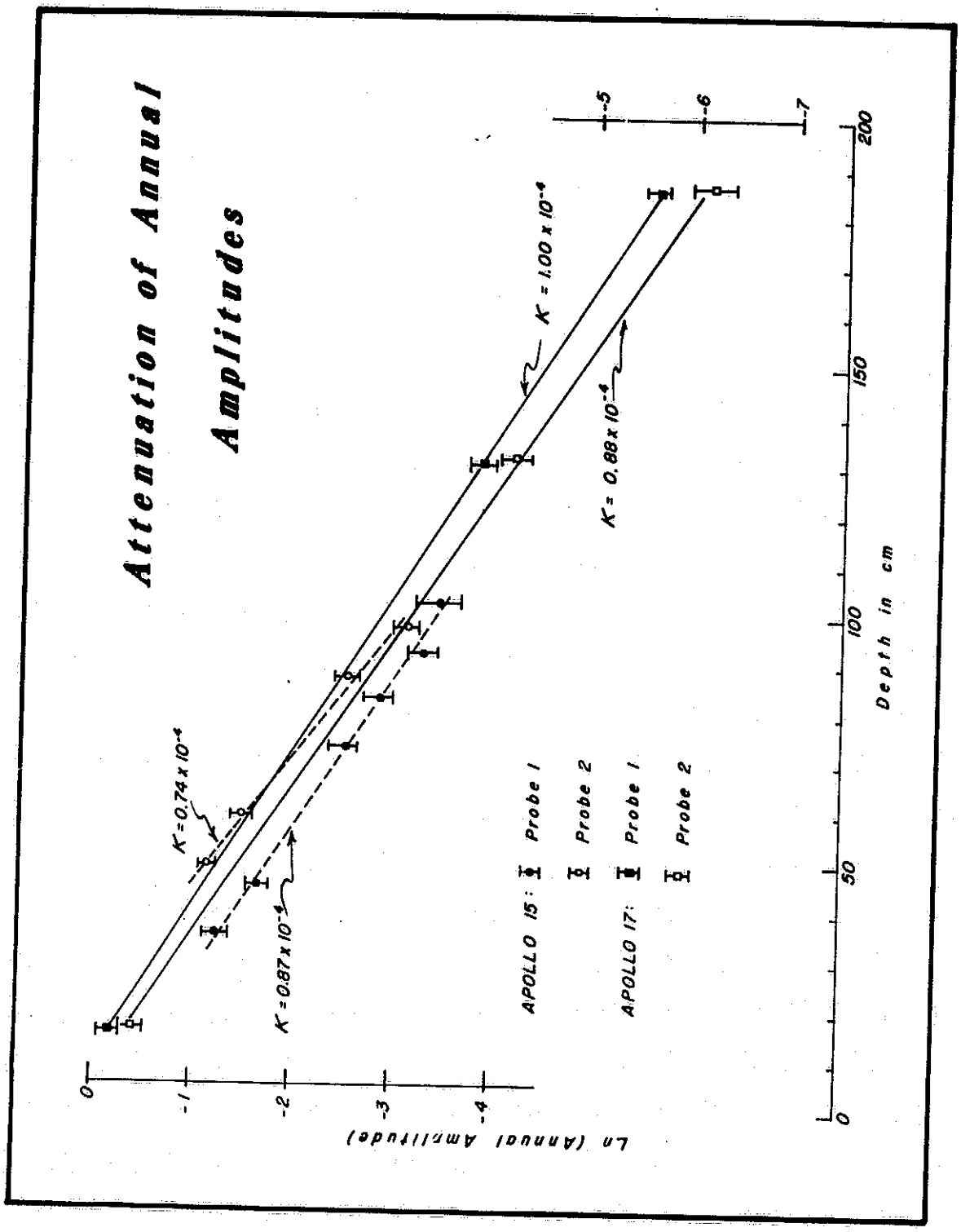

Figure 5. Annual amplitudes vs. depth at Apollo 15 and 17. Straight line fits represent best estimates of regolith diffusivity.

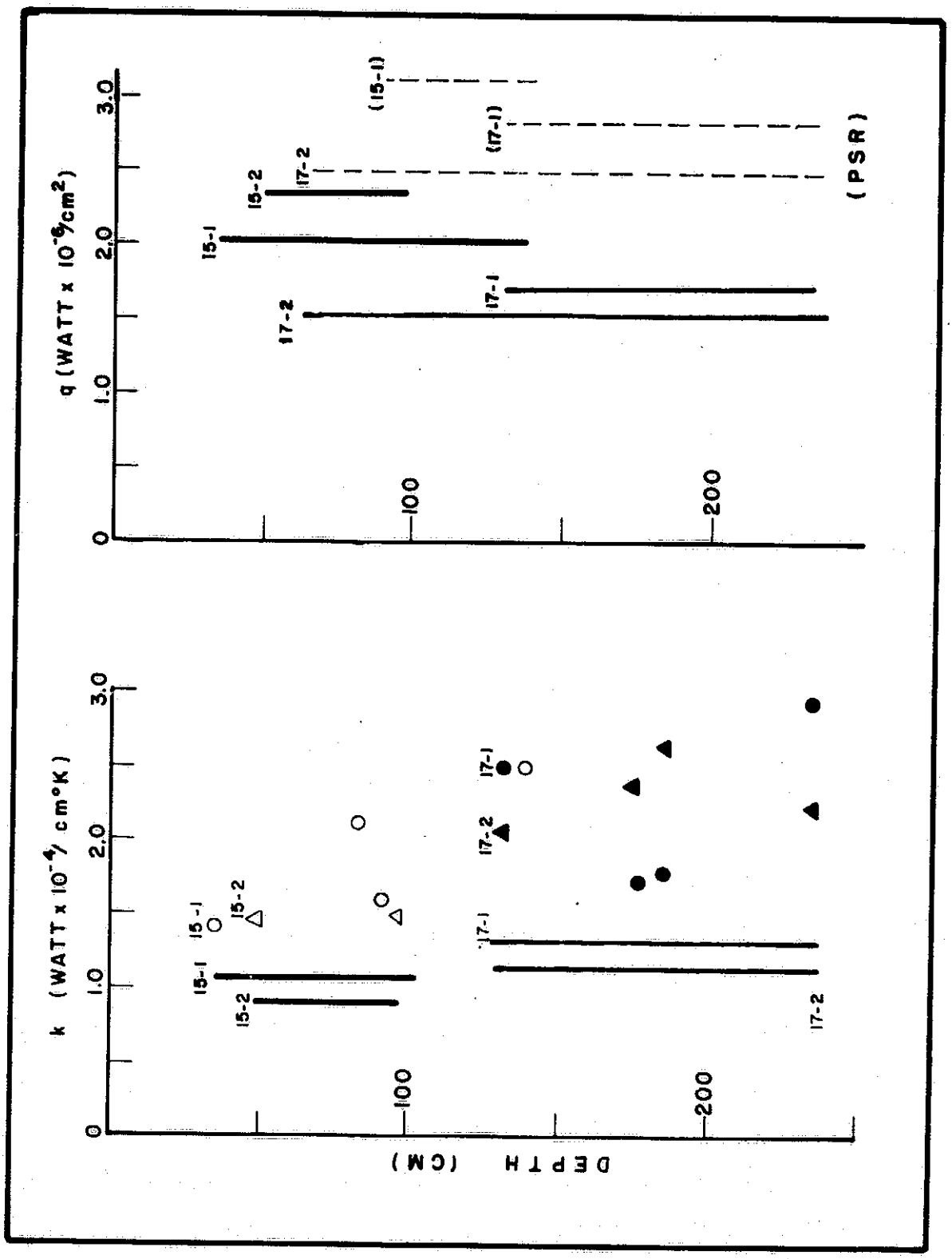

Figure 6. Preliminary (point data and dashed lines) and revised (solid lines) conductivity and heat flow deductions at Apollo 15 and 17.

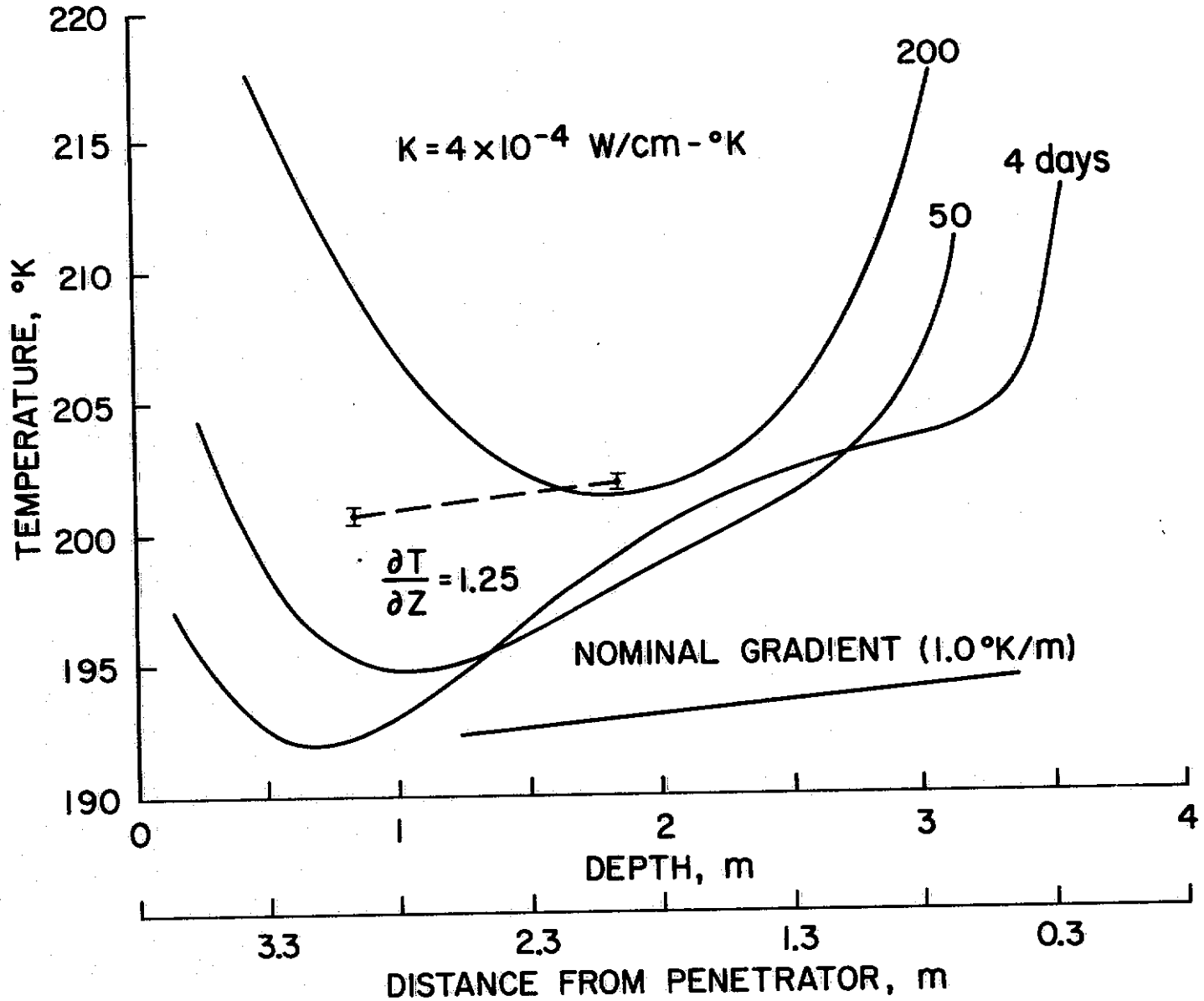

Figure 7. Hole wall temperature profiles at different times following penetration for a simulated Mars penetrator heat flow measurement. Penetration depth = 5 m. (Model M1)

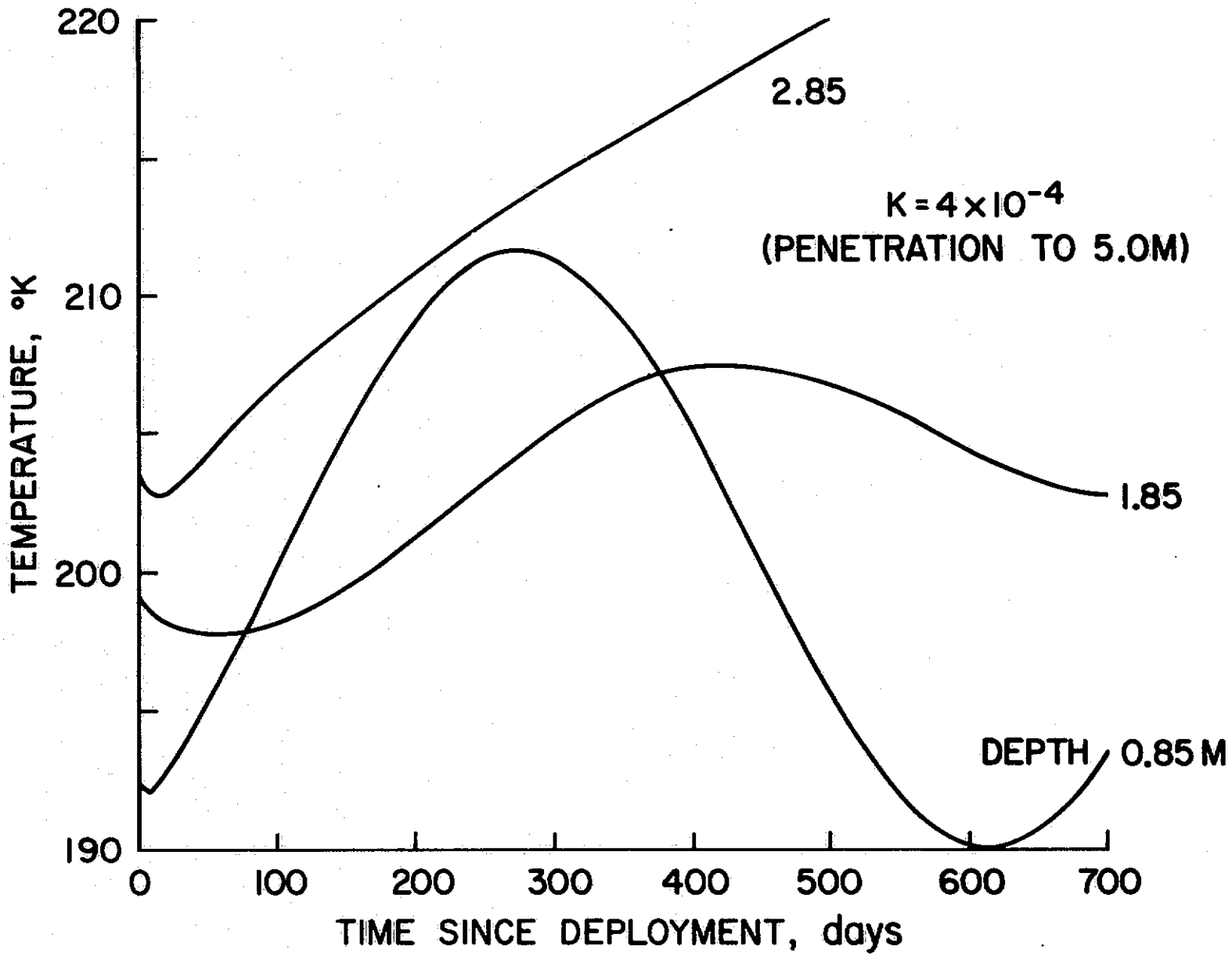

Figure 8. Subsurface temperature histories at proposed umbilicus sensor locations for Mars penetration Model M1. (See text.)

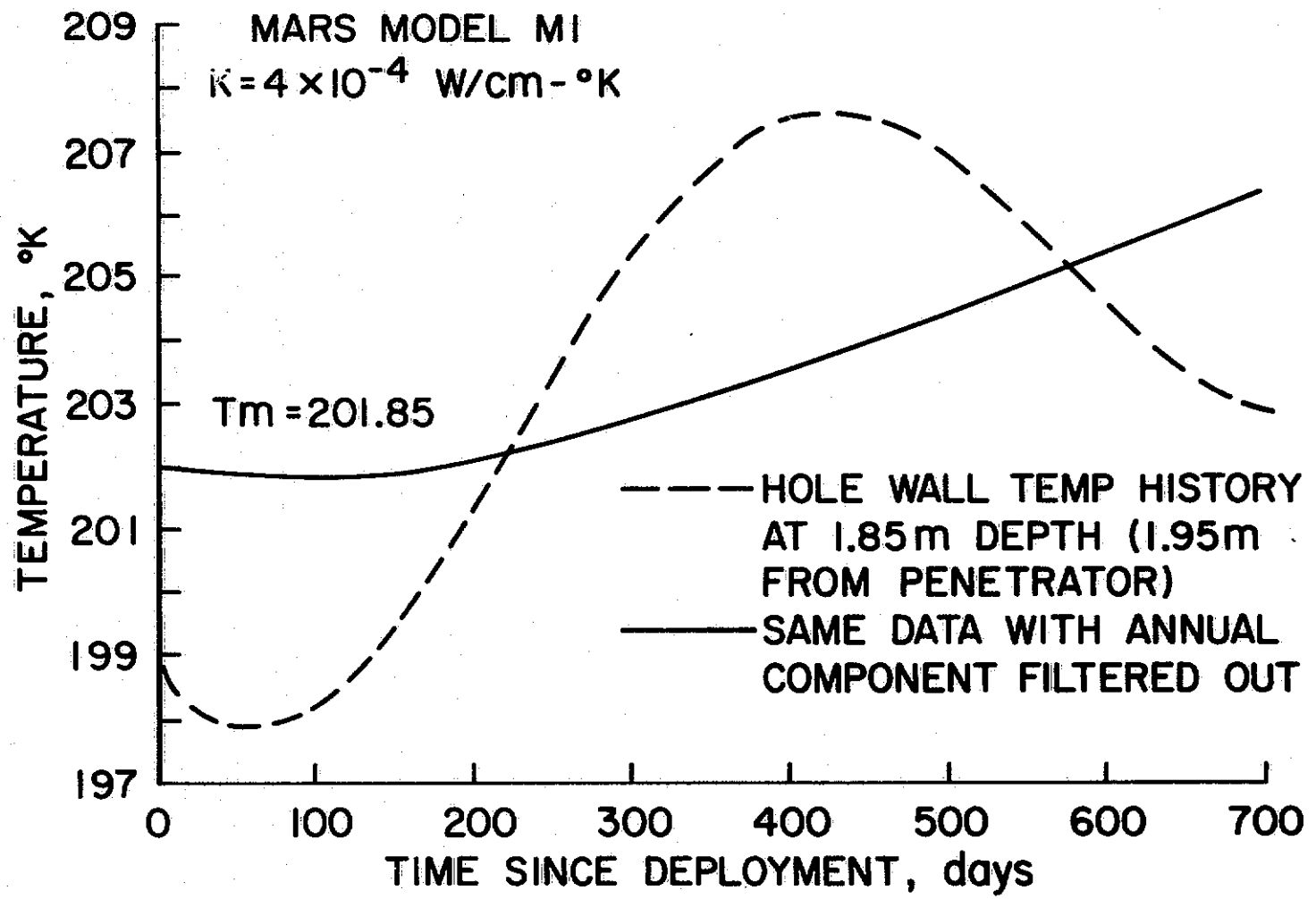

Figure 9. Raw (dashed curve) and filtered (solid curve) temperature data at the 1.85 m depth umbilicus sensor of Model M1. Removal of the large annual component allows a mean temperature to be determined prior to the onset of RTG effects.

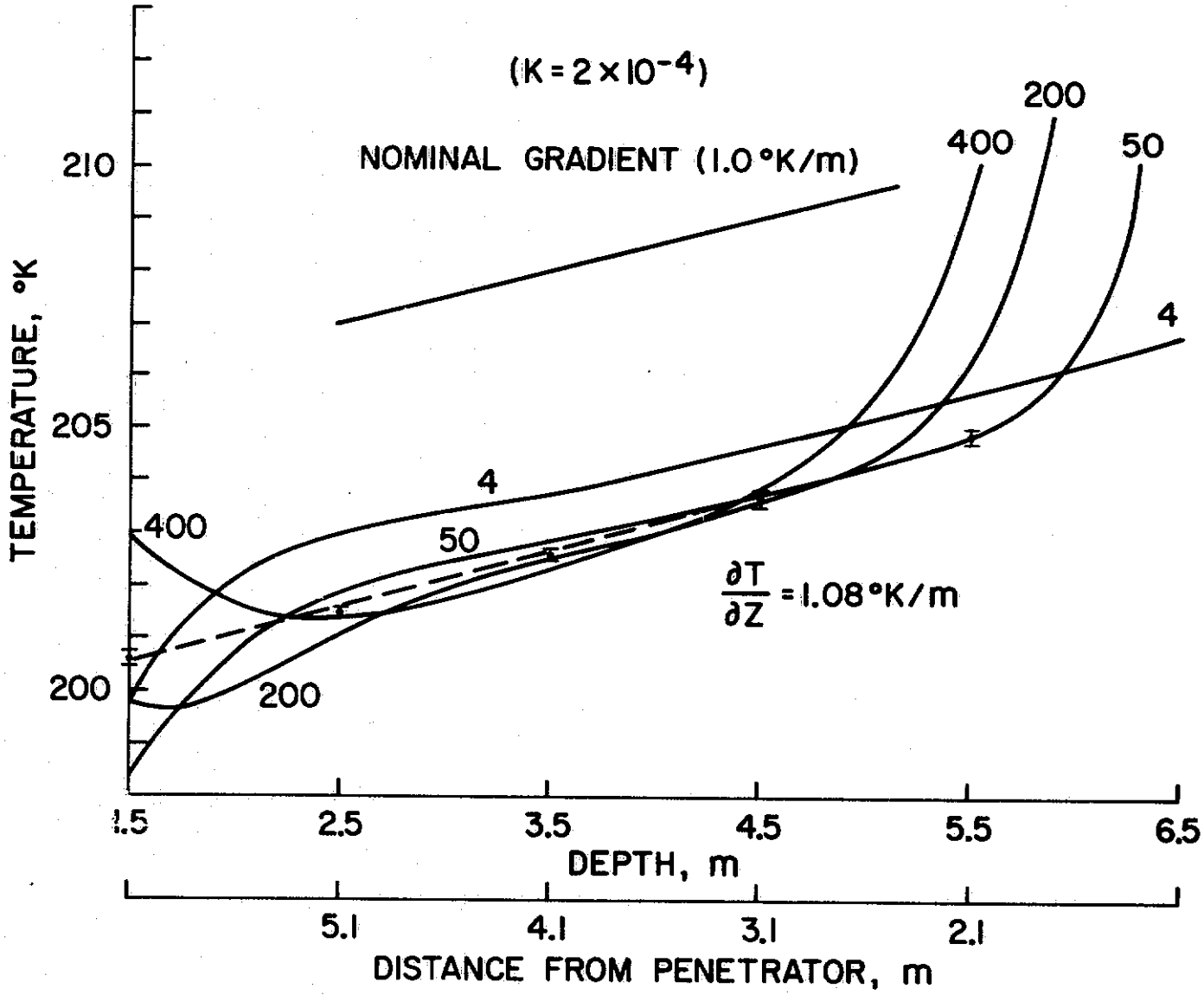

Figure 10. Hole wall temperature profiles at different times following penetration for a simulated Mars penetrator heat flow measurement. Penetration depth = 8.8 m. (Model M2)

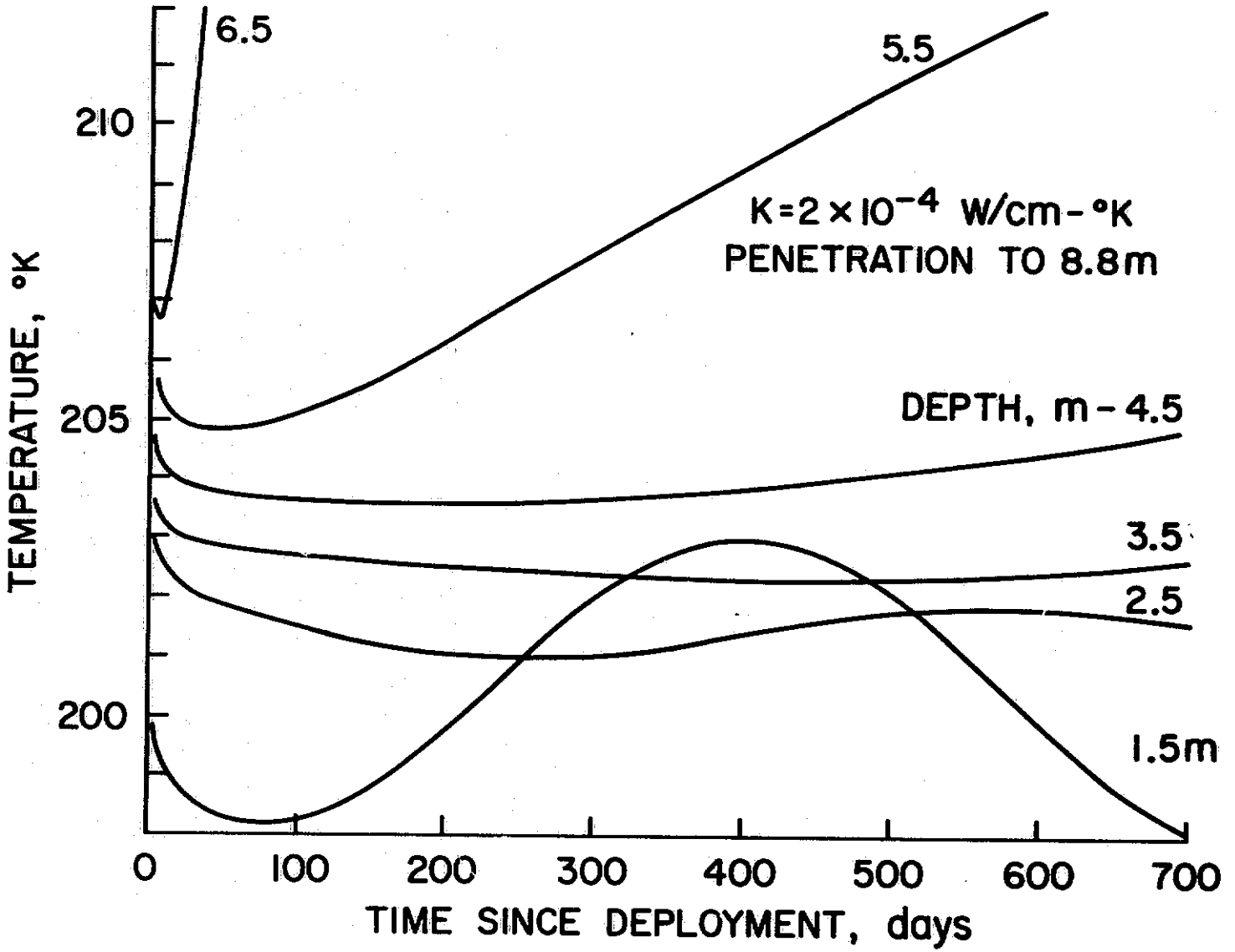

Figure 11. Subsurface temperature histories at proposed umbilicus sensor locations for Mars penetrator Model M2. (See text.)

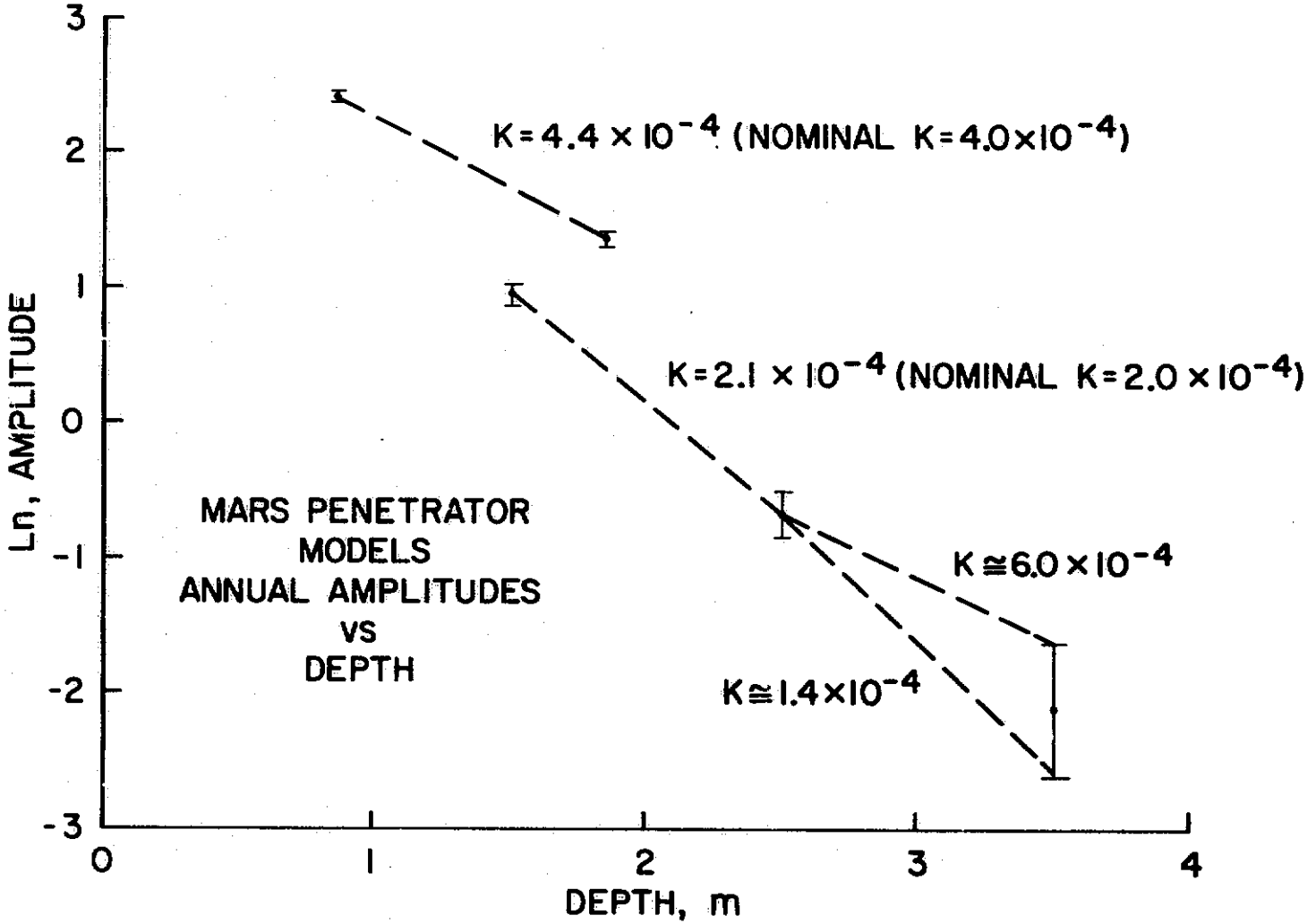

Figure 12. Diffusivity estimates based on the attenuation of annual components with depth for the 2 simulated Mars penetrator models.

APPENDIX G

MAGNETIC FIELD EXPERIMENT FOR THE MARS PENETRATOR

Palmer Dyal
Ernest Iufer
Ames Research Center

Curtis W. Parkin
University of Santa Clara

William D. Daily
Eyring Research Institute

Magnetic Field Experiment for the Mars Penetrator

I. Properties and Shock Tests of Magnetometer Sensor

A. Sensor Properties

Size	4 cm x 4 cm x 1 cm
Weight	64 grams/axis
Power	15 milliwatts/axis
Range	0 to 1000 gammas
Drive	14.5 KHz carrier
Sensitivity	66 μV/γ
Accuracy	0.2%
Core	Low-noise permalloy
Material	High-strength ceramic housing, Permalloy core Copper windings

B. Drop tests at Ames (29 March 1976)

1. Sensor mounting - Direction of shock along magnetic axis, i.e. in plane of permalloy core (structurally most vulnerable orientation).

2. Shock test and results - 2000 g's for 0.8 millisec. Properties of sensor (drive; sense winding resistances; drive voltage & current; sensitivity; etc.) unchanged by shock.

C. Air gun tests at Sandia Corp (5 April 1976)

1. Sensor mountings

a. Parallel to permalloy ring core

b. Perpendicular to permalloy ring core

2. Shock tests:

a. Parallel	b. Perpendicular
5,000 g's for 4.5 millisec	5,500 g's for 4.4 millisec
9,000 " " 3.0 "	9,500 " " 3.0 "
21,000 " " 1.1 "	21,000 " " 1.2 "

3. Results - Sensor mechanical and electrical properties unchanged by shock tests.

II. Magnetometer Properties for Mars Penetrator

Range	0 to ± 1000 gamma
Resolution	0.05 gamma
Frequency response	dc to 3 Hz
Sensor geometry	Three orthogonal flux gate sensors
Commands	5 each
Internal calibration	0, ± 25, ± 50, ± 75 percent of full scale
Power	100 mw
Weight	400 gms
Size	300 cm^3

III. Objectives and Theory of the Magnetic Field Experiment. Scientific objectives are to determine physical properties of the interior of Mars using data from a network of Mars penetrator magnetometers. The objectives are to investigate: a) internal planetary magnetic field; b) electromagnetic induction and global conductivity profile; c) crustal magnetic anomalies; and d) magnetic permeability and global iron abundance.

A. Internal Planetary Magnetic Field

(1) Known magnetic properties of Mars, from USSR Mars 3 and 5 satellite results (Dolginov et al., 1974; Gringauz et al., 1974) include the following:

a) Magnetic moment $M=2.5\times10^{22} G\cdot cm^3$, corresponding to a 64γ surface field.

b) North magnetic pole in northern hemisphere (opposite to the case of the earth).

c) Magnetic pole inclined 15 to 20° to spin axis.

d) Solar wind standoff distance approximately 1000 km altitude. (See figure 1.)

(2) Our technique utilizes the variation of the vector field confined by the solar wind to determine an accurate orientation and magnitude of the global magnetic moment. One part of this technique has been treated theoretically by Parker and by Cassen and measured by a capped-cylinder superconductor in the laboratory by the authors. The results are shown in figure 2. The ratio of the transverse component of confined field to unconfined field on the cylinder axis is

$$\left(\frac{B_c}{B_u}\right)_{trans.} = \frac{2}{R^3} \sum_{n=1}^{\infty} \frac{r^3 N_n^3 \, J_1'(0) \, f_n(r)}{(N_n^2-1) \, J_1^2(N_n)}$$

where

$$f_n(r) = \exp(-N_n|r|/R) + \exp(-N_n(r+2R)/R)$$

ϕ is the azimuthal angle measured around the cylindrical axis

r is the distance along the cylinder axis

N_n is the n-th root of $J_1'(N_n) = 0$

The ratio of the radial component of confined field to unconfined field along the cylinder axis is:

$$\left(\frac{B_c}{B_u}\right)_{axial} = \frac{1}{R^3} \sum_{n=1}^{\infty} \frac{r^3 \, K_n \, g_n(r)}{J_o^2(K_n)}$$

where

$$g_n(r) = \exp(-K_n|r|/R) - \exp(-K_n(r/R+2))$$

K_n are roots of the zero-order Bessel function

and the other quantities are shown in figure 2.

(3) This theory will be extended to the case of a magnetic dipole confined by a hemispherically capped cylinder. In order to determine the planetary moment it will also be necessary to account for contributions to the total measured surface fields from local remanent fields, ionospheric current systems, external solar wind fields, and induced Martian fields.

B. Electromagnetic Induction and Planetary Conductivity Profile

(1) Electrical conductivity analysis has been developed for a magnetometer network array for the case of a symmetric sphere in a vacuum. The analysis involves displaying magnetic data on a 20-inch IMLAC display system in a real-time interactive mode with the Ames IBM 360/67 computer.

(2) The above technique has been successfully applied to the Moon using Apollo 15 and Apollo 16 lunar surface magnetometers and the Apollo 16 subsatellite magnetometer data to infer internal lunar structure (see figures 3, 4, and 5).

(3) Depth of electromagnetic probing will be down to several hundred kilometers (for $\sigma = 10^{-2}$ mhos/m, $f = 10^{-4}$ Hz, skin depth = 500 km).

(4) Conductivity studies of Mars will likely parallel those of the geomagnetic variation method used for the earth since: (a) both planets are probably qualitatively similar in internal structure, (b) data from an array of penetrator magnetometers will be available, and (c) fluctuating ionospheric currents give rise to induced currents in the interior of both planets.

(5) The 3-magnetometer technique now used on the Moon will be generalized to use the entire array of penetrator magnetometers.

(6) The present theory for the radially symmetric case will be extended to account for the confinement of induced fields on the day side by the ionopause.

C. Surface Magnetic Anomalies

(1) Direct comparison of magnetic fields at various penetrator locations and a knowledge of the intrinsic penetrator fields will

allow determination of magnetic fields due to local sources (e.g., magnetized surface and subsurface materials). Knowledge of the magnetic properties of the penetrator housing and other on-board instruments will be obtained after the final instrument package has been developed and its field measured. The instrument fields can then be subtracted out to determine intrinsic Martian remanent fields.

(2) It will be important to compare the crustal remanent magnetization of Mars and the moon to determine if the same processes which were responsible for lunar remanent magnetism were operative during the crustal formation of Mars

D. Magnetic Permeability and Global Iron Abundance

(1) Development of techniques has begun to analyze Mars global permeability using a minimum of two magnetometer instruments: (a) one penetrator and one orbiter or (b) two (or more) penetrators.

(2) To date the technique has been developed for a symmetric case, treating the planetary body as a sphere in a vacuum. The numerical analysis technique utilizes an IMLAC television data display system, allowing rapid and accurate data selection and processing.

(3) This method has already been successfully applied to analyze magnetic permeability and iron abundance of the Moon using data in the geomagnetic tail field measured simultaneously by the Apollo 15 and 16 lunar surface magnetometers. The permeability analysis concept and theory are outlined in figures 6 and 7 .

(4) To calculate the permeability of Mars we will adapt the above analytical technique to the asymmetric confinement case (Mars global magnetization induction field confined to an asymmetric magnetosphere by the solar wind flow past the planet). The technique will be expanded to utilize three (or more) simultaneous magnetometers, using one orbiter and two (or more) penetrators.

(5) We will also generalize the analysis program to include induced global magnetization, permanent global magnetic field, and local remanent magnetization in a self-consistent analysis to demonstrate that each mode can be separated and measured. Further, we will assess effects of spurious magnetic fields produced within the penetrator and afterbody.

(6) A technique to calculate iron abundance in the Mars interior from permeability results has already been developed. The analysis requires modeling the Martian thermal profile and internal composition. Knowledge of these parameters can be gained from the Mars conductivity analysis and other experimental results.

References

(a) Dolginov, Sh.Sh., Yeroshenko, Ye.G., Zhuzgov, L.N., and Sharova, V.A., "Magnetic Field of Mars based on Data from the Mars-5 Satellite," NASA Technical Translation F-16,232, March 1975.

(b) Gringauz, K.I., Bezrukikh, V.V., Verigin, M.I., and Remizov, A.P., "Plasma in the Antisolar Region of Near-Martian Space According to the Mars-5 Satellite Measurement Results," NASA Technical Translation F-16,231, March 1975.

(c) Dyal, P., Parkin, C.W., and Daily, W.D., "Magnetism and the Interior of the Moon," Reviews of Geophysics and Space Physics, 12, 4, 1974.

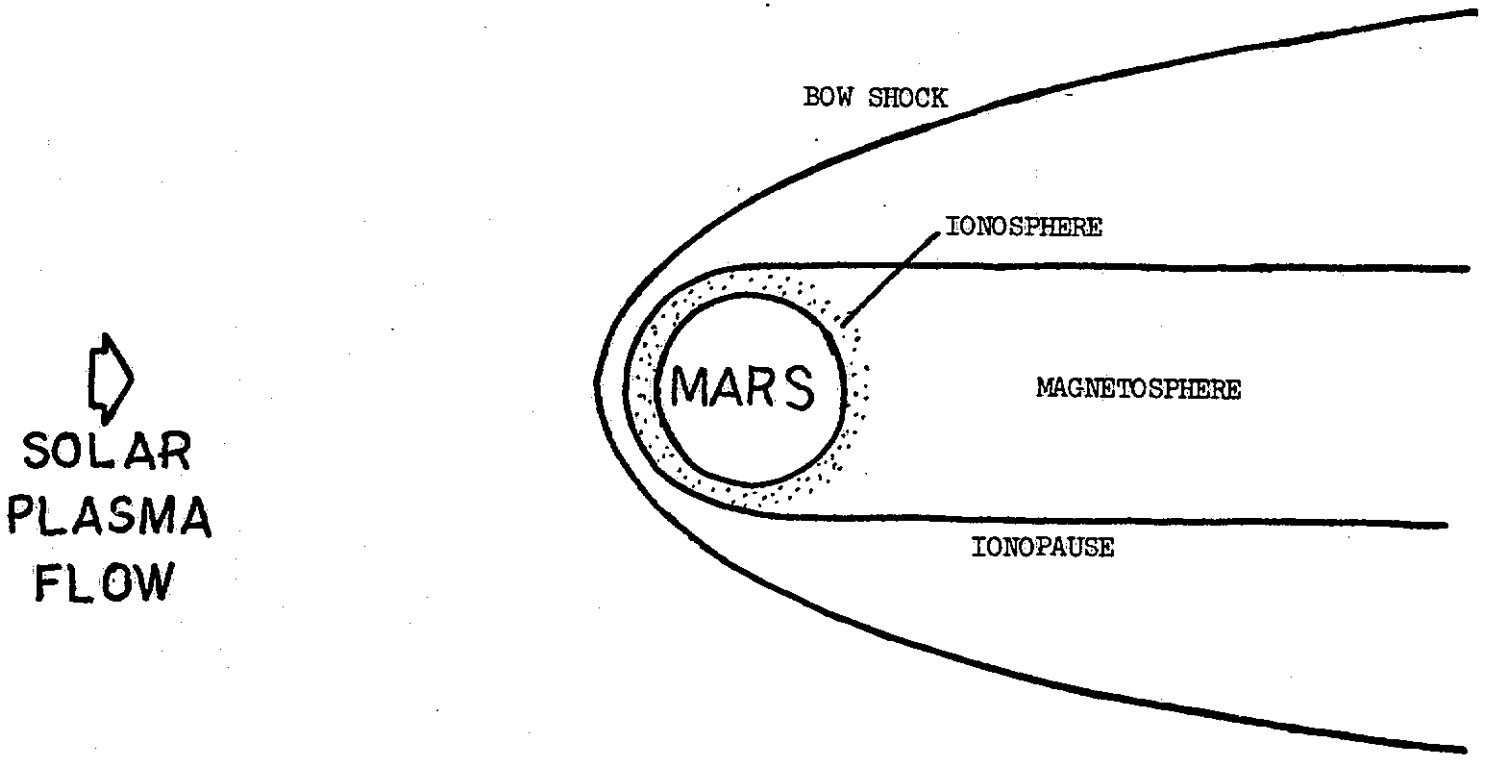

FIGURE 1 MAGNETOSPHERE OF MARS

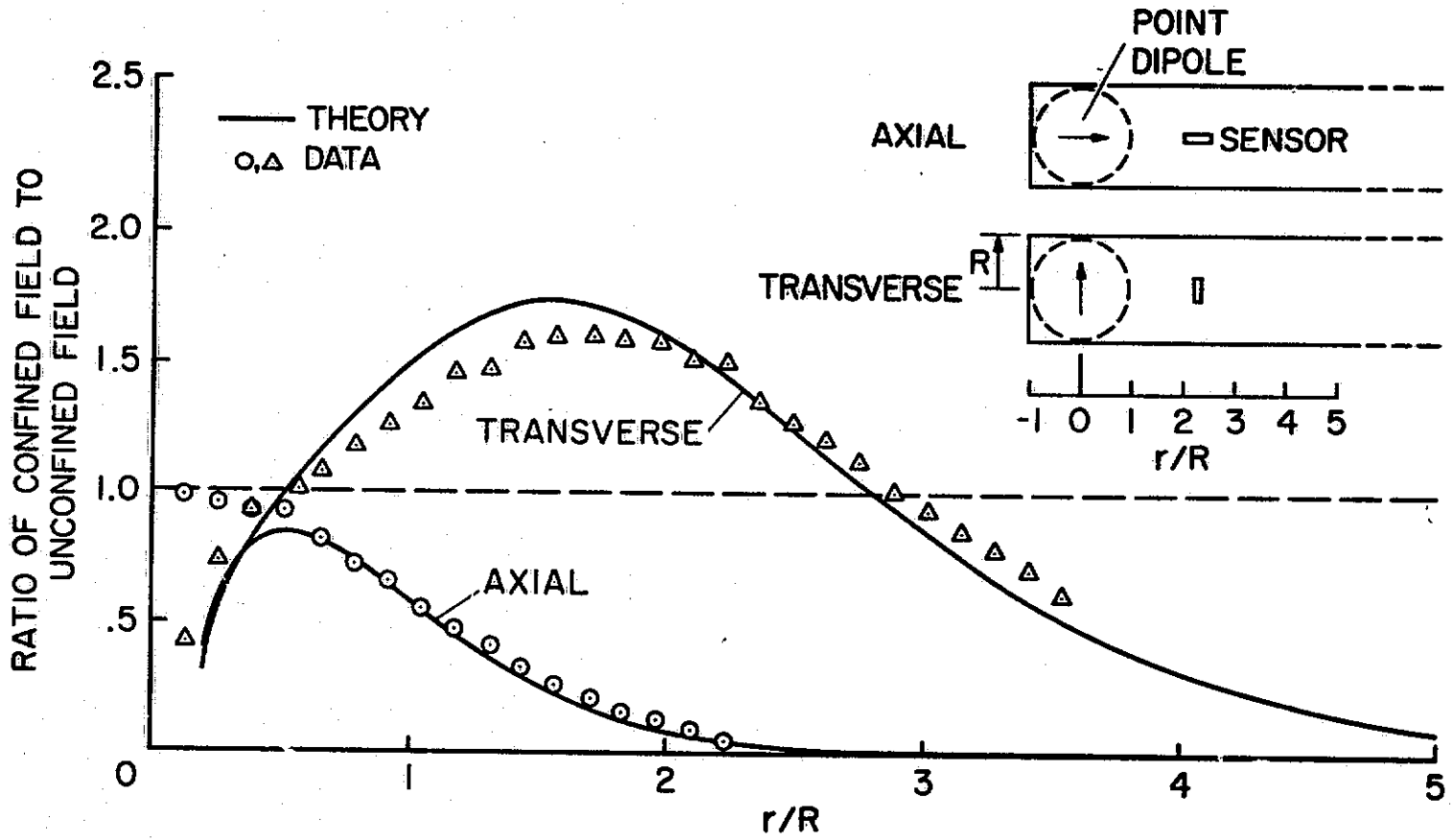

FIGURE 2 STRENGTH OF CONFINED MAGNETIC FIELD

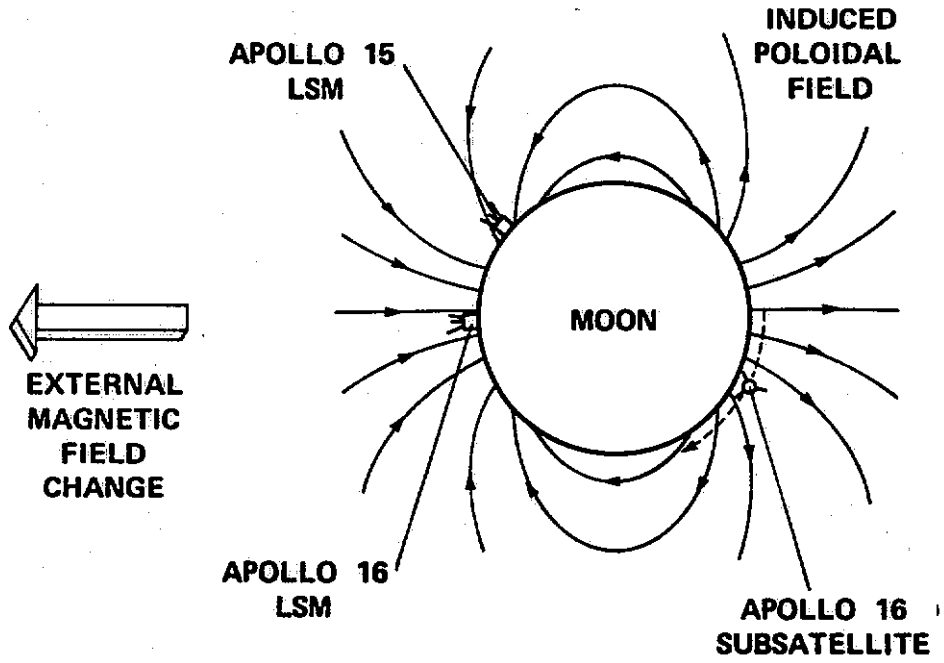

FIGURE 3 3-MAGNETOMETER CONDUCTIVITY ANALYSIS

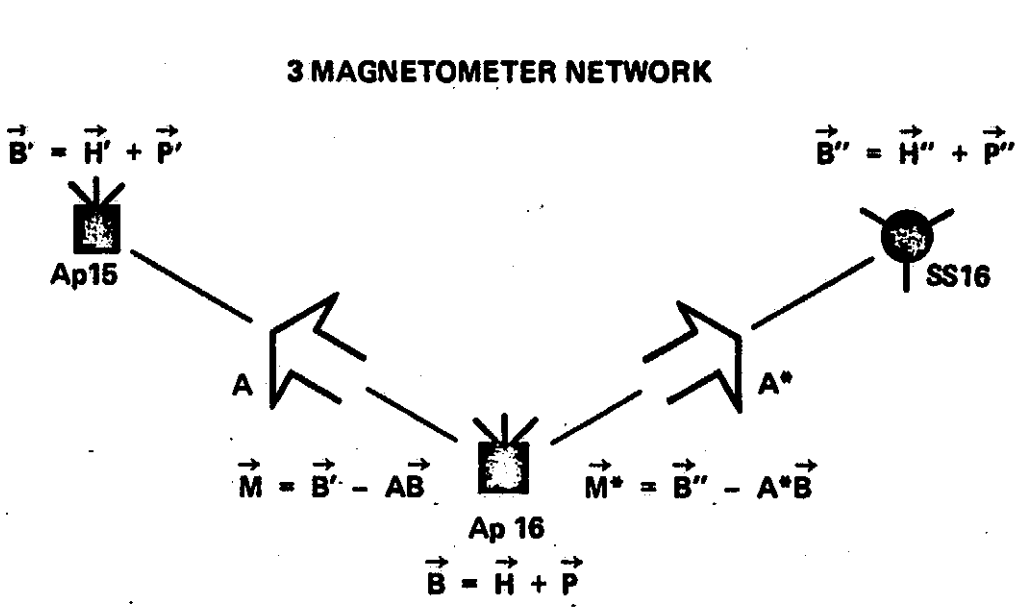

FIGURE 4 CONDUCTIVITY THEORY

3-MAGNETOMETER NETWORK

$\vec{M}(t) = D\vec{P}(t)$ $\qquad$ $\vec{M}^*(t) = D^*\vec{P}(t)$

D AND D* MATRICES DEPENDING ON GEOMETRICAL RELATION BETWEEN THE 3 MAGNETOMETERS AND THE SYMMETRY PROPERTIES OF THE INDUCED FIELD

$$P_1 = -\frac{2}{3a_{21}} M_2$$

$$P_2 = \frac{1}{3} \frac{a_{13} M^*_1 - a_{13} M_1}{a_{12} a^*_{13} - a^*_{12} a_{13}}$$

$$P_3 = -\frac{M_1}{3a_{13}} - \frac{a_{12}}{a_{13}} P_2$$

WHERE $a_{ij} = A$, $a^*_{ij} = A^*$

FIGURE 5 CONDUCTIVITY THEORY

MAGNETIZATION INDUCTION

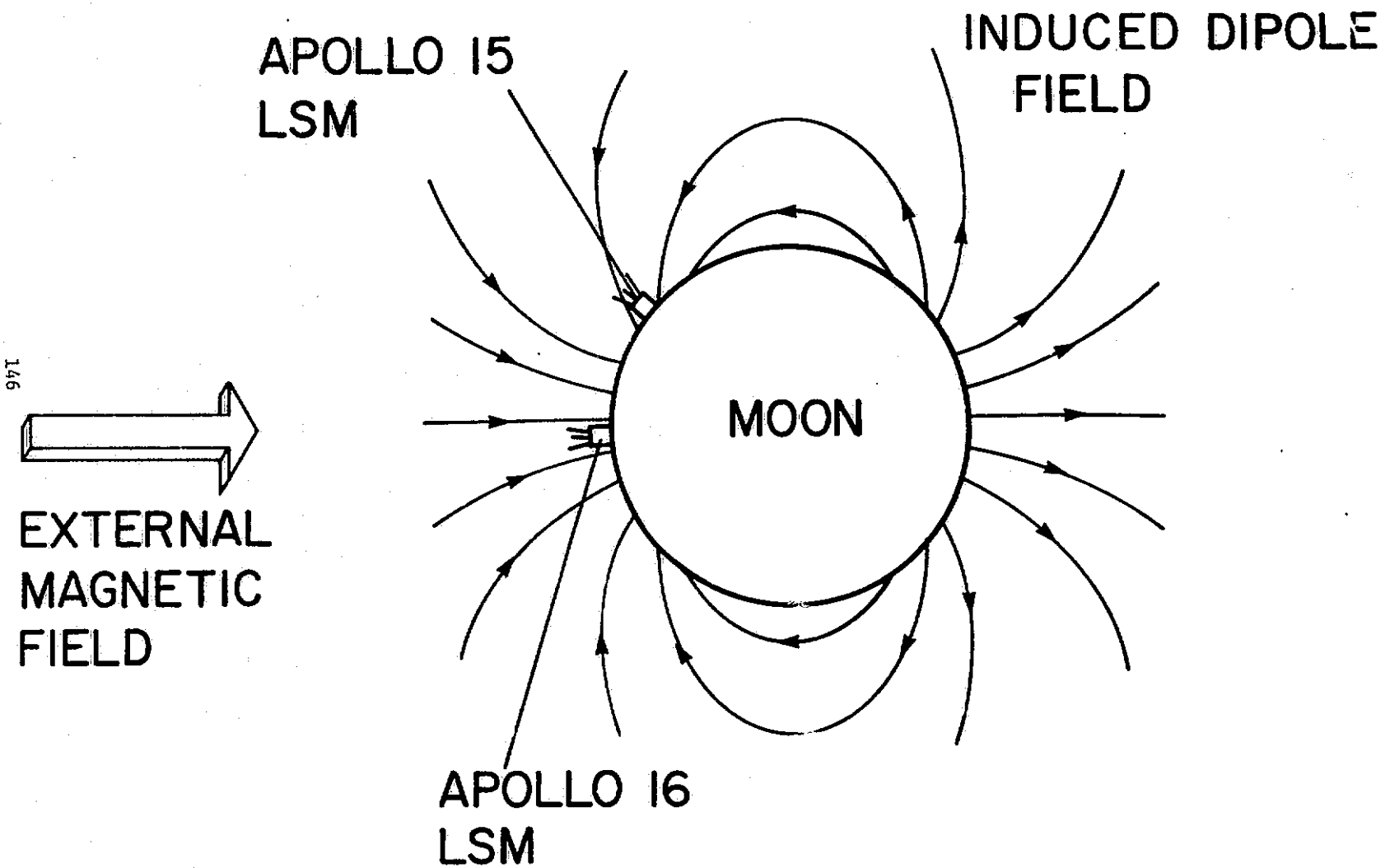

FIGURE 6 MAGNETIZATION INDUCTION

$$\vec{B} = \mu \vec{H}$$

$$\begin{cases} B_{xi}(t_j) = (1 + 2G)\, H_{xi}(t_j) \\ B_{yi}(t_j) = (1 - G)\, H_{yi}(t_j) \\ B_{zi}(t_j) = (1 - G)\, H_{zi}(t_j) \end{cases}$$

$$\left[H_2\right] = \left[a_{pq}\right]\left[H_1\right]$$

WHERE $G = (\mu - 1)/(\mu + 2)$

$i = 1$ (APOLLO 15 SITE)
$i = 2$ (APOLLO 16 SITE)

$j = m, n$

$$\mu = \Delta_1/\Delta_2$$

$$\begin{cases} \mu = \dfrac{\Delta B_{2x} - a_{11}\,\Delta B_{1x}}{a_{12}\,\Delta B_{1y} + a_{13}\,\Delta B_{1z}} \\ = \dfrac{a_{21}\,\Delta B_{1x}}{\Delta B_{2y} - a_{22}\,\Delta B_{1y} - a_{23}\,\Delta B_{1z}} \\ = \dfrac{a_{31}\,\Delta B_{1x}}{\Delta B_{2z} - a_{32}\,\Delta B_{1y} - a_{33}\,\Delta B_{1z}} \end{cases}$$

WHERE

$$\Delta B_{ik} = B_{ik}(t_m) - B_{ik}(t_n)$$

$k = x, y, z$

FIGURE 7 PERMEABILITY ANALYSIS THEORY

APPENDIX H

BIOLOGICALLY-RELEVANT EXPERIMENTS FOR A MARS PENETRATOR MISSION

Donald L. DeVincenzi

Ames Research Center

BIOLOGICALLY-RELEVANT EXPERIMENTS FOR A MARS PENETRATOR MISSION

Donald L. DeVincenzi
NASA-Ames Research Center

INTRODUCTION

A group of scientists in the Planetary Biology Division at NASA-Ames (D. L. DeVincenzi, M. R. Heinrich, V. I. Oyama, G. E. Pollock and M. P. Silverman) have been devising concepts for biologically-relevant experiments which could be performed on a Mars penetrator mission. Attention has been concentrated on experiments which can utilize the sub-surface, multi-site and long-life characteristics of the probes.

In addition to providing information relative to the goals of planetary biology (the origin, evolution and distribution of life and life-related compounds), these concepts can yield data pertinent to the geosciences also. As with other experiments proposed for a penetrator mission, these ideas may change dramatically once data is returned from Viking. However, some of the experiments actually complement the Viking science.

The concepts for the experiments described in this report were developed about a year ago. Two of them have been undergoing verification at a modest level in the laboratory. Some are outgrowths of experiments proposed by other scientists, or are based on advanced instrumentation which has recently been developed. All, however, are of significance to the continued exploration of Mars.

It has been only recently (during the past month) that these concepts have been evaluated, from an engineering point of view, for their suitability for a penetrator mission. The time for evaluation was short and judgements were based upon knowledge of state-of-the-art technology and consultation with experts where possible. The search for information was not exhaustive and recent or future developments may change the feasibility assessments. However, this study has provided extremely useful comments regarding the procedures, identification of key elements, constraints, feasibility, etc.

This report summarizes the biologically-relevant experiments, with emphasis on science rationale and objectives, experimental approach and engineering evaluation.

ORGANIC CARBON

I. Scientific Rationale and Objectives

Several classes of organic compounds which are found in soil and living things will fluoresce when irradiated with ultraviolet light. These and other organic carbon compounds, when heated to temperatures of 250°C or above for some time (several seconds at 800°C to a few minutes at 250-450°C), will produce polyaromatic compounds which fluoresce when irradiated with ultraviolet light. Inorganic carbon in the form of carbonates does not interfere since it is not measured. This experiment was proposed several years ago (Report by Dr. Joon Rho, J.P.L., 1967) and much ground work on the sensitivity and design of an instrument measuring fluorescence after ultraviolet activation was done. Sensitivity of the experiment will depend on the experimental design and the nature of the compounds encountered. In a pyrolytic mode, very small samples of 0.025g to 0.1g could be used to detect organic carbon in amounts which would be in the range of several nanograms of organic carbon, 3ng to 3μg depending on the organic carbon composition and whether optimum pyrolytic conditions were used.

Carbon found in organic matter is a prerequisite for life. Finding very little or no organic carbon would indicate little or no probability of life while large amounts of organic carbon would give reason for hope. This particular measurement has been worked on, and it is known that the instrumentation can be relatively simple and requires only a small sample (e.g., 0.1g or less). Further, this analysis would lend itself to a penetrator mission because one could obtain the organic carbon values at various depths and at various sites, thus increasing the ability to choose sites objectively for more sophisticated later missions and giving more information on the possible organic history of the planet (e.g., if large deposits of organic carbon are found at some depths beneath the surface this could indicate sedimentary deposits which could be interesting from the point of view of life detection as well as for a history of water).

II. Experimental Approach

This experiment involves acquisition of a small soil sample (e.g., 0.1g to 0.025g) followed by pyrolysis of the sample at around 450°C for a few minutes in a sealed chamber. The pyrolysate is condensed on a cooled surface, the condensate irradiated with an ultraviolet source between 300-400nm, and the fluorescence emitted from the pyrolysate measured

with a photodetector at the fluorescence maximum (~450nm). This method of operation is capable of detecting a few micrograms to a few nanograms of organic carbon present in any sample. The temperature of pyrolysis could be varied in such a way that pyrolysis started at 250°C might be increased stepwise to higher values if studies indicated that such a step program led to enhanced diagnostic capability, i.e., some ability to relate fluorescence to pyrolysate composition to the original organic compound class. Such ability might exist if variable UV wavelengths could be used for activation as well as detection of the wavelength maximum of the fluorescence. The temperature of the cold spot should be as cold as possible for maximum sensitivity, 0°C or lower if pressure is 4-5mm Hg. It should be pointed out that the pyrolysate fluorescence could be measured in the gas phase in some limited volume. This latter approach would sacrifice some sensitivity of the method, but might be more easily implementable.

III. Engineering Evaluation

Key elements associated with the experiment include sample collector, sample dump while maintaining seal, heating sample, cold collector surface, UV source, and photo-detector.

Of the key elements, only the problems associated with the sample collection and dumping appear to be difficult. One idea is an explosively driven core sampler which is driven into the soil and then retracted and the sample is dumped into the pyrolysis chamber. The pyrolysis chamber must be sealed to allow maximum pressure differential between the volatiles driven off and the cooled collector surface, but this should present no great difficulty. Maintaining the cooled collector surface at 0°C could be a problem and this should be investigated during the penetrator thermal studies. The acceleration survivability of the UV light source and the detectors could be assessed easily.

The experiment to estimate organic carbon appears quite feasible for a penetrator mission if a reliable sample collection technique can be devised. A program to develop a sample collector should start as soon as possible and available UV sources and photo-detectors should be shock tested.

WATER AND ELEMENTAL ANALYSIS

I. Scientific Rationale and Objectives

Water is essential for life as we know it. The relative abundance and location of water on Mars may be crucial to the selection of landing sites on the planet for future life detection missions, Mars sample return missions, and for a proper assessment of planetary quarantine requirements. Measurements of water are needed to determine the composition of the polar ice caps, to discover whether a permafrost or sub-surface water is present, and to delineate its areal location and extent. Knowledge of the total water content of Mars is needed for an understanding of the planet's geochemical, biological, atmospheric, and climatological history and evolution.

The principal attribute of the combined pulse neutron experiment (CPNE) is its ability to measure water without the necessity for external sample acquisition. Although the (CPNE) does not measure water directly, it measures the hydrogen atom content of the target material making the assumption that all the hydrogen is present as water. As little as 0.92% water in basalt, granite, and dunite can be detected (Caldwell, R.L., et. al., Science 152, 457-465, 1966; Mills, Jr., W.R., et. al., Mobile Research and Development Corporation, Dallas, TX, 1969).

The CPNE instrumentation can also detect gamma ray emissions from the natural radioactive elements K, Th, and U. Knowledge of the abundance of these elements will allow inferences to be drawn concerning the internal heating of the planet, its age, and the Ar content of the atmosphere. These are important to an understanding of the geophysical and geochemical history and evolution of Mars and its atmosphere, and to comparative planetology.

A third feature of the CPNE is that it can measure the elemental ratios of C, O, Si, Al, Mg, Fe, Na, Ca, and Ti in the Martian regolith. The importance of determining regolith composition is obvious and need not be expanded upon. An important capability of the CPNE is the fact that analyses will be made over distances of several tens of centimeters beyond the probe. Its importance can be recognized readily when the events accompanying penetrator entrance are considered. First, frictional heating alters the surface of the entrance hole immediately adjacent to the penetrator, forming silicate glass and volatilizing certain elements and water. Second, penetrator body surface material is abraded and mixed with bore hole surface material. Thus, analyses of only the first few millimeters of the bore hole adjacent to the penetrator may be in error regarding the true composition of the Martian subsurface regolith. The greater depth of penetration of the neutrons from the CPNE (several tens of centimeters) would minimize such errors and give a better assessment of the overall composition of the target material.

II. Experimental Approach

The CPNE instrumentation consists of a 14-Mev pulsed neutron source emitting $\sim 2 \times 10^5$ neutrons/sec, a gamma ray detector, and a neutron detector. An attenuator is positioned between the neutron source and gamma ray detector. The use of a pulsed source of neutrons and time-gated spectral measurements provide a convenient means of separating gamma rays produced in the processes of inelastic neutron scattering, neutron capture, and neutron activation. This is feasible because the resultant gamma rays are emitted in different time domains relative to the time at which a fast neutron is produced by a source. Also required are provisions for (a) controlling the frequency and duration of neutron pulses from the neutron source, (b) precise time discrimination for controlling the time at which gamma rays and neutrons are measured, (c) data acquisition, storage, and transmission, and appropriate sheilding between the RTG's and the detectors.

Radioactive elements are determined in a quiescent mode. After landing, and before the neutron source is turned on, the gamma ray detector is operated for suitable time periods to measure the gamma rays emitted by the natural radioactive elements K, Th, U.

Elemental analyses are made in high repetition rate operation. The neutron source emits ~5000 pulses/sec of 14-Mev neutrons. Each pulse is of 5 μsec duration and is followed by ~200 μsec of no emissions. The resulting gamma ray production from inelastic scattering begins and ends sharply within the same time frame as the 5 μsec neutron burst and yields information on the elemental ratios of C, O, Mg, Al, Si, Fe. The neutron detector measures the epithermal neutron intensity which builds up and then dies away during the 200 μsec following each neutron pulse from the source. The rate of this "epithermal die-away" is primarily dependent on hydrogen content and is a measure of the hydrogen (= water) density in gm/cc.

In another mode (low repetition) the fast neutron pulses are still 5 μsec in duration, but are separated by 2000 μsec of zero neutron emission. For about 50 μsec after the 5 μsec neutron burst the gamma ray detector measures the gamma rays emitted during the process of thermal neutron capture and yields elemental ratios of H, Na, Si, Ca, Ti, and Fe. After ~1200 μsec the gamma ray emissions will have decayed to a constant rate. This rate is primarily from isotopes with half-lives greater than several hundred μsec which were formed by the process of fast neutron activation. Thus, measurement of fast activation gamma rays in the time period after 1200 μsec but before the next burst yields very accurate O/Si ratios.

III. Engineering Evaluation

The CPNE requires a thin window or opening to the outside of the penetrator. Water presence is inferred by presence of hydrogen but not directly measured.

This experiment seems to offer a high probability of success. Sensitivities of absolute water content of less than 1 percent seem feasible. This experiment does not require modifications that appear to reduce the structural strength of the penetrator. The additional information gained on elemental abundance appears to be an advantage. Sandia is evaluating pulsed neutron sources for similar subsurface measurements. Further development should be pursued.

INORGANIC IONS, WATER HISTORY, LIFE DETECTION

I. Scientific Rationale and Objectives

The proposed experiment measures the concentration of water-soluble inorganic ions in the Martian soil by means of several ion-specific electrodes and electrical conductivity electrodes. A number of inorganic ions are important to living organisms, in addition to being indicators of the presence and state of oxidation of some of the elements of the atmosphere and soil. Ions like nitrate, ammonium, sulfate, and sulfide are utilized as sources of energy by some bacteria, while other bacteria produce them as metabolic end-products. Sodium, potassium, and chloride are important in maintaining functioning cell structures. One of the major unknowns in searching for life on Mars is the total lack of knowledge of the nutritional requirements of putative Martian organisms. A detailed analysis of the organic compounds in Martian soil would provide invaluable suggestions about organic nutrients, but this is very difficult. An inorganic analysis appears to be attainable, and would also be very valuable.

Knowledge about the inorganic ions in Martian soil would impact future missions to that planet. Any future life detection experiments would be greatly improved by use of that information in formulating growth media. The same conclusion applies to the search for living organisms in any Martian soil samples which are returned to Earth. In addition, the planetary quarantine estimates of the probability of terrestrial bacteria surviving on Mars would be much more accurate with any information about soil composition.

There is an obvious relationship between the composition of the atmosphere and the soil. The amount of nitrogen on Mars is unknown, but its presence is essential for the evolution of life as we know it, or for the survival of terrestrial life on that planet. The two most important ionic forms of nitrogen are nitrate and ammonia. The nitrate ion which is common in earth soil is principally the product of oxidation of ammonia by bacteria. The ammonia, in turn, could have biological origins from the fixation of atmospheric nitrogen or from the decomposition of nitrogen-containing constituents

of organisms; it could also occur in the atmosphere, or be formed chemically from atmospheric nitrogen. The presence of nitrate on Mars would suggest the presence of life, or some other process for oxidation of nitrogen.

Anomalous inorganic ion accumulations on Mars can also be indicative of the history of water on the planet. Running surface water on Earth dissolves certain components of rocks and minerals more rapidly than others. The more soluble cations and anions are transported downstream to basins where they accumulate. Subsequent evaporation of the water yields terrestrial sediments enriched in salts. If similar processes occurred on Mars, it is reasonable to expect the dry basins at the terminus of river-like channels to be more enriched in water-soluble salts than highland rocks and minerals at the source of the channels. Experiments have been performed to test this hypothesis (Silverman, M.P., and E.F. Munoz, Icarus 24, 383-387, 1975). They showed that aqueous solutions of soils from dry terrestrial basins with a history of water accumulation, as well as solutions of soils from the topographic lows of valleys, had a significantly greater ($P<.01$) mean electrical conductivity (2133 ± 718 μmhos/cm) and water soluble Na and Ca content (15.86 ± 5.29 μmoles/ml) than did solutions from highland soils (165 ± 48 μmhos/cm ; 0.67 ± 0.18 μmoles/ml) or finely divided igneous and metamorphic rocks (174 ± 15 μmhos/cm ; 0.99 ± 0.13 μmoles/ml).

The penetrator mission concept, employing multiple probes deployed along appropriate highland to basin transects, seems ideally suited to an investigation of Mars to answer the question--are those sinuous channels really dry river beds?

If Mars had surface water at one time, then the question of where did the water go is of great interest to space scientists. It may be in the polar caps or it may be present as a permafrost. The latter could react with rocks and minerals and accumulate inorganic ions at the mineral-ice interface. Seasonal sublimation of some of the permafrost would leave behind a subsurface residue of water-soluble inorganic ions. Thus, subsurface multiple site analyses may reveal anomalous concentrations of water-soluble ions which could be presumptive evidence for a permafrost. In any case, the information obtained would add a valuable dimension to the results of elemental analyses.

The environmental conditions below the surface of Mars are not incompatible with life as we know it. Indeed, viable microorganisms have been recovered from 60 foot depths in Arctic permafrost. Measurements of water-soluble inorganic ions, electrical conductivity, and pH can be used to indicate the presence of life. The indigenous microorganisms in terrestrial soils containing as little as 10^4 microorganisms/gram of soil caused dynamic changes in the electrical conductivity, pH, and water-soluble Ca and Mg of soil

solutions during glucose metabolism (Silverman, M.P., and E.F. Munoz, Applied Microbiology 28, 960-967, 1974). Sterile soils did not show these effects. The kinetics of these processes can be measured either continuously or at selected time intervals without removing samples. Other advantages are (a) the measurements are non-destructive and allow other experiments to be performed on the same soil sample, (b) the measurement of multiple parameters, i.e., electrical conductivity, pH, Ca, Mg that display parallel kinetics increases confidence in the conclusion that life has been detected.

II. Experimental Approach

The proposed experiment would measure the concentration of nitrate, chloride, sodium, potassium, and calcium ions by electrodes specific for these ions. Also required are reference electrodes for the above, a pH electrode and reference, a pair of platinum black electrical conductivity electrodes, and a temperature probe. The ion-specific electrodes were chosen because they serve the objectives of the experiment and are compatible with one another with respect to tolerable pH ranges and other interferences. The pH electrode serves experimental objectives and allows corrections to be made for pH effects on ion-specific electrode measurements. A temperature probe is required because temperature will affect ion-specific electrode and electrical conductivity measurements and must be known to make appropriate allowances. The electrical conductivity electrodes serve experimental objectives and also furnish a measure of the total ionic strength of solutions.

At launch, the measuring vessel with its component electrodes and temperature probe contains a calibrating solution of known pH with low levels of each of the ions to be determined. After landing on Mars, the pH and ion-specific electrodes are calibrated, and electrical conductivity is determined. A soil sample, after acquisition, is then added to the measuring vessel containing the calibration solution. Readings at intervals will then show increases in those ions which are being dissolved from Martian soil. When all parameters being measured reach equilibrium a dry, non-ionic nutrient such as glucose is added to the measuring vessel. All parameters are then read at intervals for evidence of metabolism and life.

III. Engineering Evaluation

Key elements associated with the experiment include miniaturized ion specific electrodes, liquid water, sampling system, sealing and pressurizing system.

Conversations with knowledgeable individuals at Sandia and Orion Research Inc., indicate that several probes in a common solution may interfere with one another. In addition, pH must be monitored and controlled to make accurate measurements. Any leak of water could create a false reading on one of the soil water measurements proposed for the penetrators, and considerable effort would have to be made to insure a low probability of leaks.

However, a start could be made on testing a system with the electrodes specified above to determine the magnitude of electrode interference, pH effects, and effect, if any, of interfering ions.

SUBSURFACE GAS COMPOSITION

I. Scientific Rationale and Objectives

Life on the Earth is sustained in the waters and in or on the land. Without deposits of liquid water, life on Mars can only be sustained on the surface and in the regolith (soil). The steady state of high oxygen and low carbon dioxide in the Earth's atmosphere reflects the activity of surficial and light reactive organisms. Mixed with the surface populations and in the soil matrix a significant biological activity exists which accounts for traces of gases in the atmosphere such as H_2S, CH_4, N_2O and CO; but more significantly the subsurface biology is sufficiently active to cause variations in the composition of the subsurface atmosphere that is significantly different from the surface atmosphere. These activities have been reported to produce subsurface carbon dioxide levels sufficient to provide steady states approaching five hundred times that of the surface atmosphere and ten times less molecular oxygen.

The objective of this experiment is to infer biological activity by comparing the subsurface gas composition to the surface gas composition. On Earth there is a reduction of oxygen and an increase in carbon dioxide. On Mars carbon monoxide, hydrogen sulfide, or nitrogen may be the differentiating phenomenon.

II. Experimental Approach

A miniature gas chromatograph in the probe forebody is used to analyze the subsurface gases. A port to the outside is required to allow the gas to enter the system. A carrier gas, such as helium, would be used to drive the sample gas through the GC. A vacuum tank would be required to pull the sample through the GC. This experiment would reply on the Viking surface gas analysis results to compare with the subsurface measurements.

III. Engineering Evaluation

Key elements of this experiment are the GC, port to the outside, pressurized carrier gas and vacuum pump. Because of diffusion problems, the measurement requires that the hole caused by the penetrator be filled. Other constraints include performing the experiment under a permafrost layer and the porosity of the soil material as it affects diffusion of gases.

Artificial sealing of the penetrator borehole is out of the question. There is no guarantee that it would fill naturally, and more importantly it would be impossible to tell whether it has filled or not. This experiment also requires that the penetrator come to rest under a very low porosity layer, such as permafrost. This seems to be an unrealistic targeting constraint. The experiment itself requires at least four valves to control the flows of gas through the GC.

More studies are needed to better understand how the bore-hole filling problem and the diffusion problem may be affected by soil temperature, water content, cohesiveness, texture, etc., using presumed Martian conditions and soil models.

OTHER METHODS FOR WATER ANALYSIS

I. Nuclear Magnetic Resonance (NMR)

This technique excites a soil sample placed in a strong magnetic field with a radio frequency signal. Changes in the resonant response of the system indicate the presence of hydrogen. Distinctive signals are given from water and from ice. Several techniques are available for excitation and detection, of which the spin-echo method appears to have advantages. A prototype system designed to monitor soil moisture under highways has been developed (Matzkanin and Gardner, Transportation Research Record, No. 532, pp. 77-87, 1975). The detector unit which holds the soil sample has been reduced to approximately 12 cu. in., including the permanent magnet, and weighs 3 1/4 lbs. The prototype instrument has been tested with bentonite, silica, and topsoil. It determines soil moisture from 0 to 200 percent with an accuracy of 1 percent up to the 25 percent moisture level, and approximately 2 percent accuracy in the 25 to 100 percent moisture region. There is some difference in response between different soil types; addition of organic matter had little effect on the response from bentonite, but a significant effect on the results with silica flour. Structured water (adsorbed, or as ice) gave a different signal than that for liquid water. It is therefore probable that ice and liquid water could be distinguished on Mars. At this stage it appears that a soil sample would have to be brought inside the penetrator and weighed in order to obtain an accurate moisture determination.

The NMR experiment appears to have some merit but requires a soil sample of known mass to make an accurate water content determination. Mass measuring techniques have not been evaluated but appear to be difficult. The sensitivity of the NMR appears to be about 2 percent by weight of water by inference from hydrogen. This experiment appears to be feasible. Considerable development would be required to produce a flight hardened unit and an adequate soil sampling system.

II. Capacitance

A pair of electrodes separated by an insulating section form a capacitor. The capacitance value is partially determined by the dielectric constant of the surrounding soil. The capacitor formed is incorporated as part of the tank circuit of an oscillator and changes in dielectric constant, and hence moisture, change the frequency of the oscillator.

The effects of a variety of parameters have been studied (Selig and Mansukhani, J. Geotechnical Engineering Div., ASCE, GT8, pp. 755-770, 1975), including soil type, salt content, temperature, adsorbed water, and oscillator frequency. Preliminary data are available on several varieties of probes which appear to be feasible for driving into the soil through an opening in a penetrator. The probes may be solid, except for a small channel for wires; a steel point can form one electrode of the capacitor, and the other electrode may be a steel band separated from the point by an insulating band. With such a probe, the calibration with respect to moisture did not vary significantly with soil type. The standard deviation in moisture determinations in the range of zero to 0.1g water/cc soil is about 7%; in the range of 0.05g to 0.5g water/cc soil, the standard deviation is less than 1%.

The capacitive probe does not offer absolute calibration of water content for varying soil conditions, although it has a high sensitivity for changes in water content.

This technique also seems feasible with some engineering development effort to either provide an insulated penetrator section (without weakening the structure) or deployable probes.

III. Microwave

The dipolar relaxation of water molecules results in an absorption of microwave energy which has been used in a variety of industrial moisture sensors. The procedure has been studied for use as an implantable soil moisture sensor under highways (Birchak, et. al., Proc. IEEE, 62, pp. 93-98, 1974).

The equipment is designed to operate for extended periods without attention. There are no moving parts in the detector, which appears to be adaptable to mounting directly in the wall of the penetrator. Although the method is attractive, it is temperature-sensitive, and has very low response to ice (an important consideration on Mars).

SPECTROPHOTOMETRY

An instrument under development which should be kept in mind for penetrator and other missions is a spectrophotometer in a total volume of about 3 cubic centimeters (D.J. Fisher, et. al., Research and Development, pp. 32-36, Jan. 1975).

In the miniaturized instrument, the light source is a light-emitting diode (LED) which is now available to provide a series of wavelengths between 500 and 900 nm. An LED is used for each wavelength to be measured. Diodes for other wavelengths are being developed, plus techniques for coating with filter material to narrow the bandwidth. Light from the diode passes through the sample chamber and is measured by a phototransistor. An additional feature of the instrument is that it uses high speed electronic switching to give pulses from the various light sources and detect the corresponding transmission, so that a large number of measurements can be made in less than a second. A prototype instrument has been built, and gives a linear response over a concentration range of 5 orders of magnitude.

No specific experiment using this miniaturized device has been formulated, but the availability of a small spectrophotometer should be recognized. One can visualize a number of biological and chemical reactions which produce color changes that can be measured by such an instrument.

APPENDIX I

PENETRATION TESTS IN LOESS AND CLAY-SILT SEDIMENTS AT McCOOK, NEBRASKA AND SOIL SAMPLE COLLECTION TECHNIQUES

Eric Reece

Sandia Laboratories

Introduction

The objectives of the penetrator tests in loess were to determine the amount of material eroded from the penetrator and deposited in the soil, and to determine the changes in the structure, composition, and physical properties of the soil caused by penetrator emplacement. The test actually consisted of three separate operations: penetrator emplacement, penetrator and bulk sample recovery, and detailed sample recovery. Four test penetrators and one practice penetrator were emplaced into a loessial deposit about five miles northwest of McCook. Each penetrator and the soil directly adjacent were recovered in a single large sample container. The containers were transported to the Denver laboratory of Woodward-Clyde Consultants, a Sandia contractor, where detailed samples were collected by NASA and Sandia for analysis. This memorandum describes the test hardware, the test site, test procedure, penetration results, recovery procedures, and detailed sampling procedure.

Test Hardware

Two full scale Mars penetrators were air dropped into the target and two 0.58 scale model penetrators were emplaced using Sandia's Mobile Gas Gun. Sketches of the penetrators are shown in figure 1. The full scale penetrators had detachable afterbodies which separated from the forebody on impact, leaving the antenna at the surface. The separation point was at the beginning of the flared section (see figure 1). An umbilical cable connected the single channel telemetry package located in the forebody to the antenna located on the afterbody. In addition to the telemetry package, one full scale penetrator, the second air-dropped unit, had a water detection device supplied by JPL onboard. The test penetrators were made of D6A-C steel. The chemical composition of D6A-C steel is given in Table I. One of the full scale and one of the subscale penetrators had ports and protrusions to simulate doors and deflectors located at the midpoint of the body. The configuration of the ports and protrusions are shown in figure 2. The .5mm (.02 in.) aluminum disks which covered the large port had four strips of temperature sensitive paint on the inboard surface. The strips of paint change colors at temperatures of 59°C, 107°C, 142°C, and 198°C. The surface finish of the test penetrators was very smooth so that abrasion could be easily detected. An additional small aluminum penetrator was emplaced with the Mobile Gas Gun. This aluminum penetrator was used to practice the primary recovery technique prior to employing the technique on the test penetrators.

Test Site

The Loess Target Test was conducted on an abandoned Army Air Corps base located five miles northwest of McCook, Nebraska. A layout of the test area, together with the approximate locations of the key equipment used

during penetrator emplacement, is shown in figure 3. The target area was a rectangle approximately 304 meters long and 152 meters wide located in the northwest corner of the area bounded by the three runways. A detailed view of the target area is shown in figure 4. The approximate locations of the penetrator impact points and four test holes which were drilled in August 1975, are shown in figure 4. The detailed drilling logs and summaries of laboratory test results for Test Holes 20 and 22 (TH 20 and TH 22) are presented in figures 5 and 6, and Tables II and III.

Test Procedure

The full scale penetrators were dropped from an U-6A "Beaver" airplane. The aircraft had six bomb racks on the wings and a telemetry receiving station onboard. For each full scale penetrator drop test, the aircraft was loaded with five practice bombs and one test penetrator. The practice bombs were ballistically similar to the full scale test penetrators and they discharged a puff of smoke upon impact. During the loading of the test penetrators, extreme care was taken not to scratch the penetrator surface. Just prior to takeoff, the test penetrators were cleaned with trichloroethylene to minimize the chances that extraneous contaminants would be introduced into the soil by the penetrator. Once the aircraft was over the test site, practice bombs were dropped until the release controller was satisfied that the test penetrator would hit the target area. After the test penetrator was dropped and located, photographs were taken, and the afterbody was removed exposing the borehole made by the penetrator. The borehole was probed to determine the depth of the penetration. Then a string of thermistors was inserted into the borehole, and the borehole vertical temperature was monitored by personnel from NASA and the University of Southern California. One scale model penetrator was emplaced approximately 15 meters from the impact point of each full scale penetrator.

Penetration Results

A summary of the penetration results, including the release and impact conditions, is presented in Table IV. The first full scale test penetrator impacted in a low lying area barren of plant growth and snow cover near Test Hole 20 (figure 5 and Table II). The practice penetrator and the first scale model penetrator were also emplaced in this area. The soil in this low lying area was more clayey, more moist and dense than the soil in the remainder of the target area. In addition, the lack of snow cover caused the soil in this area to be frozen to a greater depth than the soil in the remainder of the target area. A complete telemetry record was received from the first full scale penetrator. The deceleration and velocity versus time and displacement are shown in figures 7 and 8 respectively. The deceleration versus displacement data were used, together with Young's penetration equation for complex penetrators and layered soils, to calculate a penetrability index profile (S number) for the target. The calculated penetrability profile is shown in figure 9. The broken line shows the deceleration values used to calculate the penetrability of the three layers encountered.

No telemetry record was obtained from the scale model penetrator emplaced

in this hard area. The reason for the lack of transmission is not known for certain, however, an antenna failure is suspected. In the absence of a telemetry record, the deceleration of the scale model was estimated using the penetrability profile obtained from the full scale penetrator and Young's penetration equation. The estimated deceleration and velocity versus time and displacement for the scale model penetrator are shown in figures 10 and 11 respectively. The calculated depth of 1.65 m agrees well with the measured depth of 1.61 m.

The second full scale and scale model penetrators were emplaced in a softer area near Test Hole 22 (figure 6 and Table III). The soil in this area was a true loess, not water-deposited clayey silt as found in the low lying area where the first pair of penetrators were emplaced. No telemetry record was received from the full scale penetrator, because the umbilical broke shortly after impact. A partial telemetry record was obtained from the scale model penetrator. The partial record is shown as the solid line in figures 12 and 13. The signal was lost after about 7 feet of penetration due to masking by the soil overburden and ice cover at the surface. The remainder of the deceleration record was estimated by forcing the penetration event to be completed at the measured depth. It was necessary to assume that either a hard layer was encountered during the last 2 meters of travel or that locking occurred causing a deceleration increase at the end of the event. During recovery, it became obvious that a hard layer was not present, therefore, locking was assumed.

As in the case of the first full scale penetrator, the available deceleration versus displacement data were used to calculate the profile of the soil. The calculated penetrability profile is shown in figure 14. The profile indicates a fairly hard layer (S = 6) about two feet thick followed by soil twice as penetrable. It is interesting to note that even the hard layer in this area is almost twice as penetrable as the hard soil in the low lying area where the first two penetrators were emplaced.

The calculated penetrability profile was used to estimate the deceleration experienced by the full scale penetrator dropped in the soft area. The estimated deceleration and velocity versus time and displacement are shown in figures 15 and 16. Again, the calculated depth of 8.29 meters using the estimated deceleration, agrees quite well with the measured depth of 7.92 meters.

Penetrator and Bulk Sample Recovery

Each penetrator and the soil adjacent to it were recovered in one large sample container. The recovery procedure was designed and executed by Woodward-Clyde Consultants of Denver under contract to Sandia. The basic elements of the recovery procedure are illustrated in figure 17. Once the subsurface location of the penetrator was determined, a 1.2 meter diameter pilot hole was augered to within about .3 meter of the aft end of the penetrator. The exact location of the tail of the penetrator was established, and an 2.4 meters diameter hole was augered with the penetrator centered in the bottom of the hole. As much soil as possible was removed

from around the desired sample with a .6 meter auger. The remainder of the soil was carved away by hand. A circular plate was then placed on the top of the cylinder containing the penetrator. As each section of the desired sample was exposed, plastic was wrapped around the sample to maintain the moisture content. A split cylindrical steel container section was secured around the sample with a layer of foam rubber placed between the container and the plastic wrap to provide some confining stresses to maintain sample integrity. This procedure was continued until the sample was completely encased. The container was then attached to a crane to provide support while the bottom (forward end) of the sample was cut free. Once the sample had been cut free and the bottom cover installed, the container was lifted from the excavation and put into a foam-lined box for shipment. The aluminum practice penetrator was recovered first and the container was opened at the test site, where NASA ARC personnel obtained samples from directly adjacent to the practice penetrator. These samples were studied to see if the recovery technique had somehow changed the nature of soil near the penetrator. It was concluded that the recovery technique had not changed the soil in the area of interest, and the four test penetrators were then recovered in the same manner.

In addition to the very large samples containing the penetrator, several samples of undisturbed material were taken for moisture content, grain size distribution, and mineralogical analysis. Twelve undisturbed samples for potential use in triaxial tests were taken from area around the second full scale penetrator and shipped to NASA Ames. Thermal conductivity measurements were made by NASA contract personnel on site.

Detailed Sample Recovery

The large sample containers were transported via truck to the Denver laboratory of Woodward-Clyde. In Denver, detailed samples were obtained from the areas directly adjacent to the penetrator skin. The prime responsibility for the detailed sampling belonged to NASA Ames, with support provided by Sandia and Woodward-Clyde. Questions regarding the rationale behind, and the details of, the detailed sampling procedure should be directed to NASA Ames. Only a general description of the procedure is presented here.

The aft end of the sample container was removed, and NASA personnel made thermal conductivity measurements in the soil at various radial distances from the aft end of the penetrator. After the thermal conductivity measurements were completed, the sides of the container were removed and about one-half the soil removed. Several samples were taken for moisture content, gradation, and mineralogical analysis. A very thin layer of soil (1mm to 3mm) was left around the penetrator. Flakes of soil were removed from directly adjacent to the penetrator for surface analyses of the penetrator/soil interface. Scrappings were taken for mineralogical analyses. After sampling was completed, the penetrators were removed from the remaining soil. Peels were taken of the soil adhering to the penetrators after removal from the containers.

The results of the laboratory analyses of the soil samples are, of course, not complete. However, several pertinent observations were made during sample collection. The penetrators were not made of stainless steel and, consequently, much surface oxidation occurred. The surface of the penetrators ranged in color from orange to black, except in regions directly behind holes or protrusions where the surface was still shiny. The apparent oxidation migrated into the soil, and the interface surface of the soil was the same color as the adjacent penetrator surface. The noses of the penetrators were very smooth, with no observable indication of physical abrasion. The soil from the low lying hard area was composed of layers of varying colors. The distortion of these layers near the penetrator surface provided a vivid picture of the "viscous-like" effects of the end of the penetration event.

All penetrators and the bulk soil sample from the scale model fired into the hard area were shipped to NASA Ames. The remainder of the bulk soil samples from the two full scale penetrators were shipped to Sandia. Both NASA and Sandia retained small samples for laboratory analysis.

Concluding Remarks

With the exception of the lack of telemetry data from two test penetrators, the Loess Target Test was an unqualified success. The new recovery technique, developed by Woodward-Clyde Consultants, Denver, provided the closest thing to an undisturbed sample of the soil around a penetrator that is presently possible. The effect of the oxidation of the penetrator surface on the conduct of geochemistry is still undetermined. However, if it should become necessary to use stainless steel for the Mars Penetrator, PH 13-8 Mo stainless steel appears to have sufficient strength, toughness, and hardness to be an acceptable alternative to D6A-C.

TABLE 1

CHEMICAL COMPOSITION OF D6A-C STEEL

Fe - 96.52 to 94.95

C - 0.45 to 0.50

Cr - 0.90 to 1.20

Mo - 0.90 to 1.10

Ni - 0.40 to 0.70

Mn - 0.60 to 0.90

V - 0.08 to 0.15

Si - 0.15 to 0.30

P - 0 to 0.10

S - 0 to 0.10

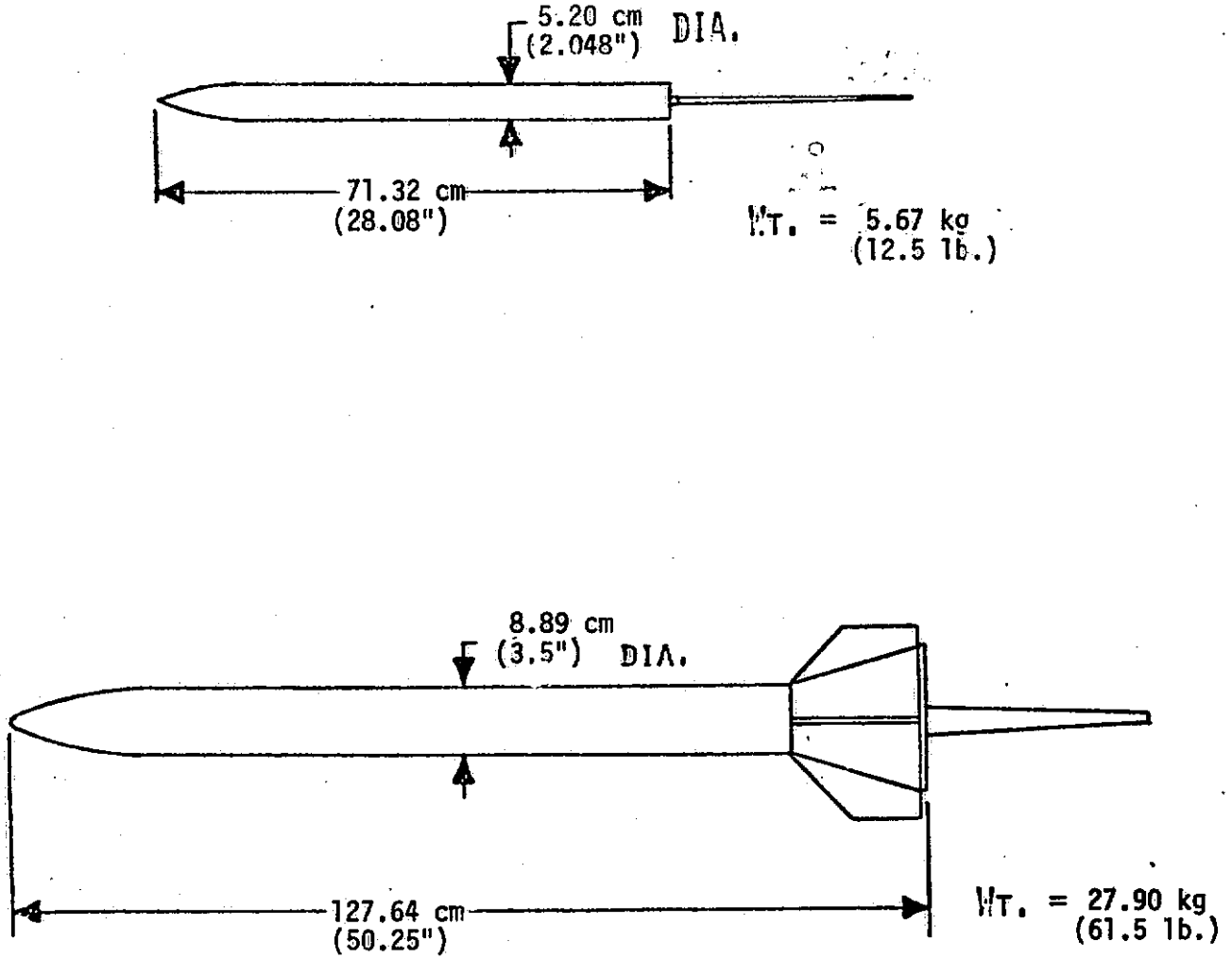

FIGURE 1. MARS PENETRATOR TEST UNITS

1.03 CM (.406 IN) DIAMETER HOLE

SMALL SCREW SIMULATING DEFLECTOR

1.03 CM (.406 IN) DIAMETER HOLE COVERED WITH .5 MM (.02 IN)

FIGURE 2. DOOR AND DEFLECTOR SIMULATIONS (FULL SCALE DIMENSIONS)

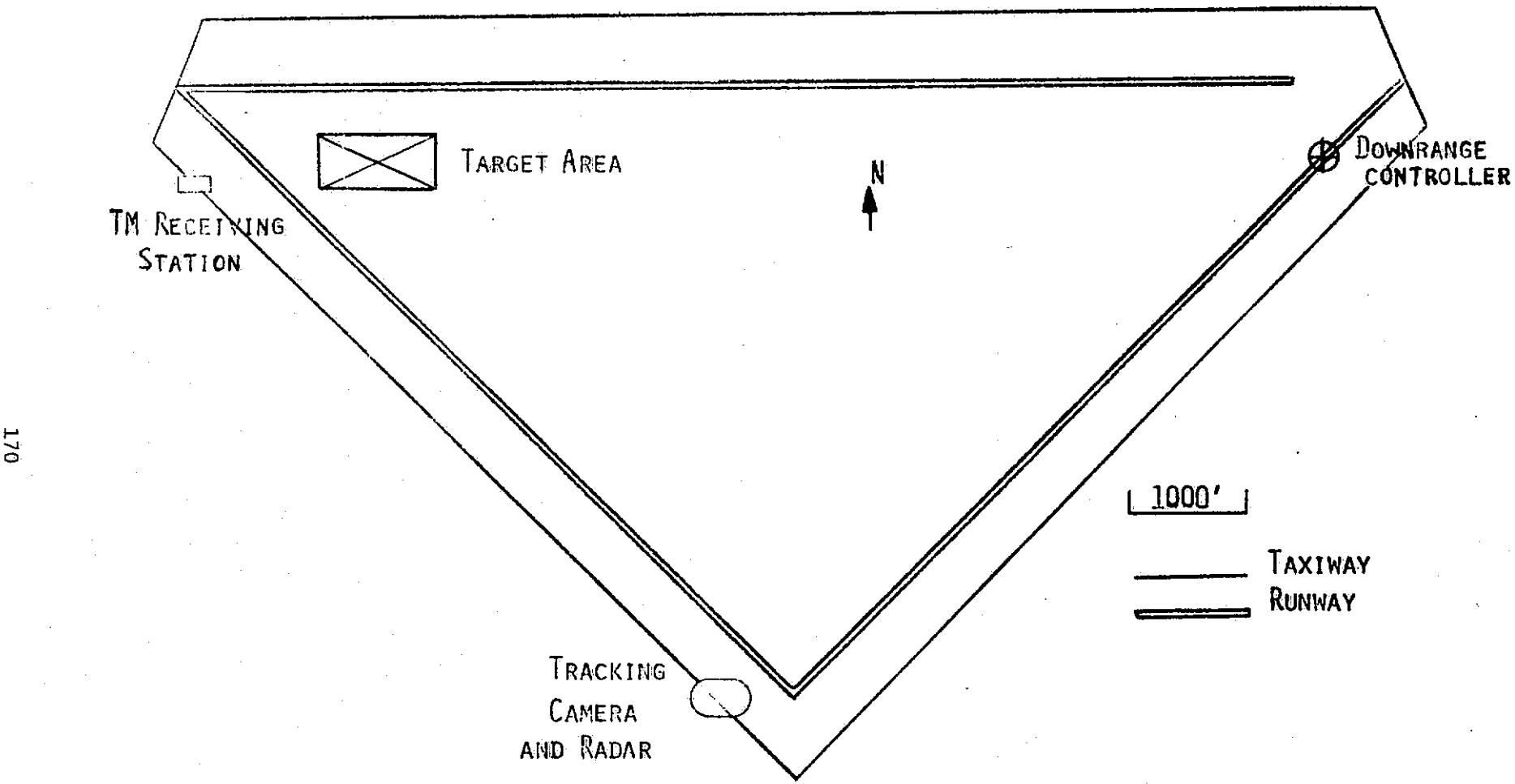

FIGURE 3. LOESS TARGET TEST AREA

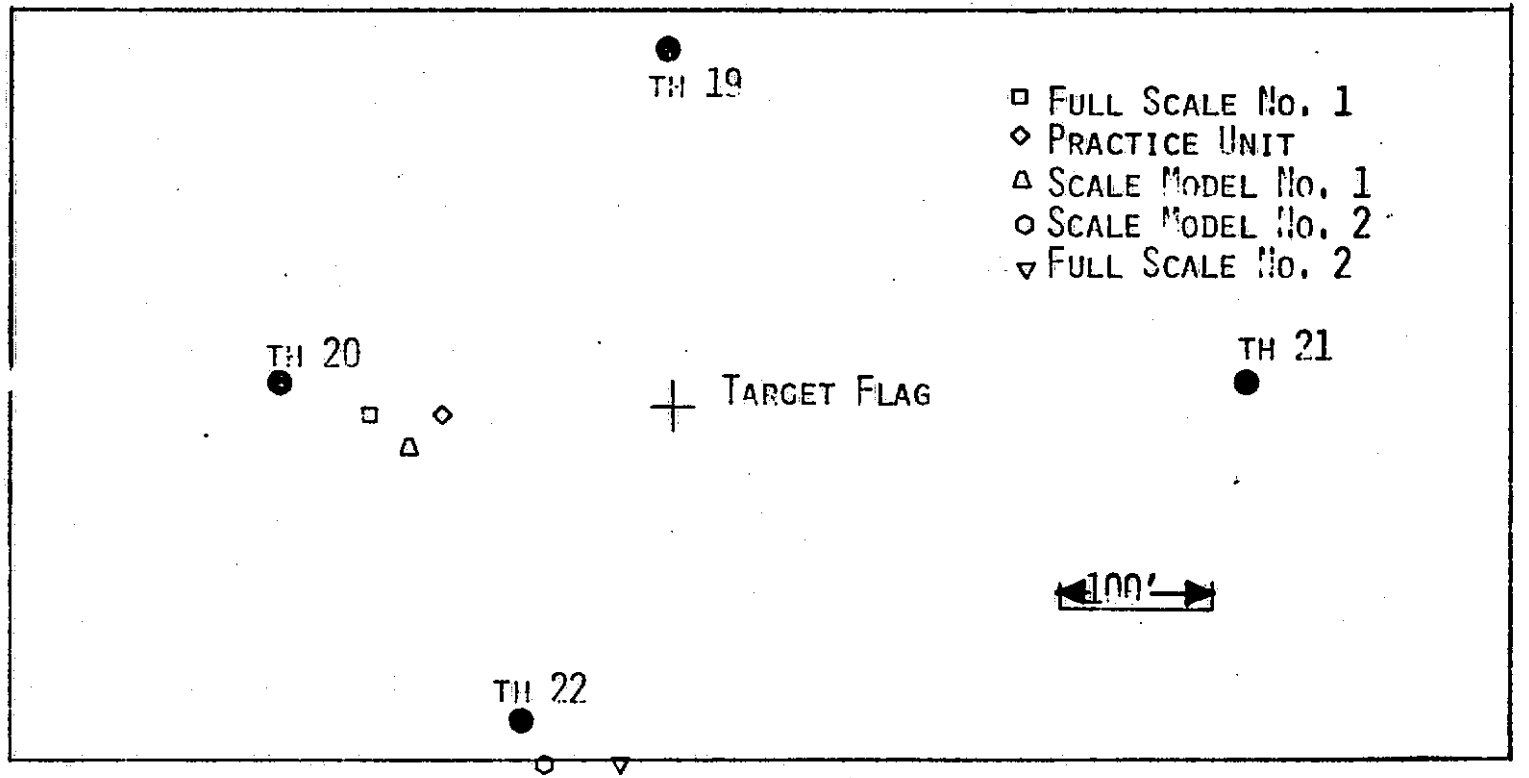

Figure 4. Target Area

WOODWARD - CLYDE CONSULTANTS
ROCKY MOUNTAIN REGION

HOLE NO. TH-20

PROJECT NO. 15335-G462
PROJECT NAME LOESSIAL SOIL TEST SITE
LOCATION : McCOOK AIRPORT
McCOOK, NEBRASKA

DETAILED DRILLING LOG

ELEVATION (MSL OR TBM) 2771.24 MSL
DATE STARTED 8-21-75 DATE FINISHED 8-21-75

DRILL MANUFACTURER AND MODEL NUMBER : CENTRAL MINE EQUIPMENT (CME-45) DRILLING RIG

DIRECTION OF HOLE : [X] VERTICAL [ ] INCLINED 0 DEGREES FROM VERTICAL

TYPE DRILL : 4-INCH CONTINUOUS HELICAL AUGER
DRILLING FLUID : NONE

SIZE AND TYPE OF BIT : 4-INCH AUGER HEAD (4 TEETH)

CASING : NONE DEPTH :
PIEZOMETER : NONE DEPTH :

WATER LEVEL : DEPTH NONE FEET DATE DEPTH FEET DATE

DEPTH (Feet)	LEGEND	CLASSIFICATION OF MATERIALS (Description)	BLOW COUNT	% CORE RECOVERY	RQD	REMARKS (Drilling time, water loss, depth of weathering, etc., if significant)
0	ST	TOPSOIL, SILT, SOFT TO MEDIUM DENSE, SLIGHTLY CLAYEY TO CLAYEY, ROOTS, POROUS, SLIGHTLY MOIST, DARK BROWN.				
10	ST	CLAY, MEDIUM STIFF, VERY SILTY, SLIGHTLY POROUS, SLIGHTLY MOIST, BROWN (CL).				
20	ST	SILT, MEDIUM DENSE, VERY CLAYEY, SLIGHTLY MOIST, BROWN (ML-CL).				
30	ST	CLAY, MEDIUM STIFF, VERY SILTY, CALCAREOUS, SLIGHTLY POROUS, OCCASIONAL IRON STAINS, SLIGHTLY MOIST TO MOIST, TAN, BROWN (CL).				
40	ST					
50						
60						
70						
80						
90						
100						
110						

LEGEND

ST INDICATES THIN WALLED SHELBY TUBE SAMPLE.

GRADUAL CHANGE IN MATERIALS. EXACT STRATA CHANGE NOT LOCATED.

NOTES :

1. MOISTURE CONTENT OF SILT WAS APPROXIMATELY 10 TO 15 PERCENT DURING DRILLING.
2. TEMPERATURE AT COMPLETION OF DRILLING WAS:
   A. 90° F. IN SHELBY TUBE FROM A DEPTH OF 35 FEET.
   B. 72° F. IN TEST HOLE AT A DEPTH OF 40 FEET.
3. TEMPERATURE IN TEST HOLE DURING THE MORNING OF AUGUST 22, 1975, WAS 62° F. AT A DEPTH OF 40 FEET.

FIGURE 5. DETAILED DRILLING LOG, TEST HOLE 20

WOODWARD-CLYDE CONSULTANTS

JOB NO. 18335

CONSULTING ENGINEERS, GEOLOGISTS AND ENVIRONMENTAL SCIENTISTS

ROCKY MOUNTAIN REGION

TABLE II

SUMMARY OF LABORATORY TEST RESULTS

HOLE	DEPTH (FEET)	NATURAL MOISTURE (%)	NATURAL DRY DENSITY (PCF)	ATTERBERG LIMITS		UNCONFINED COMPRESSIVE STRENGTH (PSF)	TRIAXIAL SHEAR TESTS		SOIL TYPE
				LIQUID LIMIT (%)	PLASTICITY INDEX (%)		DEVIATOR STRESS (PSF)	CONFINING PRESSURE (PSF)	
20	4.0	13.0	107.9						CLAY, VERY SILTY, BROWN (CL).
	9.0	24.1	89.0						SILT/CLAY, DARK BROWN (ML-CL)
	14.0	22.0	107.4						CLAY, VERY SILTY, TAN, BROWN (CL).
	19.0	17.7	110.0	33	14				CLAY, VERY SILTY, TAN, BROWN (CL).
	24.0	17.3	100.9						CLAY, VERY SILTY, TAN, BROWN (CL).
	29.0	16.1	100.4						CLAY, SILTY, TAN, BROWN (CL).
	34.0	17.7	111.9						CLAY, VERY SILTY, TAN, BROWN (CL).
	39.0	16.8	118.2						CLAY, SILTY, BROWN (CL).

WOODWARD - CLYDE CONSULTANTS
ROCKY MOUNTAIN REGION

HOLE NO. TH-22

PROJECT NO. 16339-6762
PROJECT NAME LOESSIAL SOIL TEST SITE

LOCATION : McCOOK AIRPORT
McCOOK, NEBRASKA

DETAILED DRILLING LOG

ELEVATION (MSL OR THM) 2770.71 MSL

DATE DRILLED
STARTED 8-21-75
FINISHED 8-21-75

DRILL MANUFACTURER AND MODEL NUMBER :
CENTRAL MINE EQUIPMENT (CME-45) DRILLING RIG

DIRECTION OF HOLE
[X] VERTICAL [ ] INCLINED ____ 0 DEGREES TO VERTICAL

TYPE DRILL : 4-INCH CONTINUOUS HELICAL AUGER
DRILLING FLUID : NONE

SIZE AND TYPE OF BIT
4-INCH AUGER HEAD (4 TEETH)

CASING NONE DEPTH
PIEZOMETER DEPTH : NONE

WATER LEVEL
DEPTH : NONE DATE
DEPTH DATE
DEPTH DATE

DEPTH (Feet)	LEGEND	CLASSIFICATION OF MATERIALS (Description)	BLOW COUNT	% CORE RECOVERY	RQD	REMARKS (Drilling time, water loss, depth of weathering, etc., if significant)
0	ST	TOPSOIL, SILT, SOFT TO MEDIUM DENSE, SLIGHTLY CLAYEY TO CLAYEY, ROOTS, POROUS, SLIGHTLY MOIST, DARK BROWN.				
10	ST	SILT, MEDIUM DENSE, VERY CLAYEY, POROUS, CALCAREOUS, SLIGHTLY SANDY, OCCASIONAL IRON STAINS, GRADUAL DENSITY INCREASE WITH DEPTH, SLIGHTLY MOIST, TAN, BROWN (ML, ML-CL).				
20	ST					
30	ST					
40	ST	CLAY, MEDIUM STIFF, VERY SILTY, CALCAREOUS, SLIGHTLY SANDY, OCCASIONAL IRON STAINS, GRADUAL DENSITY INCREASE WITH DEPTH, SLIGHTLY MOIST, TAN, BROWN (CL).				
50						
60						
70						
80						
90						
100						
110						

LEGEND

ST INDICATES THIN WALLED SHELBY TUBE SAMPLE.

GRADUAL CHANGE IN MATERIALS. EXACT STRATA CHANGE NOT LOCATED.

NOTES :

1. TEMPERATURE AT COMPLETION OF DRILLING WAS:
   A. 80° F. IN SHELBY TUBE FROM A DEPTH OF 38 FEET.
   B. 70°F. IN TEST HOLE AT A DEPTH OF 40 FEET.
2. TEMPERATURE IN TEST HOLE DURING THE MORNING OF AUGUST 22, 1975, WAS 60°F. AT A DEPTH OF 40 FEET.

FIGURE 6. DETAILED DRILLING LOG, TEST HOLE 22

WOODWARD-CLYDE CONSULTANTS

JOB NO. 18335

CONSULTING ENGINEERS, GEOLOGISTS AND ENVIRONMENTAL SCIENTISTS

ROCKY MOUNTAIN REGION

TABLE III

SUMMARY OF LABORATORY TEST RESULTS

HOLE	DEPTH (FEET)	NATURAL MOISTURE (%)	NATURAL DRY DENSITY (PCF)	ATTERBERG LIMITS		UNCONFINED COMPRESSIVE STRENGTH (PSF)	TRIAXIAL SHEAR TESTS		SOIL TYPE
				LIQUID LIMIT (%)	PLASTICITY INDEX (%)		DEVIATOR STRESS (PSF)	CONFINING PRESSURE (PSF)	
22	4.0	10.2	87.7						SILT, CLAYEY, POROUS, ROOTS, CALCAREOUS, TAN, BROWN (ML).
	9.0	13.4	91.2						SILT, CLAYEY, TAN, BROWN, (ML).
	14.0	13.8	90.4						SILT, CLAYEY, TAN, BROWN, (ML).
	19.0	15.3	94.0						SILT, CLAYEY, TAN, BROWN, (ML).
	24.0	15.6	98.8						SILT/CLAY, ROOTS, POROUS, TAN, BROWN (ML-CL).
	29.0	15.7	100.0						SILT/CLAY, TAN, BROWN, (ML-CL).
	34.0	7.3	107.3	32	16				CLAY, VERY SILTY, TAN, BROWN, (CL).
	39.0	11.1	109.1	39	22				CLAY, VERY SILTY, TAN, BROWN, (CL).

TABLE IV

MARS PENETRATOR

LOESS TARGET TEST DATA SUMMARY

DATE	RELEASE CONDITIONS ALTITUDE m(ft), AGL	VELOCITY (KTS)	IMPACT CONDITIONS VELOCITY (mps(fps))	ANGLE (Deg)	DEPTH TO NOSE m(ft)
1/14/76	1980(6500)	80	120(395)	8	2.46(7.5)
1/15/76	Air Gun	Air Gun	159(520)	0	1.74(5.3)
1/15/76	1526(5000)	80	133(435)	15	8.53(26)
1/15/76	Air Gun	Air Gun	136(445)	0	4.60(14)

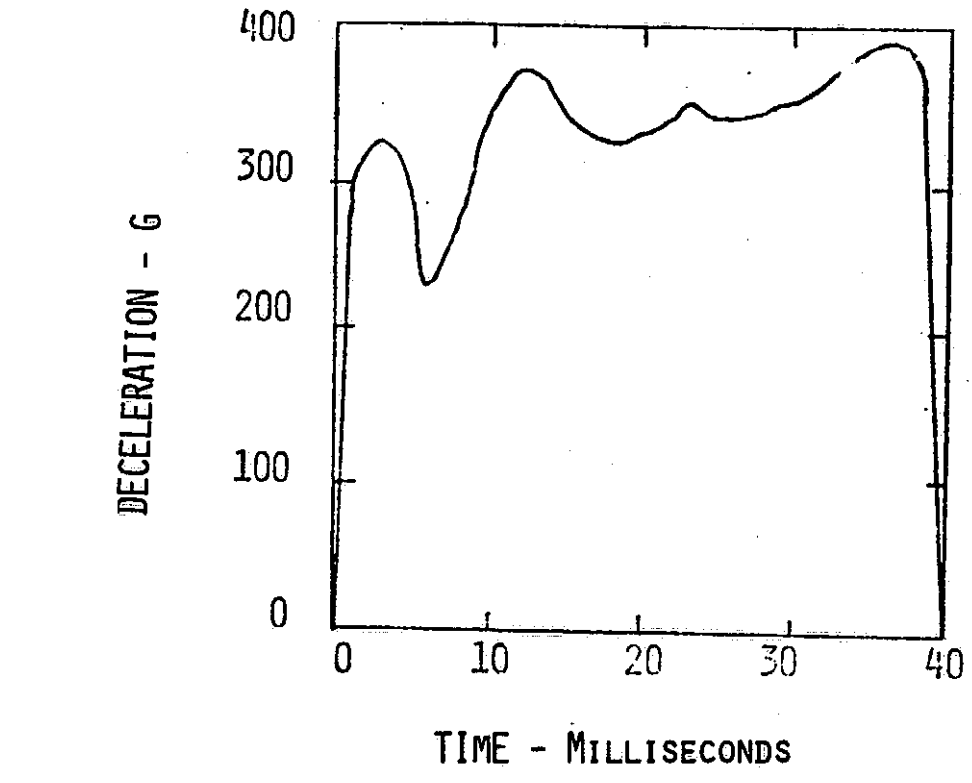

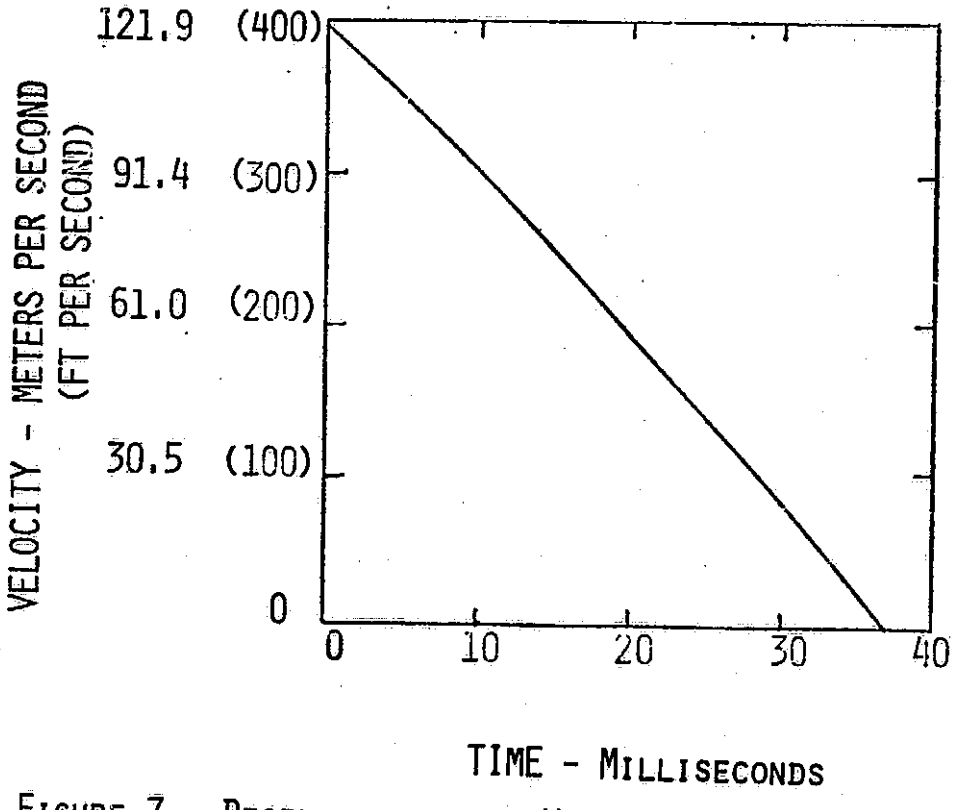

FIGURE 7. DECELERATION AND VELOCITY VERSUS TIME, FULL SCALE UNIT, HARD AREA

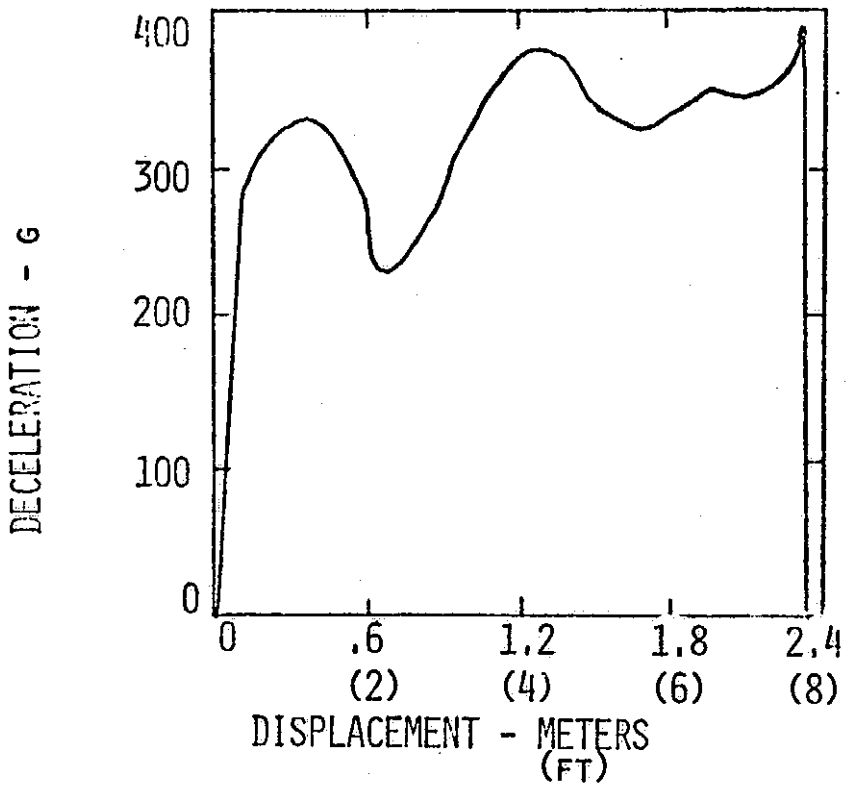

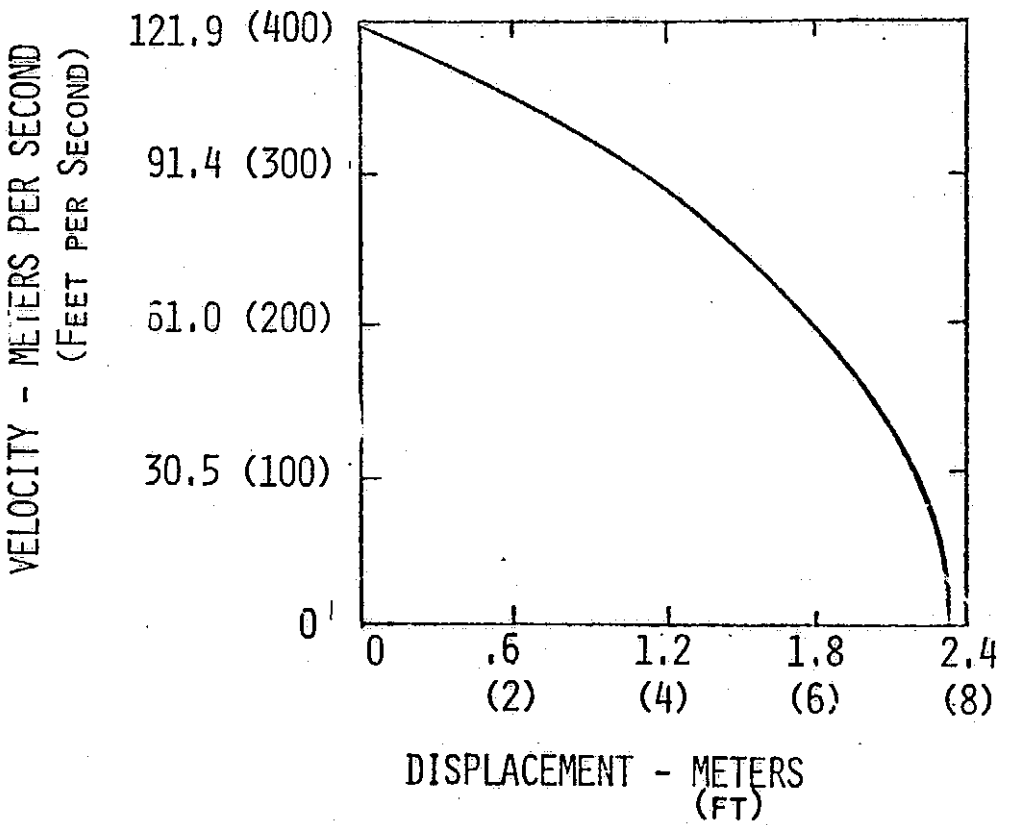

FIGURE 8. DECELERATION AND VELOCITY VERSUS DISPLACEMENT FULL SCALE UNIT, HARD AREA

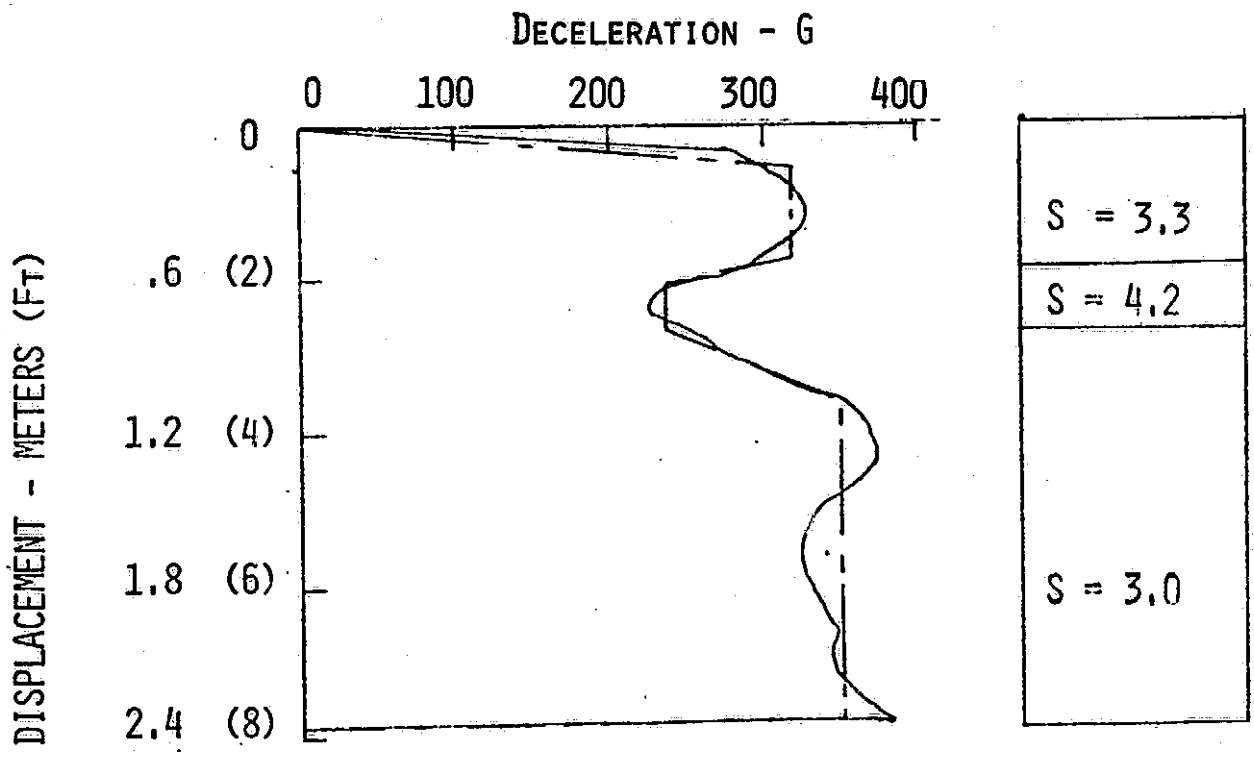

FIGURE 9. PENETRABILITY PROFILE, HARD AREA

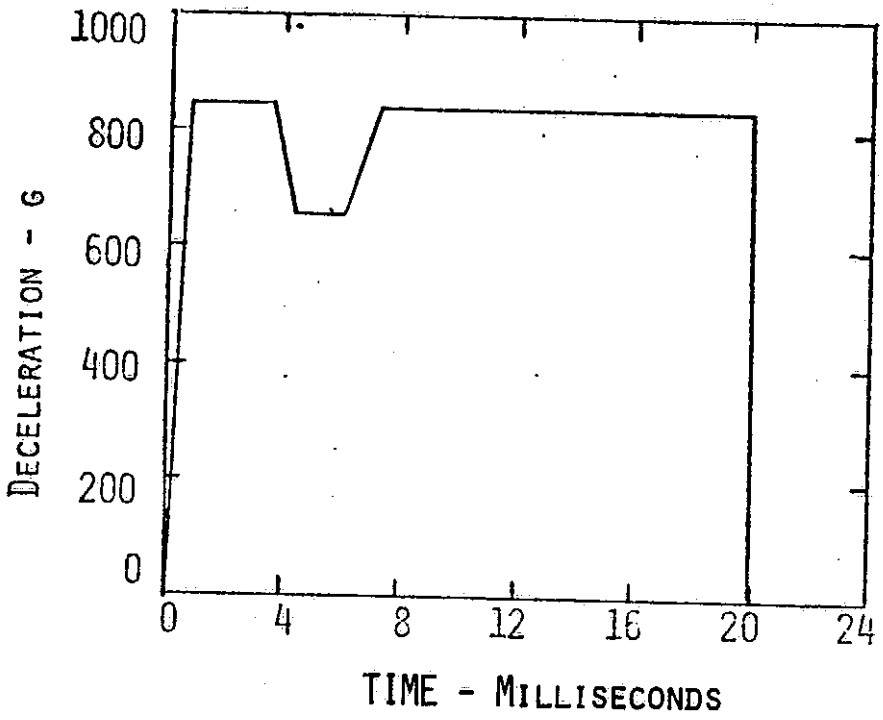

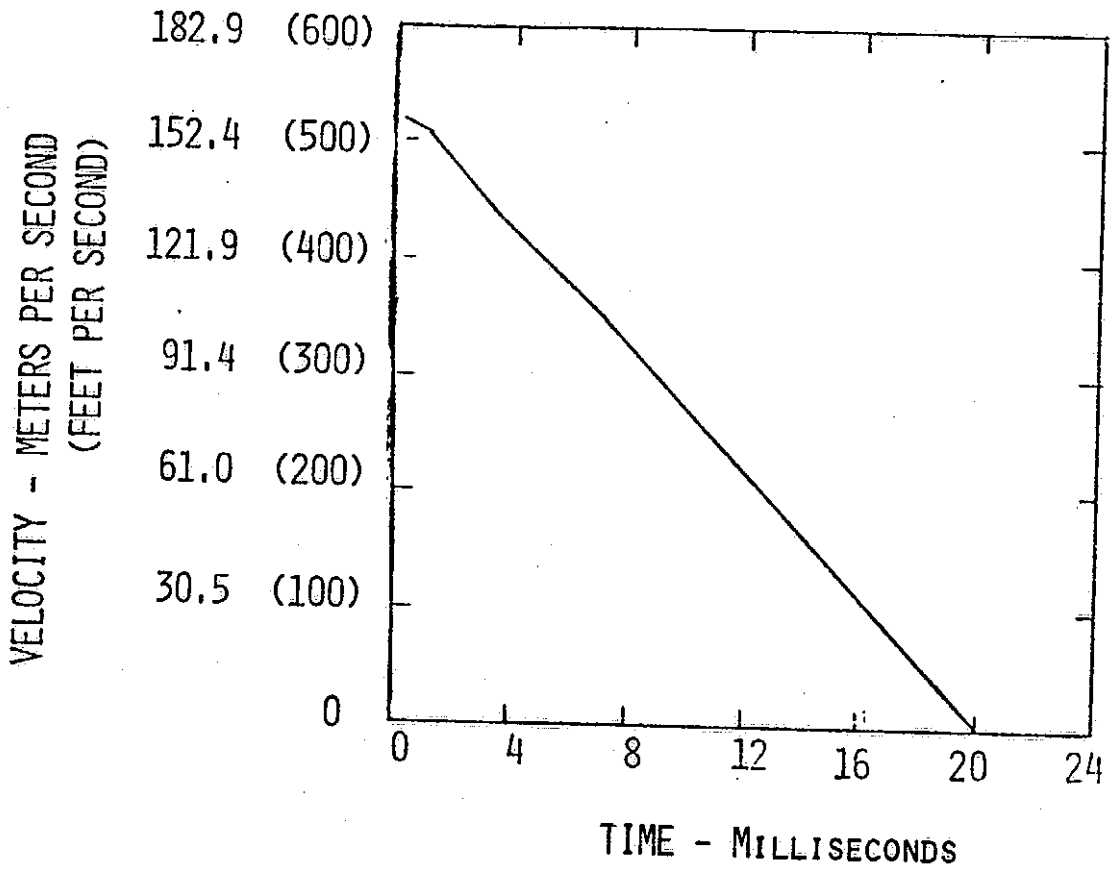

FIGURE 10. ESTIMATED DECLERATION AND VELOCITY VERSUS TIME, SCALE MODEL, HARD AREA

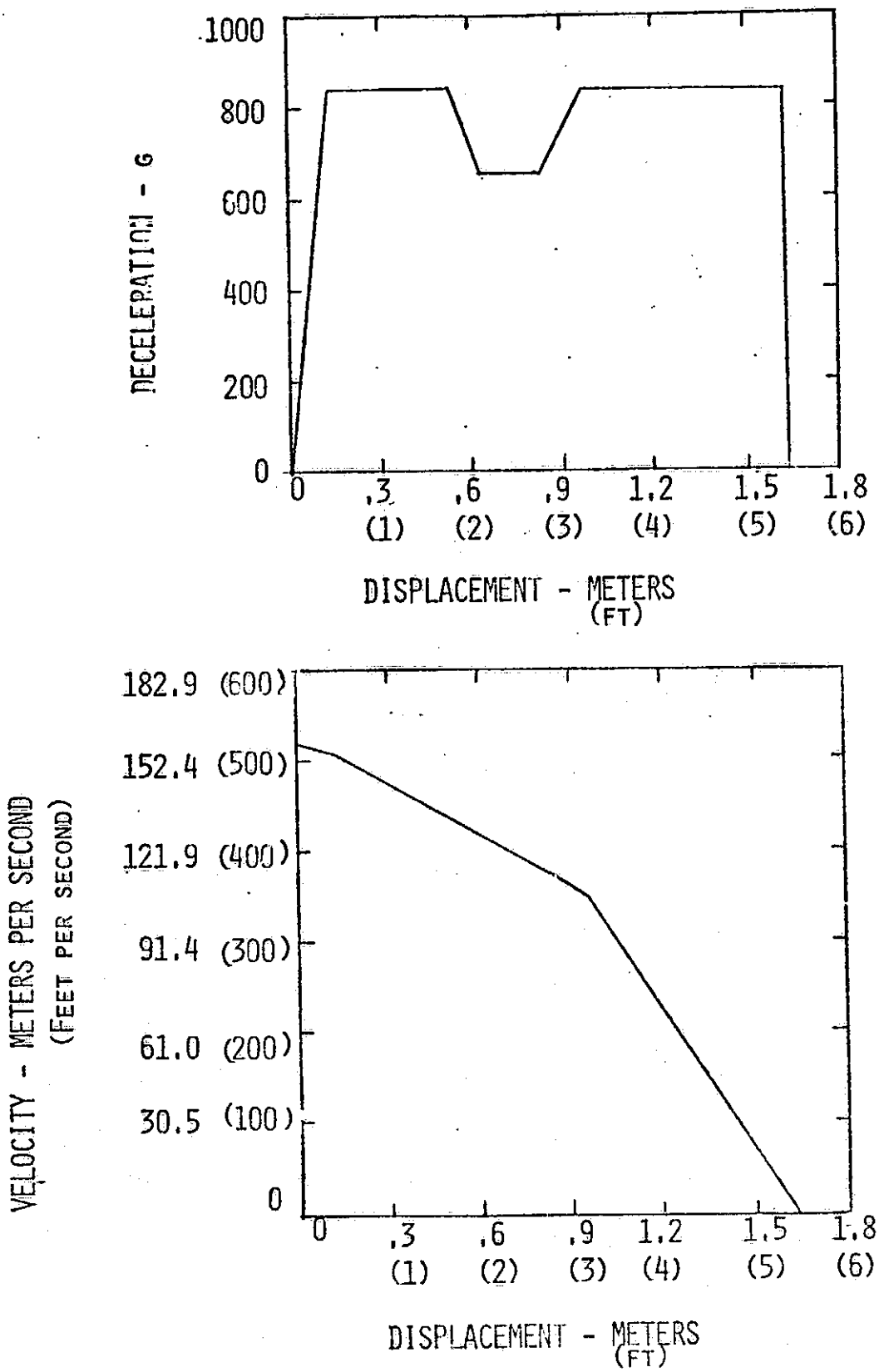

FIGURE 11. ESTIMATED DECELERATION AND VELOCITY VERSUS DISPLACEMENT, SCALE MODEL, HARD AREA

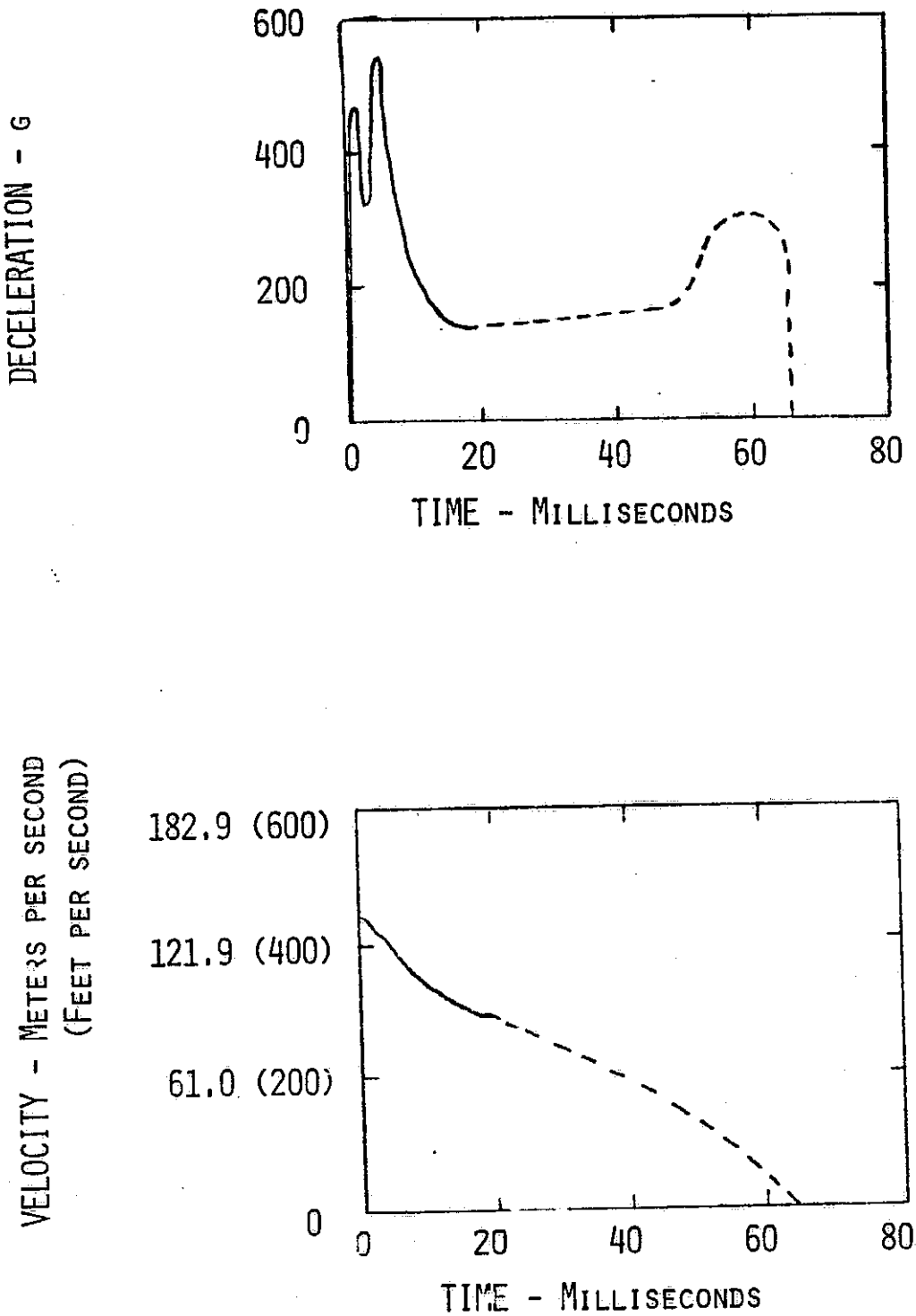

FIGURE 12. DECELERATION AND VELOCITY VERSUS TIME, SCALE MODEL, SOFT AREA

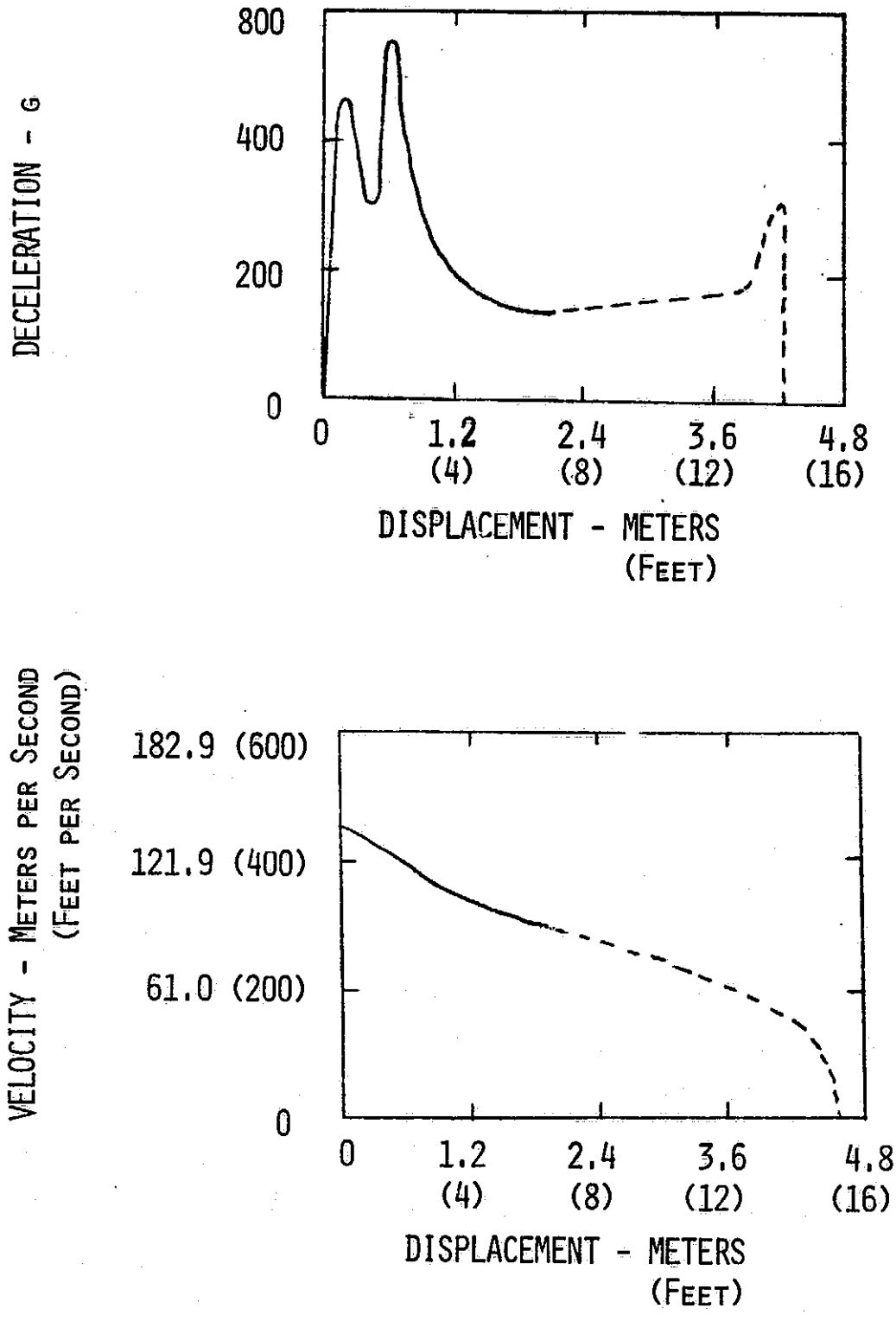

FIGURE 13. DECELERATION AND VELOCITY VERSUS DISPLACEMENT, SCALE MODEL, SOFT AREA

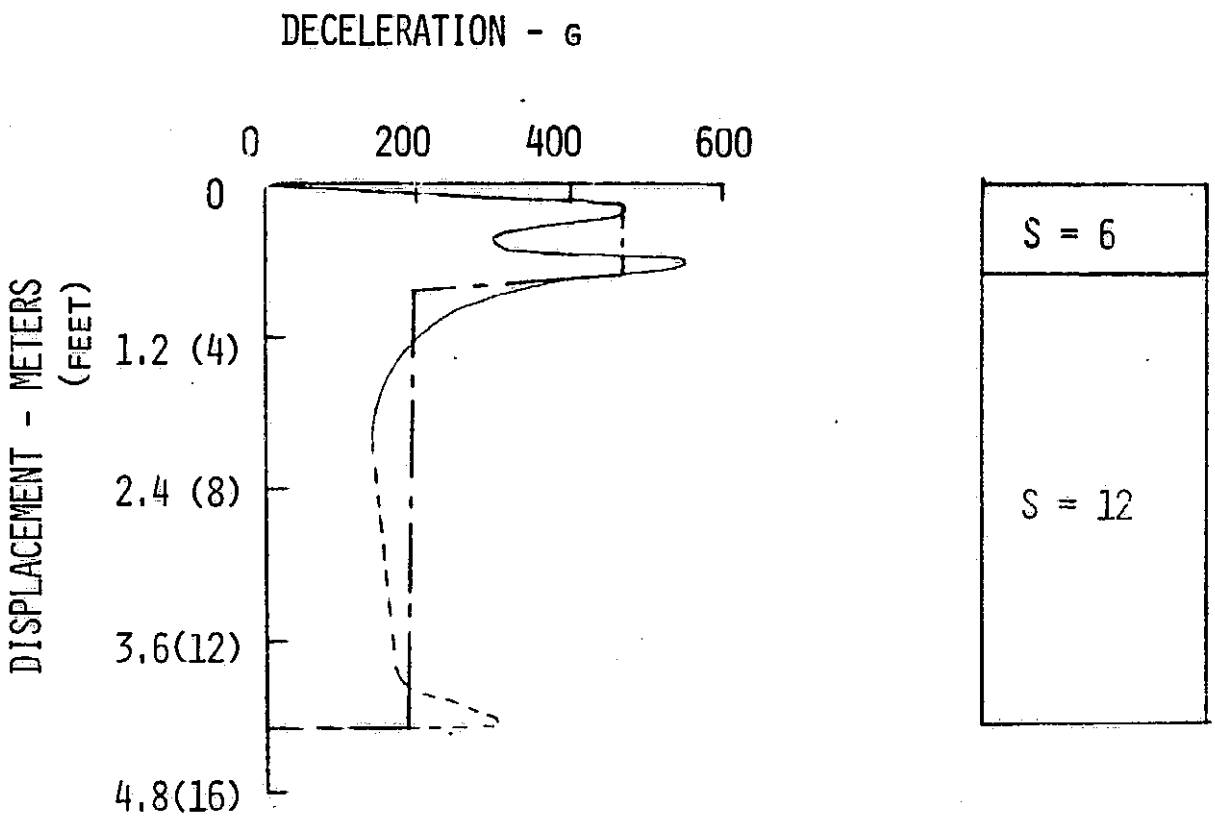

FIGURE 14. PENETRABILITY PROFILE, SOFT AREA

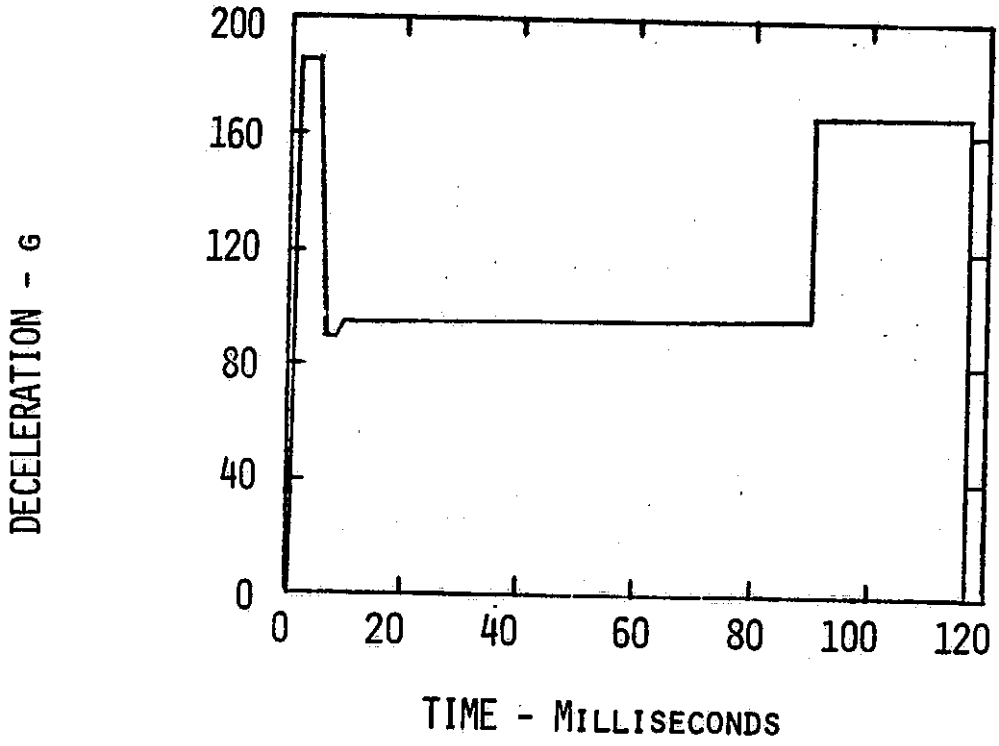

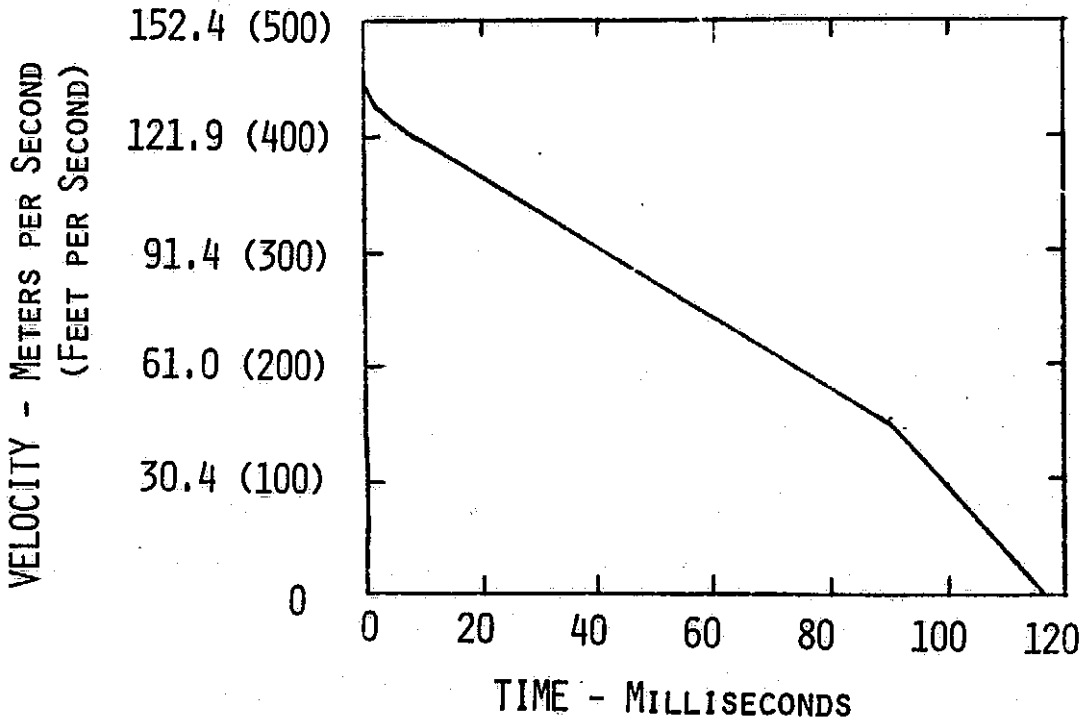

FIGURE 15. ESTIMATED DECELERATION AND VELOCITY VERSUS TIME, FULL SCALE UNIT, SOFT AREA

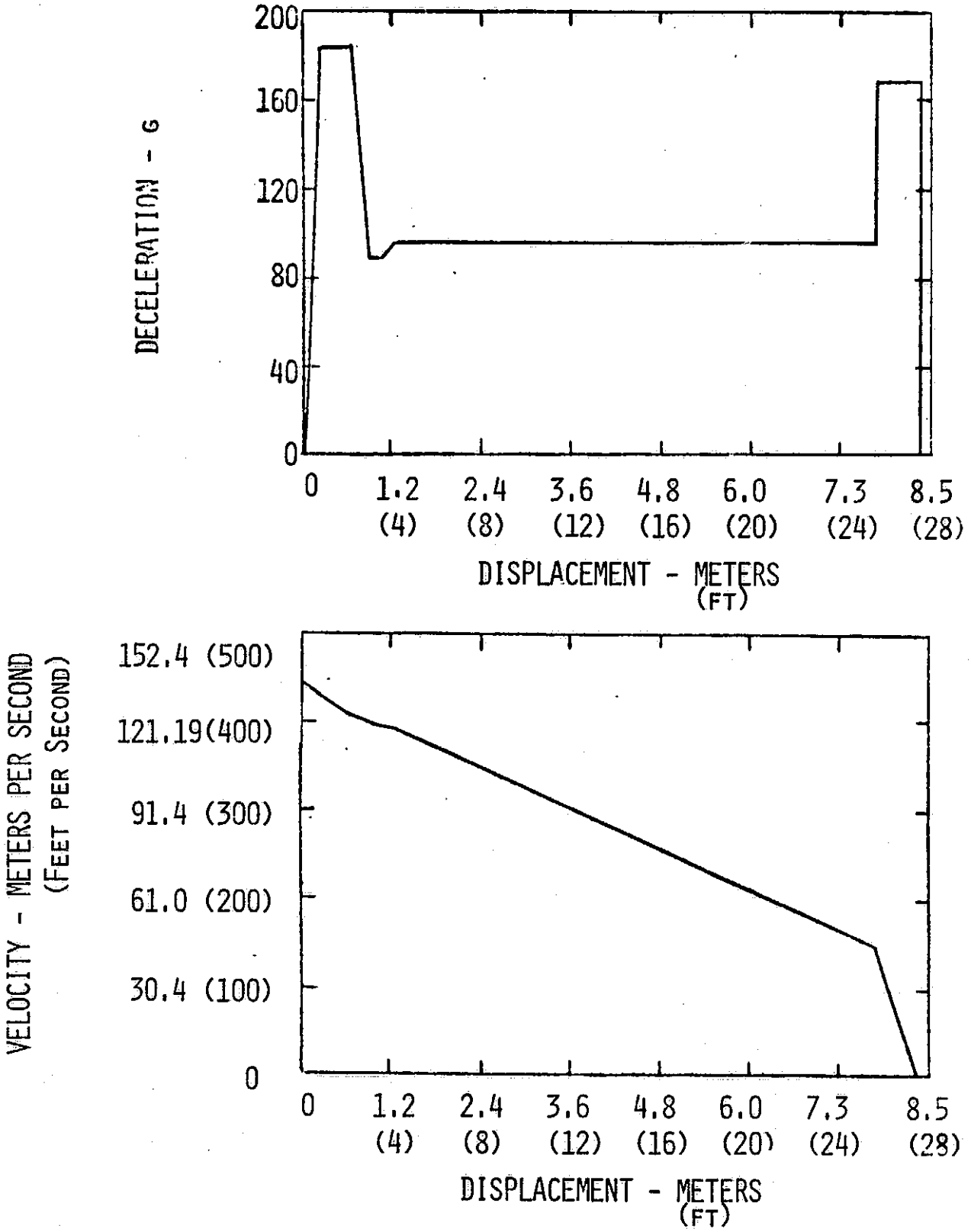

FIGURE 16. ESTIMATED DECELERATION AND VELOCITY VERSUS DISPLACEMENT, FULL SCALE UNIT, SOFT AREA

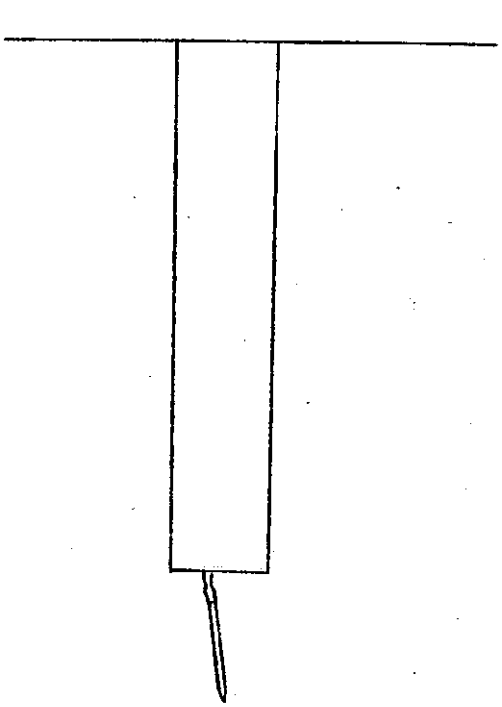

A. 1.2 M PILOT HOLE

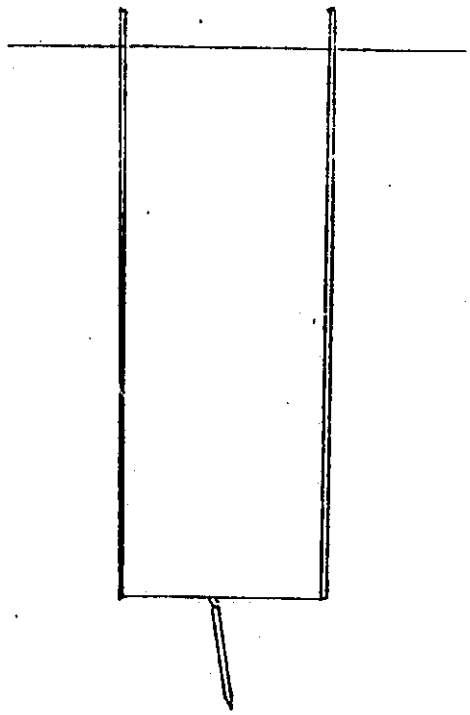

B. CASED 2.4 M HOLE

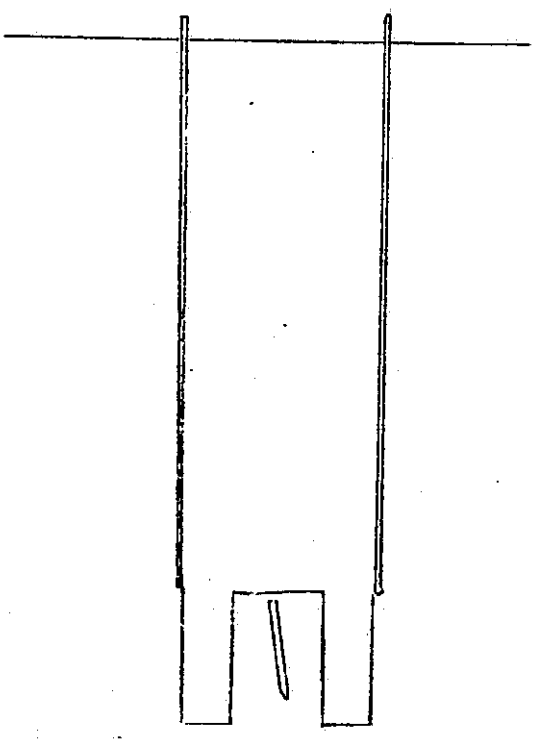

C. .6 M HOLES

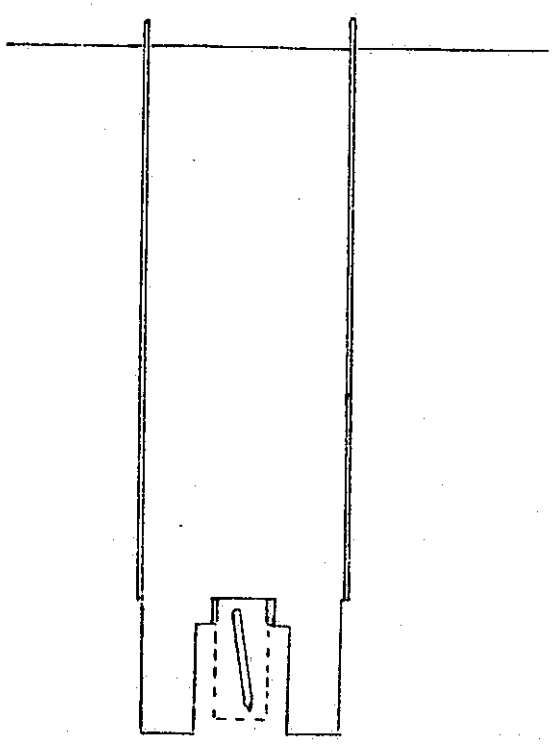

D. SAMPLE ENCASEMENT

FIGURE 17. SAMPLE RECOVERY

APPENDIX J

PRELIMINARY SOIL MODIFICATION EFFECTS IN LOESS

Maxwell Blanchard
Theodore E. Bunch
William Quaide
Kenneth Snetsinger
Ames Research Center

Harry Shade
Josef Erlichman
George Polkowski
L.F.E. Corporation

Alice Davis
Frank Kyte
San Jose State University

Gary Cunningham
University of Oregon

Gerald Nelson
Sandia Laboratories

PRELIMINARY RESULTS OF ANALYSES PERFORMED ON THE SOIL ADJACENT TO PENETRATORS EMPLACED INTO LOESS SEDIMENT MC COOK, NEBRASKA, JANUARY 1976

The penetrator and a column of surrounding soil (radius ~ 46 cm) were sealed in place and encased in a steel container before being removed from the drill hole. After being transported to Denver, Colorado, the containers were opened in the Woodward - Clyde Laboratories about 14-16 days after the drop tests occurred. In the laboratory, the nature of the physical changes were observed and soil samples surrounding the penetrator were recovered for later analytical studies. The moisture content in the soil during encasement and transportation remained largely unchanged. The moisture content just prior to encasement (see Table 1) was between 15-16% dry weight for the five impact sites. The moisture content in the soil during recovery at the Woodward - Clyde Laboratories was between 14-17% dry weight. Measurements taken on undisturbed samples indicate the soil saturates at about 22% soil moisture.

Observervations indicate the original sedimentary structures were modified by the penetrator's impact. The clay and silt layers in the sediment were deformed (see Fig. 1) by the penetrator as it passed through them. Drag folds developed about 5 cm away from the penetrator rotating some of the once horizontal layers to a vertical orientation about 1 cm away from the penetrator. In this zone (0-1 cm) the sediment was mixed and crushed so that nearly all evidence of the original layers were destroyed. A series of parallel shear planes (see Fig. 2) now characterize the only structure evident in this zone. These shear planes can be described as a series of en échelon conical-shaped surfaces having their apex pointing towards the penetrator's nose and intersecting the penetrator's skin at 5-10^{o} angles.

TABLE 1

SOIL MOISTURE AT TEST SITE IN McCOOK, NEBRASKA, JANUARY 1976

Woodward-Clyde Recovery Sequence	Penetrator Type	Depth of Penetration	Soil Moisture (% dry weight)	
			Prior to Encasement (McCook)	After Recovery (Denver)
1	Aluminum, Air Gun Launched	1.54m	16.1	16.8
2	D6AC Steel, Air Gun Launched	1.74m	15.6	17.7
3	D6AC Steel, Aircraft Dropped	2.46m	15.3	14.6
4	D6AC Steel, Aircraft Dropped	8.53m	15.3	15.4
5	D6AC Steel, Air Gun Launched	4.60m	16.1	14.4
Soil, Saturated		25mm - 150mm	23.5	
Soil, Saturated		300mm	22.1	

C-3

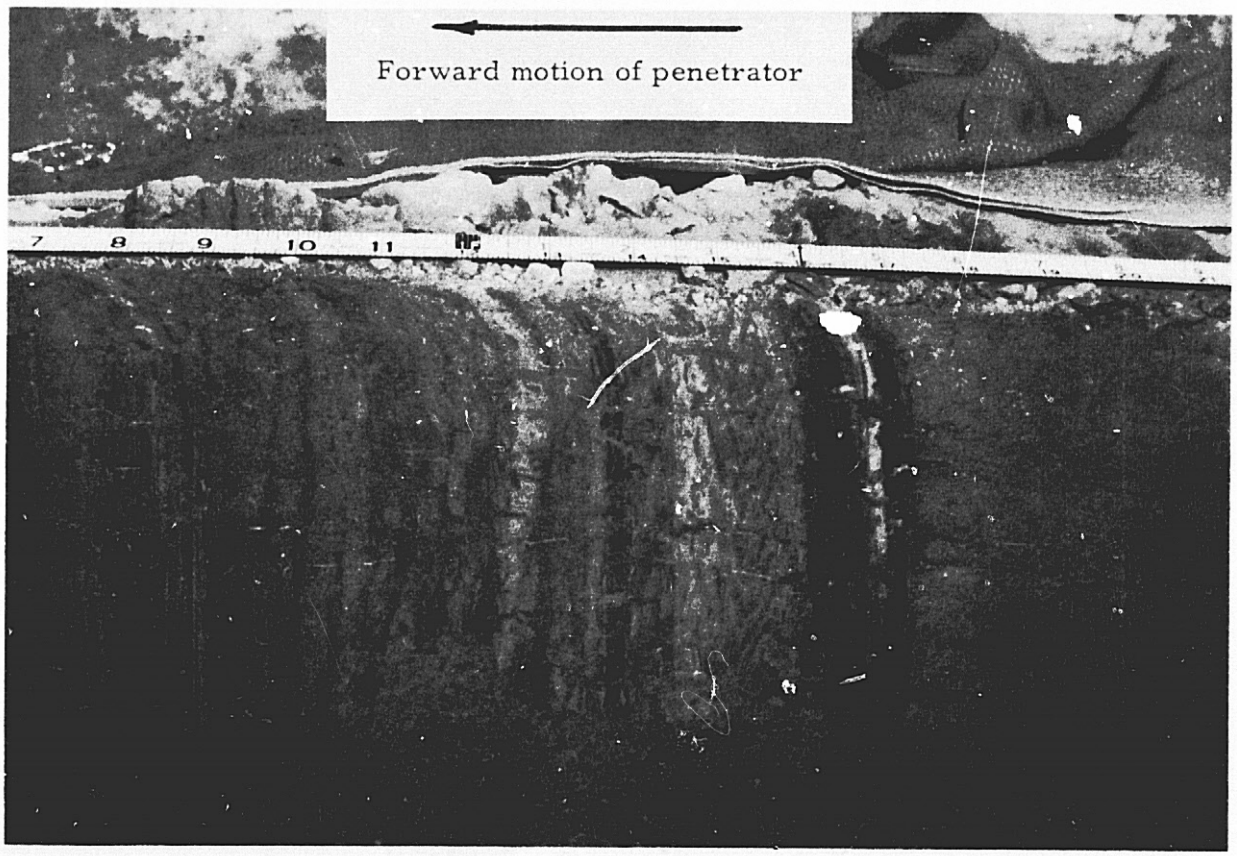

Figure 1

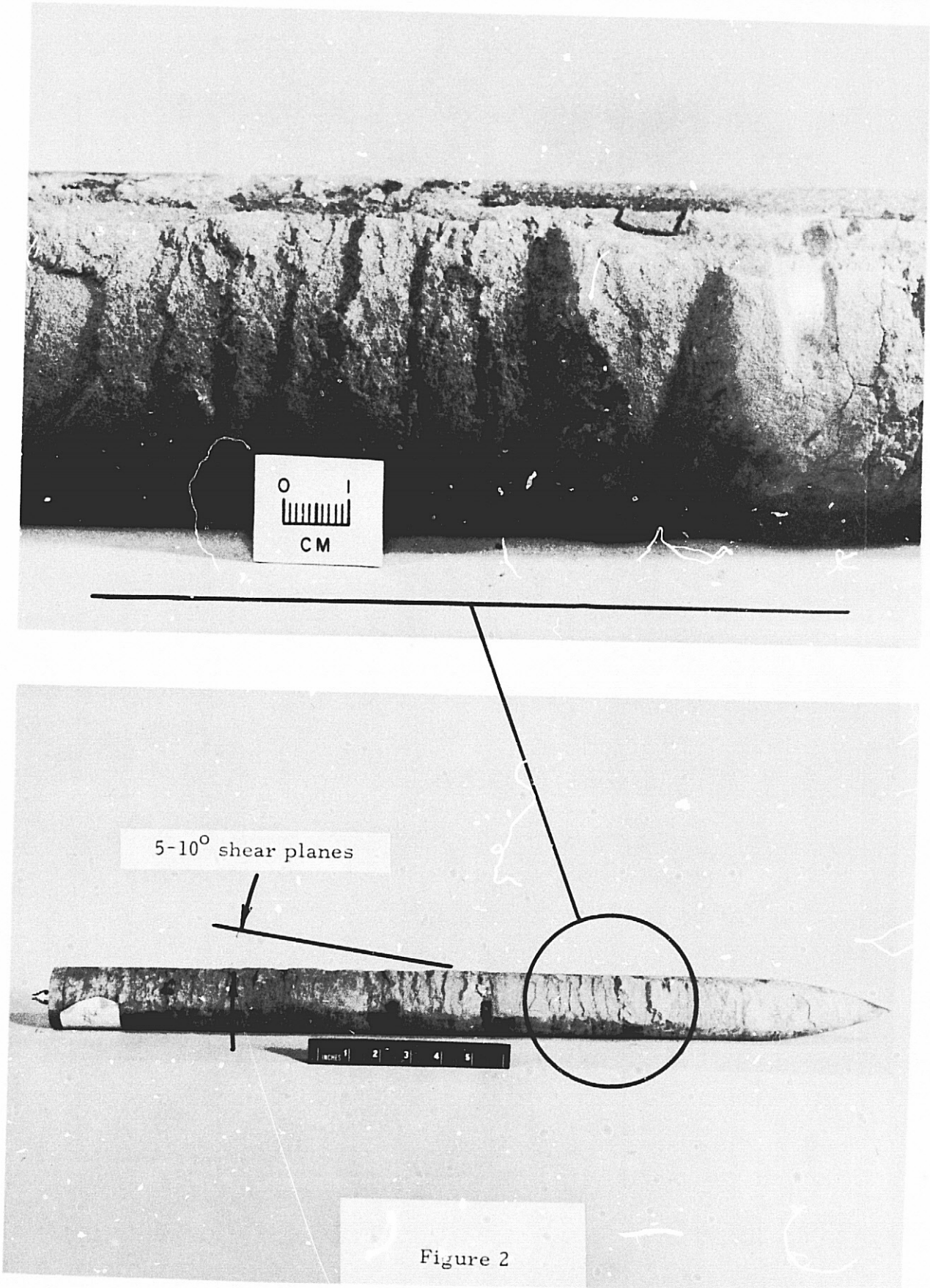

Figure 2

Soil samples were recovered in zones surrounding each penetrator. These zones were divided into the following increments: 0-1 mm, 1-2 mm, and farther than 2 mm away from the penetrator. From these zones soil samples were taken in 10-cm sections from the nose to the aft-end of the penetrator. Also, undisturbed samples of soil were recovered for comparison.

Preliminary results have been obtained from analyses performed on the soil layers immediately adjacent to the full-scale vehicle penetrating the loess sediment (WC#4 in Table 1). Size distribution studies (see Fig. 3) comparing the undisturbed loess with the modified material in the 0-1 mm zone adjacent to the penetrator's skin show that a significant increase has occurred in the particulate material larger than 125 microns in size. This material is a combination of glass and sintered sediment grains formed from the original loess and at the expense of the clay size ($<8\ \mu$) particulates.

Optical microscopy studies show that the material next to the penetrator's skin is characterized by a layer of dark brown glass approximately 50 μm thick. The elemental content of the glass layer consists of Na, Mg, Al, Si, K, Ca, Cr, Fe, Ni, and Mo. Relative to the host sediments, consisting largely of quartz, plagioclase, and K-feldspar (see Table 3), the glass is enriched in Ca, Cr, Fe, Ni, and Mo, and deficient in Al, Si, K, and Na. The Cr, Fe, Ni, and Mo came from the penetrator and Ca from the sediments (probably dissociated calcite).

A profile analysis with an electron microprobe using an enlarged beam spot size (about 30 microns) was performed on a cross section of sediment taken directly from the penetrator's skin containing the glass,

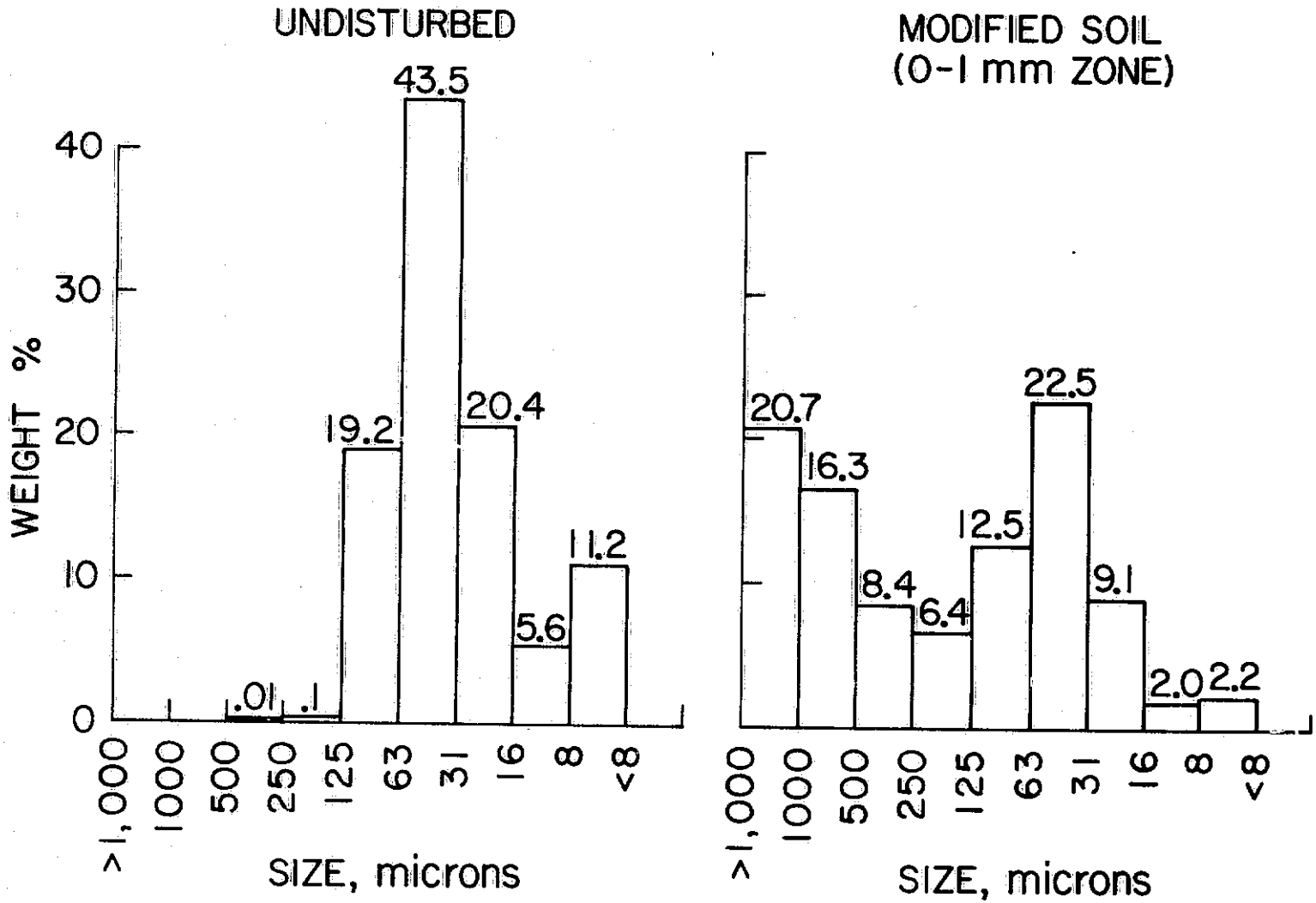
SIZE DISTRIBUTION FOR LOESS SOIL AT WC#4
PENETRATOR IMPACT SITE
UNDISTURBED
MODIFIED SOIL
(0-1 mm ZONE)
WEIGHT %
0
10
20
30
40
.01
.1
19.2
43.5
20.4
5.6
11.2
20.7
16.3
8.4
6.4
12.5
22.5
9.1
2.0
2.2
>1,000
1000
500
250
125
63
31
16
8
<8
SIZE, microns
SIZE, microns

Figure 3

TABLE 2

ELEMENTAL COMPOSITION OF PENETRATOR STEEL ALLOY

Elements	D6A-C Specifications*	Electron Microprobe Analyses (Weight %)
		Penetrator Interior
Fe	96.52-94.95	96.2
C	0.45- 0.50	
Si	0.15- 0.30	0.2
P	0.00- 0.10	0.08
S	0.00- 0.10	
V	0.08- 0.15	0.08
Cr	0.90- 1.20	1.0
Mn	0.60- 0.90	0.7
Ni	0.40- 0.70	0.6
Mo	0.90- 1.10	1.0
		99.86

*Sandia metallurgical report

TABLE 3

MINERALS IDENTIFIED BY OPTICAL MICROSCOPY IN UNDISTURBED LOESS SOIL ADJACENT TO PENETRATOR DROPPED AT WC#4 SITE

Mineral Name	Estimated % Abundance in Undisturbed Soil
Quartz (SiO_2)	60
K-Feldspar-Microcline [$(K,Na)(AlSi_3O_8)$]	10
Plagioclase-	20
Albite ($NaAlSi_3O_8$)	
Mica-	3
Muscovite [$KAl_2(AlSi_3O_6)(OH)_2$]	
Biotite [$K_2(Mg,Fe)_2(AlSi_3O_{10})(OH)_2$]	
Opaques-	3
Ilmenite ($FeTiO_3$)	
Magnetite (Fe_3O_4)	
Hematite (Fe_2O_3)	
Limonite ($FeO \cdot OH \cdot nH_2O$)	
Other Minerals-	4
Hornblende [$Ca_2(Mg,Fe,Al)_5(OH)_2[(Si,Al)_4O_{11}]_2$]	
Augite [$Ca(Mg,Fe)(SiO_3)_2[(Al,Fe)_2O_3]_x$]	
Rutile (TiO_2)	
Zircon ($ZrSiO_4$)	
Sphene ($CaTiO(SiO_4)$	
Garnet [$(Mg,Fe,Mn,Ca)_3Al_2(SiO_4)_3$]	
Tourmaline [$Na(Fe,Mg)_3B_3Al_3(OH)_4(Al_3Si_6O_{27})$]	
Calcite ($CaCO_3$)	
	100

sintered material, and adhering sediment. The results show (see Fig. 4) the Fe content immediately adjacent to the penetrator is about 30% and drops off to about 10% three millimeters away. Similarly, the Cr content immediately adjacent to the penetrator is about 2% and drops off to the ppm level about 1 mm away. However, when the electron beam size was reduced to about a 3-micron-diameter, the Fe and Cr contents were shown to be highly variable. Fe content ranged from 1% to 54%. Two trends (see Fig. 5) are evident for the Fe content: (a) a general increased Fe level in the 10-30% range caused by the introduction of metal from the penetrator, and (b) the natural Fe level in the original sediment which was about 1-2%. The Cr content was shown to be about 3% and dropped off to the ppm level within 1 mm away from the penetrator's skin. Although the abundance of Fe in the penetrator alloy was about 96%, the other elements (Cr, Ni, and Mo) occurred in the alloy at the 1% level (see Table 2). Analysis of the surface of the glass shows that the Cr, Ni, and Mo occur in greater concentrations in the glass than they were in the penetrator alloy, and Fe occurs in a greater concentration in the glass than it was in the host sediment. The Cr, Ni, Mo, and Al concentrations were compared with Fe from place to place within the glass and show (see Fig. 6) that Cr, Ni, and Mo concentrations increase with increasing Fe, whereas Al content decreases with increasing Fe. This demonstrates the Cr, Ni, and Mo were introduced along with the Fe into the host sediments.

Comparisons between the undisturbed and modified soils show (see Table 4) that important changes occurred in elemental concentrations within the glass and in the 1-2 mm zone adjacent to the penetrator. Na is less abundant in the glass than it was in the host sediment and it appears

Fe & Cr CONCENTRATIONS IN GLASS AND SEDIMENT ADJACENT TO WC#4 PENETRATOR USING ELECTRON MICROPROBE WITH 30 MICRON SPOT SIZE

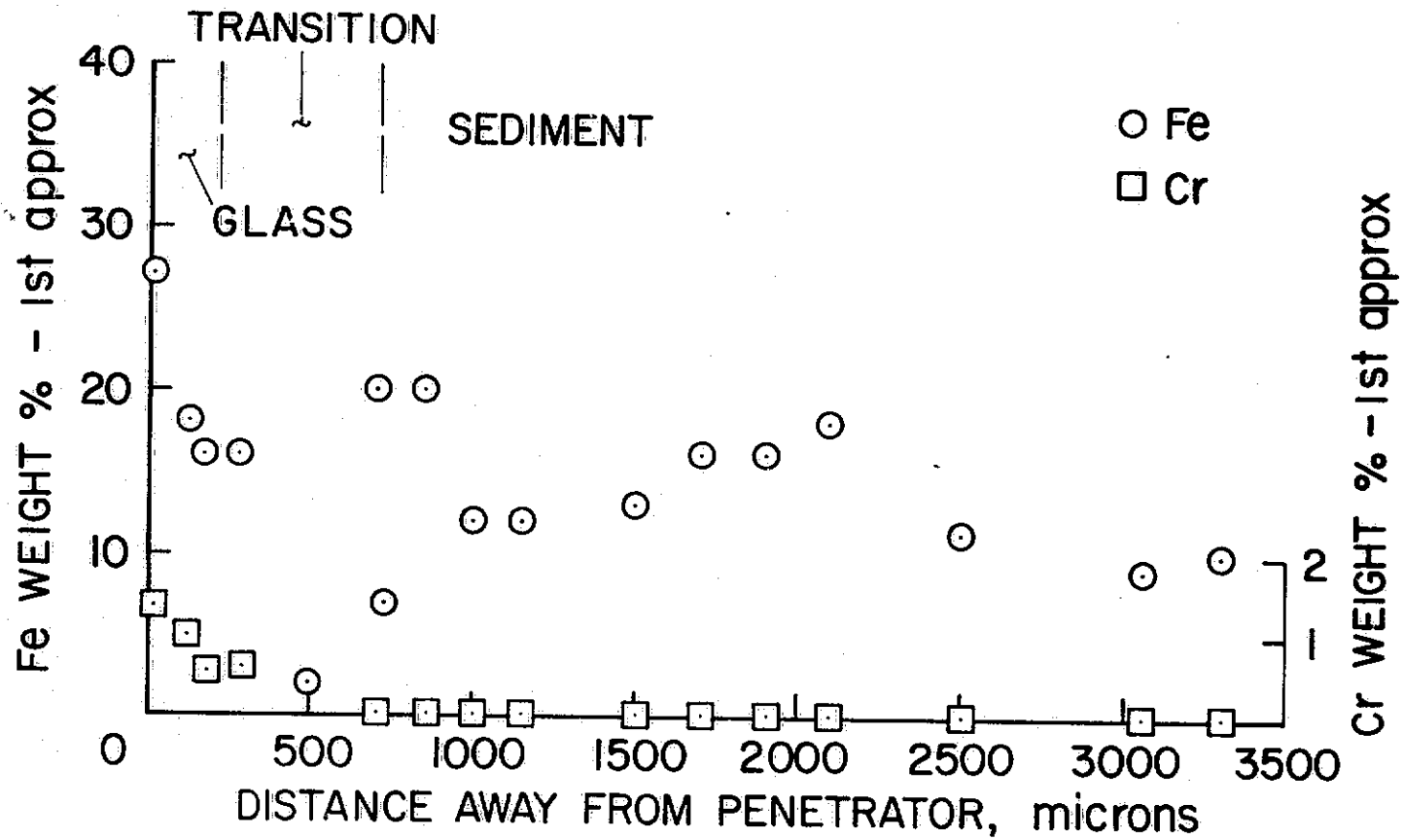

Figure 4

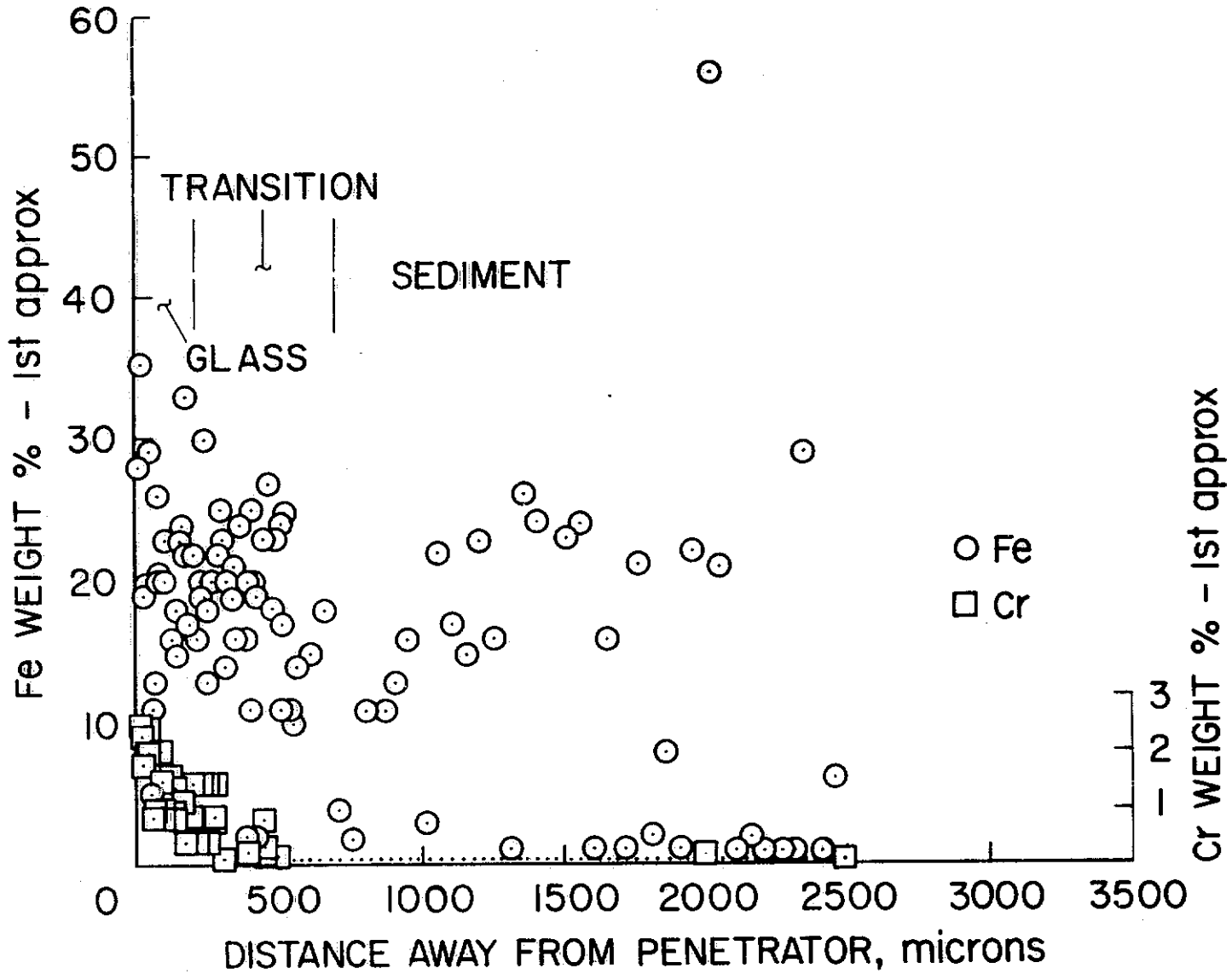
Fe & Cr CONCENTRATIONS IN GLASS AND SEDIMENT ADJACENT TO WC#4 PENETRATOR USING ELECTRON MICROPROBE WITH 3 MICRON SPOT SIZE
TRANSITION
SEDIMENT
GLASS
Fe WEIGHT % - Ist approx
Cr WEIGHT % - Ist approx
Fe
Cr
DISTANCE AWAY FROM PENETRATOR, microns
0
500
1000
1500
2000
2500
3000
3500
10
20
30
40
50
60
1
2
3

Figure 5

RELATIONSHIP BETWEEN Cr, Ni & Mo WITH CONCENTRATION OF Fe CONTENT IN GLASS ADJACENT TO WC#4 PENETRATOR USING ELECTRON MICROPROBE

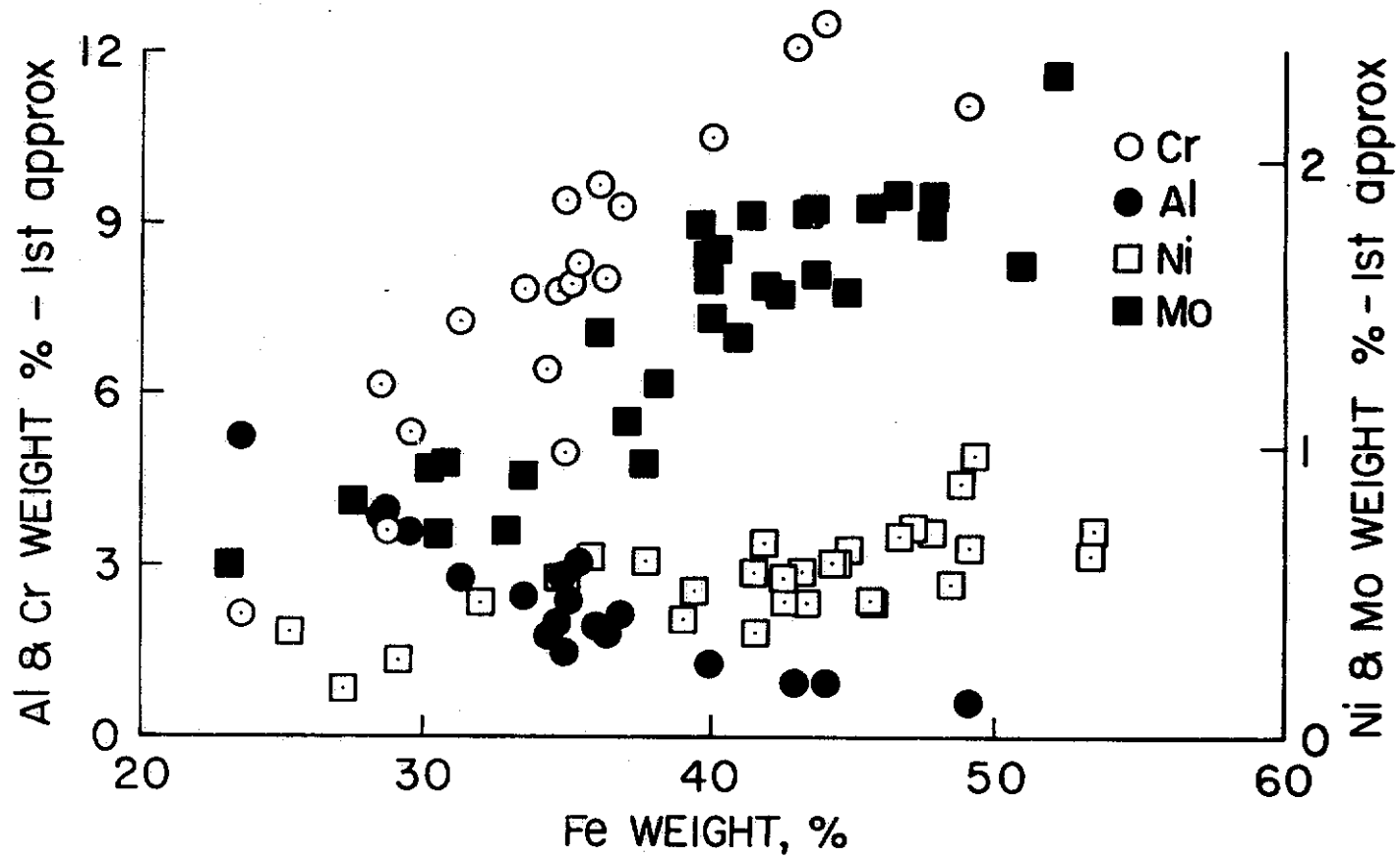

Figure 6

TABLE 4

COMPARISON OF ELEMENTAL COMPOSITION BETWEEN UNDISTURBED AND MODIFIED LOESS SEDIMENT ADJACENT TO PENETRATOR DROPPED ATWC#4 SITE

Element	Undisturbed Soil		Modified Soil Next to Penetrator			
	Sample A (1)	Sample B (1)	1-2mm Zone (1)	0-1mm Zone (1)	Glass Layer Brown (2)	Black (2)
Na	0.53	0.77	1.14	1.21	0.04-.52	0.03-.41
Mg	0.95	0.92	0.87	0.86		
Al	6.22	6.23	6.28	6.01	3.3-6.6	0.6-5.3
Si	31.85	32.11	32.55	31.35	10.5-25.7	2.4-20.7
P	0.06	0.06	0.05	0.06		
K	2.19	2.23	2.20	2.16	0.5-1.0	0.6-1.0
Ca	2.37	2.40	2.28	2.32	2.0-6.2	0.8-3.4
Ti	0.31	0.33	0.31	0.31		
Cr	0.0035	0.0034	0.0032	0.0104	0.2-1.7	2.2-12.5
Mn	0.04	0.04	0.04	0.04		
Fe	2.21	2.22	2.25	3.64	14.2-26.4	23.6-49.0
Ni	0.0015	0.0012	0.0026	0.0064	<0.02	0.02-0.17
Mo	0.0026	<0.0020	<0.0020	0.0107	<0.02	<0.02-7.4

(1) XRF - Sample averaged from forward, middle, and aft sections of penetrator.
(2) Microprobe - 25 separate analyses from each piece located forward, middle, and aft of penetrator.

to have migrated from the glass region thereby increasing its concentration in the 1-2 mm zone. Ca is more abundant in the glass than it was in the host sediment and it appears to have been depleted from the 1-2 mm zone. Fe, Cr, Ni, and Mo are all more abundant in the glass and 1-2 mm zone than they were in the host sediment.

Because most, if not all, of the Fe abraded from the penetrator into the sediment is now hydrated, there seems little chance of determining just how far these particles migrated into the sediment during emplacement. Fe is more mobile than Cr, Ni, and Mo in an aqueous environment. The limit of mechanical mixing for the abraded iron alloy may occur where the concentration of these later elements reaches the background level in the sediments. However, since the abundance of these elements is ten times less than Fe in the penetrator alloy, they may still exist but in such small grains that they are below the detection limit.

The mineralogical changes (see Table 5) characterizing the glass include: (a) introduction of numerous micron size grains of α iron and occasional grains of a Cu-Sn alloy from the penetrator; and (b) the formation of cristobalite, lechatelierite (?), and an opaline-like silica glass. The clay minerals, calcite, and mica have been depleted from the glass. The morphology of some of these abraded metal grains resembles spherules. The mineralogical changes in the sediment farther away from the penetrator (50 μ to 2 mm) include: (a) introduction of α iron particles and a number of iron oxide and hydrated iron oxide phases (e.g., hematite (Fe_2O_3), goethite ($\alpha FeO{\cdot}OH$), limonite ($FeO{\cdot}OH{\cdot}nH_2O$)); and (b) formation of reduced quantities of the opaline-like silica glass (SiO_2nH_2O), occasional droplets of lechatelierite glass (SiO_2) and aragonite ($CaCO_3$) which transformed from calcite.

TABLE 5

GENERAL ABUNDANCE OF MINERALS IDENTIFIED IN LOESS SOIL AT PENETRATOR IMPACT SITE OBTAINED BY XRD, EM, OM

Mineral Name	Undisturbed Sediment	Modified Sediment				
		Behind Screw Head (0-1mm thick)	Inside Screw Hole	Within Glass 0-50μ	50μ-1mm Zone	1-2mm Zone
Silicates						
Quartz	H	H	H	L	H	H
K-Feldspar	L	L	L	L	L	L
Plagioclase	M	M	M	L	M	M
Mica	L	t	t		t	L
Clay	L	t	t		t	L
Hornblende	t	t	t		t	t
Augite	t	t	t		t	t
Cristobalite				t		
Lechatelierite				t (?)		
Amorphous (Opal)		L	L	H	L	
Carbonates						
Calcite	L				t (?)	L
Aragonite						L
Metal						
Iron Alloy (α Fe)		L	L	L	L	L
Cu-Sn Alloy				t	t	
Metal Oxides						
Ilmenite	t	t	t		t	t
Rutile	t	t	t		t	t
Magnetite	t	t	t		t	t
Hematite		L	t	L	t	
Goethite		L	t	L	t	
Lepidocrocite		L		t		
ε Fe_2O_3		L				
Limonite	t	L	L	L	L	L
FeO-Cr_2O_3					t	

H = High M = Moderate L = Low t = trace

Formation of cristobalite demonstrates that the soil temperatures within 50 μm of the skin must have been several hundred degrees above the ambient soil temperature. It seems likely that cristobalite crystallized at the same time the opaline-like silica glass phase was formed and was metastably preserved upon cooling. Most of the glass is now hydrated except for the few small (∿10 μm) droplets of lechatelierite. An attempt was made to determine the melting temperature of the undisturbed sediment. A sample of powdered sediment was pressed and allowed to absorb 16% water and then sealed in a closed tube and heated. The mineral grains became sintered at 1100°C. However, because the closed tube volume was much larger than the sediment tested, the water content of the sediment at the time of sintering was probably 1-2%. Therefore, it appears that the near-dry sediment melts at a temperature above 1100°C, and with a 16% moisture content it will probably melt at a much lower value.

The calcite-aragonite transformation is known to occur at 2-3 kilobars at 20°C. At higher temperatures it occurs at higher pressures. Aragonite was found in this study because it was preserved metastably. However, aragonite has also been produced by prolonged grinding of calcite at 20°C. In this instance it was believed that this kind of transformation is a consequence of combining a shearing force with hydrostatic pressure. It is not certain if this kind of transformation can be produced by the transient pressures caused by the penetrator.

In attempting to reconstruct the sequence of events suggested from the data (see Table 6) obtained thus far, it seems metallic particles were abraded from the penetrator as it forced its way through the sediments. During this action the sediments became deformed and were crushed. The skin of

TABLE 6

TENTATIVE SUMMARY OF CHANGES IN LOESS AT PENETRATOR IMPACT SITE

Region	Material	Elemental Changes		Mineralogical Changes	
		Increase	Decrease	Introduced or Newly Formed	Depleted
0-50μ	Glass layer surrounding penetrator	Fe,Cr,Mo,Ni,Ca(?) (i.e.,Fe 14-49%)	Si,Al,K,Na (i.e.,Si 2-26%)	αFe(Fe,Cr,Mo) Cu-Sn Alloy Cristobalite (SiO_2) Opal ($SiO_2 \cdot nH_2O$)	Mica Calcite Clay
50μ-1mm	Crushed sediment	Fe,Cr,Mo,Ni,Na	Si,Al,Ca(?)	αFe(Fe,Cr,Mo) Hematite (Fe_2O_3) εFe_2O_3 Goethite ($\alpha FeO \cdot OH$) Lepidocrocite ($\gamma FeO \cdot OH$) Limonite ($FeO \cdot OH \cdot nH_2O$) $FeO-Cr_2O_3$ Lechatelierite (SiO_2) Opal ($SiO_2 \cdot nH_2O$)	Calcite? Clay?
1-2mm	Crushed sediment	Fe,Cr,Mo,Ni	?	Aragonite ($CaCO_3$)	Calcite

the penetrator became very hot, perhaps some of the micron size abraded metal melted and oxidized. As the vehicle travelled, the heat from the penetrator raised the temperature of the soil grains in a layer about 50 μm thick (now crushed into powder) to sufficient temperatures to oxidize most of the micron size abraded Fe particles and melt the clay particles of the host sediment. Cristobalite was formed upon cooling in the presence of water during the production of an opaline-like silica glass. Small grains (∿ 10 μm size) of the lechatelierite were also formed on the outside of the glass layer. It seems likely that the iron and iron oxide particulate material abraded from the penetrator's skin, was hydrated and oxidized by the high water content in the soil. This migrating water was also responsible for increasing the Fe content in the matrix of the sediments farther away than 2 mm from the penetrator's skin.

In conclusion, these preliminary results indicate that a sample grabber will be necessary before an onboard α-backscatter or x-ray fluorescence/diffraction experiment can make a meaningful in situ soil analysis. These results must be considered with caution since differences observed between different types of analytical studies have yet to be resolved. Detailed comparisons between x-ray diffraction, electron microprobe, scanning electron microscopy, and optical microscopy will be performed to verify the new and depleted minerals. Differential thermal analysis of the clay minerals has not been completed and will be correlated with low-angle x-ray diffraction studies. Also, additional experiments will be performed in an attempt to determine the temperature the sediments were raised to immediately adjacent to the penetrator's skin.

Additional studies are planned for the full-scale vehicle penetrating the clay layered silt sediments (WC#3). Comparisons will then be made between the two full-scale vehicles with the two 0.58 scale vehicles (WC#2&5) launched by the air gun. The purpose of these later studies is to determine if the soil modification is the same for the small-scale vehicles so that they may be used for future investigations to reduce costs.

REFERENCES

Blanchard, M. and Shade, H., 1975, The effect of a planetary surface penetrator on the soil column surrounding the impacting body, NASA TMX 62,428.

Polkowski, G., 1976, Procedures for preserving subsurface fabric and textures in soil adjacent to an impacted planetary penetrator, L.F.E. Contractor Report TLW 6149.

Shade, H. and Polkowski, G. 1976, Analysis of core samples obtained from the McCook, Nebraska, penetrator test site, L.F.E. Contractor Report TLW 6148B.

Shade, H., 1975, Preliminary analysis of soil modification found after 0.58 scaled penetrator impaction on August 4, 1975, at Sandia, L.F.E. Contractor Report TLW 6142A.

APPENDIX K

INFLUENCE OF PENETRATOR ON LOCAL SOIL TEMPERATURES

William Pitts
Thomas N. Canning
Ames Research Center

Introduction

The calculations presented by Keihm and Langseth illustrate several critical aspects of planetary-heat-flow determination using sensors deployed along the borehole of a penetrator, assuming moderately deep penetration.

A modest parallel effort was directed in the present study to obtain a detailed estimate the temperature disturbances in the soil close to the penetrator and to contrast these disturbances with those along the borehole. Interest in the nearby disturbances stems from the possibility of deploying lateral probes from the penetrator immediately after emplacement to determine undisturbed temperatures at differing depths below the ground surface. The results described herein, obtained using a multinode heat conduction program, describe the effects produced by four penetrator-associated heat sources:

a. the energy residing in the penetrator before impact by virtue of the temperature difference between it and the soil;

b. the kinetic energy of the penetrator dissipated and deposited into the soil during penetration;

c. the kinetic energy of the penetrator dissipated and deposited in the penetrator structure; and

d. the energy released by the Radioisotope Thermoelectric Generator (RTG) after impact.

The above four heat sources may be treated separately, or in combination by superposition because the influences of radiation and free convection are ignored; i.e., the equations are linear. The resulting solutions can then be used as building blocks in studying the prospects for good measurement of the natural soil temperature and thermal properties.

All solutions have been made as an incremental set; for example, when the penetrator kinetic energy is the issue, the RTG power and the initial temperature difference (relative to the soil) are made zero. In all cases the soil thermal conductivity is assumed to be 3×10^{-4} cal/cm °C sec, the highest value anticipated for Mars regolith, the soil specific heat is 0.18 and density is 1 gm per cubic cm. Contact thermal resistance between soil and penetrator skin is assumed zero.

For convenience in presenting the results, the initial soil temperature is taken to be uniform at 0°C.

LAYOUT OF SOLUTIONS

The sketch in Figure 1 shows the penetrator in its final resting position; penetration to a depth of 260 cm is assumed. The penetrator mass is taken to be 30 kg and the impact conditions are consistent with the energies described below. The key assumptions for each building-block solution are summarized and the nodes for which temperature histories are presented are identified as well. The points abreast the penetrator (numbers 1, 2, 3, and 4) typify elements accessible to probes extended immediately after emplacement. The

concept, here, is to measure the local soil temperature quickly (before heat stored and generated in the penetrator can diffuse). The key measurements must be completed in a few minutes.

Several nodes are identified in the borehole wall (numbers 5, 6, 7). These represent the potential locations of sensors mounted on the umbilical cable between the penetrator and its afterbody at the surface. The potential for measurements relatively remote from the penetrator depends on impacting reasonably penetrable regoliths. As shown below, umbilicus measurements provide very much longer test periods free of complex interference from the penetrator body, nose, and RTG than do local measurements.

MAGNITUDES OF ENERGY SOURCES

The initial temperature of the penetrator must lie in the range for good battery performance because implantation requires simultaneous operation of the data system, longitudinal accelerometer, and some of the experiments. Thus prompt operation of the system sensors demand that the initial temperature must lie between 311°K and 243°K. With soil temperature (at depth) ranging from 150°K to 225°K the temperature difference might range from 161°K to 18°K. A temperature difference of 100°K has been selected for these calculations.

The impact velocity of the penetrator, 135 to 165 meters per second, yields a specific energy of 182 to 272 x 10^6 erg/gm or 4.4 to 6.5 cal/gm. Even if all this energy were to remain in the penetrator, the average temperature rise would be only about 22 to 33°K. An experiment described later has shown, on the other hand, that the kinetic energy is divided roughly equally between soil and penetrator and that which goes to the latter is delivered on the ogival penetrator nose. This is consistent with an average temperature rise of the solid ogive of 200°K.

The other half of the kinetic energy is delivered impulsively to the soil lining the borehole; it yields a temperature rise of about 50°K averaged over the inner 1 mm of soil. This model is consistent with studies of soil modification described by Blanchard, et al.

Finally, the long-term heating resulting from RTG operation is taken to be 2.5 cal/sec (about 10 watts). This yields in three days an energy comparable to that for the initial temperature difference of 100°K.

DESCRIPTION OF RESULTS

Stored Energy Term

Conduction of the stored energy (initial bulk temperature difference between penetrator and soil before impact) into the adjacent soil results in fairly prompt and large temperature rises at points 1, 2, 3, and 4 in the lateral array as indicated in Figure 2. Clearly, a probe in such an array must equilibrate within a few hundred seconds, indicated by an estimated cooling curve for a 1 mm diameter steel probe, in order to approach the initial soil temperature before the stored-heat pulse arrives.

Similar curves for the borehole array (5, 6, 7) show that, owing to greater distance from the penetrator and situation beyond the end as well, the stored-heat pulse arrives much later, so that gauge equilibration to local temperature should present no problem.

Borehold Heating by Kinetic Energy

Deposition of half of the kinetic energy at impact in the borehole walls results in an initially high temperature in the borehold array. This temperature history is indicated in Figure 2 for point number 7 (at 35 cm from the penetrator base). The stored heat effect is perceptible in the results only after about 20,000 seconds; thereafter this effect dominates and yields a reversal in trend. Extrapolation of the cooling curve (dashed line) and use of sensors still farther from the penetrator should yield local temperatures with high accuracy, particularly because the uncertainties in the coupling between sensors and the borehole wall are of vanishing importance for such long times.

The small effects of borehole-soil heating (kinetic energy pulse) are shown in Figure 3 for the lateral array points, 1, 2, 3, and 4.

Kinetic Energy Stored in Nose

The other half of the kinetic energy dissipated during deceleration in the regolith is deposited in the ogival nose of the penetrator and is subsequently conducted outward and along the penetrator body. This effect is now shown for the borehole array because it is not felt until long after the initial stored energy pulse has dominated the history. On the other hand, the effect is quite important in the lateral array (see Figure 2, point 2) where initial temperature transients comparable to those resulting from the stored energy are realized.

RTG Power Dissipation

The 10-watt (total) emission from the RTG located forward in the penetrator body dominates over all other effects only after several days of operations as indicated in Figure 3, but its effect may be felt during the prime measuring period in the forward part of the lateral array. A 0.05°K temperature rise is calculated at 25 cm above the penetrator only after 18 hours of operation.

CONCLUSIONS

Although the interfering heat-pulse components from the penetrator compromise the lateral probe scheme for soil-temperature measurement within a few minutes, such a measurement may in fact be feasible.

The measurement of temperatures along the borehole is conceptually simpler because the various heat pulses are greatly delayed. On the other hand, use of this array requires much deeper penetration in order to deploy a sufficiently long umbilicus.

RECOMMENDATIONS

It is recommended that the subsystem development program include the qualification of a multiwire umbilicus for deployment of several thermistors or thermocouples in the borehole.

It is further recommended that numerical modelling of both umbilicus and lateral-probe measurement schemes be made more representative of realistic experiments in order to provide adequate error analyses.

A CAVEAT TO OTHER EXPERIMENTERS

It is seen that the three sources of thermal energy, stored, kinetic, and radioactive, will conspire to warm the environment of the penetrator. Depending on the impact location, the temperature can rise, fall, and subsequently rise or it can rise monotonically throughout the penetrator's operating life. Great care must be exercised to identify all important effects which this may introduce. Some possible effects are:

1. Vaporization, transport, and freezing (elsewhere) of water followed by subsequent revaporization and further transport.

2. Production of a large region of carbon-dioxide-depleted regolith in areas where permafrost (CO_2) is the natural state.

3. Transport of water vapor away from the penetrator resulting from 1 above.

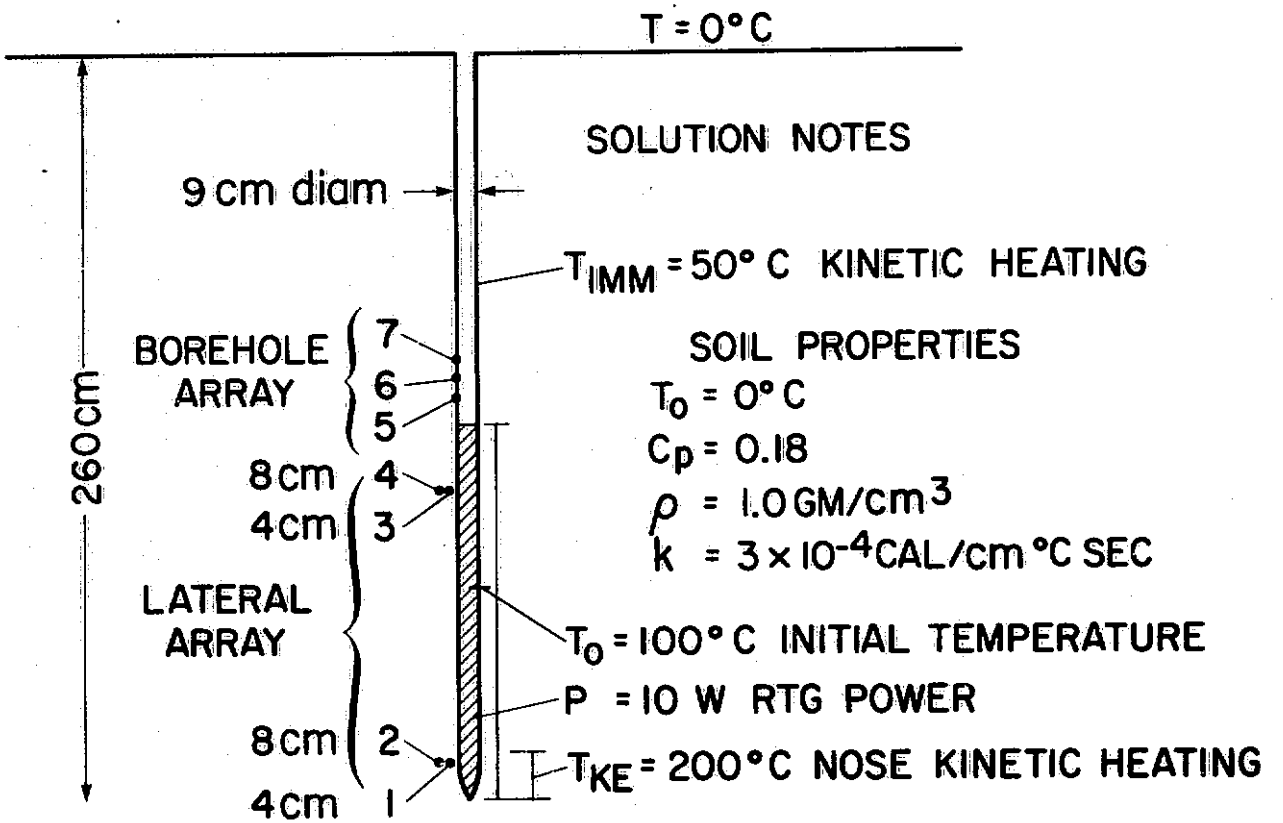

FIGURE I. SOLUTION LAYOUT

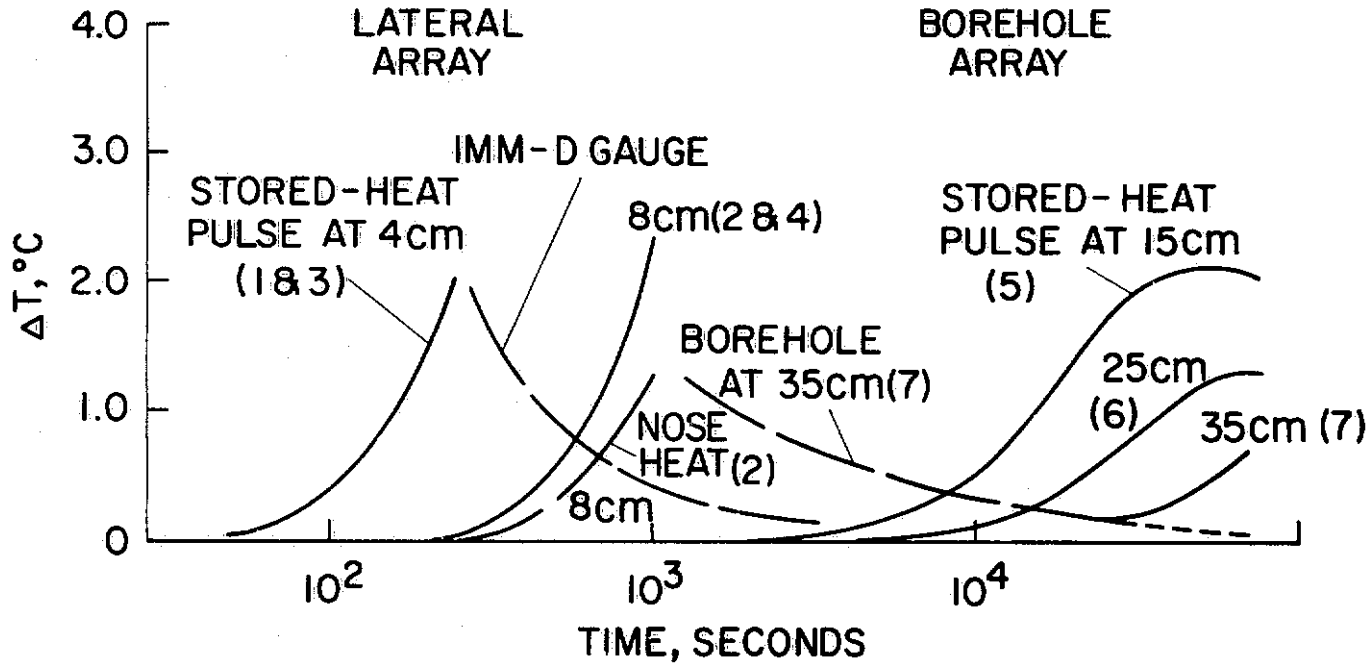

FIGURE 2. PRINCIPAL TEMPERATURE-ERROR TERMS

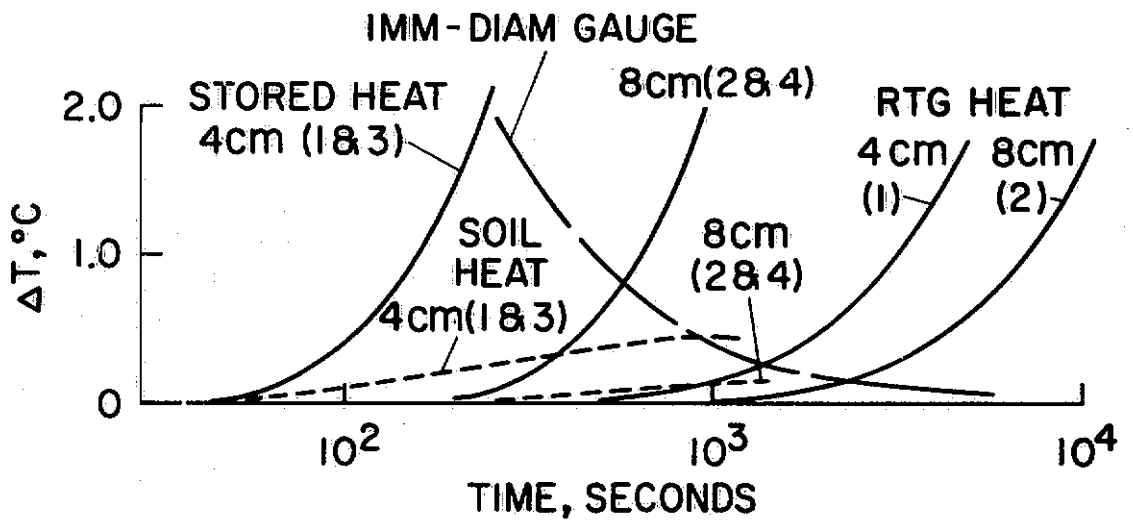

FIGURE 3. RTG EFFECT AT LATERAL ARRAY

A NOTE ON DEPOSITION OF IMPACT KINETIC ENERGY INTO THE SOIL AND PENETRATOR NOSE

By Thomas N. Canning

When a penetrator decelerates as it passes through the soil, most of the kinetic energy dissipated is deposited in a thin film of soil adjacent to the penetrator and in the skin of the penetrator. The latter part is deposited near the nose, where the pressure is high and shear stress is near its maximum. An unknown fraction of the energy (probably small) is dissipated in shear, phase changes, and particle comminution somewhat remote from the interface. If we ignore this last component, it is reasonable to treat the energy left in the soil as a pulsed line-source of energy in an infinite uniform conductive medium. The ensuing temperature variation depends on only thermal conductivity and the amount of energy released.

Reference (1) shows that

$$T = \frac{Q}{4\pi K} \quad \frac{1}{t}$$

T is temperature, °K
Q is energy deposited, cal/cm
K is thermal conductivity cal/sec °C cm
and t is time in seconds after impact.

TEST CONDITIONS

In a full-scale test a 28 kg steel penetrator was aircraft-launched at 133 meters per second into a deep loess target near McCook, NE. The projectile penetrated about 26 feet into the soil, and the deduced deceleration at the 15-foot level was 100 g's (approx.) After an hour's work, a thermistor array was inserted to the 15-foot level and a temperature history recorded for about 3 hours.

The process of inserting the thermistors introduced a delay (and time-distributed) small increment of energy; this yielded a distortion from the proper behavior plus a bias towards a high value of energy deposited.

During recovery of this penetrator, excavation was suspended at the 15-foot level to permit in-situ measurements of thermal conductivity to be made using conventional laboratory techniques adapted to the field. Thermal conductivity was found to be independent of position relative to the borehole; the mean value of 3×10^{-3} cal/sec °C cm was used in analysis of these data. The time-temperature history is shown in Figure 4. The deduced heating of the soil was found to be about 75 cal/cm. The decelerating force of 2800 kg corresponds to a total dissipation of 115 cal/cm.

(1) Carslaw and Yeager: Heat Conduction in Solids, 1959.

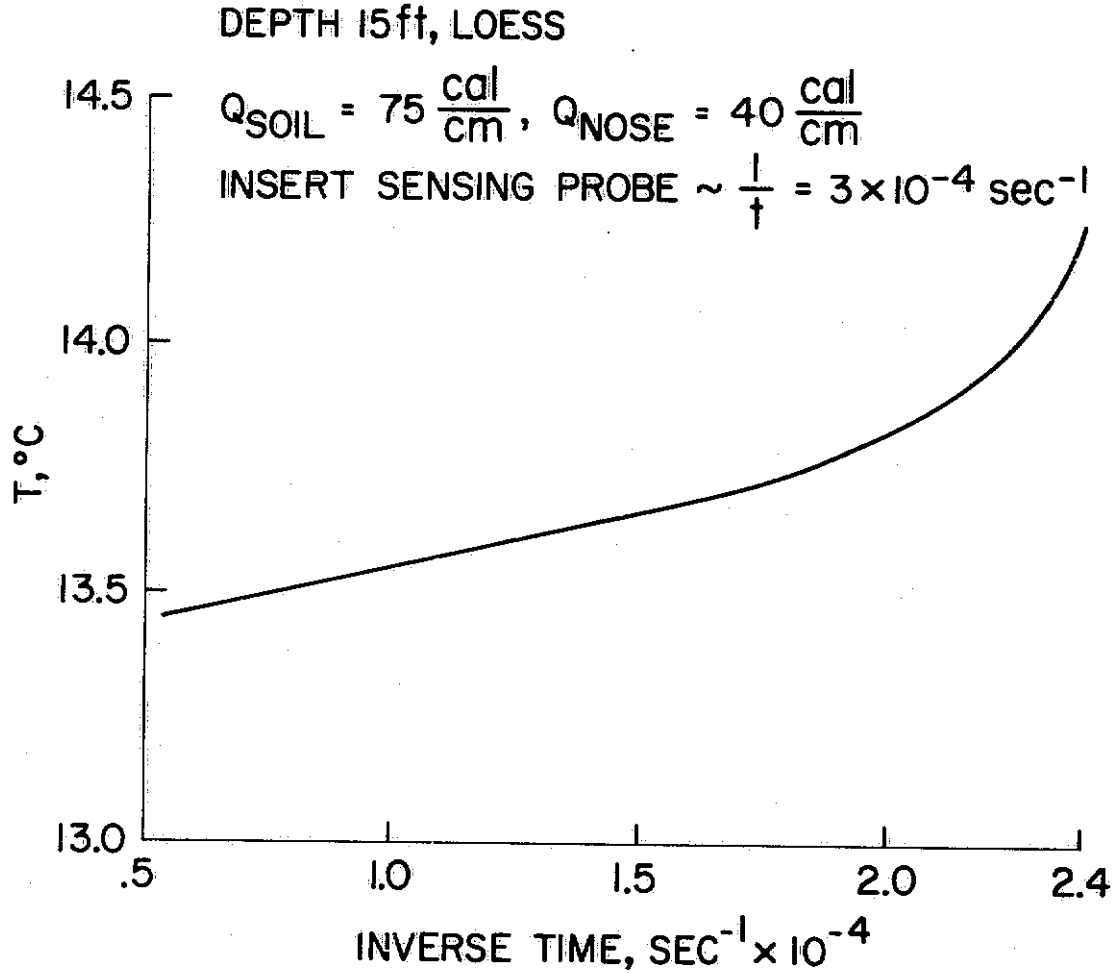

FIGURE 4. BOREHOLE COOL-OFF

APPENDIX L

PENETRATION TEST INTO INSTRUMENTED TARGET

Eric Reece

Sandia Laboratories

Introduction

On December 14, 1975, a 0.58 scale model Mars Penetrator was shot into a prepared target at Sandia Laboratories in Albuquerque. The primary objective of the test was to measure the thermal response of the target material to penetrator emplacement. Temperature data was obtained at four locations in the target. This memorandum briefly describes instrumentation, target construction, test procedures, and test results.

Instrumentation

Thermistors were used to measure the thermal response of the target. In order to achieve the greatest possible resolution, the temperature difference between two thermistors, one located near the penetrator and a reference thermistor located far away (approximately 60 cm.) was measured. It was assumed that the reference thermistor remained at a constant temperature throughout the test. Six thermistor pairs were installed in the target, three pairs each at two depths. The output of the thermistors was hardwired through a signal conditioner to a tape recorder.

Target Construction

A pit approximately 2 meters deep and 2 meters on a side was excavated. A layer of soil about 8 cm. thick was returned to the pit and tamped. Three thermistor pairs were installed by carving a small trench for the thermistor pair and hand packing the soil around the thermistors. After the first three thermistor pairs were installed, approximately 20 cm. of soil was returned to the pit and tamped, and the remaining thermistor pairs were installed. The remainder of the soil was returned to the pit in layers and tamped. The soil used in the target was a silty sand. The gradation analysis is shown in Table I.

Test Hardware

The penetrator was a 0.58 scale model of the forebody of the proposed Mars Penetrator. A sketch of the penetrator is shown in Figure 1. The penetrator was made of D6A-C alloy which is quite hard (42 on the Rockwell C scale). Four strips of temperature sensitive paint were put on the backside of the thin aluminum disc which was mounted flush with the penetrator skin. The strips of paint changed colors at temperatures of 332°K, 380°K, 415°K, and 471°K.

Test Procedure

The penetrator was shot into the target with Sandia's Mobile Gas Gun. Prior to the test the gun was carefully positioned over the desired impact point. The inside of the barrel and the penetrator were cleaned with trichloroethylene and alcohol. The penetrator was loaded into the gun, the barrel was elevated, and the gun was fired. The penetrator came to rest after travelling 1.97 meters into the target.

Test Results

Temperature rises were recorded by four of the six thermistor pairs. The temperature rises are shown as a function of time in Figures 2 and 3.

The locations of the active thermistors, as measured during recovery, are shown in Table II. There was an apparent DC shift in the output of thermistor A-3. The open triangles in Figure 3 represent the uncorrected data; the closed triangles represent the same data corrected for the apparent DC shift. The validity of the data is reinforced by the fact that all thermistors indicate the same temperature rise after 6000 seconds. The greater temperature rise experienced by the lower thermistors (A level) is probably due, in part, to the fact that these thermistors were nearer the nose of the penetrator. Visual inspection of the penetrator nose by Sandia metallurgists resulted in the opinion that the nose may have reached a temperature of 800°K, and perhaps 1000°K. The temperature sensitive paint on the backside of the aluminum disc indicated the surface temperature of the penetrator was greater than 333°K, but less than 380°K at a point midway between the nose and tail.

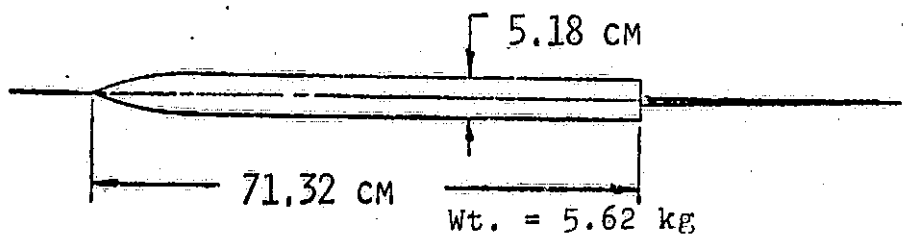

Figure 1. 0.58 Scale Model Mars Penetrator

TABLE I

Gradation Analysis

Screen Size	Cumulative % Passing
No. 4	100
No. 10	98.3
No. 40	95.1
NO. 80	61.1
No. 200	24.7
(Wash Test)	21.8

TABLE II

Thermistor Location

Thermistor	Radial Distance from Penetrator (cm.)	Distance Behind Penetrator Nose (cm)
B-1	6.19	41.58
B-2	4.70	42.54
B-3	2.18	42.69
A-1	6.11	21.74
A-2	4.33	21.74
A-3	2.46	21.74

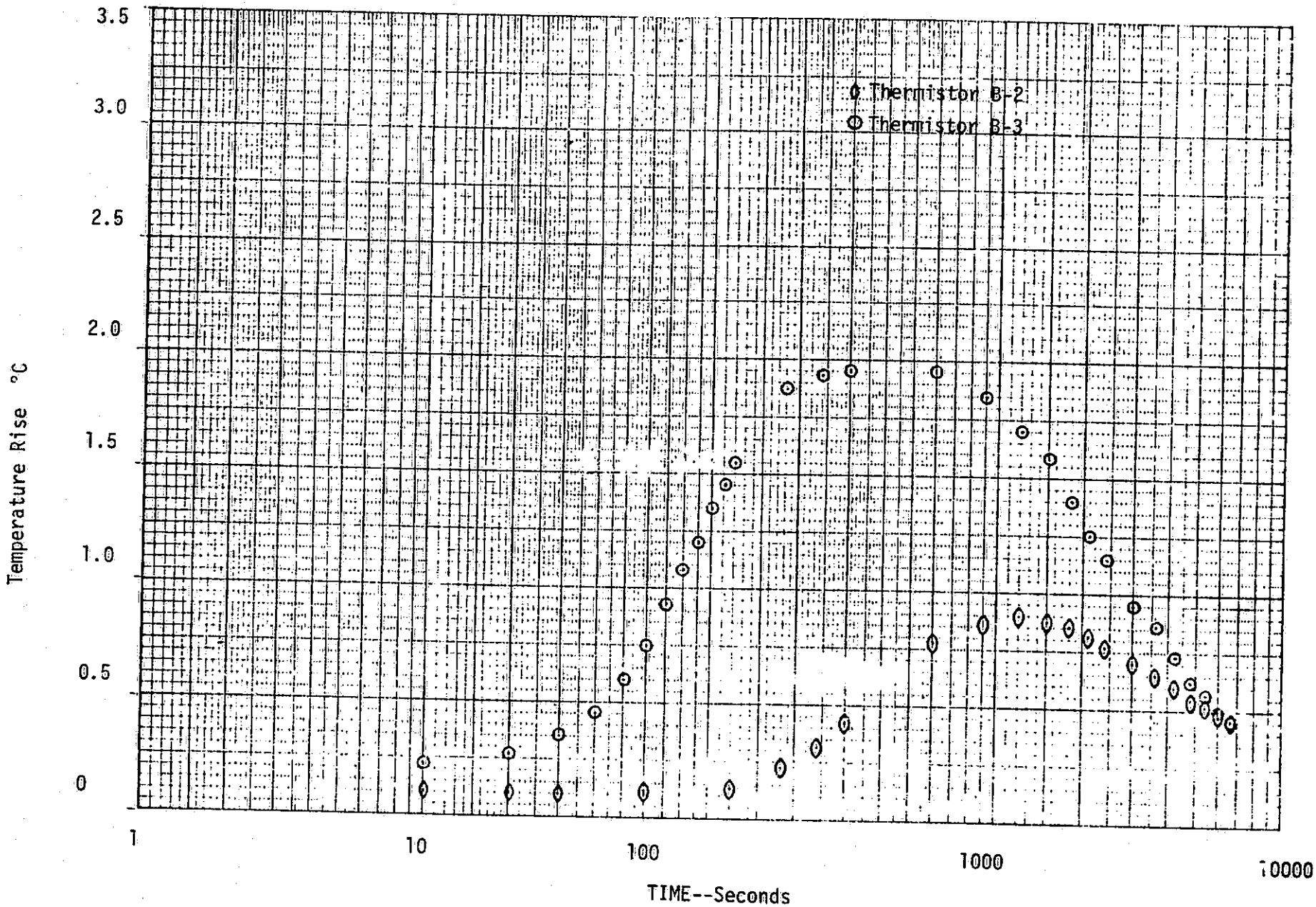

Figure 2. Temperature Rise Versus Time for B-Level Thermistors

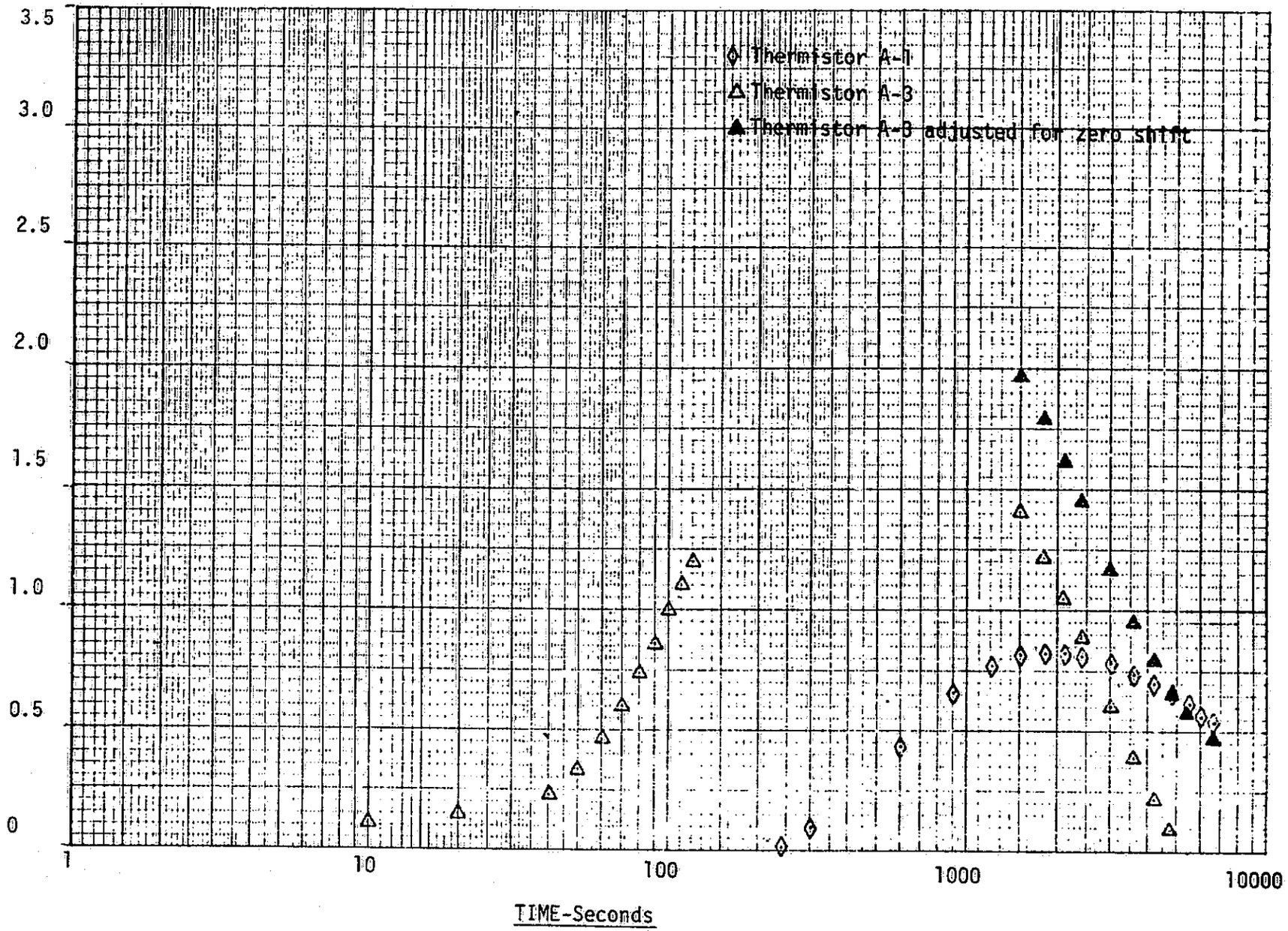

Figure 3. Temperature Rise Versus Time for A-Level Thermistors

APPENDIX M

PENETRATION TESTS IN BASALT AT AMBOY, CALIFORNIA

Eric Reece

Sandia Laboratories

Introduction

During the week of April 12, four full scale Mars Penetrators were dropped into lava near Amboy Crater, California. The purpose of the test was to evaluate the survivability of the penetrators in this hard target and to collect rock samples for contamination study. The penetrators were air-dropped from a U6-A "Beaver" airplane. The release and impact conditions a are shown in the attached Table I.

Penetration Results

The primary target was a plateau approximately 122 meter wide and 244 meter long. The underlying lava was covered by .3 to .4 meters of sand and clay containing pebbles, cobbles, and boulders. The first penetrator impacted at about 213 mps in an area with .3 meter of cover of the lava. The onboard telemetry failed after about 1.5 milliseconds. Integration of the partial record revealed that the depth at which the telemetry failed was about .3 meter. Using Young's penetration equation for layered materials, and matching the residual velocity of the penetrator obtained from the first integration of the partial acceleration record, the penetrability of the overburden was calculated to be $S \simeq 1.1$. Also using Young's equation and the measured distance of penetration, the penetrability of the lava was calculated as $S \simeq 0.70$.

The second penetrator impacted at approximately 152 mps and implanted in a depression just south of the target plateau. The second impact point had about .5 meter of overburden over the lava. The penetrability calculated for this impact point agrees very well with the penetrability calculated at impact point number one ($S \simeq 1.1$ for overburden and $S \simeq 0.70$ for lava.)

The third drop impacted at 152 mps on the target plateau. The impact point had .4 meter of overburden covering about .15 meter of fractured basalt followed by .3 meter of massive unfractured basalt. The penetrability of the lava was $S \simeq 0.65$.

The fourth penetrator was dropped in an area composed completely of material similar to the previously described overburden. The separation between the afterbody and the forebody was about .6 meter. The umbilical remained intact. The penetrability of this target area was calculated to be $S \simeq 1.6$.

All penetrators had "off the shelf" telemetry packages which were not designed to survive hard rock penetration. Consequently, the telemetry packages on the first three units failed upon impacting the lava. The fourth telemetry unit stopped transmitting before impact.

Sample Collection

The penetrators were excavated by using hand tools, jackhammer and backhoe to break up and remove the overburden and basalt. Basalt samples were collected by NASA personnel. Three types of samples were collected from around each penetrator: loose powdered basalt from a zone about 1 mm thick next to the

penetrator, loose chips and small pieces of basalt which showed signs of deformation, and powdered basalt which adhered to the penetrators. The samples were taken to NASA Ames for subsequent study.

TABLE I

AMBOY BASALT TARGET TEST RESULTS

Unit Number	Release Altitude (m(ft), AGL)	Release Speed (KTAS)	Impact Velocity (mps(fps)	Rest Angle (Deg)	Depth to Nose (m(ft))
1	2590(8500)	80	213(700)	7	1.2(4)
2	1980(6500)	80	152(500)	14	1.1(3.5)
3	1980(6500)	80	152(500)	14-1/2	.9(3)
4	1980(6500)	80	152(500)	17	1.8(6)*

*Measured to nose of forebody, .6 meter of separation between afterbody and forebody.

APPENDIX N

FINAL REPORT AND RECOMMENDATIONS OF THE AD HOC SURFACE PENETRATOR SCIENCE COMMITTEE

Douglas Currie
University of Maryland

Jon Fruchter
Batelle Northwest

James Head
Brown University

Charles Helsley
University of Hawaii

Clive Lister
James Tillman
University of Washington

John Niehoff
Science Applications Inc.

James Westphal
California Institute of Technology

FINAL REPORT

and

RECOMMENDATIONS

OF THE

Ad Hoc Surface Penetrator

Science Committee

to

Planetary Programs Division

Office of Space Science

National Aeronautics and Space Administration

Washington, D.C.

12 August 1976

Foreword

In August 1975, J.A. Westphal was asked by NASA Headquarters to organize an Ad Hoc group to look carefully at the surface penetrator concept and express its opinion as to feasibility and desirability of such missions, especially to Mars.

A group was recruited who were unlikely to be principal investigators on such a mission, and yet had expertise and experience with the potential scientific experiments. An attempt was made to find people with broad, innovative views. A committee consisting of:

Douglas Currie, University of Maryland - Physics
Jon Fruchter, Battelle Northwest - Geochemistry
James Head, Brown University - Geology
Charles Helsley, University of Hawaii - Geophysics/Geology
Clive Lister, University of Washington - Geophysics
John Niehoff, Science Applications, Inc. - Engineering
James Tillman, University of Washington - Meteorology
James Westphal, California Institute of Technology - Chairman

met first at Ames in January 1976 to familiarize themselves with the details of the penetrator concept as it was then defined. Subsequent meetings were held in Albuquerque and Pasadena dealing principally with the science capabilities of penetrators. The committee and its individual members met and talked with most of the people known to have a direct interest in penetrators. Tom Canning from Ames acted as general NASA liason. The committee also had input from Steve Dwornik, Paul Tarver and Dan Herman from Headquarters.

Committee Membership

Professor James A. Westphal, Chairman
California Institute of Technology
Pasadena, California 91125

Dr. Douglas Currie
University of Maryland
College Park, Maryland 20742

Dr. Jon Fruchter
Battelle Northwest
Richland, Washington 99352

Dr. James Head
Brown University
Providence, Rhode Island 02906

Dr. Charles Helsley
University of Hawaii
Honolulu, Hawaii 96822

Dr. Clive Lister
University of Washington
Seattle, Washington 98195

Mr. John Niehoff
Science Applications, Inc.
Rolling Meadows, Illinois 60008

Mr. James Tillman
University of Washington
Seattle, Washington 98195

Recommendations

We firmly believe that penetrators represent a valuable and necessary platform for the conduct of certain essential in situ experiments in the exploration of a majority of solid solar system bodies. Therefore:

1. We recommend that, for both science and engineering reasons, the first penetrator mission undertaken be to Mars, and that this be done during the 1981 launch opportunity;
2. We understand that the scope of a 1981 Mars Penetrator mission may necessarily be dictated by a highly constrained NASA budget. We therefore recommend that a minimum viable mission must consist of at least 4 penetrators, and that each of these penetrators must carry a seismometer, an afterbody imager, and at least one of the following additional experiments:
   a) chemical composition
   b) total water measurement
   c) heat flow
   d) afterbody meteorology.

In our opinion, with reasonable effort it will be possible to fly all of these experiments plus a few others.

Introduction

The full potential of solar system exploration will only be realized with the application of a variety of spacecraft concepts and mission modes. As our base of knowledge expands from the returns of flybys and orbiters, the quest for in situ surface measurements can be expected, and indeed has already begun on several bodies, i.e. the Moon and Mars. To date these investigations have been undertaken by the comparatively large, complex and expensive soft-landers, Surveyor and Viking. While soft-landers play an important role in surface exploration, they cannot realistically be sent to a large number of the solid bodies in the solar system. Other simpler, less expensive spacecraft will be needed.

One such device that has been successfully applied to a wide range of terrestrial problems is the penetrator - a missile-shaped object which impacts the surface at high speed and dissipates its kinetic energy by penetrating to depths of 1-15 meters with its science package and associated power and electronics. An impact-hardened afterbody remains at the surface with a transmitter to relay collected data to an orbiting spacecraft. It is connected to the penetrating forebody by an umbilical cable which is deployed during the process of penetration. Light-weight science sensors may be carried on the afterbody in addition to the main forebody payload. Nominal physical characteristics of a Mars penetrator are summarized in Table 1.

Table 1

NOMINAL MARS PENETRATOR CHARACTERISTICS

Complete Penetrator

Weight	31 kg
Principal diameter	9 cm
Frontal area	64 cm^2
Sectional density	0.5 kg/cm^2
Length	140 cm

Payload*

Weight	7 kg
Volume	4500 cm^3
Power Output (RTG)	0.3 watts
Battery Supplement	1.0 watt hrs/day
Data Storage	2×10^5 bits

Forebody Probe

Weight	28 kg
Principal diameter	9 cm
Frontal area	64 cm^2
Sectional density	0.5 kg/cm^2
Length	123 cm

Detachable Afterbody

Weight	3 kg
Principal diameter	23 cm
Frontal area	350 cm^2
Sectional density	0.01 kg/cm^2
Length	28 cm

* Includes science and supporting electronics.

The purpose of this report is to summarize the findings of the Ad Hoc Surface Penetrator Science Committee regarding the merit of proposed penetrator science experiments and their potential value to surface exploration of solid bodies in the solar system. Our efforts have been focused on assessing two of the important questions which bear directly on the present stage of terrestrial body exploration. These are:

1) Are penetrators a superior means of answering really important basic scientific questions?
2) Are there enough feasible experiments to make a mission really attractive?

We have concluded that the answer to both questions is an enthusiastic YES.

Internal global structure, surface and near-surface chemical composition, and planetary heat flow are among the most basic and essential facts one needs to begin to understand the nature, history and evolution of a solid planet. Experiments capable of acquiring this information are well suited to penetrators. Furthermore, the ability to emplace instruments in widely separate regions of a planet on one relatively low cost mission makes the penetrator a prime tool for future planetary reconnaissance. Thus one mission will yield several samples of surface morphology, heat flow and chemical composition, and allow high quality seismic measurements of the internal structure. The second question, regarding sufficient feasible experiments, is addressed in the next sections of this report. The committee has classified the experiments which have been proposed for penetrator

missions into four levels of priority. Our evaluation of experiments in the first two levels is then presented in detail. The report concludes by summarizing our assessment of the penetrator concept and its capabilities for planetary exploration.

The Committee feels that penetrators are a logical follow-on mission to Viking. For this reason, the discussions which follow are presented in the context of a Mars mission. Nevertheless, we wish to emphasize that penetrators are applicable to the exploration of many of the other solid bodies in the Solar System.

Science Priorities

A large number of experiments have been discussed for penetrator missions. A compilation of the experiments specifically proposed to the Committee is presented in Table 2.

We feel strongly that, with limited mission capability, it is essential at this early stage to develop experiment priorities so that the scientifically most important questions are addressed, and that a rational mix of experiments are flown. This also implies priorities for development and a pre-existing strategy for experiment selection.

Scientific priorities are to some extent subjective. However, we feel that rational judgements can be made more easily if they are made early and by competent scientists not likely to have vested interests in the result. We have attempted to set such priorities within our limited expertise. To this end we first developed the following experiment class definitions:

Class 1: Essential.

Class 2: To be included, if feasible.

Class 3: Highly desirable, if feasible and provided there is no major negative impact on Class 1 and feasible Class 2 experiments.

Class 4: Secondary, use as accommodation permits, if feasible and provided there is no significant negative impact on Class 1, 2 and 3 experiments.

Using these classes as a guide, each of the experiments presented in Table 2 were discussed by the Committee in the context of an early Mars mission and a censensus was reached for their classification. The resulting priority of the proposed experiment is as follows:

Class 1: Seismic Measurement
Imagery

Class 2: Chemical Composition
Heat Flow
Total Water Measurement
Meteorology (Temperature, Pressure, Wind)

Class 3: Frost and Dust Detection
Organic Geochemistry (Re-evaluate after Viking GCMS results are available)

Class 4: Ion Geochemistry
Magnetometry
Nutrient-Induced Biology
Atmospheric Relative Humidity
Soil Electrical Conductivity

It became apparent to the Committee, in the process of these classifications that a minimum Mars penetrator mission must consist of the Class 1 experiments and at least one Class 2 experiment. Detailed discussions of what Class 1 and 2 experiments should accomplish are

presented in the sections which follow. We feel that all Class 1 and most Class 2 and 3 experiments can in fact be flown if a real effort is made promptly.

Table 2

POTENTIAL PENETRATOR SCIENCE

CLASS	MEASUREMENT	INSTRUMENTS
INTERIORS	SEISMICITY	SEISMOMETERS, TILTMETERS
	HEAT FLOW	THERMOCOUPLES
	MAGNETICS	3-AXIS FLUX GATE
SUBSURFACE	ELEMENTAL COMPOSITION	α-PARTICLE (α,p, X-RAY), γ-RAY SPECTROMETER
	CHEMICAL COMPOSITION	NEUTRON FLUX ANALYZER, γ-RAY SPECTROMETER
		WATER HYGROMETERS
		PYROLITIC CHAMBER, ION CHAMBER
	MINERALOGY	α-PARTICLE/γ-RAY SPECTROMETER
	SOIL PROPERTIES	ACCELEROMETER, γ-RAY SPECTROMETER
	BIOLOGY	ION CHAMBER
SURFACE	SITE CERTIFICATION	IMAGER
	GEOLOGIC SURVEY	IMAGER
	METEOROLOGY	ANEMOMETER, PRESSURE GAUGE,
		THERMOMETER, IMAGER
	AEOLIAN PROCESSES	IMAGER
	VOLATILE TRANSPORT	IMAGER, METEOROLOGY INSTRUMENTS

Mars Penetrator Seismic Experiment

General Background

Many remote sensing experiments have been used, or have been proposed to be used, for the exploration of solid bodies within the solar system. Many of these deal with the chemistry and morphology of the surface or near surface layers. Seismic experiments permit one to extend this knowledge into the subsurface and provide general constraints on the mechanical, thermal and chemical zonation within the interior of the planet. Detailed knowledge of internal planetary structure is crucial to our understanding of the chemical and thermal evolution of the solar system.

On the earth, seismic observations made during the last century, and primarily during the last thirty years, have enabled us to develop a detailed understanding of the chemical zonations within this planet and their evolution with time. Within the past decade we have acquired a similar, though much less extensive, data set for the Moon, one that has enabled us to constrain chemical evolution models for a second planetary body. For these reasons, a seismic experiment was included on the Viking missions. Unfortunately the Viking I seismic system is not working, and even if a similar malfunction does not occur on the second Viking mission this will leave us with almost no knowledge of the structure of the interior of the planet - knowledge that is critical for our understanding of planetary evolution. Thus, it appears to be imperative to incorporate a seismic system within proposed future missions. The penetrator concept appears to be a unique means of emplacing seismic systems on Mars, or on

any other solid planetary body.

Scientific Goals

In order to understand the interior zonation of a planet, via seismic methods, at least one broadband three component instrument is necessary. Under ideal conditions for a spherically symmetric planet, one system and a very large seismic event is all that is necessary. However, on Mars an ideal spherical symmetry does not exist. Thus it will be necessary to emplace three or more instruments in order to simultaneously determine the time of origin of an event, its location, and the velocity structure between the source of the event and the detector. With such an array, one can achieve the following scientific objectives:

1) The determination of a velocity vs. depth function.
2) The distribution of seismic sources.
3) Identification of phase change and/or chemical boundaries within the planet (by means of abrupt velocity changes).
4) Identification of a liquid planetary core, if present.
5) Identification of zones with high (or low) Q.
6) Determination of a thermal profile for the interior of the planet.
7) Identification of asymmetries within internal planetary structure.
8) Identification of tectonically active zones both near surface and at depth.

All of these scientific goals can be acquired with instrumentation that is currently developed and is suitable for use on a penetrator mission.

Instrumentation

In order to accomplish the objectives stated above, it will be necessary to implant three three-component instruments on the surface of Mars. Each of these instruments should be capable of detecting signals from seismic events in the bandpass 0.01 to 10 Hz. Sensors are available that are capable of recording over this bandpass and that are sufficiently small that they can be accommodated within the space available for scientific packages within the penetrator.

Three types of sensors are currently under investigation, and all appear promising. The bubble seismometers appear to be ideal for the detection of horizontal seismic signals. A miniaturized version of a conventional seismometer, or a force-balance accelerometer appear to be most suitable for the detection of vertical motions. All three of these sensors are commercially available, and thus should not require extensive development efforts. The electronics for each, however, would have to be miniaturized.

Necessary Engineering Development

The primary need for future investigations is to design a miniaturized leveling system that would allow the establishment of local vertical after the penetrator has been emplaced, and to devise practical means of data compression so that the maximum information content can be returned to the earth without undue data requirements. This should not be overly difficult, since much of this development has already been undertaken for the Viking mission.

Mars Penetrator Afterbody Imaging Experiment

Information on the surface characteristics and process of a planet is basic to the understanding of planetary evolution and to the interpretation of data obtained from other experiments. The recent successful Viking I surface imaging experiment illustrates these points well. The initial imagery returned by Viking I shows a wealth of features indicating the variety of processes operating or previously operative at the site (impact cratering, aeolian activity, volcanism, and possible tectonism and fluvial activity). Longer-term observations will isolate and document rates of change and detailed surface modifications (aeolian activity and diurnal variation of precipitates, for instance). Viking I also illustrates the significance of imagery in supporting and interpreting other experiments (choice of sampling site, physical properties of surface material, monitoring of other equipment such as sampling arm, providing a framework for interpretation of geochemical analyses, etc.).

Examples of Scientific Objectives of an Imaging Experiment

Near Field Observations

Rock Characteristics. Analysis of the size distribution, surface characteristics (rounding, vesicularity, etc.), internal features (phenocrysts, clasts), and albedo, of surface rocks will provide important information on the geologic processes operating at the various sites.

Soil Characteristics. The observed characteristics must be related to the site context as ascertained in far field observations and orbiter imaging. Particle sorting, ripples, dunes, layering and ejecta characteristics would be studied. Sites on volcanos at sufficiently high altitude

may yield bedrock surfaces to study primary lava flow morphology and rock type. In arroyo sites the degree of rounding will be of interest in terms of studying flow regimes.

Cratering. In any areas where the bedrock is exposed, small craters may have been preserved, in which case their areal density and state of preservation would be of interest in connection with cratering rates, secondary cratering, erosional and filling processes.

Aeolian Processes. During a long mission some movement of the soil may occur as a result of winds. Repeated imaging should provide observations of how the dust is deposited and removed near small scale positive and negative topographic features. This would be relevant to the problem of Martian albedo feature generation and to local and global rates of sediment production and movement.

Condensation Processes. This analysis would be particularly significant where several sites could be observed. In winter and in the early morning hours surface condensation of water and CO_2 ices may be observed at some sites. The determination of the temporal history of ices (which would involve several images) would be of considerable interest since there are many poorly understood problems involving water processes and polar cap phenomena (e.g. does wind drifting of CO_2 ice play an important role in determining the rate of retreat of the caps).

Far Field Observations

Site Characterizations. In addition to characterization of the site for support of other experiments, penetrators could be targeted to many diverse regions on Mars where relatively detailed observations

of land forms would have significant value. Specific land forms of particular interest are dunes, rock formations, layered deposits, arroyo beds, landslides, cliffs (and associated stratigraphy), volcanic forms and polar cap features. In this way, surface observations could provide verification of the detailed characteristics of major geologic units defined from orbit. This information is a necessary prerequisite to the successful understanding of these fundamental units and to their planet-wide extrapolation.

Dust Storms. Although the Viking Lander cameras may provide the first surface images of dust storms, it is likely that penetrator cameras, operated when orbital imaging indicates the presence of dust clouds, could contribute usefully to the study of this phenomenon. The combination of orbital imaging and IR data together with the surface images could be a powerful means of understanding how dust storms begin, propagate and decay.

Condensate Clouds. The manner in which seasonal water ice clouds form in the tropical areas, typically in the vicinity of volcanos and canyons, will not be well studied by either Viking or, probably, by a Mars Polar Orbiter. Imaging at different times of day, principally in the morning, on successive days at sites where clouds occur could help understand this phenomenon, particularly if a meteorology package is included in the payload. The pictures could determine whether the clouds form at high or low altitude and whether surface condensation plays any role.

Atmospheric Properties. Quantitative analysis of sky brightness and characteristics of the sky would be extremely important information

for analysis of Martian atmospheric properties and their variation due to dust and other factors.

Examples of the Supporting Role of an Imaging Experiment

Star Observations. A penetrator imaging system could be used to determine the position and orientation of the probe. This would have particular value for the seismic experiment. The area array cameras can be used for long exposures, particularly at night when temperatures are low, and therefore should be able to detect bright stars. It is estimated that an exposure of only about 100 seconds would be needed.

Macroscopic Examination of Rock Types. This would provide an important framework for interpretation of geochemical results in terms of characterization of indigenous rock types and textures. Similarly, analysis of the vesicularity of rock types would provide important information for heat flow calculations.

Characterization of Substrate. Determination of local topography will be important for the interpretation of meteorology data. Analysis of the presence of bedrock exposures, evidence for depth to bedrock, and grain size analysis of particulate matter will be significant in establishing a framework for the heat flow and geochemical analyses. Imagery, in conjunction with the accelerometer record, will help determine whether the geochemical analysis is in local bedrock or in a winnowed or transported aeolian deposit. Such a framework will provide confidence in the ability to extrapolate local results to planet-wide units. This type of characterization will also be important in the seismic investigation.

Summary

The use of a camera on the penetrator afterbody would provide some very interesting direct scientific results, as well as provide very strong support for a number of other experiments. It would appear that this system is technically feasible, and the current developmental status of such a camera is within a 1981 launch schedule requirement.

Mars Penetrator Water Detection Experiment

Because of its essentiality to life, the presence or absence of water on planetary bodies is a question of very high priority. If water is present at the surface or in the regolith, it will nearly always be present in detectable quantities in the atmosphere. The detection of water in a planetary atmosphere therefore answers the question of first priority. However, the levels of water vapor present in the atmosphere are not at all a reliable measure of the quantities of surface and subsurface water, nor are the levels of atmospheric water of much significance in biological considerations beyond establishing its presence, as living organisms require a liquid phase which occurs most commonly on or in the surficial layer. Hence the measurement of soil water in its various forms at representative locations, and under a representative variety of climatological conditions, is an objective of the highest priority in a planetary lander mission.

One potential experiment actually measures hydrogen content rather than water directly. It uses the fact that hydrogen atoms are very effective at moderating fast neutrons, such as those emitted by the RTG. Other atoms also moderate neutrons, although they are much less effective than hydrogen. If a geochemistry experiment is on board (α-particle or x-ray), then the composition of the target will be known so that the effects of other atoms can be calculated and subtracted. Because it would be sensitive to other forms of hydrogen (organic, etc.) besides water or ice, the experiment's interpretation would be a little ambiguous.

However, hydrogen in any form is of considerable interest, and the neutron experiment is likely to be less ambiguous than other water detectors which have been proposed. It has the advantages that it samples a relatively large volume around the penetrator, that it does not require any special sampling apparatus, and that it is sensitive to water in solid or liquid as well as gaseous form. The experiment has an estimated measurement sensitivity of about 0.05% H by weight which corresponds to about 0.5% water by weight. About 1% is typical of the amount of water contained in terrestrial basaltic rocks. Since it is quite likely that rocks and soils on the surface of Mars and other planets may be somewhat lower in water content than terrestrial rocks, it would be nice to have better sensitivity than this.

No development work has yet been done on a neutron-hydrogen detector for use in a planetary penetrator. However, all of the required components are shelf items. Neutron-hydrogen detectors are in common use for terrestrial well logging operations. Thus, there would seem to be no conceptual problems. Future work would involve designing an instrument which is compatible with the spacecraft requirements, building a preliminary instrument, shock testing it, calibrating it and testing it under field conditions. Some consideration should also be given to possible interference from hydrogen-containing plastic parts in the penetrator.

Another potential water experiment proposes the procurement of a sample of the regolith by a mechanical drilling technique, sealing this sample of known volume in a crucible and then detecting the water

driven off the sample by pyrolysis. This technique utilizes a P_2O_5 electronic detector which electrolyzes the water driven off the sample. By doing the pyrolysis in steps, both the free water and the bound water released as a function of temperature can be recorded. Although somewhat more complex than the neutron method, the pyrolysis experiment yields much more valuable data for both biological and mineralogical interpretation. The development of the detector and of the sampler concept has already received considerable effort.

Mars Penetrator Chemical Composition Experiments

Knowledge of the chemical composition of a planet is fundamental to our understanding of the nature of that planet, including the processes which formed it and subsequently modified it. Two types of measurements are important. The first is determination of the chemical composition of important components such as rocks, soils and atmospheres into which the planet has differentiated. Unless the planet is completely chemically homogeneous, the composition of the planet as a whole cannot be measured directly. Instead, it must be deduced by applying geochemical principles to measurements of the various differentiated components, such as rocks. Geophysical measurements such as seismic velocity profiles are also important in ascertaining the chemical composition and phase relationships of the planetary interior. Direct chemical measurements can be made only of the accessible exterior of the planet. In the case of soft-landers and orbiters, only the top few millimeters or centimeters are accessible to measurement. Penetrators are capable of extending this depth to about ten meters, a depth at which better and more representative samples may be available. The penetrator will also be capable of sampling a large number of locations, which is important in chemically characterizing a planet. Two potential experiments, the alpha backscatter and gamma ray detector, have been proposed. Both of these detectors have had successful application on the Moon.

An alpha backscatter experiment modified to include proton and x-ray modes has the potential for measuring the largest number of chemical elements with at least adequate precision. Adequate precision

is here defined as ±3% relative for major elements (>1%) and ±10% relative for minor and trace elements (<1%). Of course, better precisions than these are highly desirable and it appears the α experiment is capable of delivering better precision for at least many of the major elements. For most of the trace elements the situation is not as clear, since the published sensitivities are in many cases quite close to the levels expected in Martian rocks. Of course, the limitations might be different for other planets. The two tables (3 and 4) on elemental precision and elemental sensitivities were taken from a paper by Turkevich, Economou and Franzgrote.

The α-proton-x-ray experiment is particularly well suited to the detection of the lighter elements (below Mg in the periodic table) which would be very important if Mars or other planets of interest turned out to be volatile rich. This feature will be important on Mars even after Viking, because the instrumentation on Viking will not be capable of making good measurements on atoms lighter than Mg. The concentrations of light elements have significant biological implications as well as importance for the geochemical nature and history of a planet.

The major limitation on the α backscatter experiment is the very shallow (~ a few microns) sampling depth caused by the fact that α particles are densely ionizing. The x-ray modification of the experiment still has the same difficulty, because the x-rays are excited by α particles. Tests showed that serious contamination of both loess and basalt targets by the penetrator extended out to a distance of almost 2 millimeters from the surface of the penetrator, and that some alteration extended out to a centimeter from the penetrator surface. Thus,

Table 3

Expected Accuracies (at 90% confidence limit) in Weight Percent for Principal Chemical Elements ("Mini-Alpha")

Element	$\alpha + p + X$ ray Modes
C	± 0.2
O	± 0.7
Na	± 0.2
Mg	± 0.8
Al	± 0.4
Si	± 1.2
K	± 0.2
Ca	± 0.2
Ti	± 0.08
Fe	± 0.2

Table 4

Examples of Expected Sensitivities
("Mini-Alpha" Instrument)
(In Weight %) for Minor Elements
(Evaluated for a Basalt Matrix)

Element	α + p + X ray (alpha and auxiliary sources
H	0.03*
N	0.2
F	0.05
P	0.2
S	0.1
Cl	0.1
K**	0.07
V	0.03
Cr	0.02
Mn	0.03
Ni	0.02
Cu	0.02
Zn	0.02
Rb	0.001
Sr	0.001
Y	0.0005
Zr	0.0005
Ba	0.001
La	0.001
Ce	0.0008
Nd	0.0008
Sm	0.0005
Pb	0.005
Th	0.005
U	0.005

* Using thermal neutron detection techniques.

** Sensitivity for K expected in the presence of a few weight % of Ca.

in the present configuration of the penetrator, an α spectrometer would view seriously contaminated material. As discussed below in the section on future work, this problem must be solved in order to make the α experiment a viable alternative. In addition to the contamination problem, the shallow sampling depth means that only a very small volume is sampled, raising serious questions about how representative a sample is obtained.

At present the status of the hardware for the α experiment is progressing satisfactorily. The basic concept has already been successfully employed on the lunar Surveyor missions. In addition, critical components of the system have been shock tested and seem capable of withstanding at least 1,800 G's. The miniaturization required for adaptation of the instrument to penetrators has not yet been demonstrated in an actual instrument, but there seem to be no conceptual difficulties. One problem is that the present x-ray detectors must be cooled by a Joule-Thompson Cryostat, which does not seem compatible with a penetrator. Another problem seems to be procurement of suitable α-particle sources. Those individuals who fabricated the α-particle sources for the Surveyor instruments are apparently no longer in business.

Future Work

The major work that remains to be done for the α-proton-x-ray experiment is to overcome the problem of contamination of the target. There seem to be three basic possibilities. One is to design a diverter which causes the contaminated material to flow away from the α-experiment sampling port. A second is to design some device to sample outside the

the contaminated zone. A final alternative, which is less desirable than the previous two, is to fabricate the penetrator out of some material which is expected to be uninteresting in the target, so that the contamination will not matter as much. Work should begin on at least the first two alternatives immediately, since this problem is critical to the experiment as a whole. Additional future work involves construction of an actual miniaturized system and shock tests of the integrated components. Finally, alternatives to cooled intrinsic germanium for the x-ray detector should be investigated because a cryostat does not seem compatible with many of the other experiments proposed for the penetrators.

Although it cannot measure as many elements as the alpha-proton experiment, a gamma ray detector has the advantage of sampling a much larger volume of the target, since the gamma rays can pentrate up to 10 or 20 centimeters of material. Thus it would measure a more representative sample and would be less susceptible to problems of contamination of the target by emplacement of the penetrator. It has the further advantage over the alpha-proton experiment of measuring the radioactive elements U and Th which are geochemically very interesting and are important to the thermal history of a planet. A major potential disadvantage is that the detector will require shielding from gamma rays emitted from the ^{238}Pu in the RTG. However, with careful design, it may be possible to provide the necessary shielding with little or no weight penalty.

As currently envisioned, the gamma-ray experiment employs a NaI(Tl) scintillation detector. These detectors have relatively poor resolution, but do not require cooling to cryostatic temperatures. They have been used for terrestrial application for many years and were successfully flown in orbit during the Apollo missions. Phototubes, which are likely to be the most fragile part of a scintillation system have survived 3500 G tests. Cd-Te detectors, which are a new class of detector, offer the hope of improved resolution without the need for cooling. However, a detector which meets the requirements for the mission in terms of size and efficiency has not yet been fabricated, so that this type of detector would need considerably more design time.

The most important need for future work is to see whether the gamma background from the RTG can be sufficiently reduced in a penetrator configuration without using heavy shielding. In addition, an integrated scintillation system should be drop tested to see whether it survives in working condition. Attempts to acquire a suitable Cd-Te detector should begin. If an alpha-proton and gamma-ray experiment are flown simultaneously, which is desirable since they complement each other scientifically, they should be designed to use as much of the electronics as possible in common.

Mars Penetrator Heat-Flow Experiment

General Scientific Background

Measurement of the geothermal heat flux has been and is an important tool for the investigation of the materials properties and internal dynamics of the Earth. The global average is a constraint on the internal composition of our planet, especially when compared with the radioactive heat production of various samples of primitive solar system material from meteorites. These come in a considerable variety, and so the amount of diversity in composition among the inner solid planets would provide valuable information on the processes at work during the accretion phase of the solar system. Heat flow measurement, being essentially a global determination of uranium, thorium and potassium content, provides complementary information to surface chemical analyses, both in being global and in being restricted to elements of high atomic weight not easily lost by evaporation.

One of the outstanding problems in evaluating the thermal history of the planets is the role of the relatively short-lived isotopes that exist still in trace amounts, but which have long since ceased to produce much radioactive heating. The Earth is so dynamic that any trace of previously different convective regimes has been wiped out, unless one can deduce something from the former existence of a single continent (Pangea). Mars, especially, is an example of a planet large enough to have significant thermal events (huge volcanos, for example), but not so large and dynamic that all trace of past events is wiped out. In contrast to Venus, it has a visible and accessible surface of moderate

temperature where measurements can be made in rationally selected areas. If the global heat flow could be estimated, and/or significant regional variations found, some deductions could be made about the accretion temperature of the planet and the time history of volcanic effusion.

The heat flow of Mars is therefore the most interesting of any other body in the solar system, for Mercury is as dead as the Moon and Venus too inhospitable for measurement in the forseeable future. The lunar heat flow was measured in holes dug and tamped by astronauts, holes whose depth proved just adequate for the measurement in the highly regular and predictable lunar environment. The penetrator is the only cheap method available to 'dig holes' by remote control, and is potentially a most attractive way of measuring the thermal properties of all solid bodies, even though only those of planetary size can be expected to have a measurable heat flow. The engineering development of viable thermal measurement techniques should therefore be a fundamental part of the planning of penetrator missions.

Measurement Feasibility

Impact penetrators provide the best hope for the medium to deep penetration needed for a viable heat flow measurement. Geothermal gradients are small, even on planetary-sized bodies, and the principal difficulty is in separating true geothermal gradients from those due to daily, annual and climatic fluctuations of surface temperature. Added to these basic environmental difficulties are those imposed by the nature of the penetrator itself, principally the frictional heat generated on impact and the steady leakage of the heat from the radioisotope thermoelectric generator (RTG).

In general, the deeper the penetration, the better the chance of obtaining a reliable heat flow measurement. If Mars has the same internal heat production rate as the Earth, the heat flux may be expected to be about half as big, or about 40 mw/m^2 (1 $\mu cal/cm^2$-sec). The thermal conductivity of dry aeolian-transported dust suffused by a few millibars of carbon dioxide is likely to lie in the range 0.0002 to 0.001 W/cm-°K, between twice those found for the lunar regolith and values some ten times higher. The lower limit is set by the conductivity of carbon dioxide gas, about 0.00012 W/cm-°K at the temperature of the Martian surface and the vague upper limit by the contact conductivity of well-settled powders of wide particle-size range. The expected geothermal gradient thus ranges between 0.4 and 2°K/m for the dry 'desert' areas of Mars. The daily cycle of temperature at the Martian (equatorial) surface is about 100°K, and the spurious gradient due to this is attenuated to 0.1°K/m at a depth of 30-50 cm, depending on the actual diffusivity of the soil. The annual cycle at a moderate latitude may be about 30°K and this is attenuated to 0.1°K/m at a depth of 5-8 m.

Climatic cycles of unknown length may also exist on Mars, since visual observations of the planet have demonstrated changes in the relative prominence of the 'markings' over periods of 30-40 years. The polar caps, of high albedo, vary in size from year to year, and there is well-stirred dust on the planet, of contrasting albedo to some of the surface. Thus there are at least two mechanisms for changing the overall absorption and re-radiation of the planet, both coupled to details of circulation in the atmosphere. It is clear that the penetrators cannot go deep enough to eliminate short-term climatic fluctuations from contributing to the measurement, and measurements cannot be

and the sensors of interest as the observation time is increased. It is probable that near-surface sensors could establish magnitude and phase of the annual wave well enough to correct apparent gradients observed by the deepest useful sensors provided that the soil was found by the entry accelerometer to be reasonably uniform in properties with depth.

The second possible method of measuring in situ temperature is the deployment of mini-probes laterally from the penetrator body immediately after impact. The transient recovery time of small diameter probes is so short that measurements can be made before significant heat from the penetrator reaches the point of measurement. Because of the low expected conductivity of the Martian soil, the principal source of heat is that conducted along the mini-probe itself. Modeling studies so far have assumed the use of solid stainless steel probes, and suggest that very thin (1 mm diameter) probes have to be extended 20 cm or so into the soil to obtain reliable in situ temperature measurements. However, the use of wound fiberglass material for the probes would reduce the conductivity contrast between probe and soil by a factor of ten, and permit satisfactory measurements to be made by probes no longer than the diameter of the penetrator body. One advantage of the lateral probes is that they permit an accurate measurement of soil diffusity using the arrival time of the penetrator temperature wave and the measured probe extension. The transients are much shorter than those in the penetration hole, and temperature measurements are needed at least every minute to delineate the curves accurately. Long term observation of the penetrator body temperature is the only method available to measure the soil conductivity in its vicinity, unless significant electrical power can be dissipated in the small lateral

continued for long enough to observe any trends. The only way to eliminate climatic error from the measurements is to repeat them at suitable intervals.

The annual temperature wave penetrates to a depth comparable to the best hoped for from the present size and impact velocity available from the mission vehicles. Long-term monitoring of the fluctuations at observation depth is precluded, both by the mission lifetime and by the heating effect of the RTG, heat that spreads out from the penetrator body. In addition to the heat generated by the pentrator, it contains a substantial component of initial heat by arriving at a much higher temperature than that of the Martian soil, and deposits considerable frictional energy both in its own surface and in the walls of the hole. There are only two approaches available to determine in situ temperatures accurately. In the first, sensors can be deployed along the umbilical to the tailpiece, and the decaying impact transient can be monitored by making approximately hourly measurements of temperature. Methods of extrapolating the transient to true equilibrium are well developed and are accurate if the temperature can be followed for about six "time constants" a^2/κ, where a is the effective hole radius and κ is the soil thermal diffusivity. Monitoring should continue for 1 to 3 days, and the thermal pulse from the penetrator body does not complicate the measurement for sensors more than $\frac{1}{2}$ m from the tail. The chief disadvantages of this method are that there is no reliable way of determining soil conductivity, and the penetration is unlikely to be so great that the annual temperature wave can be discounted. Monitoring of the annual changes during the life of the mission is feasible, but progressively greater distances must be allowed between the RTG heat source

function. If it is buried in solid dry ice in a polar cap, it will be colder still. On the other hand, if buried at depth in light soil of the lowest expected conductivity, the temperature could rise toward 170°K above the soil ambient (20 W RTG). The choice of RTG thermal power level may have to be based on some estimate of the soil conductivity expected for 'sand dune' sites since these are the prime sites for heat flow measurement. There is difficulty in making this estimate, since laboratory studies of simulated lunar regolith produced conductivity estimates nearly an order of magnitude lower than those found in the actual measurements. This thermal control problem is to a large degree soluble by insulating the battery and RTG from the rest of the penetrator, and then providing a thermally switched (mechanical switch or variable conductance heat pipe) heat path to the penetrator shell. By this means the payload temperature can be held above the minimum acceptable temperatue. The maximum allowable thermal dissipation of the RTG will be controlled by the worst combination of low thermal conductivity and high soil temperature.

The chief technical problem related to the thermal measurements is the construction of a viable sensor-containing umbilical. The sensors themselves are available with adequate stability and shock resistance, and they are easy to measure with solid state circuitry to the 0.55°K precision required. However, the feasibility of constructing a multi-wire, multi-sensor umbilical that can meet the strength, flexibility and shock-acceleration requirements of penetrator emplacement needs to be demonstrated. The heat-flow experiment is probably viable without such an umbilical, and the materials-properties aspect of the lateral probe

probes immediately after the decay of their temperature transient.

Correcting for the annual temperature wave is difficult if this method is used alone, but an estimate may be possible if the penetrator body temperature is monitored carefully and the soil is reasonably uniform. It may be feasible to select sites where the annual temperature cycle is small enough for the method to be satisfactory directly; because of the asymmetry in the Martian climate these preferred sites may not be exactly on the equator.

All the above analysis assumes that the penetrators have entered dry Martian soil. The presence of even a small amount of ice in the soil would increase the conductivity so much that useful measurements could not be obtained - the conductivity of ice is 200 times that of the low-conductivity end of the expected dry-soil range. It is also obvious that maximum penetration must be aimed for, and this, too, would argue for a 'sand dune' site, since the penetrability of permafrost is relatively low. It may have to be accepted that useful heat flow measurements will be obtained only by a minority of the vehicles deployed, especially if a variety of terrain is desired for the geochemical sampling.

Mission-Related Remarks

Associated with the question of the RTG heating effect is the ambient temperature expected for the pentrator body under various different emplacement conditions. If the penetrator is partially stuck into solid basalt, the exterior surface will follow the Martian daily temperature cycle and be much too cold (except for a short period near equatorial noon) for the Nickel-Cadmium transmitting batteries to

measurement qualifies it as an interesting standard measurement for missions to other bodies in the solar system. The deployment of the lateral probes presents its own challenges because a large fineness ratio is needed to minimize axial conduction effects. Forcing thin probes several centimeters through soils containing even small pebbles is difficult, and some redundancy (multiple probes at each level) may have to be provided.

Meteorology

Scientific Goals

As a technique for obtaining low cost global meteorological measurements, a Mars Orbiter-Penetrator experiment could provide important scientific returns. Synoptic and global measurements could be made for periods of minutes to one or more Martian years. Annual and shorter term investigations are meteorologically important for several reasons. Among these are:

1) A complete annual cycle could be observed following the progression from low to medium to high winds and the corresponding local and planetary dust evolution. With the observation of turbidity from the afterbody and orbiter (hopefully obtaining particle size and optical propriety) some hypotheses relating atmospheric temperature to these parameters could be tested.

2) A highly regular diurnal variation in wind speed, wind direction and temperature has been observed at the Viking I landing site. This variation can be attributed to the sloping terrain at the site which, with diurnal heating and cooling, would generate upslope and downslope winds respectively, modified by rotation and surface friction. Alternatively, the diurnal variability could be due to a planetary scale diurnal traveling wave driven by the traveling daily heating cycle, a diurnal tide or a combination of these. A series of three or more surface meteorology probes located within 30 degrees of the equator

could determine the extent to which the traveling wave is responsible for the Viking I diurnal observations.

3) Terrestrial observations during unstable daytime conditions indicate that stability and heat and momentum fluxes can be obtained exclusively from temperature statistics. Quantitative estimates are obtained from the mean temperature, pressure and from the standard deviation and skewness of temperature after appropriate high pass filtering. The technique is being refined in terrestrial studies. In Viking, the technique is both being used and refined by cross checking with other estimates.

However, Viking does not have adequate resolution to best utilize such estimates or to readily verify the presence of the cold quiescent downward advected air parcels on which the estimation technique is based. The higher resolution of the penetrator measurements would facilitate use of the technique and provide better verification of the structure on which such techniques are based.

4) Statistics of the turbulent properties of wind and temperature in the turbulent surface layer would be intrinsically important and of value in determining some site properties near the penetrator, especially in tropical latitudes where the diurnal cycle is predictable.

5) The Viking mission has observed water ice clouds and their motion in addition to surface ice, fog or frost. The measurement of water vapor into and out of the surface daily and seasonally is an important element in understanding these phenomena along

with the surface geochemical evolution. Humidity fluxes probably will not be adequately understood during the Viking mission partially due to the unfortunate deletion of the humidity sensor from the surface meteorology experiment.

6) A global network would provide observations against which the results of general circulation models can be checked.

With the exception of the Viking program and some earlier Voyager studies, very little meteorological sensor development has or is taking place for landed planetary probes. This lack of long term development has resulted in a Viking meteorology instrument more complex than necessary, which has in turn generated excessive operational, management and computational problems. The severe power, weight and exposure problems (shock may be less important than expected) of the penetrator require that long term development of sensors and systems begin immediately so that the decision on the inclusion of meteorology in the Penetrator Mission will not be dictated by lagging development. Also, the development of sensors for planetary surface meteorology should not be neglected and this development would serve as a focus for other planetary probe development and terrestrial applications.

Measurements

Wind speed and direction

The Viking anemometer system consists of two hot film and a heated wake sensor to measure wind speed and direction. The power requirements for these sensors are too high for consideration in a penetrator applica-

tion. On a penetrator, a hot wire instead of a hot film could be used reducing the power by an order of magnitude for the two wind sensors. Viking sensor power requirements of .5 to .7 watts per sensor could be reduced to the 0.05 watt level, but Knudsen number effects would have to be incorporated in the processing. Alternatively, a spherical bead thermistor of 250 to 500 micron diameter could be used for wind speed but wind direction would require other methods. A drag sphere anemometer could provide two components and low power, but it would have to be leveled or its orientation determined.

Another potential wind system is the ion flow anemometer which can be made very rugged and low in power consumption. Commerical units are available and there does not appear to be any fundamental limitation. There are unknown effects related to gas composition and instrumental parameters that need to be investigated, but this could be a promising transducer. It is recommended that studies and tests of heated anemometer and ion flow instruments be started.

Temperature

The logical choice for temperature measurements is a thermocouple sensor of a design similar to the Viking system. The exposure and mounting would differ but the size and material could be the same. An important requirement is to provide an order of magnitude better resolution than was provided by Viking.

Pressure

Pressure can be measured either by capacitance or variable reluctance diaphram pressure transducers. For mechanical rigidity, a capacitance transducer is preferable. To obtain the absolute accuracy, a significant development effort may be required. If the absolute accuracy cannot be attained, an effort should be made to obtain long term stability of 0.01 millibars. The least stringent requirement would be for 0.01 millibar stability over one day.

Humidity

The importance of humidity should not be downgraded too much even though it is of secondary meteorological importance. However, the sensor requirements are very stringent and the transducer choices few. The Aluminum Oxide sensor responds at low humidity but with long time constants. The other sensor which is sensitive enough is the quartz crystal microbalance, the King sensor. This sensor was under development for Viking and has undergone a considerable amount of testing. The drawbacks of this transducer are the complexity, power consumption and size, which make it a doubtful choice for a penetrator.

Summary

The wide dispersal possible with a multi-penetrator mission makes it attractive as a meteorological program, provided that at least two and preferably more penetrators can be located 30 degrees or more apart. If large spacing cannot be used, then small arrays could be used to study synoptic processes. For this purpose, it would be desirable to move away from

the equator to obtain the most interesting weather. Within the general penetrator concept, there are several interesting scales and types of phenomena that can be profitably studied.

Summary and Conclusions

The Committee is convinced that penetrators can play a significant role in the exploration of the Moon, Mars, asteroids and the Galilean satellites. From previous studies it is clear that the engineering requirements of the Mars penetrator are considerably less severe than those for all these other targets. Penetrator missions have also been studied for the exploration of Venus and Mercury. These studies indicate that the Venus environment is unacceptably hot for a penetrator mission. Unfortunately Mercury is also problematical, again because of high subsurface temperatures (except near the poles) and further study is needed to determine if alternate "rough" surface landers might not be preferred.

It is, therefore, the opinion of the Committee that Mars is the prime first objective for application of penetrators to planetary exploration. We submit that this would be a truly significant beginning to the understanding of the planet as a whole. By comparison, an Earth penetrator mission would have brought us to the level of understanding of our planet as a whole not achieved until recently (see Appendix). The prospects for Mars are fully as good.

We believe that the seismic, geochemical and afterbody imaging experiments are far enough along to insure their feasibility for an early launch. The heat flow, total water and meteorological techniques are still not fully developed. In view of the extreme scientific interest in these measurements, we feel that intensive developmental effort in these areas should begin promptly so that, if feasible, the measurements can be made on Mars.

We conclude that there is a high probability that an adequate instrument package can be flown which addresses the many important basic scientific questions remaining after Viking. We therefore recommend that:

1) Immediate steps be taken to plan and implement a 1981 Mars Penetrator Mission;
2) Development of Class 1 and 2 experiments be started immediately so that a FY 1979 new start can immediately begin construction of flight hardware with demonstrated experiment concepts. We feel that the heat flow, total water and meteorological experiments, in particular, require immediate attention;
3) An advisory group be empaneled promptly to set scientific priorities, review progress and guide mission planning to maximize the science return from this mission. Members selected to this group should be both scientists and engineers, with particular care taken to insure that the majority of individuals do not have vested mission interests;
4) Immediate work be started to find workable solutions to the identified engineering and operational problems, particularly in the thermal control, umbilical deployment and data storage/processing areas.

Appendix

As an aid in appreciating the potential usefulness of a penetrator mission to a solid planet, we have reviewed what would be learned if 4 penetrators were emplaced on the Earth and operated for 1 year.

For this exercise we have assumed that the penetrators are emplaced on land, and that the penetrators have all the Class 1 and 2 experiments. We have also assumed orbital imaging and other remote sensing data exist.

After 1 year of operation, we would know the surface characteristics of a variety of major surface geologic units defined with earth orbital resolution (@ 100 m). Thus, the detailed morphology and topography of continental shield, ocean basin, folded mountain, and other global geologic units would provide significant data for the general interpretation of these units (rock types, structure, stratigraphy, surface weathering, etc.).

Imaging would provide information on the surface processes operating at the different sites, such as aeolian activity, fluvial and water-related modification, volcanism, biologic activity, etc. Images of rock and soil samples at local sites would add to this information. Extended observations would establish the characteristics of these processes, and their relative significance at each site. Observations over the lifetime of the mission would document transient events and establish rates of processes at specific sites. Processes that operated over wide portions of the planet would be monitored (snowstorms, weather fronts, dust storms, etc.). Specifically, a survey of surface vegetation, documentation of seasonal variations, and evidence of erosional agents such as rainfall and running water would be obtained.

Surface imaging results would also be important in the interpretation of other surface and orbital experiments, providing information on the substrate and environment in which surface geochemical, seismic, and heat flow experiments were being undertaken. Information on the grain size, block distribution, bedrock exposure, and local topography of the surface would be of significant interest to orbital remote sensing experiments.

We would be aware of the considerable geochemical heterogeneity of the earth's crust. It would at least be possible to detect the contrast between silicic continental crust and mafic oceanic crust. The penetrators would probably get few analyses of the true bedrock, because of effective surface modification processes and complications caused by sediment transport, but it would still be possible to see fundamentally different rock compositions which affect the final compositions. In addition, these complications would give fundamental insights into the nature of the processes which shape the earth's surface such as weathering, erosion, transport and sedimentation. If any bedrock were encountered, it would be possible from its analysis to begin drawing conclusions concerning the differentiation processes occurring on earth.

At least one of the penetrators might hit a more unusual rock type, such as limestone, giving an idea of the great range of chemical composition of rock on the earth's surface. Finally, the precise chemical analyses would provide valuable ground measurements for an accompanying orbiting geochemical experiment.

From the seismic stations, we would expect to record at least 10 large events on all instruments as well as a number of smaller events that would be recorded on one or more instruments. Assuming each major event would contain 10 or more phase arrivals as well as a surface wave train (with dispersion), one could expect to obtain some 400 or more data points to be used in the construction of a travel timetable. Such a data set should enable the identification of all of the major discontinuities within the earth, i.e. inner core, core, lower mantle, upper mantle, low velocity zone, and crust, as well as enable the identification of velocity changes and gradients within these regions. The difference between continental and oceanic upper mantle structure should also be identifiable. Moreover, one could probably identify one or more regions in which major tectonic activity was taking place, e.g. the subduction zones along the western margin of the Pacific Ocean.

From four heat flow measurements, the planetary heat flow could be deduced to an accuracy of about 50%. Variability among the measurements would demonstrate either that the earth is highly heterogeneous in the distribution of radioactive elements on a global scale, or that it has a dynamic surface. Comparison with the seismic results and orbiter data would eliminate the first possibility, and confirm that something like plate tectonics is occurring.

From orbiter imaging of cloud structure and with surface wind, temperature and pressure observations, the two two major meteorological regimes, tropical and subtropical would be deduced.

In the tropics, daily temperature variations of 10°C around 300°K would be discovered with weak pressure fluctuations on the order of 0.1% daily with few long-term fluctuations observed. A quite repeatable daily pattern of wind speed and direction variation would be observed with small seasonal variations. In other words, the tropics are predictable and for this reason are quite important in studying basic diurnal variations unobscured by other complicating processes. The annual movement of the intertropical convergence zone would be observed and the predominant easterly motions would be measured.

In the middle latitudes, the pattern of several days repeatable diurnal temperature variation would be dramatically interrupted by large and rapid pressure changes. With the rapidly decreasing pressure and temperature, wind speed increases and wind direction changes markedly. Coupled with the orbital imaging, the presence of low and high pressure centers and their motion would be observed and the development of frontal systems could be deduced.

The general wind direction would be from the west as opposed to the easterlies of the low latitudes in the northern hemisphere. Also it would be observed that fluctuations of temperature are much larger in the daytime than night, and the phenomena of unstable turbulent convective exchange would be observed. With a long period of observation, dust devils (and tornados?) might be observed, with their excessively large velocity compared to the mean wind. Clouds, fog and frost would be observed with

the imaging, demonstrating the wide variability of the weather as observed from the surface and an orbiter.

In summary, after one year of operation, we would have a level of understanding of the earth as a planet only reached in recent times. The prospects for Mars are surely as good.

☆ US GOVERNMENT PRINTING OFFICE: 1976-789-018/102